

**Morphological analysis of the
Golgi apparatus in
*Schizosaccharomyces pombe***

Thesis submitted towards the degree of Doctor of
Philosophy in the University of London

Kathryn Rachel Ayscough

University College London,
London WC1E 6BT

Imperial Cancer Research Fund,
Lincoln's Inn Fields
London, WC2A 3PX

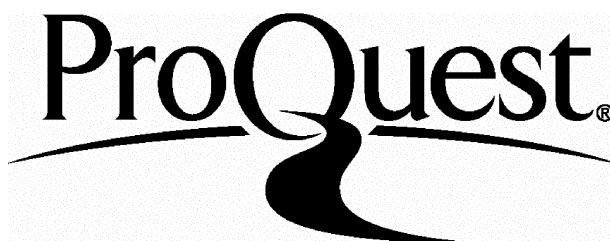
ProQuest Number: 10046094

All rights reserved

INFORMATION TO ALL USERS

The quality of this reproduction is dependent upon the quality of the copy submitted.

In the unlikely event that the author did not send a complete manuscript and there are missing pages, these will be noted. Also, if material had to be removed, a note will indicate the deletion.



ProQuest 10046094

Published by ProQuest LLC(2016). Copyright of the Dissertation is held by the Author.

All rights reserved.

This work is protected against unauthorized copying under Title 17, United States Code.
Microform Edition © ProQuest LLC.

ProQuest LLC
789 East Eisenhower Parkway
P.O. Box 1346
Ann Arbor, MI 48106-1346

Abstract

The most striking, morphological aspect of the Golgi apparatus is its stack of cisternae. How this distinct structure relates to its known function in the processing of secretory proteins, is however, not known.

During the course of my work I have made an intensive investigation of the morphology of the Golgi apparatus in *Schizosaccharomyces pombe*. This yeast contains stacks of membranes resembling the Golgi stacks of mammalian cells suggesting that certain fundamental processes underlying formation of the stack may be conserved.

I have demonstrated that the Golgi cisternae can be reversibly unstacked in vivo and that stacking required intact cytoplasmic microtubules. This was revealed by use of microtubule disrupting drugs and tubulin mutants. The functional consequences of this morphological change were addressed.

Inhibition of protein synthesis and a mutation in a gene product required early in the secretory pathway resulted in breakdown of the Golgi apparatus.

The action of Brefeldin A was investigated and resembled its effect in mammalian cells with Golgi disruption and redistribution to the ER.

Finally, specific cross reactivity with an antibody to mammalian Golgi structures showed that some epitopes have been conserved over the evolutionary period of divergence from *S.pombe* to mammalian cells.

This study has highlighted many aspects of the Golgi structure and further research at a genetic level would reveal molecules involved in the maintenance of the stack. Such work would in turn increase our understanding of the role of cisternal stacking.

Contents

	Page
Abstract	
Chapter 1. Introduction	12
1.1 Introduction	13
1.2 The secretory pathway	17
1.2.1 Outline of the pathway	17
1.2.2. The endoplasmic reticulum	20
1.2.3. Exit from the ER	21
1.2.4. Recycling between the ER and the Golgi apparatus	22
1.2.5. Glycosylation in the Golgi apparatus	24
1.2.6. Compartmentalization of the Golgi apparatus	25
1.2.7. Retention of proteins in the Golgi stack	28
1.2.8. Sorting in the trans Golgi network	29
1.2.9. Vesicular traffic in the secretory pathway	30
1.3. Structural aspects of the Golgi stack	36
1.4. Microtubules and the organization of the Golgi apparatus	37
1.5. The secretory pathway in <i>S.cerevisiae</i>	39
1.5.1. Introduction	39
1.5.2 The <i>SEC</i> genes and the genetics of the secretory pathway	40
1.5.3. Glycoprotein modifications in the secretory pathway	46
1.5.4 Compartmentalization in the secretory pathway	47
1.5.5. Diverting proteins from the default pathway	47

1.5.6. The structure of the Golgi apparatus in <i>S.cerevisiae</i>	48
1.6. Reasons for a stack	52
1.6.1. Introduction	52
1.6.2. Stacking to maximize efficiency of transport	52
1.6.3. Stacking to maximize recovery of protein lost from the ER	56
1.7. Using <i>Schizosaccharomyces pombe</i> to facilitate understanding of the Golgi apparatus	57
1.7.1. Introduction	57
1.7.2. The Golgi apparatus in <i>S.pombe</i>	58
1.7.3. Functioning of the Golgi apparatus in <i>S.pombe</i>	58
1.8. The aims of this project	62
Chapter 2. Materials and Methods	63
2.1. Materials	64
2.1.1. General laboratory services	64
2.1.2. Chemicals	64
2.2. Yeast procedures	65
2.2.1. Strains	65
2.2.2. Media	66
2.2.3. Growth	67
2.2.4. Storage	68
2.2.5. Measuring cell number	68
2.2.6. Spheroplasting cells	69
2.2.7. Preparation of yeast homogenates and microsomes	69
2.2.8. Drugs used in the study	70
2.3. Antibodies	71

2.3.1. Primary antibodies	71
2.3.2. Secondary antibodies	71
2.3.3. Preparation of a fusion protein using the pUEX system and raising antibodies to the overexpressed product	72
2.4. Immunofluorescence	73
2.4.1. Solutions	73
2.4.2. Immunofluorescence using methanol fixation	74
2.4.3. Mounting cells for fluorescence microscopy	74
2.4.4. Preparation of coverslips	75
2.4.5. Viewing stained cells	75
2.4.6. Confocal microscopy	75
2.5. Fluorescence staining of cell organelles	75
2.5.1. Golgi apparatus staining	75
2.5.2. Nuclear staining	76
2.5.3. Vacuolar staining	76
2.5.4. Viewing stained cells	77
2.6. Electron microscopy	77
2.6.1. Solutions	77
2.6.2. Fixatives	77
2.6.3 Processing and embedding	78
2.6.4. Immuno-electron microscopy	79
2.6.5. Quantitative Analysis	80
2.7. Protein Procedures	82
2.7.1. Preparing <i>S.pombe</i> protein extracts	82
2.7.2. Measuring the level of protein synthesis by incorporation of ³⁵ S-trans label	83

2.7.3. Measuring protein concentration	83
2.7.4. Sucrose gradients	84
2.7.5. Endoglycosidase H digestion	84
2.7.6. SDS-PAGE gels	85
2.7.7. Western Blotting	86
2.7.8. Western blotting (alternative protocol)	87
2.8. Enzyme assays	88
2.8.1. Acid Phosphatase	88
2.8.2. Hexokinase	89
2.8.3. α -1,2-galactosyltransferase (GalT)	89
Chapter 3. The Golgi apparatus in wild type cells	91
3.1. Introduction	92
3.2. Light Microscopy	92
3.2.1 Fluorescent probes for cellular organelles	92
3.2.2 Fluorescent probes for the Golgi apparatus	95
3.2.3 Immunofluorescence microscopy	99
3.2.4 Characteristics of the Golgi apparatus revealed by fluorescence microscopy	111
3.3. Electron Microscopy	117
3.3.1 Characteristics of the Golgi apparatus revealed by electron microscopy	120
3.3.2. Factors affecting the morphology of Golgi stacks in wild type cells	134
3.4. Discussion	139
Chapter 4. Stacking of Golgi cisternae requires intact microtubules	140
4.1. Introduction	141

4.2. Results	142
4.2.1. The effect of nocodazole on <i>S.pombe</i> cells	142
4.2.2 Investigating the use of chemically related alternatives to nocodazole	145
4.2.3. The effect of TBZ on growth and division	145
4.2.4. The effect of TBZ on polarized growth	148
4.2.4 The effect of TBZ on microtubules	151
4.2.6. Effect of TBZ on the Golgi apparatus - quantitation	151
4.2.7. Tubulin mutants	168
4.2.8. The functional consequences of microtubule disruption and Golgi unstacking	174
4.3. Discussion	183
Chapter 5. Inhibition of protein synthesis disrupts the Golgi apparatus in fission yeast	186
5.1. Introduction	187
5.2. Results	187
5.2.1. Inhibitors	187
5.2.2. Immunofluorescence microscopy	190
5.2.3. Electron microscopy	195
5.2.4. Changes in Cell Proteins	200
5.2.5. Disruption of the Golgi apparatus is reversible	208
5.3. Discussion	211
Chapter 6. The effect of Brefeldin A on the Golgi apparatus in <i>S.pombe</i>	218
6.1. Introduction	219
6.2. Results	220

6.2.1. Effect on growth	220
6.2.2 Immunofluorescence	223
6.2.3. Electron microscopy and quantitation	226
6.2.4. Reversibility of the BFA effect on the Golgi apparatus	231
6.2.5. Effect on Golgi marker proteins	234
6.3. Discussion	240
Chapter 7. Changes in the Golgi apparatus of mutant strains of <i>S.pombe</i>	242
7.1. Introduction	243
7.2. Secretory mutants	244
7.2.1. Background	244
7.2.2. Results	245
7.2.3. Discussion	253
7.3. Cell cycle mutants	254
7.3.1. Background	254
7.3.2. Results	258
7.3.3. Discussion	263
Chapter 8. Recognition of the Golgi apparatus in <i>S.pombe</i> by antibodies raised to mammalian Golgi structures	269
8.1. Introduction	270
8.2. Results	271
8.2.1. Western Blotting	271
8.2.2. Immunofluorescence microscopy	271
8.2.3. Factors affecting the TEX staining pattern	276
8.3. Discussion	279

Chapter 9. Concluding remarks	280
9.1. Summary introduction	281
9.2. Structural conservation between the mammalian and fission yeast Golgi apparatus	281
9.3. The Golgi apparatus at mitosis and the effect of microtubule disruption	284
9.4. The effect on the Golgi apparatus of blocking the secretory pathway	285
9.5. The effect of Brefeldin A on the Golgi apparatus	286
9.6. Summary	287
Acknowledgements	289
References	291

For James

" walk out with me toward the unknown region"

Abbreviations

ANS	anisomycin
β -gal	β -galactosidase
BiP	Immunoglobulin binding protein
BFA	Brefeldin A
CGN	cis Golgi network
CHX	cycloheximide
CPY	carboxypeptidase Y
DNA	Deoxyribonucleic acid
DMM	Defined minimal medium
e.m.	electron microscopy
ER	Endoplasmic reticulum
gal	galactose
GalT	galactosyltransferase
Glc	glucose
GlcNac	N-acetylglucosamine
kDa	kiloDalton
NEM	N-ethylmaleimide
NSF	NEM sensitive factor
Man	mannose
TBZ	thiabendazole
TGN	Trans Golgi Network
s.d.	standard deviation
VSV	vesicular stomatitis virus
YES	Yeast extract + supplements

Chapter 1

Introduction

1.1 Introduction

The Golgi apparatus was first recognized as a unique cellular entity nearly one hundred years ago (Golgi, 1898). Since this time it has been the subject of much controversy regarding both its structure and its function. Although its existence as a distinct organelle is now fully accepted many aspects of how its complex structure relates to its recognized function in protein processing have yet to be revealed.

The initial observations of the Golgi apparatus were made with the light microscope using specimens impregnated with salts or heavy metals. In many instances structures other than what is currently defined as the Golgi apparatus were stained including lysosomes and parts of the endoplasmic reticulum (ER). These uncertainties led many to believe the Golgi apparatus was an artifact of the preparative methods.

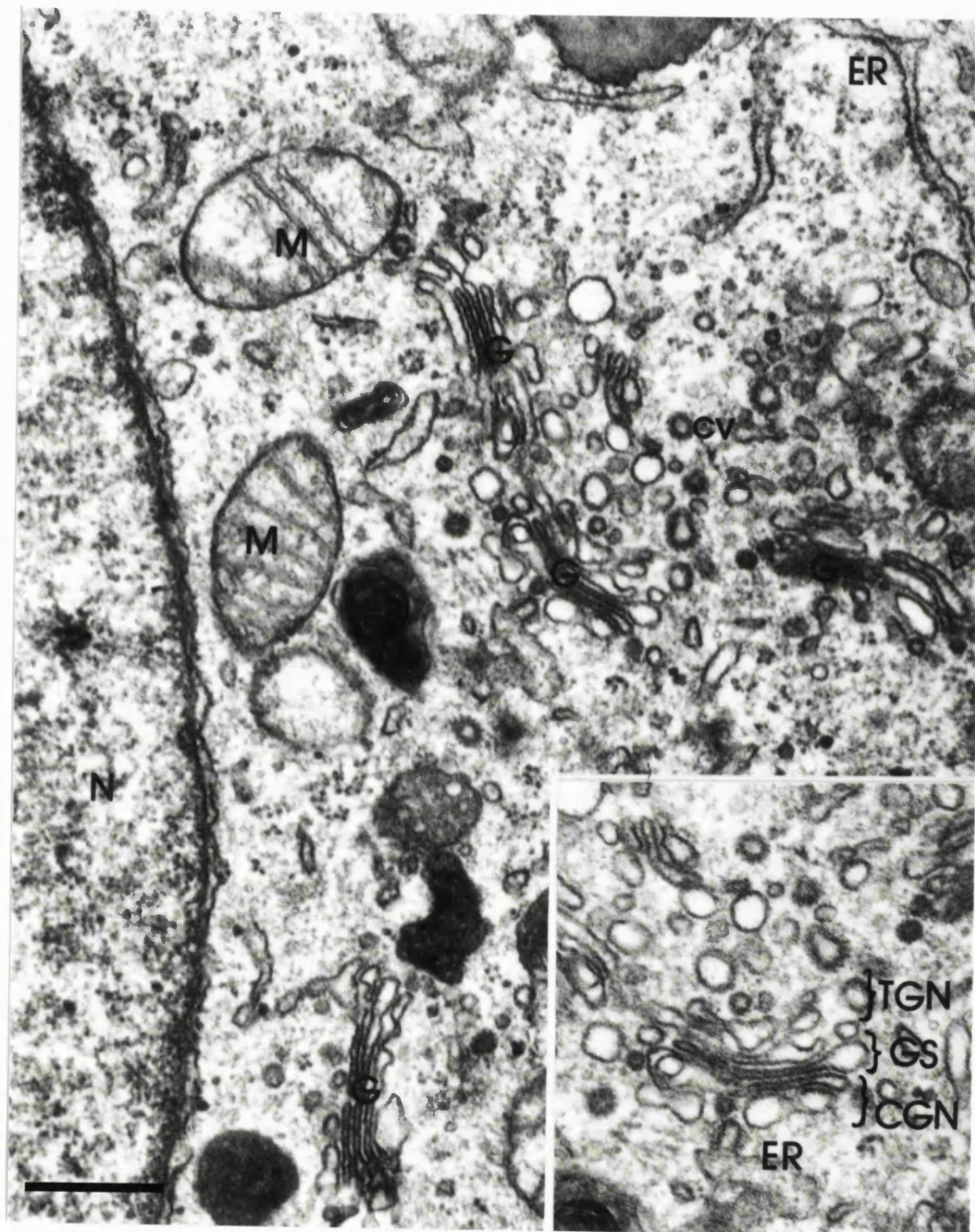
The advent of the electron microscope however, erased the controversy over the ubiquity of the organelle. Electron micrographs illustrating the Golgi apparatus as it is now known were published by Dalton and Felix (1954, 1957) and by Sjöstrand and Hanzon (1954).

In the classic electron microscope image the Golgi apparatus appears as a structure consisting of stacks of flattened membrane compartments known as cisternae and occupies a juxtanuclear position (Farquhar and Palade, 1981). Surrounding this stack are numerous vesicles thought to be involved in transporting proteins from one cisterna to another. The rims of the stacks are usually dilated and are proposed to be the sites of vesicle budding (Palade, 1975). Figure 1.1 clearly shows the distinctive stack structure we now associate with the Golgi apparatus.

Figure 1.1. The Golgi apparatus in a mammalian cell

Electron micrograph of a HeLa cell illustrating the classic image of the Golgi apparatus. Inset shows a single stack (GS) with the compartments of the stack labelled, CGN = cis Golgi network, TGN = trans Golgi network. Bar = 0.45 μm .

G = Golgi apparatus, ER = endoplasmic reticulum, N = nucleus, M = mitochondria



Another aspect of the Golgi structure highlighted in the figure is its polarity. The stack is thought to be traversed in a unidirectional manner with proteins being exposed to sets of processing enzymes in the different compartments. The first compartment, the cis Golgi network (CGN) and the final compartment (TGN) are more reticular and can be distinguished visually (Fig. 1.1 inset). These compartments are thought to be primarily involved in sorting processes. The CGN may have a role in the retrieval of ER proteins that have escaped their resident compartment whilst the TGN is involved in the sorting of proteins to their final destinations.

In order to comprehend the functional role of the Golgi apparatus it is easiest to describe it in the context of the whole secretory pathway since its function is inherently tied to that of other compartments lying both downstream and upstream of it in this pathway. I shall initially describe the secretory pathway in mammalian cells because this is the system that is most fully understood. Many of the individual processing reactions have been characterized and certain stages of the vesicular transport between the compartments have been elucidated at the molecular level.

I shall then briefly discuss what is known about structural components involved in stacking Golgi cisternae in mammalian cells, thus illustrating our lack of knowledge concerning factors responsible for forming and maintaining the stacked structure. I will also consider the relationship between microtubules and the structure of the Golgi apparatus since changes in Golgi structure in mammalian cells are often associated with alterations in the microtubular network.

Following this I will introduce the secretory pathway in the yeast, *S.cerevisiae*. This highlights the current Golgi controversy concerning

the requirement for a stack. Whilst the various functions of the Golgi apparatus in processing and sorting seem to be universal amongst eukaryotes, not all eukaryotes appear to have the distinctive Golgi stack structure. Some possible reasons for cisternal stacking will be considered in light of the known role of the Golgi apparatus.

The uncertainty concerning the role of the stack emphasizes the need for a simple system in which to study the structural and functional relationships of the Golgi apparatus. I conclude the introduction with a summary of what was known about the Golgi apparatus in the fission yeast, *S.pombe*, at the outset of my research.

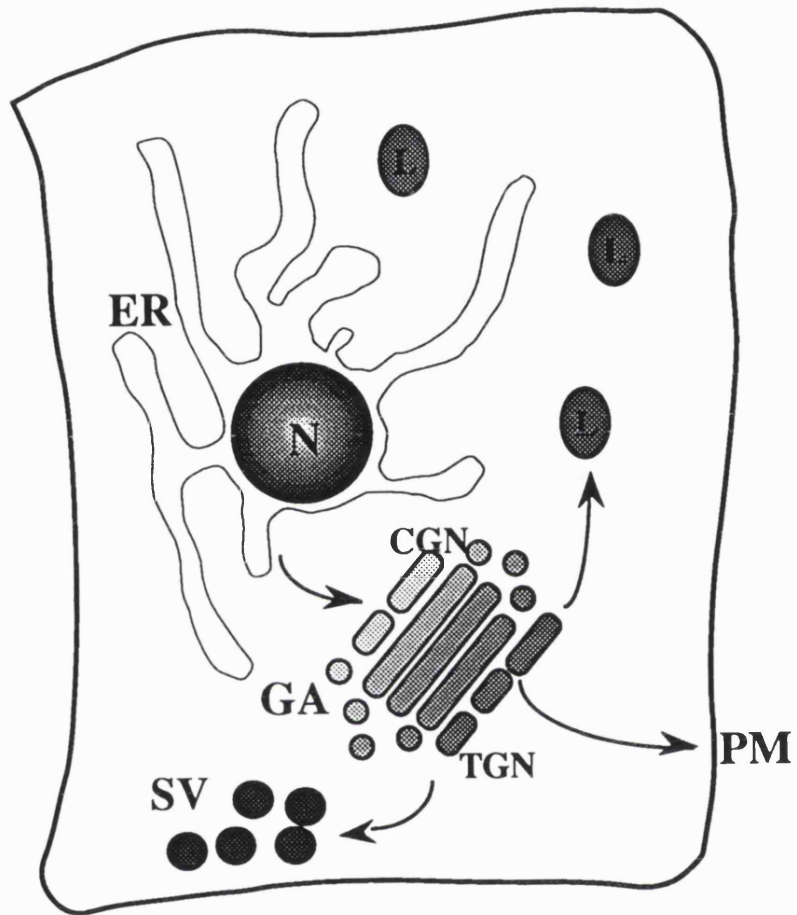
1.2 The secretory pathway

1.2.1 Outline of the pathway

The secretory pathway of eukaryotes consists of a set of membrane bound organelles; the endoplasmic reticulum (ER), the Golgi apparatus and the secretory vesicles (Fig. 1.2). Proteins destined for secretion from cells pass through these compartments where they receive post translational modifications before they are sent to the cell surface. Other proteins may remain resident in one of the compartments or can be diverted after traversing the Golgi apparatus to hydrolytic compartments, lysosomes in animal cells or vacuoles in fungi and plants. Whilst in transit through the compartments of the secretory pathway proteins can be post-translationally modified by specific sets of enzymes in each of the different compartments. At all stages, the secretory pathway is thought to operate by the budding of a vesicle from a donor membrane and targeting it to the correct acceptor membrane, and subsequent fusion of the two compartments. This exposes the contents of the vesicle to the lumen of

Figure 1.2. The secretory pathway in a typical mammalian cell

A schematic diagram of a mammalian cell showing the organelles of the secretory pathway. Arrows indicate the route of a secretory protein from the endoplasmic reticulum (ER), via the Golgi apparatus (GA), to the plasma membrane (PM). Certain proteins are directed, when they reach the trans Golgi network (TGN) to the lysosomes (L), or to secretory vesicles (SV). Certain proteins of the ER may escape their resident compartment and then be retrieved from the cis Golgi network (CGN).



the acceptor organelle and the enzymes there, or to the exterior of the cell.

1.2 The endoplasmic reticulum

Secretory proteins segregate from cytoplasmic proteins at translation. Translation of secretory proteins takes place on ribosomes associated with the ER. The association of these ribosomes with the ER gives a studded appearance of these regions when observed by electron microscopy and they are known as the rough endoplasmic reticulum (RER). Translation is accompanied by simultaneous translocation of the nascent polypeptide into the lumen of the ER (Blobel and Dobberstein, 1975).

On entry to the ER, secretory proteins become subjected to a range of modifications. Amongst ER specific modifications are, cleavage of the signal sequence, disulphide bond formation, and oligomerization (Copeland, et al., 1986). This compartment is also where proteins with certain consensus sequences can be modified by the addition of core oligosaccharides. Both asparagine (N-) linked and serine, threonine (O) linked oligosaccharides are first added in the ER lumen. N-linked sugars are added co-translationally whilst the addition of O-glycans is mostly thought to be post-translational. The oligosaccharides bound to proteins have provided invaluable tools for work on the secretory pathway since the extent to which they become modified indicates the parts of the pathway which are operational and also the parts of the pathway that are in common between different systems. The N-linked oligosaccharide is added to certain asparagine residues in the sequence Asn-X-Ser/Thr where X is any residue except proline. The core oligosaccharide transferred from a dolichol lipid precursor is Glc₃-Man₉-GlcNAc₂ (Behrens, et al., 1971; Behrens, et al., 1973; Bause and

Lehle 1979). This is illustrated later in figure 1.3. The enzyme responsible for transfer of the core glycan, oligosaccharyltransferase, has recently been purified (Kelleher, et al., 1992). After transfer these N-linked oligosaccharides are acted on by processing enzymes which trim the structure to a Man₅-GlcNAc₂ structure before the proteins exit the ER (Kornfeld and Kornfeld, 1985).

1.2.3. Exit from the ER

A mechanism exists in the ER to allow only the export of proteins which have achieved the correct three dimensional conformation. Misfolded proteins, or those which have not associated with relevant partners to form oligomeric structures are retained in the ER. In animal cells many of these proteins are associated with the protein BiP. This protein was first identified as a heavy chain immunoglobulin binding protein. It was found associated with this protein when light chains were not produced so preventing the necessary oligomer from forming and leaving the ER (Machamer, et al., 1990). BiP may also bind transiently to proteins, possibly to stabilize them in the course of folding or oligomerization (Pelham, 1989a; Rothman, 1989a). When folding is complete, BiP is released and the protein is free to exit the ER (Gething, et al., 1986).

Proteins leave the ER in vesicles which bud from regions of the ER that are free of ribosomes, known as transitional elements. Several lines of evidence indicate the existence of vesicle carriers. The first report was from electron microscope studies showing vesicles budding from the transitional region of the ER (Palade, 1975; Saraste and Kuismanen, 1984). Fractionation of membrane preparations from tissue culture cells led to the identification of vesicles proposed to be specific for ER to Golgi transport (Lodish, et al., 1987) and incubation of ER membranes

with ATP and cytosol also caused production of vesicles (Paulik, et al., 1988).

The nature of the budding and fusion of transport vesicles is discussed more fully in 1.2.9.

1.2.4. Recycling between the ER and the Golgi apparatus

Several groups are currently investigating the facets of a protein which allow it to reside in the ER rather than being transported with the majority of protein through the Golgi apparatus. Most evidence suggests that movement toward the cell surface is by default whereas retention requires special signals (Burgess and Kelly, 1987; Rothman, 1987). Thus cytoplasmic proteins introduced into the ER lumen will be secreted efficiently provided they can fold.

Several specific signals have been identified in proteins considered to be permanent residents of the ER. Many of the soluble ER proteins in mammalian cells bear a carboxy terminal tetrapeptide sequence, KDEL, which has been shown to be necessary and sufficient for at least one of these proteins, BiP (Munro and Pelham, 1987). The growing number of luminal proteins that bear this sequence implicate it as the distinctive feature that signals residency of the ER. The KDEL motif appears to operate mainly by signalling a protein for retrieval if and when a protein bearing this tag escapes from the ER to the cis Golgi network (CGN). Evidence for a salvage mechanism from a post-ER compartment came from an experiment in which the sequence HDEL (the *S.cerevisiae* equivalent of the mammalian signal KDEL) was attached to the C terminus of a protein normally secreted from yeast. The HDEL protein was localized to the ER, yet was also modified by the addition of mannose residues, modifications characteristic of early

Golgi apparatus compartments. The changes in glycosylation pattern did not occur when transport from the ER was blocked in mutant strains, confirming that proteins must leave the ER in order to receive the observed modifications (Dean and Pelham, 1990).

The signals causing ER residency of certain membrane proteins have also been investigated. The sequence KX(X)KXX, where this final X is the cytoplasmically exposed terminal amino acid, has been identified as necessary for residency (Nilsson, et al., 1989; Jackson, et al., 1990). There is a report that this signal also specifies retrieval from the CGN and possibly later compartments (Rothman and Orci, 1992; Jackson, 1993).

A receptor responsible for salvaging the KDEL bearing proteins has also been identified. The yeast homologue was firstly found in a mutant screen and called *erd2* (for ER retention defective). It confers specificity for HDEL tagged proteins. The human *erd2* gene is predicted to encode a 26 kDa protein that may span the bilayer seven times (Lewis and Pelham, 1990a). Immunofluorescence indicates that the human gene product is localized to the Golgi apparatus (Lewis and Pelham, 1990a). More recently a second KDEL receptor gene has been sequenced and its gene product shown to function in retrograde transport from the Golgi to the ER. Whether this receptor has the same function in vivo is not known (Lewis and Pelham, 1992b).

The mechanisms so far discovered indicate that ER residency is achieved by retrieval from post-ER compartments. There may however be further systems which operate within the ER to deter loss of resident proteins. This is suggested by the observation that removal of the KDEL sequence from a protein normally resident in this compartment

e.g. BiP, results in its secretion but at a much slower rate than for routinely secreted proteins (Munro and Pelham, 1987).

Although several components necessary for retrieval of ER proteins have been identified, the mechanism by which the proteins are returned to the ER is not clear. Studies using the fungal metabolite, Brefeldin A (BFA) have highlighted a retrograde pathway from the Golgi apparatus to the ER (Klausner, et al., 1992). In the presence of BFA, Golgi enzymes from the cis, medial and trans compartments but not from the TGN reversibly redistribute into the ER, leading to the disappearance of the typical Golgi morphology of stacked cisternae (Doms, et al., 1989; Lippincott-Schwartz, et al., 1989; Chege and Pfeffer, 1990). At the same time transport beyond this mixed ER/Golgi compartment becomes blocked and ER proteins experience a range of Golgi specific modifications. Microscopically, tubules can be seen to emanate from the Golgi apparatus following BFA addition and these travel along microtubules to the ER (Lippincott-Schwartz, et al., 1990). There is no direct evidence however, that these membrane tubules involved in the Golgi reorganization in the presence of BFA, are the elements responsible for the selective retrieval of KDEL tagged proteins.

1.2.5. Glycosylation in the Golgi apparatus

The passage of proteins through the Golgi apparatus is best reflected in the modifications that such proteins receive. Glycosylation is the most fully characterized of the various post translational modifications occurring in the secretory pathway. Other processes known to occur in the Golgi apparatus are acylation (Dunphy, et al., 1981), phosphorylation (Lang, 1984) and sulphation (Huttner, 1987; Niehrs and Huttner, 1990)

As mentioned earlier two types of glycosidic linkage are made, called N- and O- linked, according to which residue the sugars are added. The best understood processing involves the N-linked oligosaccharides. These are firstly added in the ER from a preformed structure transferred from a lipid precursor (see 1.2.2). Entry into the Golgi stack exposes the oligosaccharides to an array of enzymes some of which, firstly trim these structures from $\text{Man}_8\text{GlcNAc}_2$ to a $\text{Man}_5\text{GlcNAc}_2$ form and then further reactions occur to allow a variety of more complex structures to be assembled. An example of oligosaccharide processing for the construction of biantennary N-linked sugars in mammalian cells is shown schematically in figure 1.3.

Several factors determine the final oligosaccharide structures. These include the level of different enzymes in the various subcompartments of the stack, and the degree to which the oligosaccharide is exposed in the folded polypeptide (Williams and Lennarz, 1984; Dahms and Hart, 1986; Schacter, 1986).

1.2.6. Compartmentalization of the Golgi apparatus

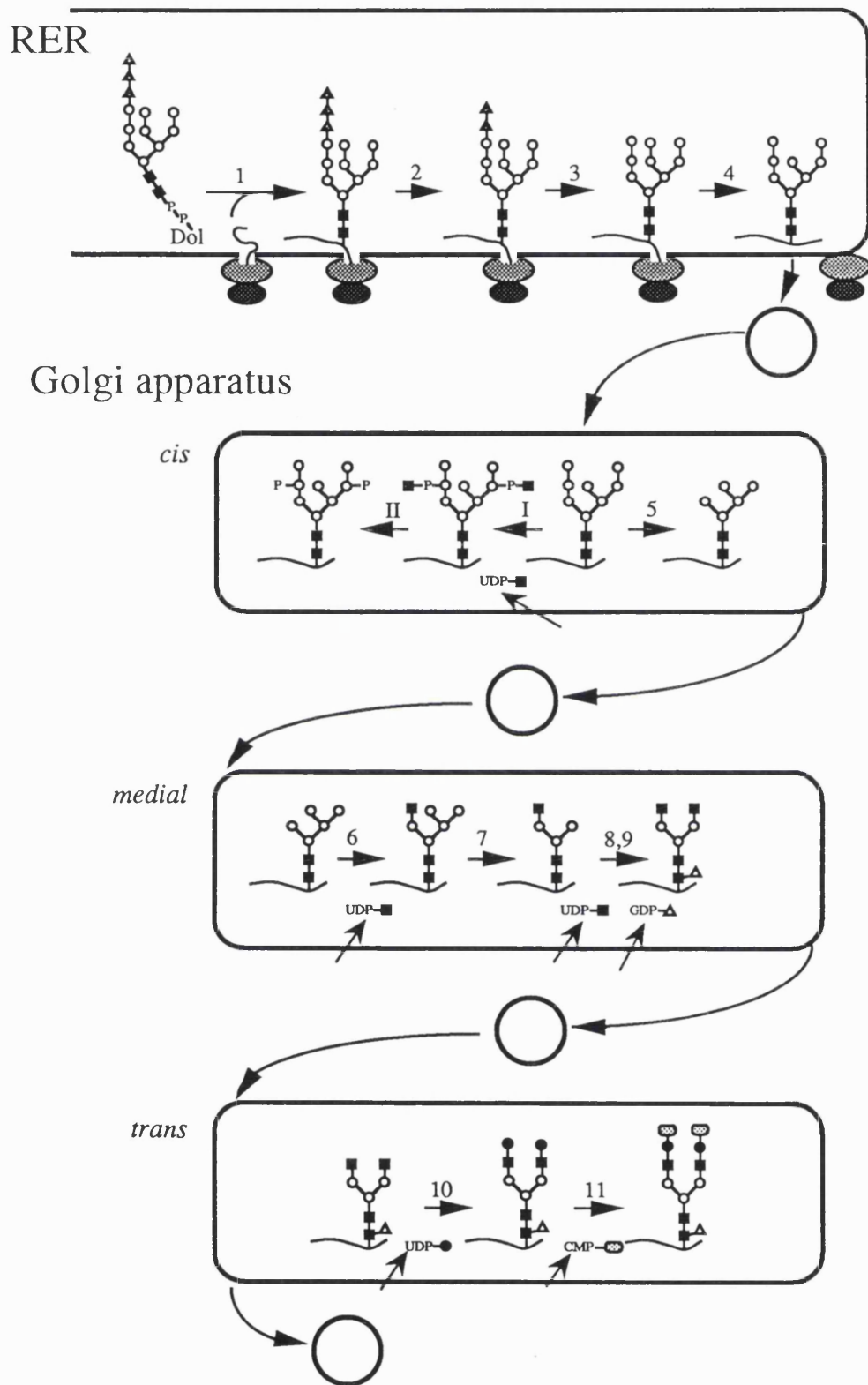
A variety of techniques have been employed to localize oligosaccharide processing reactions to specific subcompartments of the Golgi apparatus. The most definitive method to emerge involves immunocytochemical labelling of ultrathin sections to localize specific proteins within the cells at the electron microscope level. Using colloidal gold particles coated with Protein A as the marker, Roth and Berger (1982) showed that $\beta 1,4$,galactosyltransferase was localized in only two or three cisternae at the trans side of Golgi stacks in HeLa cells whereas Slot and Geuze (1983) using ultrathin cryosections from human hepatoma cells localized the same enzyme to a single trans cisterna. The enzyme, *N*-acetyl glucosaminyltransferase was localized using immunoperoxidase to the

Figure 1.3. Schematic pathway of oligosaccharide processing on newly synthesized glycoproteins

Proteins are translocated into the ER as they are translated. On entry into the lumen they may be modified by the addition of a preformed oligosaccharide. This structure is then trimmed and processed as the protein traverses the secretory pathway. The processing depicted is a simple example of a set of reactions which a glycoprotein might encounter.

The reactions are catalyzed by the following enzymes: (1) oligosaccharyltransferase, (2) α -glucosidase I, (3) α -glucosidase II, (4) ER α 1,2-mannosidase, (5) Golgi α -mannosidase I, (6) N-acetylglucosaminyl transferase I, (7) Golgi α -mannosidase II, (8) N-acetylglucosaminyl transferase II, (9) fucosyltransferase, (10) galactosyltransferase, (11) sialyltransferase. Proteins to be directed to the lysosomes may be modified in the first compartment by enzymes: (I) N-acetylglucosaminylphosphotransferase, (II) N-acetylglucosamine-1-phosphodiester α -N-acetylglucosaminidase.

The symbols represent: ■, N-acetylglucosamine; ○, mannose; ▲, glucose; △, fucose; ●, galactose; ▨, sialic acid.



medial cisternae (Dunphy and Rothman, 1985). From these original immunocytochemical experiments it was not clear whether each enzyme was found in a single type of compartment or whether there was some degree of overlap. More recently double labelling has been achieved of two glycosyltransferases in the Golgi apparatus of HeLa cells. This demonstrated an overlapping distribution of N-acetylglucosaminyl transferase I (medial) and galactosyltransferase (trans and TGN) (Nilsson, et al., 1993). These data suggests that the differences between cisternae are determined not by distinct sets of enzymes but by different mixtures.

Other approaches have provided convincing albeit less direct evidence for compartmentalization of the Golgi apparatus. By using sucrose density fractionation various groups demonstrated separation of up to four different enzyme activities (Dunphy, et al., 1981; Dunphy and Rothman, 1983; Goldberg and Kornfeld, 1983). Other workers have mapped the distribution of oligosaccharides by using lectins that bind to specific carbohydrate structures (Griffiths, et al., 1982; Tartakoff and Vassalli, 1983).

1.2.7. Retention of proteins in the Golgi stack

All of the Golgi resident enzymes characterized are integral membrane proteins. These proteins must be retained in their correct compartment so that they are able to function at the appropriate time in the sequence of processing events. They must also be retained against the general bulk flow of traffic destined for the cell surface, secretory vesicles or for lysosomes. Various groups have recently demonstrated the importance of the transmembrane spanning domain in the retention mechanism (Munro, 1991; Nilsson, et al., 1991; Swift and Machamer, 1991; Wong, et al., 1992). When the membrane-spanning domain of a

construct, reporter molecule is replaced by that of a Golgi protein the protein not only resides in the Golgi apparatus but in the correct cisterna (Nilsson, et al., 1991; Burke, et al., 1992). The simplest model to explain retention using this domain is to suggest that Golgi enzymes interact with their neighbours through their membrane spanning domains forming oligomers so large that they cannot enter vesicles budding from the dilated rims.

1.2.8. Sorting in the trans Golgi network

The trans most side of the Golgi apparatus in the animal cell consists of a tubular membrane structure and is the site of sorting secretory proteins. (Griffiths and Simons, 1986). Secretory proteins can be sorted into three categories: 1) bulk flow plasma membrane and secretory proteins; 2) proteins of the regulated secretory pathway; 3) lysosomal proteins. Secretory animal cells secrete proteins simultaneously along the regulated and constitutive pathway (Kelly, 1985). In the regulated pathway the secretory proteins are stored in granules which release their contents by fusing with the plasma membrane as a response to an extracellular stimulus e.g. secretion of histamine from IgE-sensitized rat basophilic cells after antigen stimulation.

The signal to target soluble proteins to the mammalian lysosome is phosphorylation in the cis Golgi of specific mannose residues of high mannose type oligosaccharide chains at position C₆ (von Figura and Hasilik, 1986; Lazzarino and Gabel, 1988). The sorting signal is recognized by one of two different mannose phosphate receptors, the 46 kDa or the 215 kDa receptor (Tong, et al., 1989; Tong and Kornfeld, 1989). The 215 kDa receptor is located in the TGN, endosomes and at the plasma membrane. In addition to directing newly synthesized proteins to lysosomes, it also harvests escaped lysosomal proteins from

the cell surface and directs them to the lysosome by endocytosis (Willingham, et al., 1981).

The TGN appears to be the only site in the Golgi apparatus of animal cells where clathrin is present (Griffiths, et al., 1981; Orci, et al., 1985). Clathrin coated vesicles appear to function in steps of the pathway that require selection of vesicle cargo. i.e. selection of proteins destined for lysosomes or for secretory granules.

1.2.9. Vesicular traffic in the secretory pathway

The current paradigm for transport through the secretory pathway is that of bulk flow. In this model, constitutive secretion from the ER through the Golgi apparatus to the cell surface occurs by default i.e. no sorting signal is required. All diversions from this pathway to other compartments must be signal mediated. Initial evidence for a default pathway for secretion was reported by Wiedman (1984), who showed that a bacterial protein, β -lactamase could be secreted from oocytes. Further confirmation for the bulk flow model came from experiments in which a tripeptide of the N-linked glycan motif, Asn-X-Ser/Thr was introduced into cells. This could enter various compartments but on entry to the ER could be modified by the addition of the N-glycan core motif which confined the molecule to the lumen of the ER and therefore also the secretory pathway. This molecule was found to be secreted from cells so showing that passage through the secretory pathway to the plasma membrane was not signal mediated, the glycopeptide carrying no other motifs than that for N-linked glycosylation (Wieland, et al., 1987). In addition, recognition signals for diversion from this default route have been found for delivery to lysosomes (von Figura and Hasilik, 1986; Lazzarino and Gabel, 1988), to the regulated secretory pathway (Burgess and Kelly, 1987) and for

recycling of escaped ER proteins (Munro and Pelham, 1987). The bulk flow model does not explain measured differences in the rates of export of endogenous secretory proteins from the ER (Lodish, 1988; Rose and Doms, 1988) though differences are most likely to be accounted for by differential rates of folding.

Early evidence for vesicle mediated transport in the secretory pathway was obtained from pulse chase studies using pancreatic exocrine cells which showed that transport of labelled material between the ER and Golgi apparatus involved small vesicles (Jamieson and Palade, 1967). More recently transport vesicles mediating certain steps of the pathway have been isolated and their specificity demonstrated in vitro (Groesch, et al., 1990; Rexach and Schekman, 1991).

The last few years have seen great advances in our understanding of the budding and fusion events and the identity of many of the molecules involved in these reactions is known. The molecular nature of the transport vesicles and the processes of budding and fusion have been most clearly delineated for those steps in the transport of material between successive compartments of the Golgi stack.

When isolated Golgi stacks are incubated with ATP and cytosol many uniform vesicles form from all cisternae. These 75 nm vesicles are proposed to be transport vesicles since they can be shown to contain the VSV G-protein when Golgi stacks are prepared from VSV infected cells (Orci, et al., 1986). Transport of this G-protein in the stack is monitored by changes in glycosylation.

The transport vesicles are either coated with an electron dense material (not clathrin) or uncoated. The use of various inhibitory agents such as non-hydrolysable analogues of GTP and N-ethylmaleimide (NEM) has

permitted stages of the process to be distinguished (Glick and Rothman, 1987; Melancon, et al., 1987). The present model suggests that coat proteins assemble on a Golgi cisterna where coated vesicles form. The vesicles bud, lose their coat and can then fuse with the acceptor compartment (Fig. 1.4). The Golgi-derived coated vesicles have been purified and components of the coat analyzed. The major coat proteins ('COPs') are α -COP (170 kDa), β -COP (110 kDa), γ -COP (99 kDa), δ -COP (61 kDa) and a small GTP binding protein called ADP ribosylation factor (ARF) of 21 kDa (Malholtra, et al., 1988; Serafini, et al., 1991a; Serafini, et al., 1991b). It is suggested that several of these COPs are recruited to the membrane, from cytosolic pools, by the ARF-GTP complex (Orci, et al., 1991; Serafini, et al., 1991a).

The signal for a bud to form at a particular site is as yet not known. The reaction requires ATP but whether the formation of a vesicle is driven by conformational changes in coat proteins or whether the material to be transported reaches a threshold concentration in the region which then triggers bud formation is not yet determined (Orci, et al., 1986).

The rab family of small GTP-binding proteins (which include the yeast, ypt proteins) appear to be localized to distinct compartments. Their differential localization has given rise to the idea that rab proteins are involved in determining the specificity of a compartment and thus somehow involved in the targeting of vesicles to the correct location (Bacon, et al., 1989; Zahraoui, et al., 1989; Plutner, et al., 1991). More recently, the trimeric G proteins have also been shown to affect secretion and they may be involved in regulating the rate of bulk flow (Barr, et al., 1991; Balch, 1992). The G proteins are known to be involved in intracellular signalling from the cell surface and may

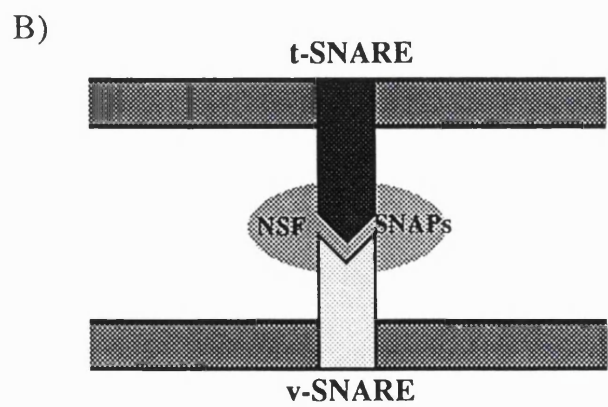
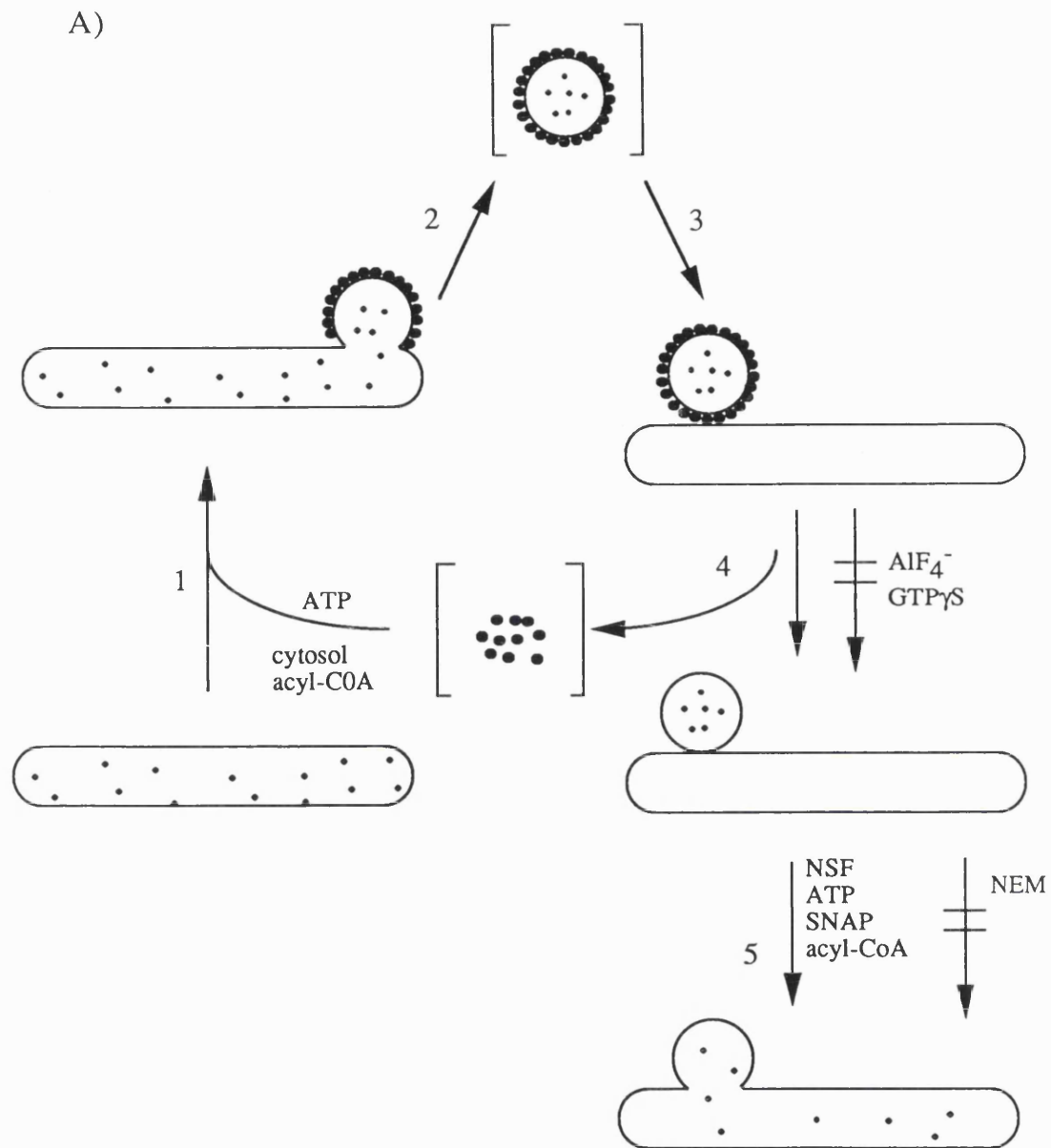
Figure 1.4. The steps involved in a round of vesicular transport

A) The figure depicts a simplified version of the steps involved in a round of vesicular transport. Successive steps of (1) assembly of coated buds, (2) pinching off, (3) targetting, (4) uncoating, and (5) fusion constitute a round of transport.

Known requirements and inhibitors are indicated. AlF_4^- = aluminium fluoride, NSF = NEM sensitive fusion protein, SNAP = soluble NSF attachment proteins.

● = soluble protein being transported; ● = coat proteins

B) Several of the molecules thought to be involved central to the fusion reaction have recently been isolated. The figure shows how these molecules might be brought together to ensure specificity of the targeting reaction. Each fusion step would require a different v-snare and t-snare pairing.



integrate the rate of secretion with the rate of protein synthesis and the need for cell growth.

Recent findings have greatly increased our understanding of the mechanism of vesicle fusion. Several of the molecules which allow this reaction to occur with the necessary specificity have now been reported. The N-ethylmaleimide-sensitive fusion protein (NSF) was purified on the basis of its ability to restore intercisternal Golgi transport in a cell free assay (Fries and Rothman, 1980; Balch, et al., 1984). It is required for membrane fusion since vesicles accumulate at the acceptor membrane in its absence (Malholtra, et al., 1988; Orci, et al., 1989). NSF requires additional cytoplasmic factors to attach to Golgi membranes. Three species of soluble NSF attachment proteins (SNAPs) have been purified, termed α , β , γ SNAP (Clary and Rothman, 1990a).

SNAPs bind to distinct sites in membranes which have recently been purified from bovine brain and called SNAREs (for SNAP receptors)(Sollner, et al., 1993). These SNAREs when cloned and sequenced were shown to be the previously isolated proteins, syntaxin and synaptobrevin (Sudhof and Jahn, 1991; Bennett, et al., 1992). This has led to the proposal of a model for vesicle targeting and fusion (Fig. 1.4B). The vesicle is thought to carry a receptor, v-SNARE (synaptobrevin-like) and the acceptor compartment a t-SNARE (syntaxin-like). These can specifically pair in a reaction mediated by NSF and SNAPs. Only when appropriate binding is achieved can the fusion of the membranes occur. Each stage of transport is proposed to have a different pair of v- and t-SNAREs so ensuring specificity of fusion at each step.

1.3. Structural aspects of the Golgi stack

As already stated, the most visually striking feature of the Golgi apparatus is its stacked structure. It therefore seems appropriate to describe what little is known about the elements which may be responsible for maintaining this stacked form.

Until recently the components involved in stacking have been a complete mystery. Several early reports showed evidence of filamentous elements between cisternae in invertebrate and plant Golgi stacks (Mollenhaur, 1965; Turner and Whaley, 1965). The nature of these parallel arrays observed as electron dense regions lying midway between adjacent cisternae was not however known and no similar elements were observed in Golgi stacks of mammalian cells or those in fungi (reviewed in Mollenhaur and Morre, 1991). Other reports were of regularly spaced intercisternal cross-bridges which were found between Golgi cisternae and also connecting membranes of organelles such as the ER and chloroplast thylakoid membranes (Franke, et al., 1971; Franke, et al., 1972).

More recently, work has shown that some proteinaceous matrix can be found between the cisternae of certain mammalian Golgi cisternae. Cluett and Brown (1992) purified rat liver Golgi stacks and treated these with a variety of agents to induce the separation of intact cisternal elements. Treatment of these intact stacks with certain proteolytic enzymes resulted in a dose and time dependent unstacking of the cisternae. Electron microscopic studies with negatively stained Golgi complexes revealed the presence of highly structured, intercisternal 'bridges'. These bridges (8.5 nm in width and 11 nm in

height) were found in the stacked regions of the Golgi but not at the dilated rims. Furthermore, the proteases which dissociated cisternae also removed these structures. This work was therefore highly indicative of stacking being specifically associated with protein complexes between adjacent cisternae.

Work by P.Slusarewicz (1993, submitted) also on rat liver Golgi stacks has shown the existence of a proteinaceous matrix which specifically associates with enzymes of the medial Golgi compartment. This work not only demonstrates the existence of a matrix necessary for cisternal association but also suggests a mechanism whereby polarity of the stack can occur with different matrix components necessary between the biochemically distinct compartments.

There are however, no reports of factors which are able to cause unstacking of the cisternae of these mammalian Golgi in vivo, nor of the effect this unstacking might have on the cell.

1.4. Microtubules and the organization of the Golgi apparatus

Electron microscopic and cytochemical studies indicate that microtubules play an important role in the organization of the Golgi apparatus in mammalian cells. During interphase the Golgi has a restricted juxtanuclear localization (Farquhar and Palade, 1981). Exposure of cells to microtubule disrupting drugs such as nocodazole or colchicine causes the Golgi to fragment into small stacks of cisternae which are dispersed in the cytoplasm (Robbins and Gonatas, 1964; Thyberg and Moskalewski, 1985). These are often accompanied by disturbances in intracellular trafficking and processing of secretory

proteins. These observations suggest a role for microtubules in the maintenance and functioning of the Golgi apparatus, possibly by organizing its stacks of cisternae within the cell and in relation to other organelles.

The most dramatic morphological change in the Golgi apparatus in mammalian cells occurs during mitosis (Warren, 1993). At pro-metaphase the Golgi apparatus firstly fragments into small stacks of cisternae dispersed in the cytoplasm. This alteration is concomitant with breakdown of microtubules. In metaphase the stacks then disassemble further and Golgi vesicles or clusters of vesicles are predominant. Once the separation of the chromosomes is complete and nuclei reform the stacks of flattened cisternae reassemble from the vesicles. These small stacks then congregate in a peri-centriolar region and fuse to form the single copy interphase organelle. The reason for the fragmentation is not clear but it may ensure equal partitioning of Golgi material between daughter cells.

Reports in the last year have documented the re-organization of dispersed Golgi stacks to the nuclear region (Corthésy-Theulaz, et al., 1992). Using semi-intact cells Golgi stacks were introduced into cells and were shown to interact with cellular constituents. Stable associations in the cell required ATP and intact microtubules. The Golgi stacks are found in the nuclear region only if cytoplasmic dynein is present suggesting a role for this molecule in movement of the stacks near to the centrosomes of recipient cells.

Golgi stacks have also been demonstrated to associate with microtubules in vitro. This association was inhibited by addition of crude microtubule associating proteins (MAPs), purified MAP2, or 1

mM ATP (Murata, et al., 1992) and was sensitive to addition of trypsin or NEM (Karecla and Kreis, 1992).

The interaction between microtubules and the Golgi apparatus in other organisms has not been widely reported. However, in both plants and fungi there are multiple stacks, which remain dispersed in the cytoplasm throughout the cell cycle. This resembles the situation in mammalian cells during mitosis. This might indicate a need in mammalian cells to localize its Golgi apparatus in this nuclear region or equally that this positioning occurred and conferred some advantage in evolution. A possible reason for forming a single-copy organelle by fusion of stacks is to allow co-ordinate movement of the whole organelle and thus permitting directional control of secretion (Moskalewski and Thyberg, 1992).

1.5. The secretory pathway in *S.cerevisiae*

1.5.1. Introduction

The yeast, *S.cerevisiae* has been a very popular organism to use as a model system for complex cell biological problems. By all accounts, many of the fundamental processes of eukaryotic life are carried out by identical systems. Many of the proteins involved in processes such as cell cycle control and secretion are extremely well conserved and in many cases can functionally replace each other in heterologous systems.

The major advantage of using yeast is that they provide a genetically tractable system. The most commonly used yeast can live in a haploid or a diploid state depending on the growth conditions used. Mutations

can be easily generated by exposure of large numbers of yeast to mutagens such as nitrosoguanidine or u.v irradiation. The phenotype of a genetically altered organism can then be analyzed and the effect of a specific mutation on the cell observed.

Like other eukaryotic cells, *S.cerevisiae* secretes proteins to its cell surface many of which are modified by addition and processing of oligosaccharides presumably whilst in transit through the Golgi apparatus. The secretory pathway has been studied in considerable detail in this yeast and the findings have made a major contribution to our present understanding of the functioning of the pathway at a molecular level.

1.5.2. The *SEC* genes and the genetics of the secretory pathway

In 1980 Novick and colleagues devised a mutational screen for defects in the secretory pathway. This, and later screens led to the isolation of many genes (*sec* genes) essential for the transport of proteins from cells (Novick, et al., 1980; Newman and Ferro-Novick, 1987). Many of the *SEC* genes have been cloned and sequenced and the intracellular location of the protein defined. Figure 1.5. shows the position in the pathway that some of the secretory mutants act. The functions of many of these gene products are now known and several have recognized mammalian homologues. Table 1.1 lists some of the yeast proteins involved in secretion and their mammalian homologues where known.

The Sec61p, Sec62p and Sec63p function in the translocation of nascent polypeptides across the ER membrane (Rothblatt, et al., 1989; DeShaies, et al., 1991). When in the ER the yeast homologue of BiP, KAR2, facilitates protein folding (Nguyen, et al., 1991).

Figure 1.5 The secretory pathway of *S.cerevisiae*

A schematic diagram of a yeast cell showing the organelles of the secretory pathway. Arrows indicate the route of a secretory protein from the endoplasmic reticulum (ER), via the Golgi apparatus (G), to the plasma membrane. Certain proteins are diverted from this pathway to the vacuole (V).

The *sec* mutants blocking particular stages of transport or sorting are marked. Many vacuolar protein sorting (*vps*) mutants have also been isolated.

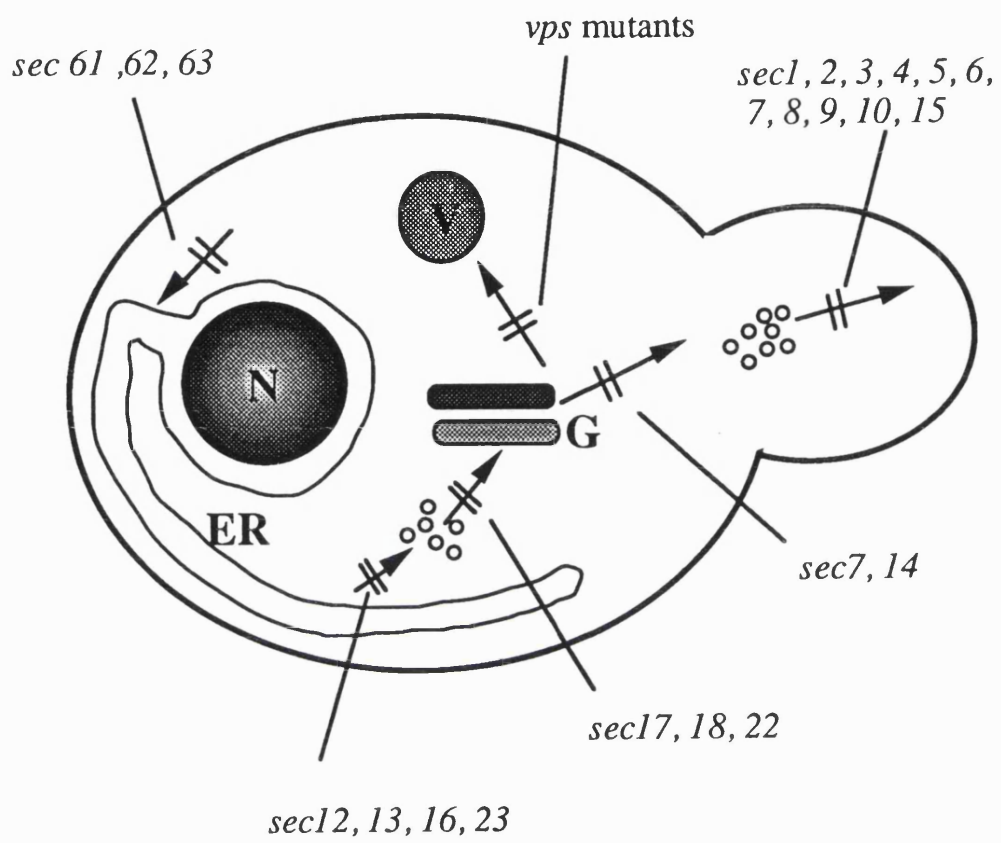


Table 1.1 Protein homologues implicated in the secretory pathway

Many of the *SEC* genes have been sequenced and found to be homologous to certain mammalian genes in both sequence and in function. Several of these are known to be able to functionally complement their homologues in heterologous systems.

Yeast cells	Mammalian cells	References
Sec18p	NSF	Wilson et al 1989
Sec17p	α -SNAP	Clary et al, 1990
Sec16p	α -COP	Rothman and Orci, 1992
Sec23p	γ -COP	Rothman and Orci, 1992
sec21p	δ -COP	Rothman and Orci, 1992
sec12p	p20	d'Enfert et al, 1991
sec13p	p36	Pryer et al, 1990
SAR1p/ARF	ARF	Rexach and Schekman, 1991
sec14p	PI/PC exchange	Bankaitis et al, 1990
Bos1p, Sec22p	v-SNARE / synaptobrevin	Newman et al, 1992
Sed5p	t-SNARE / syntaxin	Hardwick and Pelham, 1992

Mutations in 12 genes have been shown to disrupt transport between the ER and Golgi apparatus (Novick, et al., 1980; Newman and Ferro-Novick, 1987). At the non-permissive temperature, these mutants accumulate excess ER-like membrane structures filled with core glycosylated forms of secreted and vacuolar proteins (Stevens, et al., 1982; Julius, et al., 1984). A subset of the mutants accumulate small membrane enclosed vesicles which may represent transport vesicles (Novick, et al., 1981).

Various activities have been isolated in *S.cerevisiae* as necessary for vesicle budding from the ER. At least four proteins are needed to mediate vesicle formation (Sec12p, Sec13p, Sec16p, Sec23p) (Kaiser and Schekman, 1990). An additional factor, Sar1p is a GTP binding protein that interacts with Sec12p to promote budding in vitro (d'Enfert, et al., 1991). Sec17p, Sec18p, and Sec22p are required for vesicle fusion with the first Golgi compartment. In yeast, the SEC18 gene encodes NSF and can replace the mammalian NSF in an in vitro assay (Wilson, et al., 1989). Sec17p is functionally equivalent to α SNAP (Clary, et al., 1990b). Homologues to the recently described v-SNAREs and t-SNAREs involved in vesicle targetting and fusion have also been identified, thus further illustrating the generality of the proposed mechanism for vesicle mediated transport. Sed5p is related to syntaxin (Hardwick and Pelham, 1992) whilst Sec22p, Bet1p and Bos1p are related to synaptobrevin (Shim, et al., 1991; Newman, et al., 1992).

Two *SEC* genes when mutated show a disruption of the Golgi apparatus. The *SEC7* gene product functions at multiple steps of intercisternal transport and the Sec14p is needed for exit from the Golgi (Achstetter, et al., 1988; Franzusoff and Schekman, 1989). The *SEC7* gene has recently been shown to encode a coat component of transport

vesicles and is essential for budding from Golgi cisternae (Franzusoff, et al., 1992). The *SEC14* gene codes for a phosphatidylinositol / phosphatidylcholine exchange protein (Bankaitis, et al., 1990) though the mechanism by which this protein is involved in supporting secretion is not known.

Several gene products are required for the final step of the pathway from the Golgi apparatus to the plasma membrane (Novick, et al., 1981). Of these *SEC4* has been shown to encode a small GTP binding protein which may be involved in catalyzing fusion of the vesicle with the plasma membrane (Walworth, et al., 1989).

1.5.3. Glycoprotein modifications in the secretory pathway

As in mammalian cells, proteins translocated into the ER may be modified by the addition of N- or O-linked glycans. The N-linked moiety is transferred from a dolichol linked precursor and has exactly the same Glc₃Man₉GlcNAc₂ structure. O-linked structures appear to be less complex with chains of 2-5 mannoses attaching directly to serine or threonine residues. The N-linked structure, as with mammalian cells is trimmed to a Man₈GlcNAc₂ form before cells exit this compartment.

When proteins enter the Golgi apparatus the oligosaccharides are trimmed probably to the same extent ^{as} ~~of~~ those of mammalian proteins i.e. to a Man₅GlcNAc₂ structure (T. Chappell, pers. comm.). Following this, mannose residues are added by enzymes of the Golgi apparatus. There are two broad classes of mannoproteins, Man₈₋₁₄GlcNAc₂ and Man_{>50}GlcNAc₂ (Orlean, et al., 1991). These long mannose chains are comprised of α 1-6 linkages with short side chains in α 1-2 and α 1-3 linkage (Ballou, 1976).

1.5.4. Compartmentalization in the secretory pathway

Work by Graham and Emr (1991) using mutant strains blocking at different points of the pathway has elegantly demonstrated the existence of distinct Golgi apparatus compartments.

Both the Sec18 and the Sec23 protein functions are rapidly inactivated upon shifting mutant cells to the non-permissive temperature. This permitted an analysis of transport events distal to the ER. The transport of alpha-factor and carboxypeptidase Y (CPY) biosynthetic intermediates present throughout the secretory pathway was monitored in temperature shift experiments. Sec18p/NSF function was required sequentially for transport through Golgi compartments to the cell surface. In contrast Sec23p function was required in the Golgi apparatus but only for the transport of alpha factor out of an early compartment. These studies define three distinct compartments, from cis to trans these compartments contain: 1) α 1-6 mannosyl transferase; 2) α 1-3 mannosyltransferase; 3) Kex2 endopeptidase which is responsible for proteolytic processing of certain secretory proteins.

1.5.5. Diverting proteins from the default pathway

The hydrolytic organelle of yeast which corresponds to the lysosome is called the vacuole. No TGN-resembling structures have been observed in *S.cerevisiae* though it is known that proteins destined for the vacuole diverge from other secretory proteins in the Golgi apparatus or shortly after traversing it (Stevens, et al., 1982; Johnson, et al., 1987; Klionsky and Emr, 1989; Roberts, et al., 1989). Unlike mammalian lysosomal proteins which are tagged on their N-glycans with a phosphate group to signal diversion to the lysosome the vacuolar sorting information for yeast seems to reside in the amino acid sequence and varies for

different proteins. In the cases of the soluble vacuolar proteases, carboxypeptidase Y (CPY), protease A (PrA), and protease B (PrB), targeting information resides in the propeptide of the precursor, which is processed in the vacuole (Johnson, et al., 1987; Valls, et al., 1987). In CPY and PrB, four amino terminal amino acids, QRPL and QNPL, respectively constitute the signal (Valls, et al., 1990). Vacuolar membrane proteins are targeted with a different mechanism. For vacuolar alkaline phosphatase, a sorting signal, both necessary and sufficient for vacuolar targeting, lies in the trans-membrane region and/or cytoplasmic tail (Klionsky and Emr, 1990). Isolation and characterization of vacuolar protein sorting (*vps*) mutants have identified at least 49 gene activities required for this sorting event (Banta, et al., 1988; Rothman, et al., 1989b).

As with mammalian cells there is evidence of clathrin playing a role in the sorting of vacuolar proteins. Cells harbouring a temperature sensitive allele of the heavy chain of clathrin when shifted to the non-permissive temperature displayed a severe defect in the sorting of soluble vacuolar proteins. Vacuolar membrane proteins and transport to the cell surface were not affected (Seeger and Payne, 1992).

1.5.6. The structure of the Golgi apparatus in *S.cerevisiae*

Most of the aspects of the secretory pathway discussed so far for *S.cerevisiae* indicate a sequence of processes highly homologous to those seen in mammalian cells. This would suggest that both systems contain the necessary facets of an efficient secretory mechanism. There is, however one very striking difference between the two which is, the lack of a stack of cisternae in *S.cerevisiae*.

One paper has characterized at a morphological level the form of the Golgi apparatus throughout the cell cycle in *S.cerevisiae* (Preuss, et al., 1992). This paper shows that in this yeast the compartments of the Golgi apparatus are present mainly as single, isolated cisternae and not stacks. It is not uncommon to see two apposed cisternae though more than two was not shown. By using immuno-electron microscopy the location of the Golgi structures was monitored. Several Golgi compartments, randomly distributed were seen in mother cells. During the initiation of new daughter cells, additional Golgi structures clustered next to the site of bud emergence. These Golgi entered daughter cells at an early stage. During cytokinesis, the Golgi compartments were located close to the sites of cell wall synthesis suggesting localization of the structures close to the sites of secretion. Examples of Golgi cisternae in *S.cerevisiae* are shown in figure 1.6.

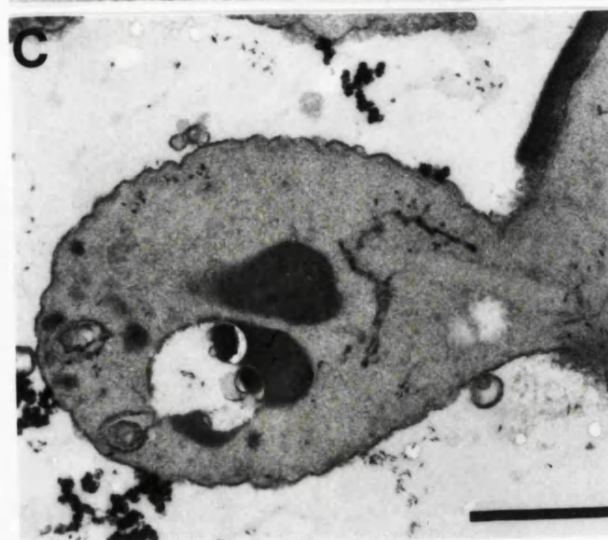
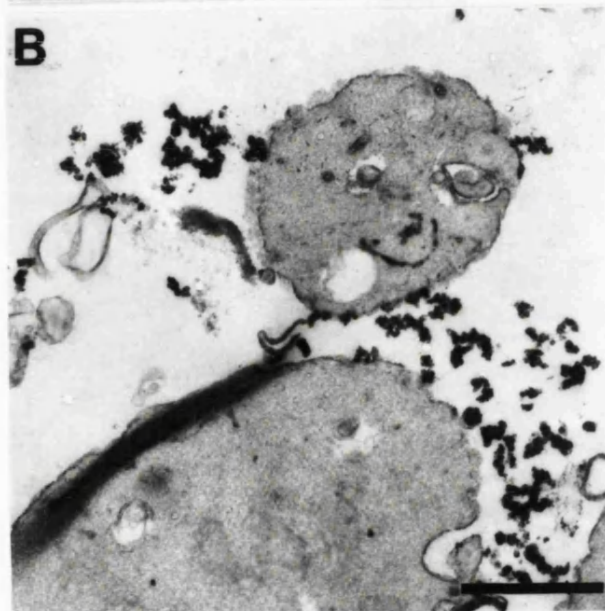
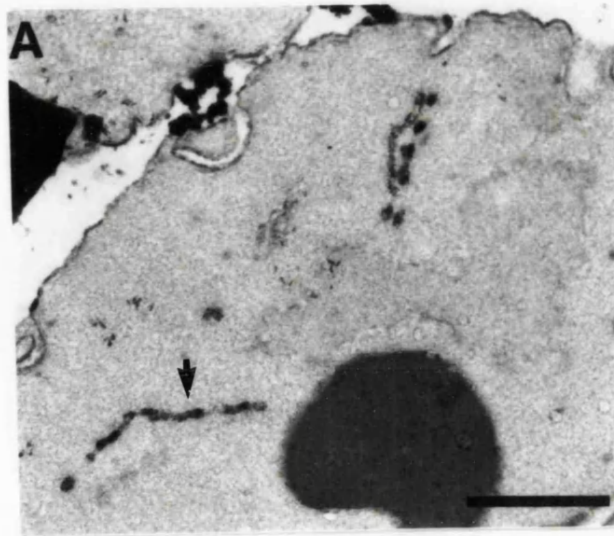
Other work however, does illustrate the existence of a stacking mechanism for the cisternae in *S.cerevisiae* but suggests that it might be a more transient association than observed with mammalian cells.

Morphological studies using electron microscopy of the *sec7* mutant strain at the non-permissive temperature showed identifiable stacks of Golgi cisternae. These were not seen in cells at the permissive temperature (Novick, et al., 1981; Franzusoff and Schekman, 1989). Thus, a stacking mechanism appears to be present in *S.cerevisiae*. Perhaps stacked cisternae and single cisternae exist in some sort of equilibrium with the unstacked state normally predominant. Only when the equilibrium is upset, for example by shifting *sec7* mutants to the non-permissive temperature, does the stacking of Golgi cisternae become apparent.

Figure 1.6. The morphology of the Golgi in *S.cerevisiae* by electron microscopy

S.cerevisiae cells were grown to log phase and then fixed using 3% glutaraldehyde and 0.5% paraformaldehyde. The fixed cells were post fix osmicated to stain putative Golgi compartments. The cells were then processed for electron microscopy. The figure shows example of cells containing stained membrane that is presumed to be Golgi cisternae.

Bar = 0.5 μm (A), 0.3 μm (B,C)



1.6. Reasons for a stack

1.6.1 Introduction

The work described on the secretory pathway in *S.cerevisiae* certainly questions the requirement by cells for an intact Golgi stack. Several other fungi also do not have their Golgi cisternae in a stacked form. Both *Allomyces macrogynus* (Sewall, et al., 1989) and *Sclerotium rolfsii*, (Roberson and Fuller, 1988) do not appear to have Golgi stacks but they nevertheless carry out a sequence of modifications to proteins undergoing transport which are most easily explained as vesicles budding from one cisterna and fusing with one containing a different set of enzymes (Sewall, et al., 1989).

It remains, however, that many eukaryotes do associate their Golgi cisternae in the form of a stack and even *S.cerevisiae* seems to have the capacity to form a stack under certain conditions. Two models have been proposed to explain the reason for stacking in the Golgi apparatus.

1.6.2. Stacking to maximize the efficiency of transport

The most obvious possibility for a function for stacking is that it would facilitate transport of newly-synthesised proteins (Palade, 1975). Vesicles bud from the dilated rims of one cisterna and fuse with the next cisterna in the stack towards the trans side (Rothman and Orci, 1992). The close proximity of cisternae in a stack would ensure rapid and efficient transport and reduce or even eliminate the need to target vesicles specifically to the next cisterna. Budded vesicles would simply fuse with the nearest cisterna. The cup-shaped structure of the Golgi in many cells would even ensure fusion with the next cisterna rather than the one from which it had just budded. Unfortunately, there is much

evidence against this interpretation. Rothman and colleagues have shown, both in vivo and in vitro, that budded vesicles will fuse with the correct cisterna even when it is present in a different stack and do so with the same speed and efficiency.

In one set of experiments two different cell types were fused in order to demonstrate transport between the two Golgi populations (outlined in Fig. 1.7). A mixed monolayer was formed containing VSV infected clone 13 CHO cells, which are unable to add galactose onto N-glycans, and uninfected clone 15B CHO cells, which can add galactose (gal) but not N-acetylglucosamine (GlcNAc). VSV G-protein was labelled with tritiated glucosamine ($^3\text{[H] GlcNH}_2$) which was incorporated into GlcNAc. These clone 13 cells were then fused to 15B cells. Transfer was monitored by the addition of Gal to tritiated GlcNAc labelled G-protein. The addition of galactose required the transport vesicles to fuse with the Golgi apparatus from the 15B cell thus beyond the stack from which it was derived. The kinetics of transport to the cell surface were measured under various conditions and this demonstrated that transport in the Golgi within a single cell and transport between Golgi populations from different cells occurred at similar rates. Furthermore, by immunofluorescence it was shown that the time required for transport was less than time it took for the Golgi populations to fuse into a single organelle with a mixed population of enzymes (Rothman, et al., 1984a,b).

An in vitro system was also set up, again using Golgi populations from different cell lines which differed in their ability to perform certain oligosaccharide modifications. Transport of the VSV G-protein between successive compartments was reconstituted in a cell free system and

Figure 1.7. Cell fusion experiment to detect transfer between two Golgi populations

A mixed monolayer was formed containing VSV infected CHO clone 13 cells and uninfected CHO clone 15B cells. VSV G protein was labelled in the Golgi of clone 13 cells with [^3H]glucosamine, incorporated as [^3H]GlcNAc. The clone 13 Golgi is unable to add galactose. These cells were then fused to neighbouring clone 15B cells (by brief exposure to pH 5) whose Golgi are able to add galactose but not GlcNAc. Transfer of G protein from clone 13 to clone 15B Golgi population was monitored by the addition of Gal to [^3H]GlcNAc labelled G protein after fusion.

VSV infected clone 13 cell

Will add [^3H]GlcNAc to G protein in Golgi

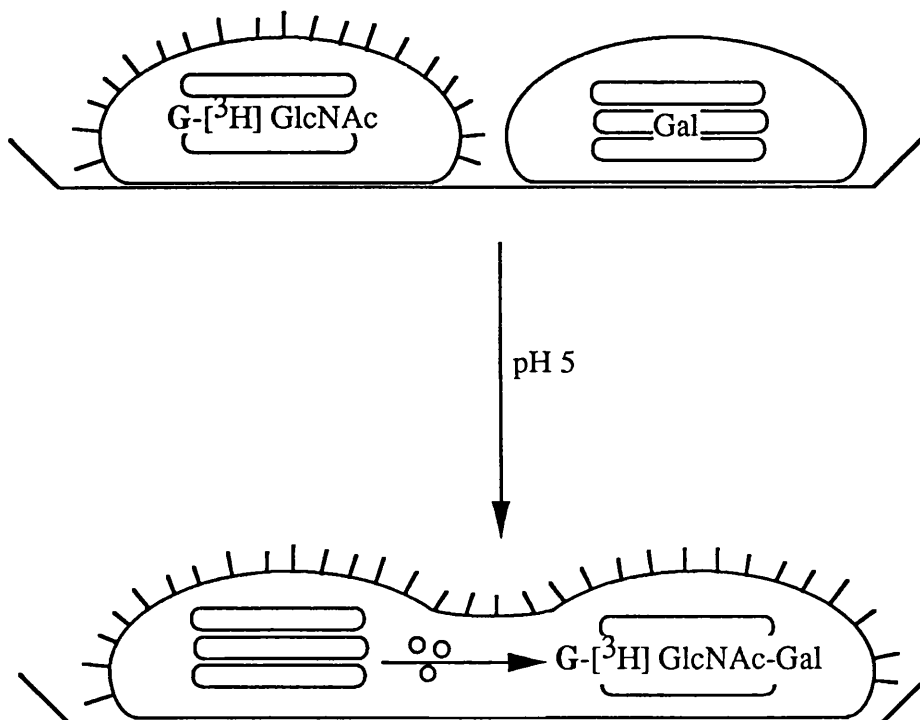
Won't add Gal to G protein in Golgi

Pulse labelled with [^3H]GlcNH₂

Uninfected clone 15B cell

Won't incorporate GlcNAc in its Golgi

Will add Gal in its Golgi



system and transport measured by the incorporation of tritiated GlcNAc. This glycosylation occurred when G protein was transported during mixed incubations from the donor compartment in Golgi from VSV-infected CHO 15B cells (missing a GlcNAc transferase) to the acceptor compartment (containing the GlcNAc transferase) in Golgi from wild type CHO cells. Transport in this in vitro system was almost as efficient as in the cell (Balch, et al., 1984). The donor and acceptor stacks were examined by electron microscope autoradiography during the transport assay and shown to remain as discrete populations for the duration of the assay (Braell, et al., 1984).

1.6.2 Stacking to maximize recovery of protein lost from the ER

Another possible function for the stack is to recover proteins that have been lost from the ER (Rothman, 1981). Stacked cisternae would allow repeated attempts to recover the lost proteins and return them to the ER. This model, termed the distillation model, was originally proposed for ER membrane proteins but no supporting evidence was found at that time (Brands, et al., 1985; Yamamoto, et al., 1985). More recent work shows that ER membrane proteins are lost and can be recovered (Jackson, et al., 1993) as can soluble ER proteins (Pelham, 1989b)(see section 1.2.4. for a fuller discussion on ER retrieval mechanisms). At the level of light microscopy the mammalian retrieval receptor protein, *erd2*, appears to be throughout the Golgi apparatus and not just the CGN suggesting the capacity to retrieve might exist in several Golgi compartments (Lewis and Pelham, 1992b). The post translational modifications, however, found on such retrieved ER proteins do not resemble more complex oligosaccharides found on proteins for the cell surface (Pelham, 1989b) suggesting that they are not exposed to the full range of Golgi enzymes. More recently, studies on the retrieval of ER

proteins in rat liver has shown that the protein, calreticulin, which carries a C terminal KDEL sequence has terminal galactose added. This modification is characteristic of the trans Golgi compartment suggesting that this protein has penetrated deep into the stack and was not simply retrieved at the CGN (Peter, et al., 1992).

The absence of stacked cisterna in *S.cerevisiae* which has an effective retrieval mechanism would also argue against a role for stacking in the salvage operation. The situation in *S.cerevisiae* however might not reflect the norm and possibly its own retrieval system is so efficient that this precludes the need to associate cisternae for repeated attempts at retrieval. Other eukaryotes might not have such effective retrieval of escaped proteins and so have stacks of cisternae to minimize loss of proteins.

1.7. Using *Schizosaccharomyces pombe* to facilitate understanding of the Golgi apparatus

1.7.1. Introduction

The main experimental difficulty in determining the function of the Golgi stack has been the lack of an experimental system. Conditions which separate the cisternae in mammalian cells invariably vesiculate them. These include treatment with ionophores such as A23187 (Blomfield, et al., 1983) and physiological states such as mitosis during which the entire Golgi apparatus is converted to thousands of small vesicles (Warren, 1993). A simple system to study the structural and functional relationships of the Golgi apparatus might facilitate our understanding of this complex organelle.

1.7.2. The Golgi apparatus in *S.pombe*

The Golgi apparatus as a morphological entity was recognized in *S.pombe* over twenty five years ago. Initial electron microscopy studies only detected stacks of cisternae in protoplasts of *S.pombe* which were regenerating their cell walls (Havelkova and Mensik, 1966). Later studies, also using electron microscopy observed these stacks in normal cells as well as in protoplasts of *S.pombe* but the authors still doubted the necessity of the organelle for cells in normal vegetative growth (Smith and Svoboda, 1972). Since this time Golgi stacks have been detected and reported in *S.pombe* cells by a range of techniques; Streiblova (1984) showed stacks of cisternae using freeze etching, whilst Johnson (1982) showed the same by thin section and staining of cells. Whilst all these reports recognized that the stacks observed comprised the Golgi apparatus, no in-depth studies were made on its morphology, or its behaviour in response to factors affecting the cell.

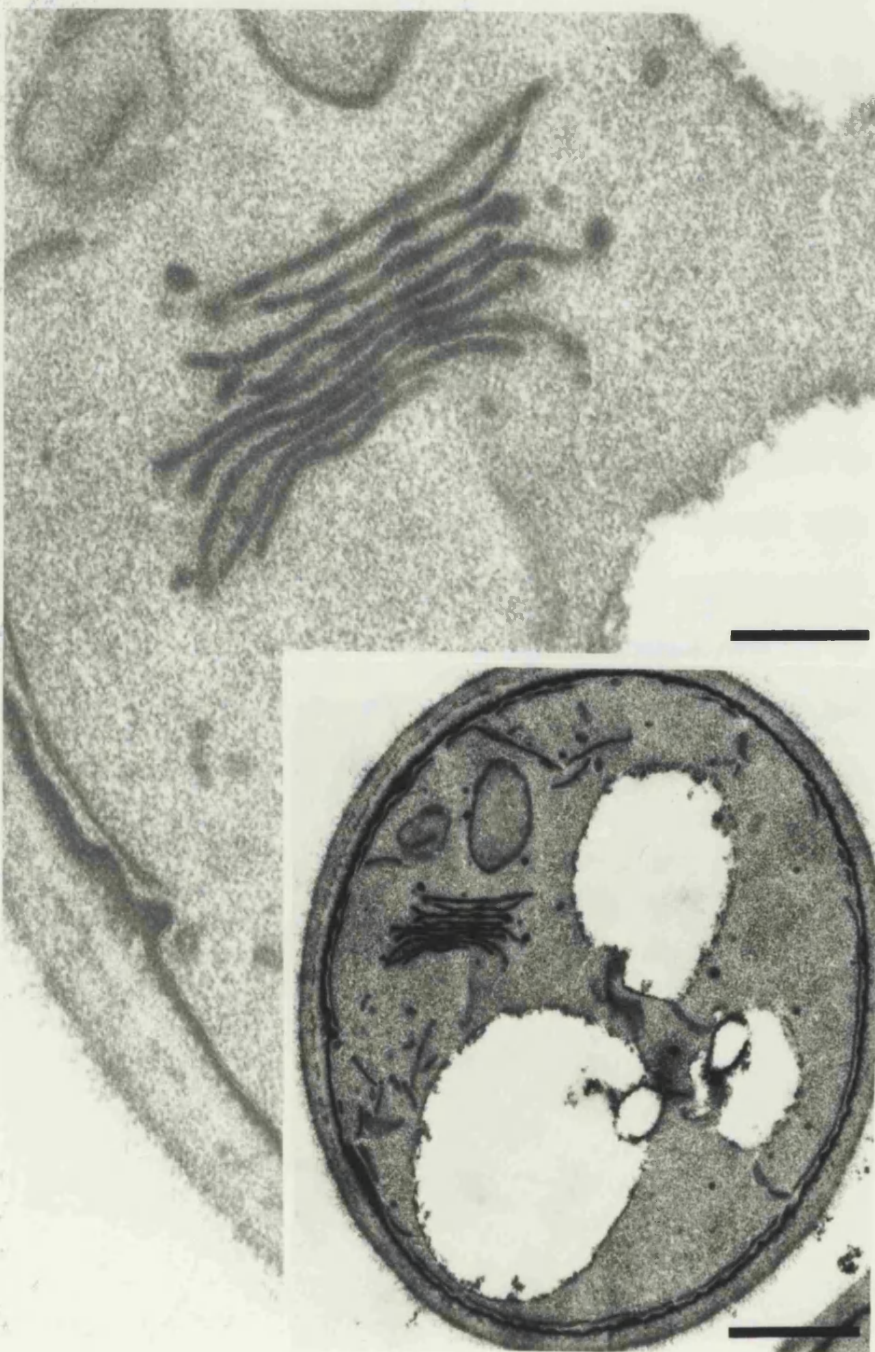
The importance of these studies to my work is that they illustrated the existence of a stack of cisternae in wild type cells, thus indicating that the Golgi apparatus in this organism was in a form comparable to that in higher eukaryotes. Figure 1.8 shows an electron micrograph of a Golgi stack in *S.pombe*.

1.7.3. Functioning of the Golgi apparatus in *S.pombe*

As with the other eukaryotes thus far characterized, proteins to be secreted from *S.pombe* cells enter the ER and may be modified by the addition of an N-glycan moiety. This structure is the same as that for mammalian cells i.e. $\text{Glc}_3\text{Man}_9\text{GlcNAc}_2$. The glucose residues are trimmed whilst in the ER though it seems that most proteins leave the ER with no mannose trimming (T.Chappell, pers. comm.).

Figure 1.8. The Golgi stack in *S.pombe*

S.pombe cells were grown to log phase and then fixed using 2% permanganate. The cells were processed for electron microscopy and sections cut and stained. The figure shows a Golgi stack and the inset shows the cell in which it was detected. Bars = 0.2 μm and 0.75 μm (inset).



The transport of proteins in vesicles from the ER is presumed to be similar to the process in mammalian and *S.cerevisiae* cells though the only protein homologues identified so far are small GTP binding proteins (Miyake and Yamamoto, 1990; Fawell, et al., 1992). In the Golgi apparatus the variation in oligosaccharides formed on secreted proteins such as invertase is greater than in *S.cerevisiae* with both mannose and galactose being added and a wider range of linkages being formed (Moreno, et al., 1990).

To date, only the purification of one Golgi protein has been published. This protein, α -1,2-galactosyltransferase (GalT) was purified to homogeneity from a microsomal preparation of *S.pombe* cells (Chappell and Warren, 1989). Antibodies raised to the purified protein gave a pattern of staining by immunofluorescence which reflected the image seen by the electron micrographs. The GalT gene has subsequently been cloned and sequenced (T.Chappell, 1993 submitted).

1.8. The aims of this project

At the outset of this work it was not clear to what extent the Golgi apparatus in *S.pombe* would resemble that in higher eukaryotes in terms of its behaviour in the cell and in response to various factors known to affect the structure of the mammalian Golgi apparatus. It was already known that cell contained structures identifiable as Golgi stacks and a specific marker protein had been purified and shown to localize by immunofluorescence to compartments presumed to be Golgi stacks.

The aim of my work was to characterize the Golgi apparatus in wild type cells and then to test the effect of a range of agents on the morphology of Golgi stacks. Factors found to affect the Golgi apparatus in *S.pombe* could highlight new approaches to studying the relationship between structure and function in this complex organelle.

Chapter 2

Materials and Methods

2.1.1. General laboratory services

I.C.R.F. central services provided sterilized glassware, pipettes, bacterial media and a range of the most commonly used buffer solutions, including sterile water and PBS. The laboratory water supply for experiments was from a MilliQ™ system.

2.1.2. Chemicals.

All chemicals used were from Sigma or BDH Ltd unless stated otherwise, and were of analytical grade or better.

Abbreviations used for chemicals

DMF	Dimethyl fluoride
DMSO	Dimethylsulphoxide
DTT	Dithiothreitol
EDTA	Ethylenediaminetetra-acetic acid (disodium salt)
EGTA	Ethleneglycolbis(β-aminoethylether)tetra-acetic acid
HEPES	N-[2 Hydroxyethyl] piperazine-N'-[2-ethanesulphonic acid]
IAA	Iodoacetic acid
MOPS	3-[N-morpholinio] propane sulphonic acid
PFA	paraformaldehyde
PIPES	Piperazine-N'N'-bis (2-ethanesulfonic acid)
PMSF	Phenyl-methyl-sulphonyl-fluoride
TCA	Trichloroacetic acid
SDS	Sodium dodecyl sulphate
TEMED	N, N, N',N'-Tetramethyl-ethylenediamine
Tris	Tris(hydroxymethyl)aminomethane
Tween-20	Polyoxyethylenesorbitan monolaurate
UDP gal	Uridine diphosphate galactose

2.2. Yeast procedures

2.2.1. Strains

Strain	Phenotype	References
<i>972 h⁻</i>	wild type	Provided by P.Nurse
<i>556 h⁺</i>	auxotrophic mutant, ade 6 ⁻ , ura4 ⁻ , leu1 ⁻	Provided by J.Armstrong
<i>cdc2-33 leu2¹-32 h⁻</i>	ts mutant, cell cycle block in late G2	(Nurse, et al., 1976) Provided by P.Nurse
<i>cdc10 leu2¹-32 h⁻</i>	ts mutant, cell cycle block at 'start' in G1	(Aves, et al., 1985) Provided by P.Nurse
<i>cdc11-123 h⁻</i>	ts mutant, cell cycle block early in septation	(Nurse, et al., 1976) Provided by P.Nurse,
<i>cdc12-112 h</i>	ts mutant, cell cycle block in septation	(Nurse, et al., 1976) Provided by P.Nurse,
<i>cdc25-22 leu2¹-32 h⁻</i>	ts mutant, cell cycle block in late G2	(Russell and Nurse, 1986) Provided by P.Nurse
<i>nda3-Km311</i>	cold-sensitive β-tubulin mutant	(Hiraoka, et al., 1984) Provided by J.Hyams
<i>nda2-Km52</i>	cold sensitive α-tubulin mutant	(Toda, et al., 1984) Provided by J.Hyams
<i>gma1-12</i>	carries a gene deletion for α-1,2, GalT	Provided by T.Chappell
<i>ypt1-1</i>	ts mutant, defective in <i>ypt1</i> function	Provided by M.Craighead

2.2.2. Media

Yeast extract with supplements (YE/S) - used for vegetative growth

To make 1 litre YE/S 500 ml 2x glucose Stored at 4°C
500 ml 2x YE/S

2x glucose 30 g D(+) glucose Autoclaved
500 ml dH₂O

2x YE/S 5 g YE Autoclaved
250 mg of each of
adenine, histidine,
leucine, uracil, lysine
hydrochloride
500 ml dH₂O

YE/S - Agar - solid growth medium, for plating strains.

To make 1 litre 20 g Bacto agar (Difco)
added to 2x YE/S. Then
as above

Defined minimal medium (DMM) - used for vegetative growth

To make 1 litre DMM 2x glucose 500 ml Store at 4°C
2x BSM 500 ml
vitamins 1 ml
supplements added at
250 mg/l as required

2x glucose 20 g glucose Autoclave
500 ml dH₂O

2x BSM 5 g NH₄Cl Autoclave
2.2 g Na₂HPO₄
3 g phthallic acid
20 ml 50x salts
100 µl 10,000^x minerals
500 ml dH₂O

50x salts	26.3 g $\text{MgCl}_2 \cdot 6\text{H}_2\text{O}$	Autoclave, store at 4°C
	0.37 g $\text{CaCl}_2 \cdot 2\text{H}_2\text{O}$	
	25 g KCl	
	1 g Na_2SO_4	
	0.01 g $\text{MnSO}_4 \cdot \text{H}_2\text{O}$	
	500 ml dH ₂ O	
10,000x minerals	0.5 g Boric acid	Store at 4°C
	0.4 g $\text{ZnSO}_4 \cdot 7\text{H}_2\text{O}$	
	0.2 g $\text{FeCl}_3 \cdot 6\text{H}_2\text{O}$	
	0.305 g molybdic acid (NH_4^+ salt)	
	0.1 g KI	
	0.04 g $\text{CuSO}_4 \cdot 5\text{H}_2\text{O}$	
	1 g citric acid	
1000x vitamins	100 ml dH ₂ O	Filtered and stored at -20°C
	0.1 g pantothenic acid	
	1 g nicotinic acid	
	1 g inositol	
	1 mg biotin	
	100ml dH ₂ O	

Freezing solution - used for long term storage of strains

For 25 ml	17.5 ml YES media	Autoclaved and stored at room temp.
	7.5 ml glycerol	

2.2.3. Growth

To start a liquid culture a sterile loopful of the relevant strain was taken from a freshly streaked plate and inoculated into 10 ml of YE/S (rich) medium. This was left for up to 2 days at 25 - 32°C to form a stationary phase culture.

This preculture would then be used to re-inoculate into fresh YES or DMM medium to grow the cells as required. Cells were grown in glass flasks with shaking in an air incubator usually at 32°C.

The generation times for growing cells in the different media and at the range of temperatures used were as follows (for wild type cells).

Temperature	Generation time YE/S	Generation time DMM
25°C	3 hr	4 hr
29°C	2 hr 30 min	3 hr
32°C	2 hr 10 min	2 hr 30 min
36.5°C	2 hr	2 hr 20 min

cdc strains which are temperature sensitive were grown at 25°C, they were shifted to 36°C to express the *cdc* phenotype.

ypt1-1 was grown at 29°C and shifted to 37°C for its mutant phenotype.

nda2 and *nda3* were grown at 32°C and shifted to 19°C to express their mutant tubulins.

2.2.4. Storage

Strains were stored on YES plates at 4°C for up to 3 weeks before re-isolating. Long term storage was achieved by growing cells at 32°C in a small volume of YES until the cells were in stationary phase. Cells were added to an equal volume of freezing solution. The culture was then snap frozen on dry ice and ethanol.

2.2.5. Measuring cell number

For most experiments it was necessary to have cells in mid-exponential (log) phase between 2×10^6 and 1×10^7 cells/ml. For wild type strains an OD_{595nm} of

0.1 is equivalent to 2×10^6 cells/ml. This is however a turbidity measurement and is therefore not reliable to assess cell number for strains which are not of the average, wild type size.

Actual cell number was measured using a haemocytometer. The cells covered by the central 25 square region were counted and this number multiplied by 1×10^4 to give the cells/ml. This was done for at least two samples at each time point to allow for non-homogeneity in culture samples.

2.2.6. Spheroplasting cells

SP1 1.2 M sorbitol, 50 mM, Na citrate, 50 mM Na phosphate, 40 mM EDTA, pH to 5.6 . Autoclaved.

SP2 1.2 M sorbitol, 50 mM Na citrate, 50 mM Na phosphate pH to 5.6. Autoclaved.

SP3 1.2 M sorbitol, 10 mM Tris-HCl pH 7.6. Autoclaved.

Cells from a log phase culture were harvested and washed once in SP1. Cells were resuspended in SP2 including 1 mg/ml Novozym (NovoBioLabs Ltd.) and 0.3 mg/ml Zymolyase-100T (Seikagaku Kogyo Co., Tokyo, Japan) and incubated at 37°C for 30 min. Spheroplasts were spun down at 1200 g and washed once in SP3.

2.2.7. Preparation of yeast homogenates and microsomes

Homogenization buffer (HB) 0.1M sorbitol, 50mM KOAc, 2mM EDTA, 1mM DTT, 20mM HEPES-KOH pH7.2, protease inhibitors

Microsome resuspension buffer 0.25 M sucrose, 50 mM KOAc, 1 mM DTT, 20 mM HEPES pH7.2 + protease inhibitors

Protease Inhibitors 1000x 1 mg/ml aprotinin, 1 mg/ml leupeptin, 1 mg/ml pepstatin, 1 mg/ml antipain, 1 mM benzamidine.

Spheroplasts were made from log phase cells as in 2.7.6 and washed once in SP3. The pellet was gently resuspended in homogenization buffer at 10^9 cells/ml.

Cells were transferred to a chilled glass dounce and broken with 20 strokes. Breakage was checked under the light microscope. A slow spin (500g) allowed removal of unbroken cells and cell wall debris without pelleting the released cellular contents. This low speed supernatant was taken as the cell homogenate and stored at -20°C .

The homogenates could be spun at 35,000 g for 20 min to pellet membranes including those of the ER and Golgi apparatus. A volume of microsome resuspension buffer equal to the pellet size was added with mixing. Microsomes were stored at -20°C .

2.2.8. Drugs used in the study

A range of drugs was used in the course of my work. These were all applied to log phase cells in suspension.

Drug	Stock concentration	Final concentration
Thiabendazole (TBZ)	10 mg/ml in DMSO Made freshly	100 $\mu\text{g/ml}$
Cycloheximide (CHX)	10 mg/ml in EtOH Stored at -20°C	100 $\mu\text{g/ml}$
Anisomycin (ANS)	10 mg/ml in EtOH Stored at -20°C	100 $\mu\text{g/ml}$
Brefeldin A (BFA)	10 mg/ml in MeOH Stored at -20°C	100 $\mu\text{g/ml}$

2.3. Antibodies

2.3.1. Primary antibodies

Name	Dilution	Notes
GTF2	1 in 50 for immunofluorescence	Prepared as described 3.2.3
TAT1	1 in 10 for immunofluorescence	Monoclonal against trypanosome α -tubulin. Provided by K.Gull
JARM13	1 in 1000 for Western blotting	Polyclonal against <i>S.pombe</i> BiP. Provided by J. Armstrong
7B4	1 in 10 for Western blotting	Monoclonal against <i>S.pombe</i> acid phosphatase. Provided by E.Schweingruber.
TEX	1 in 25 for Western blotting; 1 in 50 for immunofluorescence	Polyclonal antiserum against Triton extracted rat liver Golgi. Made in the laboratory by P.Slusarewicz.

2.3.2. Secondary antibodies

All antibodies were purchased from TAGO Immunochemicals Inc. except for the alkaline phosphatase conjugated antibody which was from BioRad.

Technique	Antibody	Dilution
Immunofluorescence	Fluorescein conjugated goat anti-rabbit	1 in 100
	Rhodamine conjugated goat anti-rabbit	1 in 100
	Fluorescein conjugated goat anti-mouse	1 in 100
Western blotting	Horseradish peroxidase conjugated goat anti-rabbit	1 in 1000
	Horseradish peroxidase conjugated goat anti-mouse	1 in 1000
	Alkaline phosphatase conjugated goat anti-rabbit	1 in 2000

2.3.3. Preparation of a fusion protein using the pUEX system and raising antibodies to the overexpressed product

A description of the work carried out in order to generate the fusion plasmid is given in 3.2.3 General points and technical details are noted below.

Constructing the fusion plasmid

The pUEX plasmids available are termed pUEX 1, 2, and 3. They differ in their reading frames for the lacZ gene. In this case pUEX 2 was selected as the plasmid required to generate an in frame fusion of the lacZ and the GalT genes (Bressan and Stanley, 1987). In order to construct the fusion plasmid, a range of molecular biological techniques were employed. Restriction digests, agarose gel running, CIP treatment of cut plasmids, ligation, transformations and mini preps of plasmid DNA were all performed according to Sambrook (1989).

Overexpression

10 ml LB-Amp broth was inoculated with a single bacterial colony which had been transformed with the pUEX2 plasmid or a derivative of it. This was grown overnight at 30°C with vigorous agitation.

20 ml of LB-Amp was inoculated with 200 µl of the overnight culture. This was incubated with shaking until the OD_{560nm} reached 0.1-0.2 (~60minutes).

10 ml of the culture was removed and 10 ml fresh medium was added. This was left to grow further at 30°C. 10 ml of LB-Amp, prewarmed to 54°C was added to the other 10 ml of culture and this was transferred immediately to a water bath at 42°C. The cultures were shaken for 2 hours before processing the cells.

Processing of Cells

The 10 ml cultures were spun at 1730 g for 10 minutes at 4°C.

Pellets were resuspended in 1 ml of 10 mM Tris-HCl pH8.0, 0.5 mM EDTA, 10 mM NaCl and transferred to eppendorf tubes.

Samples were spun at full speed in the Eppendorf centrifuge for 2 minutes.

Bacterial pellets were then lysed in 100 µl 2x sample buffer (2.7.6.).

The samples were loaded onto SDS-PAGE gels (section 2.7.6) and blotted onto nitrocellulose (2.7.8.).

Preparation of antigen and injection

The relevant bands were excised from the nitrocellulose and dissolved in 300 µl of DMSO at 37°C. Vortexing was required to dissolve the nitrocellulose.

An equal volume of complete Freund's adjuvant was added. An emulsion was formed by further vortexing.

This was injected subcutaneously into the lymph region of a rabbit's neck.

The rabbit was boosted at monthly intervals, with an emulsion of 300 µl antigen in an equal volume of incomplete Freund's adjuvant, and bled one week after each boost.

2.4. Immunofluorescence

2.4.1. Solutions

PEM 0.1 M PIPES-NaOH pH6.9 (Boehringer Mannheim), 1 mM MgSO₄, 1 mM EGTA

PEMS PEM + 1.2 M sorbitol

PEMF PEM + 2% fish skin gelatin

Cell wall digestion mix PEMS + 1 mg/ml Novozym (NovoBioLabs Ltd.) and 0.3 mg/ml Zymolyase-100T (Seikagaku Kogyo Co., Tokyo, Japan)

2.4.2. Immunofluorescence using methanol fixation

10 ml of log phase cells was poured into a filtration unit prechilled in the freezer and cells collected on a 2.4 cm round GFC filter discs (Whatman).

These were plunged into 10 ml methanol at -20°C and quickly shaken to remove cells from the filter. Cells were fixed for 8 mins.

The filter discs were removed and the fixed cells spun at 1200 g, 4°C and washed three times in PEM buffer.

Cell walls were digested by resuspending the cells in 2ml cell wall digestion mix for 25 mins at 37°C.

The digestive enzymes were removed by washing three times in PEMS.

The cells were resuspended in PEMF and sites blocked for at least 2 hours at room temperature or overnight at 4°C.

The primary antibody was added at 1:10 to 1:100 dilution in PEMF and incubated overnight at 4°C with rotation on a Spiramix™.

Cells were washed three times in PEMF, resuspended in the secondary antibody and incubated either overnight at 4°C or for at least 1 hr at room temperature.

Cells were washed three times in PEMF before mounting.

2.4.3. Mounting cells for fluorescence microscopy

At the end of the experimental procedure the cell pellet was resuspended in sufficient buffer to give a thick suspension. The suspension was applied to a prepared coverslip and excess suspension withdrawn with a pipette. The monolayer of cells was air dried. The cells were then inverted onto a 4 µl drop of Citi-fluor antifade (Agar Aids) containing 1 µg/ml DAPI (4'6'-diamidino-2-phenylindole dihydrochloride). Coverslips were sealed with nail varnish.

2.4.4. Preparation of coverslips

13 mm diameter coverslips were washed free of dust and grease by immersing sequentially in the following : 5% Teepol detergent, dH₂O (twice), acetone. They were air dried. Finally they were coated with either application of 0.1% poly-L-lysine or with chrome alum gelatin and left to dry before being stored.

2.4.5. Viewing stained cells

Fluorescence staining was observed using a Zeiss Axiophot microscope and photographs taken with Ilford HP5 film (black and white), Ektar 1000 (colour print) or Fujichrome 400 ASA (slides).

2.4.6. Confocal microscopy

Confocal fluorescence microscopy was performed with a BioRad Lasersharp microscope MRC600, using a 60 X objective. Images were collected with a Polaroid Quick Print video printer on Plus-X 125 film (Kodak) or using Ilford FP4 film.

2.5. Fluorescence staining of cell organelles

2.5.1. Golgi apparatus staining

NBD-ceramide was made up at 10 mg/ml stock solution in 95% EtOH.

1 µl stock was taken and to it added 10 µl defatted BSA (Sigma) from a 68 mg/ml stock solution. 1 ml DMM was added.

Log phase cells were fixed with 3% formaldehyde for 60 minutes at 30°C. 5% toluene/ethanol (20:80 ratio) was added with shaking for 5 minutes at room temperature. They were spun down gently at 1500 g for 5 minutes,

resuspended in 500 µl DMM with NBD-ceramide and incubated with rotation for 45 minutes at room temperature.

Cells were then washed in 2% BSA in DMM. 10 µl sample was dropped onto coverslips precoated with 0.1% poly-L-lysine and mounted onto a 4 µl drop of Citi-fluor antifade (Agar Aids) containing 1 µg/ml DAPI. Cells were viewed with suitable filters for fluorescein (Lipsky and Pagano, 1985; Pagano, et al., 1989).

2.5.2. Nuclear staining

DAPI (4,6-diamidino-2-phenylindole) was made up as a 1 mg/ml stock in water and kept in the dark at -20°C.

Live Cells: DAPI was added to growing cells at 1 µg/ml. Labelling of the nucleus was rapid (~ 10 minutes). Cells were mounted and viewed with u.v.

Fixed Cells: cells having been fixed for immunofluorescence and exposed to the primary and secondary antibodies were mounted onto slides. Cells dried onto coverslips were inverted onto a drop of DAPI-antifade solution (1 µg/ml DAPI in Citi-Fluor antifade, Agar Aids). The DAPI was taken up almost immediately by the fixed cells.

2.5.3. Vacuolar staining

CDCFDA (Carboxydichlorofluorescein diacetate) was bought from Molecular Probes Inc. It was kept as a 1mM stock in DMSO.

Cells were grown with shaking to log phase. Cells were spun down and resuspended at 1×10^7 cells/ml in 1 ml of a low pH medium (YES + Na citrate final pH 3.5). 5 µl CDCFDA was added from the stock solution. Cells were incubated with rotation for 30 minutes at 30°C. Cells were washed and mounted, then viewed with fluorescein filters. (Adapted from (Pringle, et al., 1989).

2.5.4. Viewing stained cells

Mounting and viewing of fluorescently cells was performed as for immunofluorescence (2.4.5).

2.6. Electron microscopy

2.6.1. Solutions

2% potassium permanganate 200mg KMnO_4 was dissolved in 10 ml dH_2O and vortexed. The fixative was made freshly for each experiment.

Uranyl acetate 2% solution (w/v) made up in 50% (v/v) ethanol.

Lead citrate (Reynolds, 1963) 1.33 g lead nitrate and 1.76 g Na citrate were placed in 30 ml dH_2O and dissolved. After 30 min 8ml 1M NaOH was added and the volume made up to 50 ml.

PEMS 0.1 M PIPES-NaOH pH6.9 (Boehringer Mannheim), 1 mM MgSO_4 , 1 mM EGTA, 1.2 M sorbitol

Cell wall digestion mix PEMS containing 1 mg/ml Novozym (NovoBioLabs Ltd.) and 0.3 mg/ml Zymolyase-100T (Seikagaku Kogyo Co., Tokyo, Japan)

Cacodylate buffer 0.1M Sodium cacodylate pH with HCl to pH7.4

Osmium tetroxide (Taab Laboratory Equipment Ltd.) 1% solution made up in cacodylate buffer.

2.6.2. Fixatives

Potassium permanganate fixation:

This method fixes cells rapidly and gives a high level of membrane contrast which was of use when studying an organelle such as the Golgi apparatus. The method was adapted from that of Luft (1956).

Log phase cells (about 10 mls) were spun down, washed extensively in dH₂O and then resuspended at 5×10^7 - 1×10^8 cells/ml in freshly prepared 2% potassium permanganate for 45 minutes at room temperature. The cells were then washed again in water.

Glutaraldehyde/paraformaldehyde fixation

This was used a more conventional fixative giving good preservation of cell architecture. Adapted from van Rijn et al (1975)

Log phase cells were spun down and resuspended in 3% glutaraldehyde (Fluka-BioChemika) in PEMS buffer for 30 minutes at room temperature.

Cells were washed three times in PEMS then resuspended at 10^8 /ml in cell wall digestion mix for 30 minutes at 37°C.

Cells were washed in cacodylate buffer then fixed in 3% glutaraldehyde, 0.5% paraformaldehyde (Agar Scientific Ltd.) for 30 minutes.

Pellets were post-fixed in osmium tetroxide in cacodylate buffer for 30 minutes, then dehydrated and processed.

Paraformaldehyde/ / glutaraldehyde fixation

Taken from Karnovsky (1965).

Cells were grown to log phase, spun down at 12000g for 2 minutes, and resuspended in 3% paraformaldehyde, 2% glutaraldehyde in cacodylate buffer.

Cells were fixed overnight at 4°C, then washed in cacodylate buffer.

Pellets were post fixed in 1% (w/v) osmium tetroxide in cacodylate buffer for 30 minutes, then dehydrated and processed.

2.6.3 Processing and embedding

Pellets were processed by dehydration in a graded series of ethanol from 70%-100%. Processing was performed in the eppendorfs in which fixing had taken place or in 15 ml glass bottles.

The sections were dehydrated with the 70% and 90% ethanol, twice in each for 15 min, then in the 100% ethanol for at least 45 minutes. The pellets were dehydrated further by leaving them in propylene oxide for 10 min. Epon resin (Taab Laboratories Equipment Ltd.) was mixed with an equal volume of propylene oxide and the pellets left in this for 1 hour. Finally, the pellets were rotated in neat Epon resin for 2 hours with a change of the resin after 1 hour. The pellets were embedded in this resin using a mould and the resin allowed to cure by leaving overnight in an oven at 65°C.

Sections were cut with a diamond knife and mounted on carbon/formvar coated grids.

Sections were stained for 10 minutes in uranyl acetate and for 4 minutes with a solution of lead citrate.

They were viewed in a Philips CM10 electron microscope.

2.6.4. Immuno-electron microscopy (performed by Nasser Hajibagheri, ICRF EM unit)

S. pombe cells were grown to log phase in YES and fixed with 1% monomeric glutaraldehyde in 0.1 M Sorensen's phosphate buffer pH7.4 for 1 hour at room temperature.

Cells were treated with 0.5 M ammonium chloride in phosphate buffer for 4 hours and washed overnight in buffer at 4°C.

The cells were dehydrated in a graded series of methanols at progressively lower temperatures and infiltrated with Lowicryl HM20 at -50°C. The resin was polymerized by uv light for 48 hours at -50°C.

Ultrathin sections were mounted on carbon coated grids and labelled as follows: after 5 min on a drop of PBS and 1 hour preincubation on 5% normal goat serum plus 5% BSA in PBS, the grids were transferred onto drops of GTF2 immune serum (1 in 10 dilution) overnight at 4°C. The sections were washed 3 times over a 15 min period with PBS and then

incubated with immunogold conjugates (goat anti-rabbit; 10nm gold) for 2 hours. After three 5 min washes in PBS and three 5 min washes in water, the sections were air-dried and contrasted with uranyl acetate and lead citrate.

2.6.5. Quantitative Analysis

Cisternal stacking:

Cell sections were selected at low magnification (x1100) and at random on an electron microscope grid (n>100).

The magnification was then increased to x13,500 and each cell in a field analyzed in turn. Every cisterna in a cell was scored as being single or associated with one or more cisternae.

Single cisternae could not always be assigned unequivocally. A short length of ER in the cell cytoplasm and a single Golgi cisternae could, for example, be confused morphologically. For this reason I adopted a fairly rigorous definition, a single cisterna being scored as such only if it was of the appropriate length (between 0.4 and 1 μm) with dilated rims at both its ends.

Stacked cisternae were easily distinguishable from all other cellular membranes.

Surface Density Measurements:

Fields of cells on the sections were selected at random and a series of photographs were taken at a magnification of 8900x and then printed at a final magnification of 22000x.

A disector (Griffiths, et al., 1989; Sterio, 1984) was made. For this series of measurements the disector was a 15mm square grid printed on a clear acetate sheet. This size was selected because at the magnification of micrographs used (22,000) this would ensure that most Golgi stacks present would be intersected by grid lines.

The disector was placed across the section micrographs and with a random start point membranes lying on the grid lines, of the disector were scored (Σi). The grid lines were followed both vertically and horizontally.

The categories of membrane counted were: stacked Golgi cisternae, nuclear envelope, peripheral ER and internal ER which included all stretches of non-peripheral membrane in cells that were not mitochondrial or vacuolar in origin, this would however include any single Golgi cisternae.

The area of the cells counted per micrograph was also measured by counting all grid intersections lying over cells (Σp). Surface density was then calculated as follows:

$$\text{Surface density} = S_{v_{mb/cell}} = \Sigma i / d \Sigma p$$

where d is the distance between grid lines expressed in μm .

The values were assessed for each micrograph, a mean value obtained over at least 10 micrographs and standard deviations calculated.

Intercisternal distances

These were measured from electron micrographs of Golgi stacks at a magnification of 75,000. The measurements were made with a pair of dividers and a 0.5mm ruler. Measurements were only made in the central third of any stack since the structure towards the dilated rims seems to be looser and would not give an accurate reflection of the distance.

Distribution of gold particles in cells and in the Golgi stacks

A 10 mm disector grid was placed over a set of micrographs obtained from immuno-e.m experiments. The micrographs were at a magnification of 60,000.

Each square of the grid was analyzed in turn as to whether it contained a majority of cytoplasm, mitochondria, vacuole, Golgi stack, or cell wall. The number of gold particles in each square was also counted.

To look at the distribution of gold within Golgi stacks the grid was laid over micrographs of Golgi stacks at 105,000 magnification.

Gold particles were scored as to whether they were in the central region of the stack or at the dilated rims.

Some Golgi stacks were sectioned through the centre of the stack so it was not clear whether they were from the rims or the central region. Gold particles in these areas were scored as lying in indeterminate regions of the Golgi stack.

2.7. Protein Procedures

2.7.1. Preparing *S.pombe* protein extracts

Stop buffer 150 mM NaCl, 50 mM NaF, 10 mM EDTA, 1 mM NaN₃, pH8.0

Homogenization buffer 25 mM MOPS pH7.2, 60 mM β -glycerophosphate, 15 mM *p*-nitrophenylphosphate, 15 mM MgCl₂, 15 mM EDTA, 1 mM DTT, 0.1 mM sodium vanadate, 1% Triton X-100, 1 mM PMSF, + stock protease inhibitors

Protease Inhibitors 1000x 1 mg/ml aprotinin, 1 mg/ml leupeptin, 1 mg/ml pepstatin, 1 mg/ml antipain, 1 mM benzamidine.

Procedure - based on (Moreno, et al., 1991)

A 50 ml culture was grown up to an OD of 0.2-0.3 in minimal medium.

The cells were harvested at 1500g for 5 minutes and washed once in ice cold stop buffer.

The cells were then spun at 2000g and the pellet drained. The cells were resuspended in 20 μ l of HB buffer.

1.5 ml acid washed 0.5 mm glass beads were added and the tube vortexed vigorously for 1 minute.

The beads were washed with 1 ml HB and the extracts centrifuged 12000g, 4°C for 15 minutes.

2.7.2. Measuring the level of protein synthesis by incorporation of ³⁵S-trans label

Log phase cells were incubated with ³⁵S trans label (NEN) for at least 30 mins (500 µCi/10⁷ cells, used 2 ml sample cultures) at 32°C to allow its incorporation into new proteins in cells.

Protein extracts were made as above. To assess the incorporation into protein rather than tRNAs the proteins were precipitated as follows (Mans and Novelli, 1961).

10µl of each extract was spotted onto a pencil marked Whatman 3MM (2.4cm) filter. Filters were also made for no extracts, the hot medium not exposed to cells and for the homogenization buffer alone. The filters were transferred to several hundred ml of ice cold 10% TCA and the protein left for 1-2 hours to precipitate. The filters were then transferred to a large volume of boiling 5% TCA and boiled for 10 min. The filters were washed with 50:50 ether:ethanol for 10 min and then in ether alone for a further 10 min. They were then air dried on a paper towel. They were transferred to scintillation vials and 5 ml Beckman scintillation cocktail added.

The TCA precipitates the labelled protein and tRNA allowing free label to be washed away. Boiling breaks down the tRNA but leaves the protein intact.

2.7.3. Measuring protein concentration

The BCA Protein Assay Kit (Pierce) was used with their standard protocol.

Standards were prepared from 2% BSA and covered the range 200-1200 µg/ml. The assay reagent was made up with 1 part solution B to 50 parts solution A.

50 µl of each standard or sample was then added to 1 ml mixed assay reagent and these incubated at 37°C for 30 min. The absorbance was then read at 562nm of each tube. A control assay contained 50 µl of an appropriate buffer solution and 1 ml assay reagent.

The concentration of samples was then calculated from a standard curve.

2.7.4. Sucrose gradients

Heavy sucrose solution. 50 mM KOAc, 20 mM HEPES pH7.2, protease inhibitors, 1 mM PMSF, 1.8 M sucrose.

Light sucrose solution. 50 mM KOAc, 20 mM HEPES pH7.2, protease inhibitors, 1 mM PMSF, 0.5 M sucrose

Protease Inhibitors x1000 1 mg/ml aprotinin, 1 mg/ml leupeptin, 1 mg/ml pepstatin, 1 mg/ml antipain, 1 mM benzamidine.

Procedure

Sucrose gradients were used to separate cellular components from yeast homogenates.

100 µl of homogenate was combined with 100 µl light sucrose solution and layered on top of a continuous sucrose gradient from 0.5-1.8 M sucrose. The gradients were spun 17 hours at 62,000 g 4°C.

150 µl fractions were removed and assayed for % sucrose using a hand held refractometer and for protein concentration .

2.7.5. Endoglycosidase H digestion

N-linked oligosaccharides were removed by endoglycosidase H treatment.

10 µl protein homogenate in 2x sample buffer (2.7.6) was added to a reaction mixture containing 1 µl 3 M Na acetate pH5.5, plus protease inhibitors in a total volume of 50 µl. Reactions were incubated overnight at 37°C in the presence or absence of 1 µl endoglycosidase H. 30 µl of 2x

sample buffer was added and samples heated to 95°C for 5 min before loading on an SDS-PAGE gel (see 2.7.6.).

2.7.6. SDS-PAGE gels

Solutions

Gel solutions	stacking gel	running gel
40 % acrylamide:bis solution 29:1	2.5 ml	10 ml
0.5M Tris-HCl pH6.8 at room temp.	2.75 ml	-
2M Tris-HCl pH 8.8 at room temp.	-	8 ml
20% SDS	50 µl	100µl
TEMED	10 µl	20 µl
dH ₂ O added to	20 ml	40ml
10% Ammonium persulphate (w/v)	50 µl	50 µl

Running buffer 5xRB For 1 litre 30 g Tris base, 144 g glycine, 5 g SDS, made up to 1 litre with dH₂O

Sample buffer 2xSB 2% SDS (from 20% stock), 50 mM Tris-HCl pH6.8, 2 mM EDTA, 10% w/v glycerol, 0.03% bromophenol blue, 2% β-mercaptoethanol

Preparation of gels

The running gel solution was made up and poured between glass plates separated by 0.75 mm spacers. The gel was covered by a layer of water saturated tertiary butanol and left to set.

When the gel was polymerized the top of the gel was washed clear of butanol, the stacking gel poured and an appropriate comb put in place.

Sample preparation

An equal volume of 2xSB was added to each sample. Dithiothreitol was added to a final concentration of 10 mM (1 µl from a 0.5 M stock added to a 50 µl sample) and heated to 95°C for 5 min.

The samples were transferred to a waterbath at 37°C for 30 min before adding iodoacetamide to a final concentration of 50 mM (5 µl of a 0.5 M stock into 50 µl sample).

Samples were left at room temperature for 15 min, then centrifuged before loading onto the gel.

Gel Running

Gels were run either overnight at constant current (4mA/gel) using BioRad gel equipment or at 20 mA for 1-2 hours using Pharmacia mini-gel kits. Both were run in 1x RB made up with dH₂O from the 5x RB stock.

2.7.7. Western Blotting

Solutions

PBS 8.06 mM Na₂HPO₄, 134 mM NaCl, 1.47 mM KH₂PO₄, 68 mM KCL (pH 7.2)

Ponceau S 2 g/l Ponceau S in 3% TCA

Tris Glycine buffer 25 mM Tris HCL (pH 8.3), 192 mM glycine.

Western blot transfer buffer (TB) 25 mM Tris HCl (pH 8.3), 192 mM glycine, 20% v/v methanol, 0.1% w/v SDS.

Western blot blocking buffer (BB) 5% Marvel milk powder, 0.1% Tween-20 in PBS.

Western blot washing buffer 1x PBS, 0.2% Tween 20.

Procedure

Proteins were transferred to Hybond-C-super nitrocellulose membrane (Amersham) using a Hoeffer Semi-Dry Electroblotter.

The membrane was floated on H₂O then soaked in TB and placed on top of 3 sheets of TB-soaked 3MM paper. An SDS gel was placed on top of the membrane, followed by 3 more sheets of TB soaked 3MM. As each layer was added, bubbles were rolled out using a Pasteur pipette.

Transfer of proteins to the membrane was accomplished using a constant current of 100 mA for 1 hour.

The membrane was washed in H₂O, then in Ponceau S to ensure that proteins had transferred.

The membrane was rinsed in PBS then blocked in 5% Marvel milk powder, 0.1% Tween-20 in PBS (BB) for 1 hour at room temperature.

The blot was incubated in a 1 in 10 to a 1 in 2,000 dilution of primary antibody in BB for 1 hour with agitation. Excess antibody was removed by washing for 5x10 min in 0.1% Tween in PBS.

The blot was then incubated in a 1 in 1000 dilution of HRP-coupled secondary antibody in BB for 45 min with agitation. Washes were performed as before.

The blot was rinsed briefly in PBS and proteins detected using the Enhanced Chemi-Luminescence system (ECL) (Amersham). A 1:1 mixture of detection reagents 1 and 2 was poured across the surface of the blot. After 1 min it was removed and excess liquid drained. The blot was dried, wrapped in clingfilm and exposed to film for 1 sec to 30 min.

2.7.8. Western blotting (alternative protocol)

This method of Western blotting was used in the lab before the development of the more sensitive Amersham ECL system. It was used for the blots involving the TEX antibodies.

Solutions

Tris/Salt buffer (TBS) 200 mM Tris-HCl pH7.4, 150 mM NaCl

Block 5% Marvel milk powder in TBS + 0.5% TX-100.

Developing substrate I *p*-nitro blue tetrazolium 75 mg/ml in 70% DMF.

Stored -20°C, darkened.

Developing substrate II 5-bromo,4-chloro,3-imidoyl phosphate, 50 mg/ml in 100% DMF. Stored -20°C, darkened.

Developing buffer 100 mM Tris, 100 mM NaCl, 2 mM MgCl₂ pH8.8.

Developing solution 12.5 µl I then 75 ml II per 25 µl developing buffer.

Procedure

Transfer of proteins was as above except that transfer was onto nitrocellulose (Schleicher and Schuell™). The blot was stained with Ponceau S to show transfer. The blot was washed in TBS buffer and blocked in 5% milk powder in TBS.

Primary antibody incubation was as above but using the TBS buffer. The blot was washed in TBS for 10 min, 20 min in TBS with 0.1% TX-100, then 10 min in TBS. The secondary antibody, alkaline phosphatase-conjugated goat anti-rabbit was used at 1:2000 dilution. The blot was washed as just described.

Developing solution was added to the blot and agitated until bands appeared in purple. Developing should not take more than 15 mins at room temperature. Development was stopped by washing with copious amounts of water. The nitrocellulose was dried and the colour remained stable.

2.8. Enzyme assays

2.8.1. Acid Phosphatase

Log phase cells in DMM were spheroplasted and then washed and resuspended at 10 times the original cell number in YES containing 1.2 M sorbitol.

100 μ l samples were taken at recorded time points and centrifuged at 1200g. The supernatant was then assayed for acid phosphatase secreted into the medium according to the method of Schweingruber (1986b).

For the assay: 50 μ l supernatant was added to 0.5 ml 2 mM *p*-nitrophenyl phosphate in 0.1 M NaOAc pH 4.0 and incubated 5 min 30°C.

The reaction was stopped by addition of 0.5 ml of 1 M NaOH.

The OD of the samples was read at 405nm.

2.8.2. Hexokinase

The activity of this cytoplasmic enzyme was measured in a coupled enzyme assay (DeLaFuente and Sols, 1970).

Log phase cells were grown and the hexokinase activity of intact and permeabilized cells assayed. Cells were permeabilized to release cytoplasmic contents by vigorous vortexing of 1ml of cells in the presence of 10% toluene, ethanol (in 20:80 v/v) for 1 minute (Serrano, et al., 1973). 20 μ l of intact or permeabilized cells was added to 0.98 ml of reagent (50 mM HEPES-NaOH pH7.0, 1 mM glucose, 2 mM ATP-NaOH (from 50 mM pH 6.8 stock), 3 mM MgCl₂, 0.5 mM nicotinamide adenine dinucleotidephosphate (NADP), 0.5U Glucose 6 Phosphate dehydrogenase (G6PDH).

The OD_{340nm} increase was measured at room temperature.

2.8.3. α -1,2-galactosyltransferase (GalT)

This assay determined GalT activity by measuring the transfer of tritium label from UDP-Gal, which is a charged molecule, to an uncharged substrate methyl mannose. Charged species were separated by running the reaction mix, after an appropriate incubation time, over an anion exchange column. To distinguish the transferase activity from other activities which would simply degrade the UDP-Gal to UDP and galactose it was

necessary to measure each sample in the presence and absence of the substrate, methyl mannose (Chappell and Warren, 1989).

Solutions

Stock solution	Volume added per assay	Final assay concentrations
1M HEPES-NaOH pH7.0	5 μ l	100 mM
1M MgCl ₂	0.5 μ l	10 mM
100 mM MnCl ₂	0.5 μ l	1 mM
10% Triton X-100	5 μ l	1%
10 mM UDP-galactose	2.5 μ l	500 μ M
Tritiated nucleotide sugar	0.25 μ l	
1 M methyl mannose	10 μ l	200 mM
dH ₂ O added to	45 μ l	

Procedure

5 μ l samples were added to 45 μ l reaction mix and incubated at 37°C for 60 min. The samples used were intact cells, permeabilized cells, homogenates and microsomes. The control samples incubated in the absence of methylmannose had dH₂O added in place of this substrate. 150 μ l dH₂O was added and each sample was then applied to a 0.8 ml Dowex anion exchange column. The unbound (and therefore uncharged) material from each column was collected in a scintillation vial.

The columns were washed twice with 1 ml water and this run through was collected in the same vials. 4 ml scintillation fluid was added to each vial and the counts measured in a Beckman LS-60001C scintillation counter.

The columns were regenerated by washing with 2 ml of 5 M NaCl, 2 ml of 0.1 M HCl and twice with 2.5 ml of water.

Chapter 3

The Golgi apparatus in wild type cells

3.1 Introduction

This chapter introduces the tools available for studying cell biological problems in *Schizosaccharomyces pombe* and how I have adapted them to study the behaviour of the Golgi apparatus. An initial investigation, looking at the Golgi apparatus in wild type cells, was necessary since very little work was documented concerning its normal morphology and behaviour.

3.2 Light Microscopy

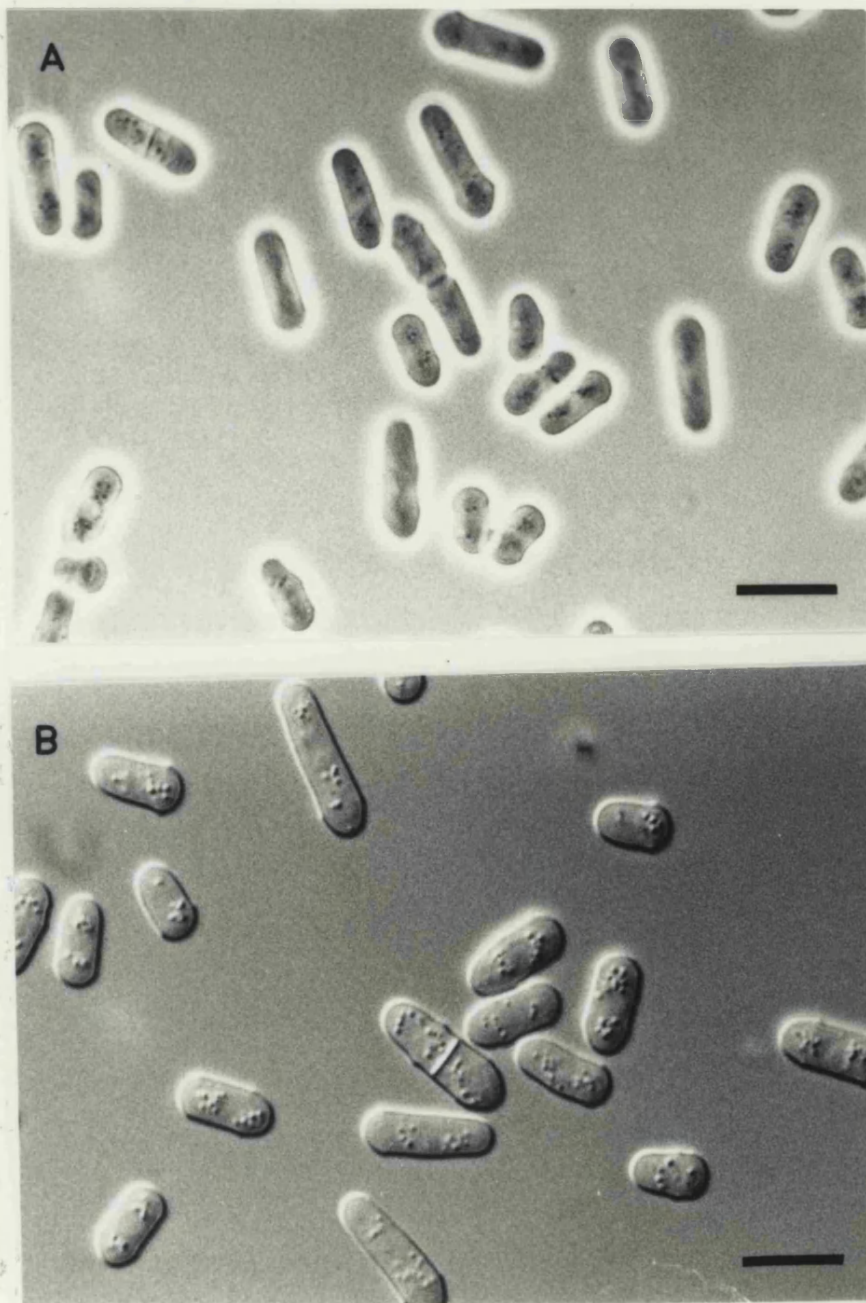
The most straightforward approach to studying organelle behaviour in cells is by light microscopy. However it should be noted that due to the size of a *S.pombe* cell (~10 µm) only large scale changes would be observable at this level. The Golgi apparatus itself is not visible by phase contrast or Nomarski optics. Organelles which may be discerned at this level are the nucleus, vacuoles and storage inclusions involved in storage of lipids and starch compounds (Fig. 3.1).

3.2.1 Fluorescent probes for cellular organelles

Some compartments can be visualized by the use of vital stains which accumulate in the relevant compartment of live cells. The best studied of these include; for vacuoles, CDCFDA (Pringle, et al., 1989) and quinacrine (Pringle, et al., 1989; Weisman, et al., 1987) and for the nucleus, DAPI (Alfa, et al., 1993). DAPI also labels the nuclei in fixed cells. I have used these fluorescent probes as markers of organelles in cells when trying to monitor the selectivity of any changes I observed on the Golgi apparatus.

Figure 3.1. Wild type *S.pombe* cells under the light microscope.

Cells were grown to log phase, spun down at 12000 *g* and resuspended in one tenth volume of PBS. A 10 μ l sample was mounted on coverslips and viewed using (A) Phase contrast optics and (B) Differential interference contrast (DIC), Nomarski optics. Few organelles are observable without the use of fluorescent markers. Bar = 11 μ m



3.2.2 Fluorescent probes for the Golgi apparatus

NBD-Ceramide: Work by Lipsky and Pagano (1985) showed that certain truncated lipids carrying fluorescent labels, such as C₆-NBD-ceramide, could be taken up by mammalian culture cells. These would initially stain many cell membranes but on washing only the Golgi apparatus would be stained. The method can be used as a vital stain or on fixed cells. The basis for the localization of NBD-ceramide in the Golgi apparatus in fixed cells has been investigated and is still not clear (Pagano, et al., 1989). The best evidence supports a localization due to interaction with Golgi apparatus lipids since use of chemicals interfering with these lipids disrupts the normal pattern of staining.

No work has been published on the use of these stains to observe the Golgi apparatus in yeast. Discussion with R. Pagano led me to attempt to stain the Golgi apparatus in the yeast, *S.pombe* using the fluorescently derived analogues utilized in his studies on cultured cells. Immunofluorescence staining of the Golgi apparatus in *S.pombe* had been carried out by this stage (Chappell and Warren, 1989) and so the expected staining pattern, of multiple, discrete spots, was known.

C₆-NBD-ceramide was added to log phase cells and a range of conditions were tried to optimize the staining seen. Both fixed and live cells were stained; the effect of removing the cell wall was assessed; the time of incubation with NBD-ceramide was changed, and the amount of washing with BSA which back exchanges the NBD-ceramide was varied. In some cases cells were permeabilized with 10% toluene/ethanol (20:80 v/v). The optimal staining conditions tried are described in section 2.5.1. In summary, the staining was best with fixed cells, incubated for at least 30 minutes with NBD-ceramide, permeabilized for 5 minutes with toluene/ethanol. The effect of

washing the cells for back exchanging non-specific NBD-ceramide staining in cells was minimal.

Figure 3.2 shows the staining pattern obtained with NBD-ceramide on *S.pombe* cells. A punctate staining pattern was observed which was consistent with the pattern obtained by immunofluorescence against a specific Golgi marker protein. Several spots were visible in each cell indicating multiple Golgi stacks consistent with e.m. images.

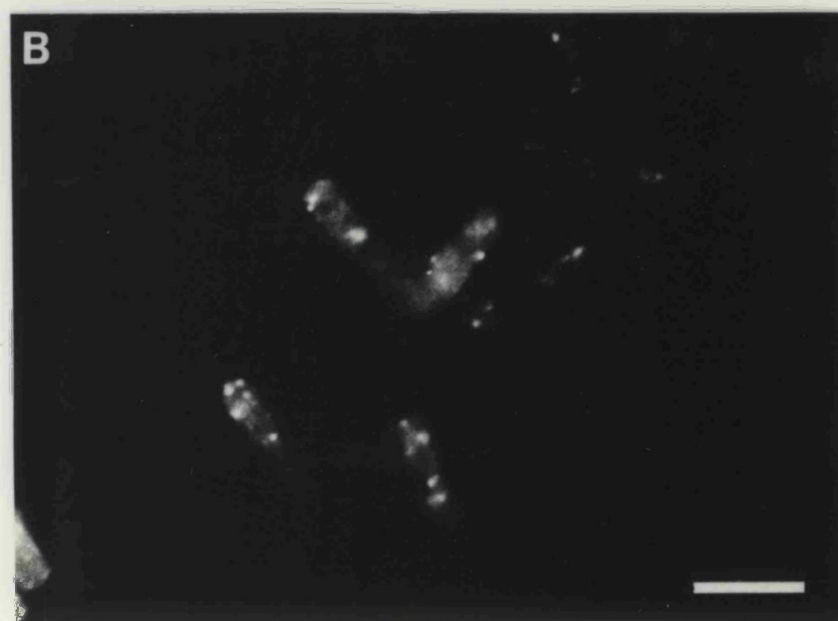
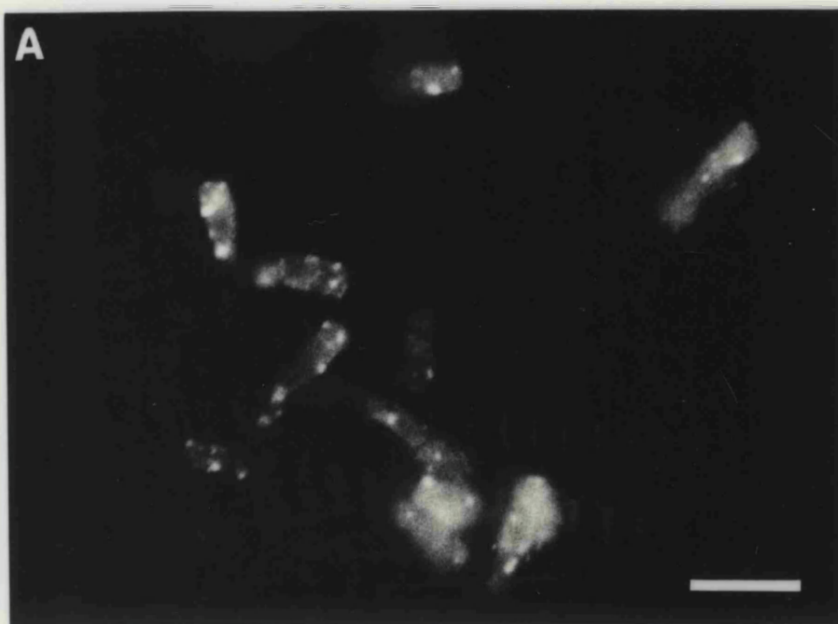
The overwhelming problem with the method was the extremely rapid bleaching time. This had been a problem in the work on mammalian culture cells with times of 5-10 seconds before bleaching. However, the problem in this case was even more severe with the majority of fluorescence bleaching after 2-3 seconds. Attempts to overcome this problem by using various antifade solutions and by the use of lipid derivatives more closely resembling those in yeast, such as NBD-phytosphingosine did not improve the staining nor the speed of photobleaching.

Fluorobora II - Another fluorochrome reported to stain the Golgi apparatus is FluoroBora II (*m*-darpsylamidophenylboronic acid). Fluoroboras are boronic acid derivatives which are highly fluorescent when taken up into certain environments. In the phytoplankton, *Prorocentrum*, a single juxtanuclear organelle presumed to be Golgi apparatus is stained (Klut, et al., 1989).

When used under a range of conditions based on those discussed by Gallop, (1982) no clear punctate staining was observed. The label was excluded from the nuclear and vacuolar regions but within the rest of the cell showed no obvious compartmentalization.

Figure 3.2. NBD-ceramide staining of cells.

(A,B) Log phase cells were grown in minimal medium (DMM) and fixed with 3% PFA for 60 minutes at 30°C. 5% toluene/ethanol (20:80 v/v) was added with shaking for 5 minutes at room temperature. Cells were spun down gently and resuspended in 500 µl DMM with 10µg/ml NBD-ceramide and incubated with rotation for 45 minutes at room temperature. Cells were washed in 2% BSA in DMM. 10 µl sample was dropped onto coverslips precoated with 0.1% poly-L-lysine. Note the multiple spots of NBD-ceramide staining in each cell. Bar = 10 µm



3.2.3 Immunofluorescence microscopy

The basis for the localization of fluorescent probes to the Golgi apparatus is poorly understood and when coupled with the problems of rapid bleaching an alternative approach seemed appropriate. An antibody probe for a protein of the Golgi apparatus in *S.pombe* would give specific labelling of the compartment and therefore would be more suitable for my investigations.

The only other available method for detecting changes in the morphology of the Golgi apparatus was by electron microscopy. It was however considered necessary to have two complementary methods for the work. Immunofluorescence would be a more rapid method of looking at cells and could detect large scale changes in the Golgi apparatus structure. An additional aspect of immunofluorescence is that whole cells are observed. Focusing through cells or the use of confocal microscopy would allow the three dimensional organization of organelles to be observed. By electron microscopy, unless cells are serially sectioned and then reconstructed it is only possible to look at a single section of a cell so no idea of numbers and distribution of organelles is possible.

Prior to this work a protein of the Golgi apparatus in *S.pombe* was isolated in our laboratory. It is an α -1,2-galactosyltransferase purified originally from *S.pombe* microsomes. Antibodies were raised to this purified protein and by immunofluorescence staining showed multiple spots in cells (Chappell and Warren, 1989). In this respect the staining is different from that seen for Golgi proteins in mammalian cells where the Golgi is a single juxtanuclear organelle.

Purification of the α -1,2-galactosyltransferase (GalT) was a lengthy process and very little protein was recovered from large quantities of cells (700 g wet weight cells yielded 200 μ g of purified protein). The supply of antiserum to

the purified protein was limited, particularly after attempts at affinity purification. In addition the antiserum could not be successfully used for immuno-electron microscopy because a large population of the antibodies were immunoreactive against carbohydrate portions of the purified enzyme rather than the protein itself.

An alternative strategy was necessary to raise a population of antibodies to a protein antigen that could be produced in large quantities and which would not be predominantly against carbohydrate epitopes. The approach adopted therefore was to raise antibodies in a bacterial system where oligosaccharides would not be added. A fusion protein could be generated and because it could be overproduced in a bacterial system the quantities that could be raised were greater.

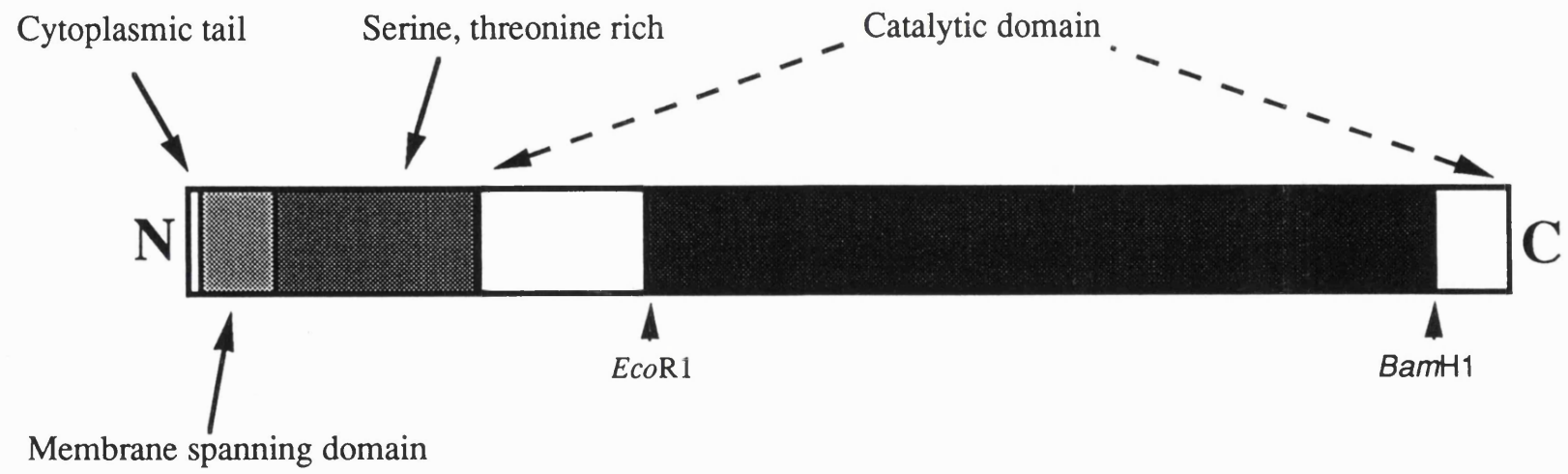
Raising antibodies to a GalT fusion protein

A construct was made in the pUEX vector system (Bressan and Stanley 1987) of a portion of the GalT gene and the lac Z gene for β -galactosidase (β -gal). The GalT had been sequenced (Chappell, et al., submitted) and the predicted amino acid sequence obtained. A hydropathy plot indicated the region most likely to be the transmembrane domain and thus determined the orientation of the protein in the membrane. Figure 3.3 illustrates schematically the major domains in the protein. The transmembrane domain is flanked by a short cytoplasmic tail and, on the luminal side by a serine, threonine rich region, probably heavily glycosylated *in vivo*., and the catalytic domain.

Restriction sites in the gene were mapped in order to make the fusion construct. A *Cla* 1/*Pst* 1 fragment which carried the entire gene was cut with *Eco* RI and *Bam* HI. This released a fragment carrying about 60% of the gene which included most of the catalytic domain (Fig 3.3.).

Figure 3.3. Structural domains of GalT

GalT was sequenced and a combination of prediction techniques and biochemistry allowed a model of its domain structure to be made. It has a very short cytoplasmic region of 7 or less amino acids, a transmembrane domain, a stretch high in serines and threonine residues, and a catalytic domain. It was this latter domain that was selected for making the fusion protein. The part of the gene used for the construct was that lying between the *Eco* R1 site and the *Bam* H1 site.



The pUEX plasmid carrying the lac Z gene was cut at the same sites and the fragments ligated to create an in-frame fusion (Fig. 3.4). To verify that the putative fusion plasmids contained the correct piece of DNA several tests were undertaken. Firstly, the plasmid was cut with *Eco* R1 and *Bam* H1 and the size of the fragments assessed. In this case 2 bands of 650 bp and 6500 bp were obtained. That of 650 bp was the GalT insert required. Secondly, from the sequence of GalT we knew that there was a *Sal* 1 site within this fragment. Repeat digests of *Eco* R1 and *Bam* H1 in the absence or presence of *Sal* 1 were performed and gave the necessary fragments of about 100 and 550 bp in the presence of *Sal* 1. Finally, using 18mer oligonucleotides corresponding to sequence within the GalT gene the correct size fragment was obtained by PCR from the fusion plasmid.

The resultant gene fusion plasmid was transformed into competent bacteria and overexpressed by shifting the cells to 42°C for 2 hours. The bacterial lysate was run on a gel as shown in figure 3.5. The overexpression caused by heat shock is clear for both the pUEX2 control and the fusion plasmid. The pUEX2 plasmid alone generated β -gal at 116 kDa whereas the fusion plasmid produced a protein of 135 kDa. This is about the size expected for the fusion of 650 bp onto the lacZ gene. After gel separation the bacterial lysate was blotted onto nitrocellulose. The relevant bands were excised and dissolved in DMSO before adding Freund's Adjuvant and injecting subcutaneously into rabbits. The antisera obtained from two rabbits were called GTF1 and GTF2 (for Galactosyl Transferase Fusion protein).

Blotting with the antiserum

The antisera were tested by blotting microsome preparations for GalT. However, the level of this enzyme in cells is low and it was not detected.

Figure 3.4. Protocol for construction of the fusion protein.

A schematic summary of the steps involved in making the fusion construct between the genes for α -1,2 galactosyltransferase and β -galactosidase in the pUEX vector.

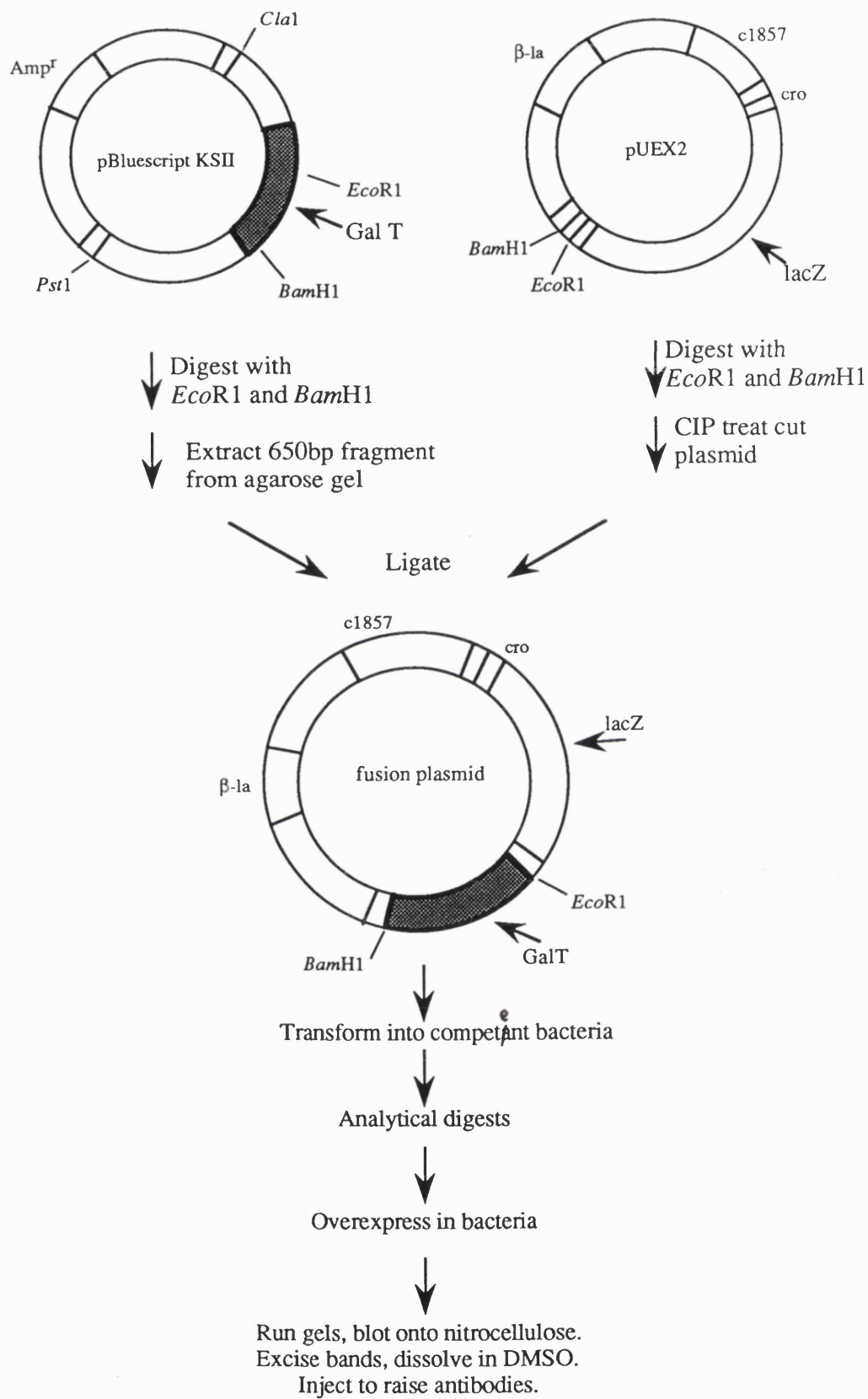
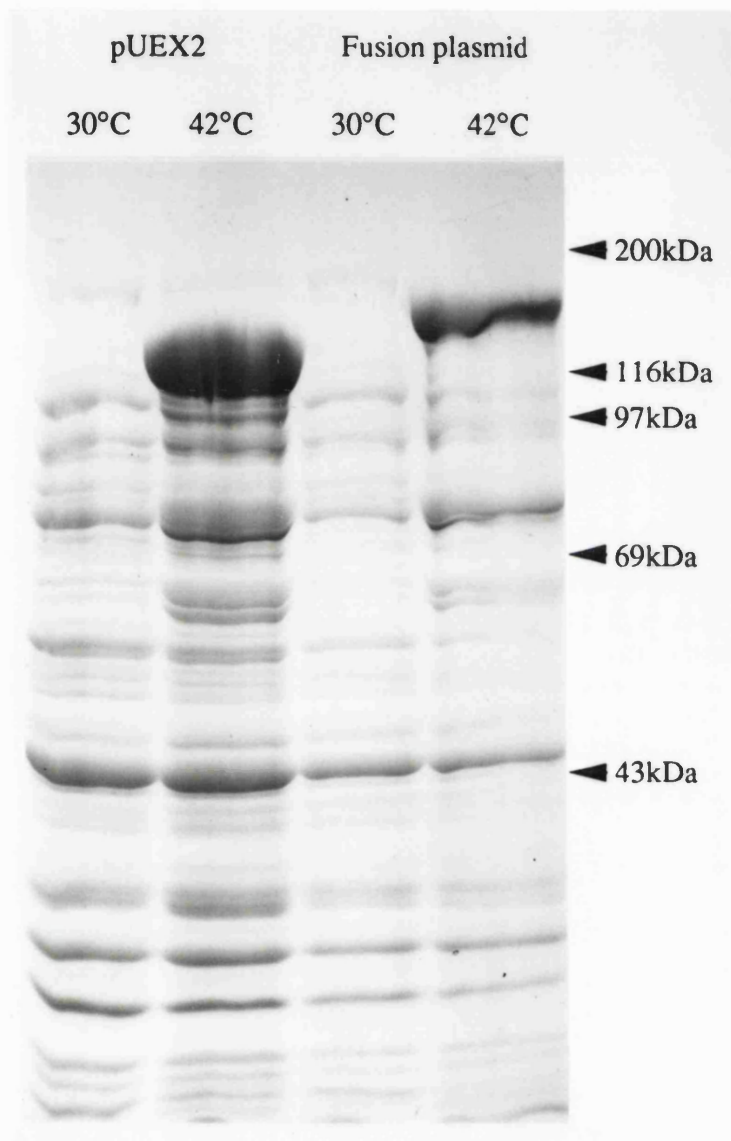


Figure 3.5. The fusion product expressed from the constructed plasmid.

The plasmid construct of GalT and lacZ was transformed into competent bacteria. Cultures were shifted to 42°C for two hours to cause overexpression of the product. Bacterial lysates were made and run on 10% SDS PAGE gels. The expressed proteins can be seen at 42°C but not at 30°C. The overexpressed protein from the original pUEX vector is 116 kDa. This is β -gal alone. The overexpressed product from the bacteria transformed with the fusion plasmid is bigger and at 135 kDa is the size expected for the protein expressed from the 650 bp fusion of GalT sequence onto the lacZ gene.



No purified GalT protein was available to test the specificity. Later bleeds were tested for blotting the fusion protein itself. The fusion protein was recognized in a bacterial lysate run on a gel and no corresponding band was blotted by the preimmune serum (data not shown). However, in this experiment it was not clear whether the population of antibodies recognizing the protein band was against the GalT or the β -gal part of the fusion.

The staining pattern with GTF antiserum

Immunofluorescence was tried despite the initial lack of a signal by blotting. The first fixative employed was paraformaldehyde since much published immunofluorescence staining in *S.pombe* has used this method. However, the results with this were not promising and no clear staining pattern was observed. An alternative method using methanol at -20°C was then used with far greater success. All of the results described were obtained using this technique.

Fixed cells were labelled with the antiserum, GTF2, followed by rhodamine tagged secondary antibodies. They were mounted in DAPI-antifade and observed using the Axiophot microscope. Cells were seen to contain multiple spots distributed throughout the cytoplasm (Fig. 3.6.A). Double labelling was also undertaken with GTF2 and anti-microtubule antibodies to show that the fixation conditions preserved other structures in cells (Fig. 3.6B).

Several lines of evidence indicated that the staining of the Golgi apparatus was specific. Firstly, the staining pattern obtained with the antiserum was very similar to that obtained by Chappell and Warren (1989) with punctate staining in the cytoplasm. In addition, the spots did not co-localize with any of the organelles visible by Nomarski optics or using available vital stains. The pre-immune serum did not give the punctate pattern, simply a low level cytoplasmic smear. Incubating the primary antibodies in the

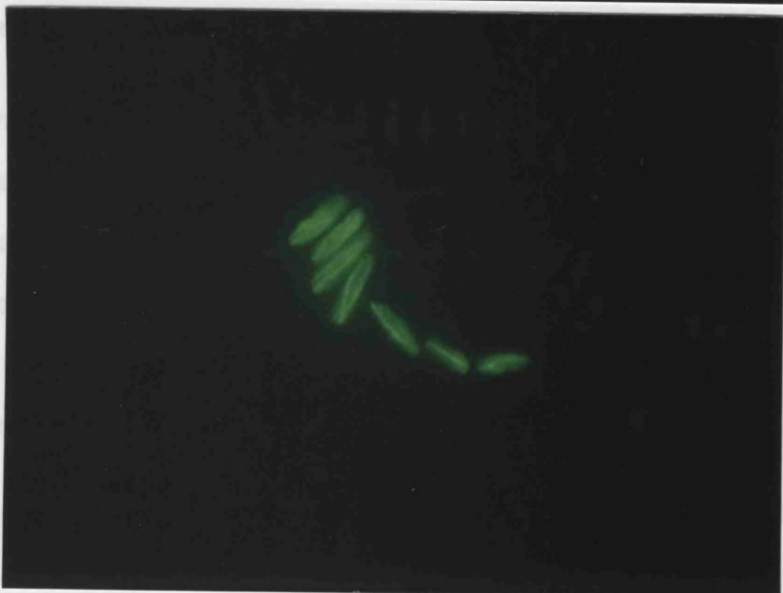
Figure 3.6. Immunofluorescence of *S.pombe* with antibodies against the fusion protein.

Log phase cells were fixed using methanol at -20°C and labelled with antibodies. (A) Using GTF2, against the fusion protein of GalT and β -gal and rhodamine-conjugated secondary antibodies. (B) Using TAT1 against microtubules and fluorescein-conjugated secondary antibodies. (C) Cells were mounted in a solution of DAPI-antifade which stains nuclei . Bar = 10 μ m.

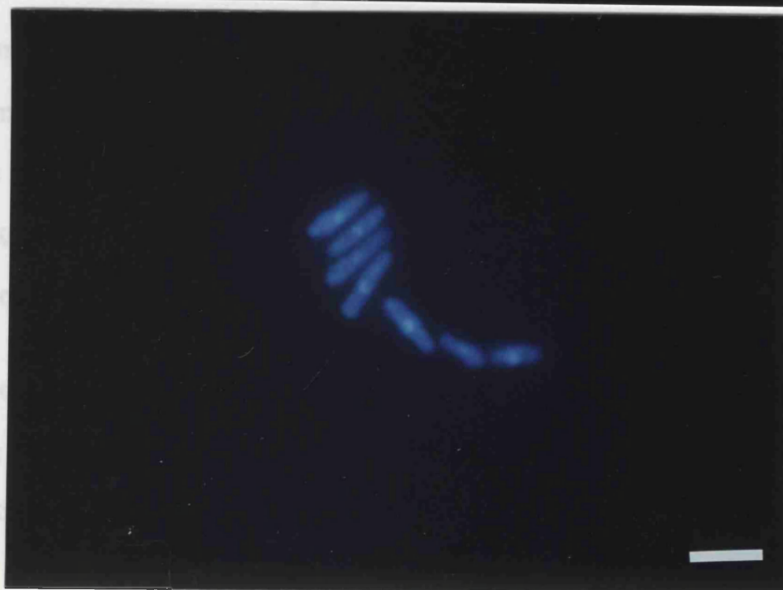
A



B



C



presence of sugars (100 mM methylmannose and 100 mM methylgalactose) did not diminish the staining showing that it was not due to any carbohydrate recognizing antibodies the rabbits may have had. Finally, the presence of β -galactosidase during labelling did not affect the staining pattern showing that antibodies to this part of the fusion protein were not interfering. Further supporting evidence for specific Golgi apparatus localization came from immuno-electron microscopy (see section 3.3.1 and Fig. 3.12).

3.2.4 Characteristics of the Golgi apparatus revealed by fluorescence microscopy

Numbers of Golgi stacks

It was of interest to know how variable the number of Golgi stacks in cells were and whether the number increased with increasing cell size. Since the approximate size, number and distribution of the 'spots' obtained on immunofluorescence staining corresponded to the stacks that could be seen by e.m it was assumed that a single spot was a Golgi stack. From this point on the spots observed by immunofluorescence are referred to as Golgi stacks.

By focusing through cells the numbers of Golgi 'spots' were counted. Cells were scored as, small (in the process of cytokinesis or just divided), medium (chromosome condensed as assessed by DAPI staining but no septum formed), and long (condensed chromosomes or septa forming). These results are shown in figure 3.7. As the cell size increased the number of spots counted also increased. Small cells, following cell division contained 11 ± 3 Golgi stacks whilst cells in mitosis and commencing cell division contained 21 ± 2 .

There was a problem in this counting method due to the level of resolution of the available tools. A Golgi stack in *S.pombe*, from e.m images measures about 0.5-1 μm in transverse section which is at the limit for resolution using

Figure 3.7. Correlation of cell size and number of Golgi stacks

Cells were labelled with GTF2 antibodies and the Golgi stacks stained were counted by focusing slowly through cells in turn. The size of the cell was scored as being small (—□— cells just breaking down their septa), medium (—●— nuclei condensed but no septa formed) or long (—■— nuclei condensed and septa beginning to form). Frequency scored was taken as the percentage of a particular number of Golgi stacks at each cell size.

the Asteroid micrographs. It was difficult, for example, to distinguish a large spot from one spot overlapping or close to another.

Confocal microscopy was performed and this confirmed the initial observations made. Again larger cells contained more Golgi stacks with about 20 or more spots. Smaller cells contained correspondingly fewer (Fig. 3.6).

The figure shows small cells with a single large peak appearing and peaking in the same area as the medium sized cells. This shows the

relationship of the stack

relationship of Golgi stacks

The Golgi stacks were found to be arranged in a regular pattern. There

was no obvious evidence of any

link between the Golgi stacks and the nucleus. It was not clear what

was moving in the Golgi stacks. It was not clear what was moving in the

Golgi stacks. It was not clear what was moving in the Golgi stacks.

so one would or possibly a Golgi stack which had grown and was dividing to

form two individual Golgi stacks.

By confocal microscopy an image of the arrangement of the Golgi stacks in

cells was obtained. There was no evidence for linkages between individual

stacks though such a link might not be detected using a resident cytosolic

marker such as TdMT.

Partitioning of Golgi stacks at cytokinesis

An attempt was made to count the spots in cells which were undergoing

cytokinesis in order to determine the accuracy of partitioning. This was

made difficult by the relatively few numbers of these cells in a

preparation. Furthermore, confocal microscopy could not be specifically

employed to overcome this problem because the main determinant of a

dividing cell as two overlapping new nuclei could not be detected since the

new nuclei could not be detected since the

new nuclei could not be detected since the

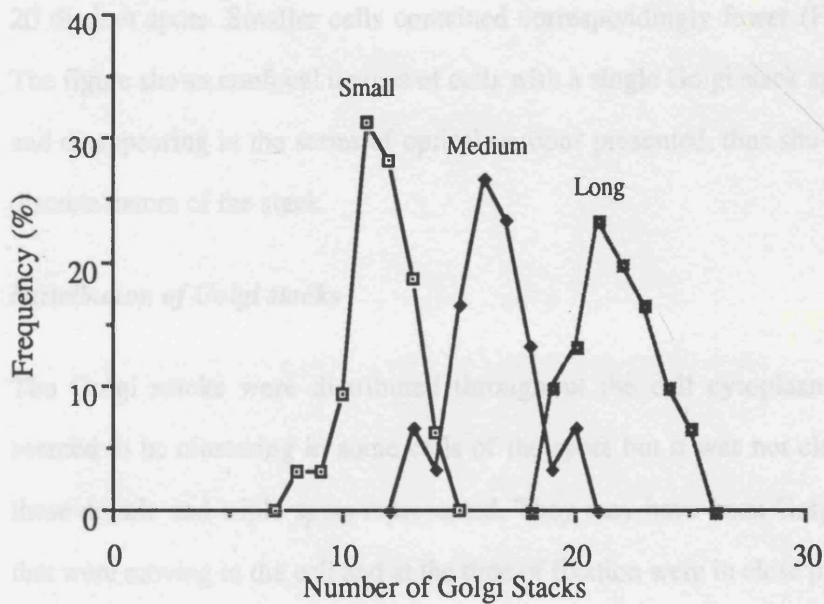
new nuclei could not be detected since the

new nuclei could not be detected since the

new nuclei could not be detected since the

new nuclei could not be detected since the

new nuclei could not be detected since the



the Axiophot microscope. It was difficult, for example, to differentiate a 'large' spot from one spot overlying or close to another.

Confocal microscopy was performed and this confirmed the initial observations made. Again longer cells contained more Golgi stacks with about 20 distinct spots. Smaller cells contained correspondingly fewer (Fig. 3.8). The figure shows confocal images of cells with a single Golgi stack appearing and disappearing in the series of optical sections presented, thus showing the discrete nature of the stack.

Distribution of Golgi stacks

The Golgi stacks were distributed throughout the cell cytoplasm. There seemed to be clustering in some cells of the spots but it was not clear what these double and triple spots represented. They may have been Golgi stacks that were moving in the cell and at the time of fixation were in close proximity to one another or possibly a Golgi stack which had grown and was dividing to form two individual Golgi stacks.

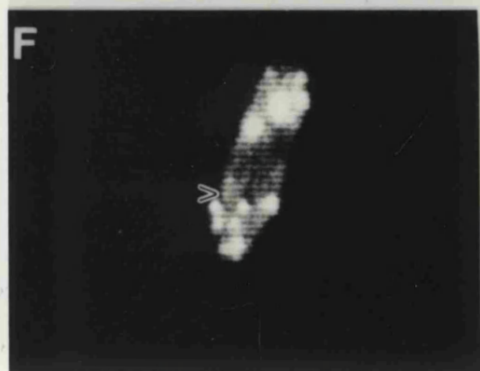
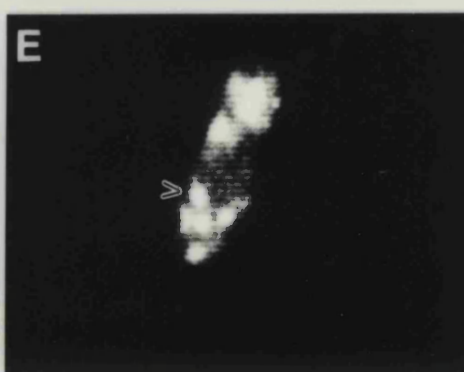
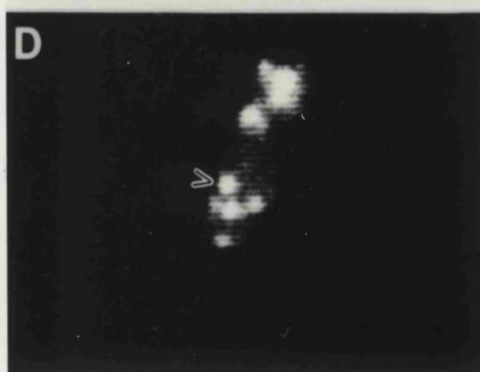
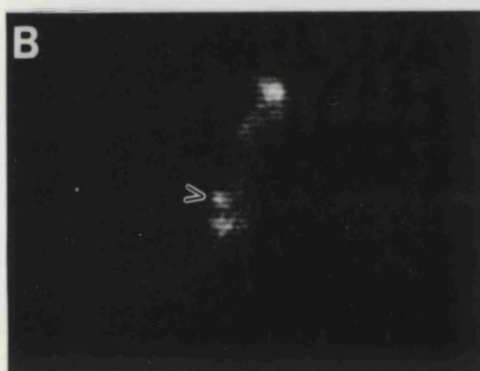
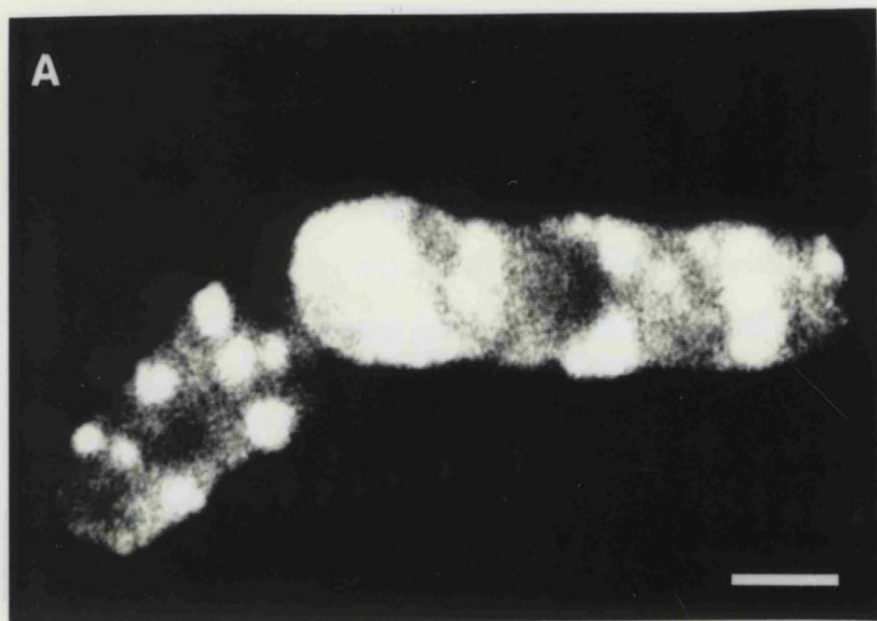
By confocal microscopy an image of the arrangement of the Golgi stacks in cells was obtained. There was no evidence for linkages between individual stacks though such a link might not be detected using a resident enzyme marker such as GalT.

Partitioning of Golgi stacks at mitosis

An attempt was made to count the spots in cells which were undergoing cytokinesis in order to determine the accuracy of partitioning. This was made difficult by the relatively few numbers of these cells in a preparation. Furthermore, confocal microscopy could not be specifically employed to consider this problem because the main determinant of a dividing cell as one containing two nuclei could not be detected since the

Figure 3.8. Confocal images of cells stained with GTF2 antibodies.

Cells were fixed and labelled with GTF2 antiserum. After mounting on coverslips cells were viewed using a BioRad MRC-600 Confocal microscope. (A) A single section through a cell showing labelling of discrete Golgi stacks. (B-G) A series of sections through a cell with images collected 0.5 μm apart. Note spots appearing and disappearing through these sections, such as that marked by the arrowheads. Bar = 2 μm (A), 5 μm (B-G).



confocal microscope was not equipped with suitable objectives necessary for viewing DAPI.

Despite these problems, counting by focusing through cells on the Axiophot suggested that the accuracy was high (Fig. 3.9). Simply studying a population of cells on a slide supported this view since the pattern of staining was always throughout the cell. No cells were seen in which just one or two Golgi stacks were in one half and the remaining stacks in the other.

Since the nuclei in *S.pombe* can be seen to condense slightly and various stages of mitosis are visible using DAPI staining the fate of the Golgi apparatus at this point in the cell cycle could be analysed. Perusal of a population of cells shows that 5-10% of cells are at some stage of mitosis. In no cases was the Golgi apparatus observed to have broken down into dispersed vesicles as is seen in mammalian culture cells at mitosis (Burke, et al., 1982).

3.3 Electron Microscopy

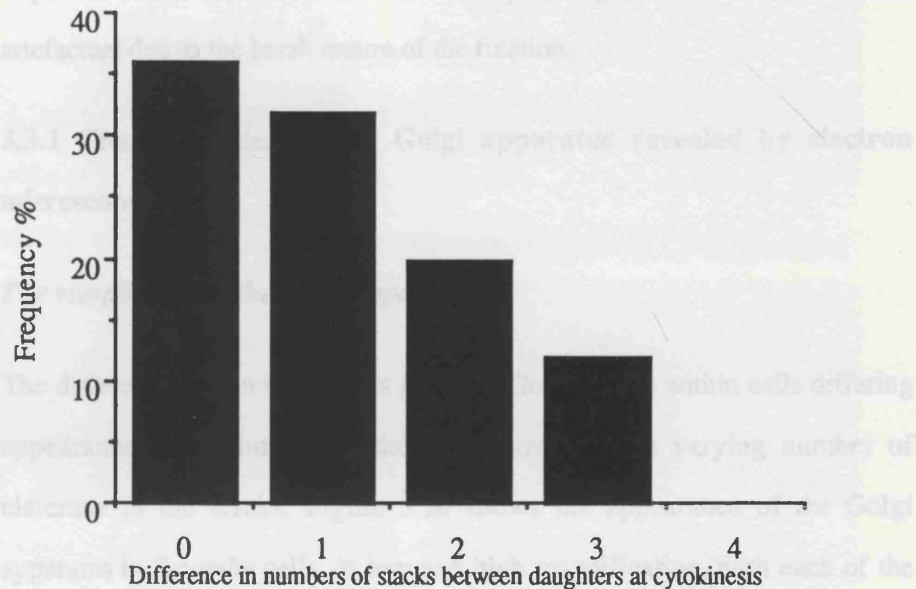
Electron microscopy was a necessary complementary approach in this work. Only large scale changes in morphology were detectable at the level of immunofluorescence and even when such a change was observed the nature of the change could not be determined. Electron microscopy therefore provided a tool to study, more precisely, morphological alterations of the Golgi apparatus in cells.

The fixative chosen initially was permanganate. This fixes cells rapidly and it gives a high level of membrane contrast which was of use when studying an organelle such as the Golgi apparatus. The contrast is partly due to the harshness of the fixation which tears out regions of the cytoplasm.

Figure 3.9. Accuracy of partitioning of Golgi stacks.

Cells were fixed and labelled with GTF2 antibodies to allow visualization of the Golgi stacks in cells. Cells which contained formed or nearly formed septum were assessed. In each cell the number of Golgi stacks on either side of the septum was counted by focusing through cells. The difference in number of stacks between daughters at cytokinesis was then calculated.

Other fixatives were used later in the course of this work which gave improved preservation of cytoarchitecture in cells. The use of osmium tetroxide gave enhanced visualization of the Golgi apparatus but overall these fixatives did not give such a high level of contrast. They were however important to show that effects observed in permanganate fixed cells were not artefacts due to the harsh nature of the fixation.



Those fixed with permanganate (Fig. 3.10 A,B) were highly contrasted over the background. However, it was uncertain that the lumina were discernible and the appearance was more of highly stained but collapsed membranes. Fixation with 3% glutaraldehyde and 0.5% paraformaldehyde gave well preserved stacks with visible lumina and also the Golgi stacks were clearly delineated from the background cytoplasm and other organelles (Fig. 3.10 C,D). Fixation with 3% paraformaldehyde, 2% glutaraldehyde gave the lowest level of contrast and also the poorest preservation of the whole cell often with tearing between the cell and cell wall (Fig. 3.10 E,F).

The differences in the fixatives were reflected when the interlamellar widths of the Golgi stacks were measured (Table 3.1). The 3% glutaraldehyde, 0.5% paraformaldehyde fixation gave good preservation and also had the largest interlamellar distances within Golgi stacks. Permanganate which gave

Other fixations were used later in the course of this work which gave improved preservation of cytoarchitecture in cells. The use of osmium tetroxide gave enhanced visualization of the Golgi apparatus but overall these fixatives did not give such a high level of contrast. They were however important to show that effects observed in permanganate fixed cells were not artefactual due to the harsh nature of the fixation.

3.3.1 Characteristics of the Golgi apparatus revealed by electron microscopy

The morphology of the Golgi apparatus

The different fixation techniques gave the Golgi stacks within cells differing appearances. All showed stacked structures with a varying number of cisternae in the stacks. Figure 3.10 shows the appearance of the Golgi apparatus in *S.pombe* cells, at low and high magnification, with each of the fixatives used.

Those fixed with permanganate (Fig. 3.10 A,B) were highly contrasted over the background. However, it was uncommon that the lumina were discernible and the appearance was more of highly stained but collapsed membranes. Fixation with 3% glutaraldehyde and 0.5% paraformaldehyde gave well preserved stacks with visible lumina and also the Golgi stacks seen were clearly definable from the background cytoplasm and other organelles (Fig. 3.10 C,D). Fixation with 3% paraformaldehyde, 2% glutaraldehyde gave the lowest level of contrast and also the poorest preservation of the whole cell often with tearing between the cell and cell wall (Fig. 3.10 E,F).

The differences in the fixations were reflected when the intercisternal widths of the Golgi stacks were measured (Table 3.1). The 3% glutaraldehyde, 0.5% paraformaldehyde fixation gave good preservation and also had the largest intercisternal distances within Golgi stacks. Permanganate which gave

Figure 3.10. The appearance of the Golgi apparatus by electron microscopy using different fixation techniques.

Cells were grown to log phase and then fixed and processed for electron microscopy. Each fixation technique is illustrated with a low (A,C,E) and high (B,D,F) magnification image. (A,B) Cells fixed with 2% potassium permanganate which gives high contrast of membranes over the background. (C,D) Cells were fixed with 3% glutaraldehyde and 0.5% PFA. Cells were post-fix osmicated to enhance visualization of the Golgi apparatus. (E,F) Cells were fixed using 3% PFA and 2% glutaraldehyde. The cells were post-fix osmicated. Bar = 0.9 μm (A) ; 0.3 μm (B).

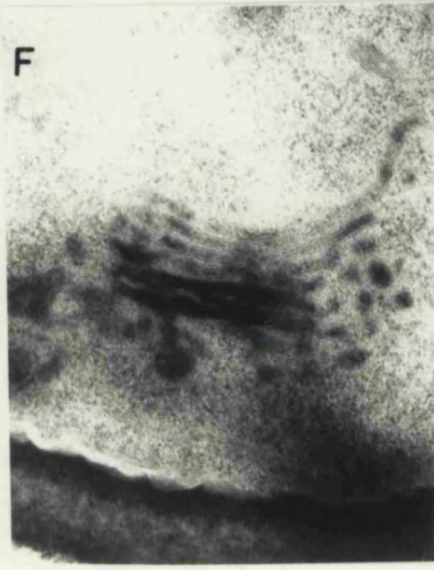
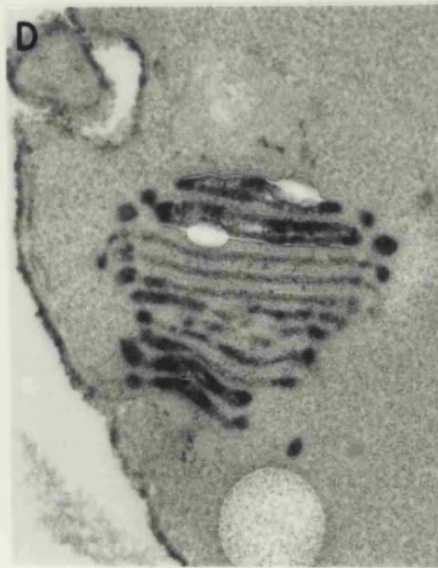
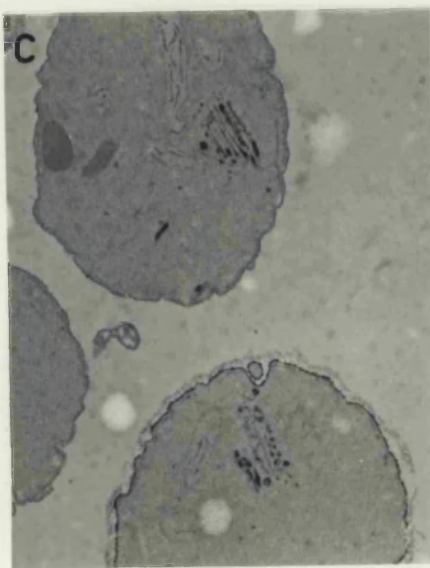
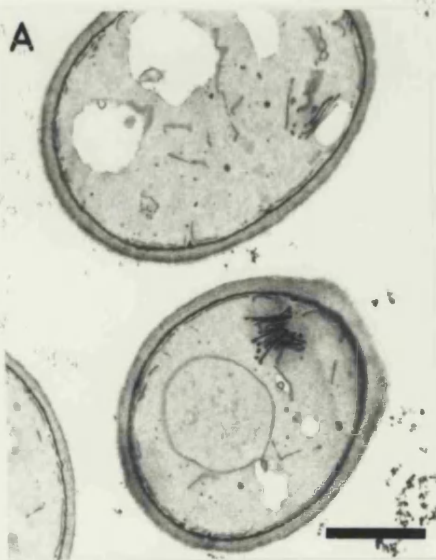


Table 3.1. Comparison of the measurable intercisternal widths in the Golgi apparatus under various fixation conditions.

Cells were fixed using the various methods listed. The cell pellets were then processed for e.m. Electron micrographs were taken at random from cell sections on grids. The intercisternal distances within Golgi stacks on these micrographs were then measured.

Fixation procedure	Intercisternal width
Permanganate	12.3 nm \pm 6.3 (s.d.)
3% Glutaraldehyde 0.5% paraformaldehyde	21.8 nm \pm 3.7
3% Paraformaldehyde 2% Glutaraldehyde	10.0 nm \pm 3.6
1% Glutaraldehyde	14.4 nm \pm 2.7

contrasted but collapsed cisternae had relatively smaller intercisternal distances. It was apparent that the Golgi stacks in all cases contained a variable number of cisternae. Within a single cell transverse sections of stacks revealed between 2 and 9 cisternae. The reason for this variability is not clear.

Polarity of the Golgi apparatus

A noted feature of the Golgi stack in mammalian cells is its polarity. Vesicles carrying proteins destined for secretion, lysosomes or for the Golgi itself, enter the stack on one side, called the cis-face. Proteins then pass through the Golgi in a unidirectional manner, employing vesicles to travel between the biochemically distinct compartments, to the trans face where they are sorted and sent to appropriate cell destinations (Palade, 1975; Rothman et al. 1984; Griffiths and Simons, 1986). It was therefore of interest whether this facet of the Golgi apparatus was conserved.

Polarity in morphology

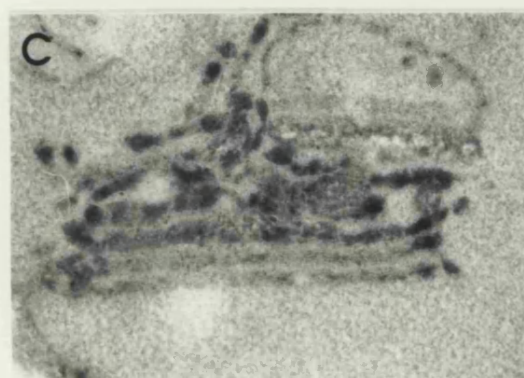
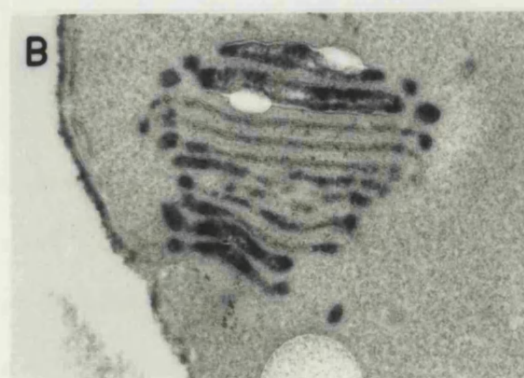
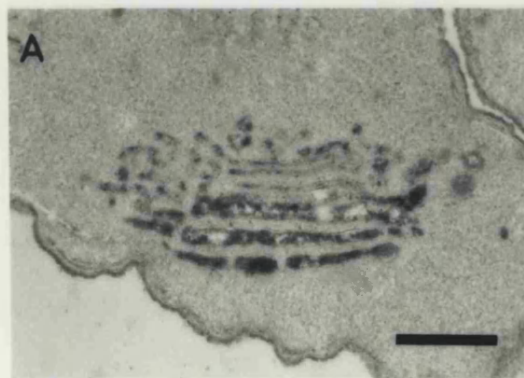
Visually, the trans side of the mammalian Golgi apparatus is more reticular in nature and is most often called the trans Golgi network (TGN). In permanganate fixed cells of fission yeast the morphology of the two sides of a stack do not seem to differ with neither face being reticular in appearance. In the 3% glutaraldehyde, 0.5% paraformaldehyde fixed cells some differences were observed with one face, on occasion being reticular or more distended (Fig. 3.11). However, since there was no method of testing the face of entry of material from the ER it was not clear whether these differences were consistently on one side of the stack.

Polarity in histochemical and chemical staining

Another way of distinguishing the faces of the Golgi in mammalian cells is the use of histochemical stains. These have been used with varying

Figure 3.11. Morphology of the Golgi apparatus.

Cells fixed with 3% glutaraldehyde and 0.5% PFA showed the best preservation of structure. In some cases the Golgi apparatus in these cells showed apparent differences in morphology across the stack i.e morphologically polarized. (A) shows unequal distribution of osmium in the stack with heavier staining on one side. (B) shows staining on both sides of the stack but not in all cisternae. Bar = 0.2 μm .



success to label the Golgi in mammalian cells. For example, thiamine pyrophosphatase can be used to label the trans side of a Golgi stack (Novikoff and Goldfisher, 1961). Use of these methods in *S.pombe* has not been widespread and there is no published data. I have looked for the localization of acid phosphatase in cells with *p*-nitrophenylphosphate as a substrate. The results were not clear and the appearance of the membranes did not change in the presence of sodium fluoride which abrogates the histochemical staining reaction. It may be that the level of acid phosphatase in cells normally is very low and this stain not sensitive enough with the conditions that I used.

Osmium is used as a stain on fixed cells and impregnates the Golgi apparatus. Mammalian cells show a selective localization of osmium reduction at the cis side of the stack (Friend and Murray, 1965). Osmium labelling after *S.pombe* cell fixation was shown in figures 3.10 C,D and 3.11. In some cases one side appeared to be labelled more predominantly than the other which could indicate some level of polarity (Fig. 3.11A,C). However, it was also common to see both sides with some labelling (Fig. 3.11B).

Polarity of a specific marker of the Golgi apparatus

To address the question of polarity and intra-Golgi organization I turned to immuno-electron microscopy using antibodies to the Golgi marker enzyme, GalT. The pattern these gave by immunofluorescence has already been shown (Fig. 3.6A).

The pattern of labelling by the GTF antibodies by electron microscopy showed that there was clear recognition of the Golgi apparatus (Fig. 3.12). Some staining of the cell surface was also apparent. Quantitation of the labelling to assess the level of specificity clearly showed preferential labelling of the Golgi apparatus (Fig. 3.13A). The gold on the cell surface was above

Figure 3.12. Immuno-electron microscopy using the GTF antiserum.

Cells were fixed and processed. The antiserum was applied to sections of cells on grids. Secondary antibodies were conjugated to 10 nm gold particles. (A) Golgi labelling in wild type cells using the GTF2 antiserum. Labelling was performed in the presence of 0.25 M methylgalactose and 0.25 M methylmannose to abrogate any binding to carbohydrate epitopes in cells. Note the lack of staining on the mitochondria and cytoplasm. (B) Higher magnification micrograph of a single Golgi stack with labelling using GTF2. Note that there is staining in some but not all cisternae. (C) Labelling using the GTF2 antiserum on the *gma-12* strain which is deleted for GalT. Labelling was still found but the distribution of gold was altered with most gold particles being found in the dilated rims of the cisternae. Bar = 0.5 μm (A); 0.2 μm (B); 0.15 μm (C).

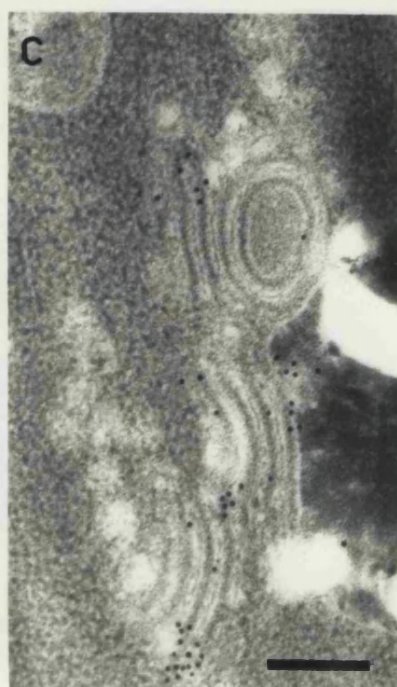
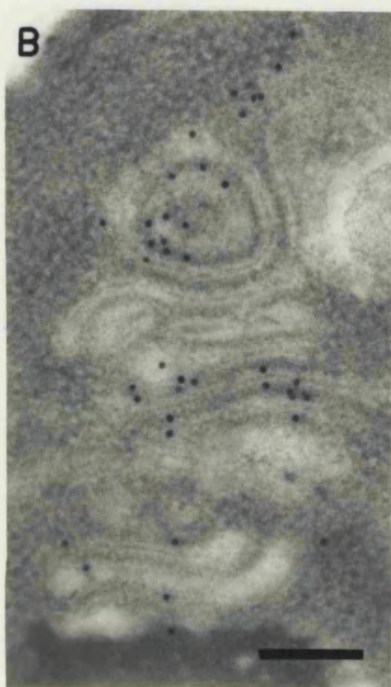
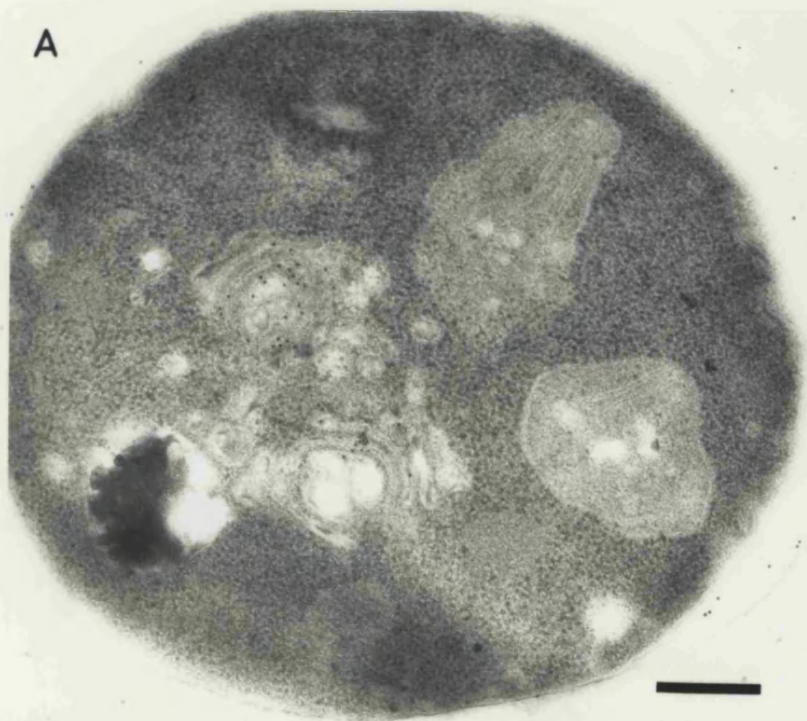
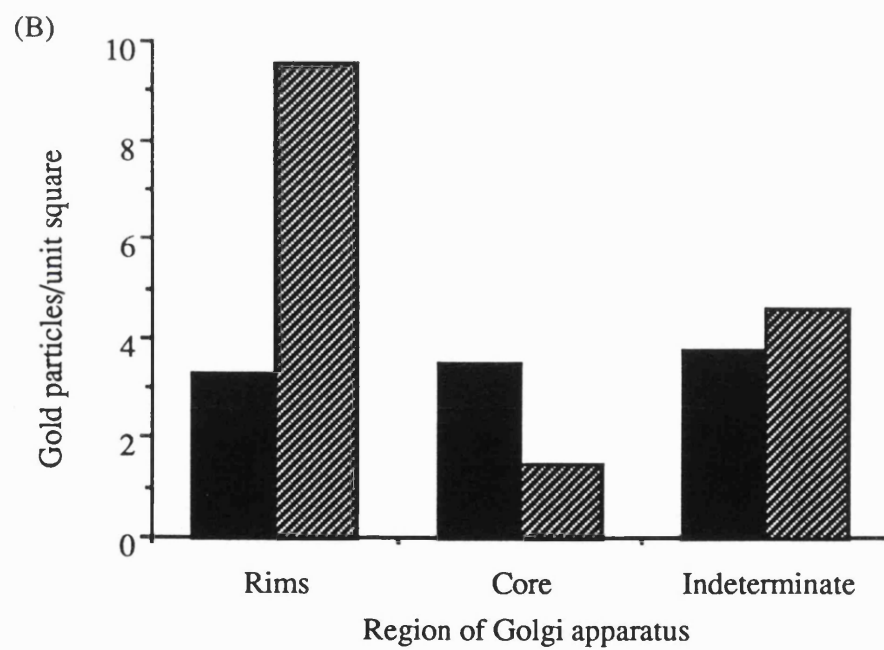
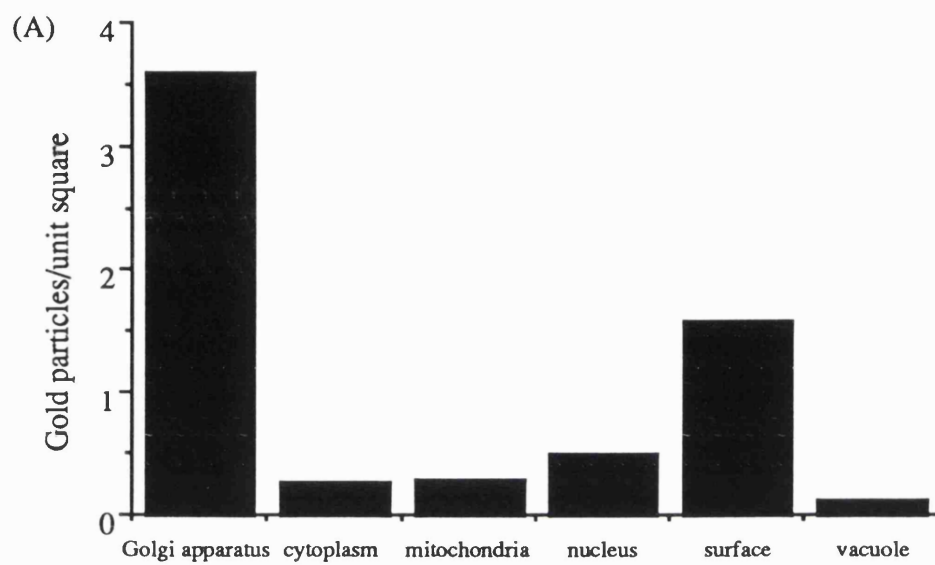


Figure 3.13. The distribution of gold particles in immunolabelled cells.

A 10 mm grid was laid over electron micrographs of immunolabelled cells and the area occupied by different organelles was assessed and the number of gold particles in each square was counted. (A) The distribution of gold over whole cells. Comparison of the level of gold particles lying over regions of the cells containing Golgi apparatus and areas of cytoplasm or other organelles. (B) Comparison of the distribution of gold in the Golgi stacks of wild type cells (■) and in the *gma-12* strain deleted for the GalT (▨).



the background levels of other organelles but this could partly be attributed to the presence in the immuneserum of some anti-carbohydrate antibodies. The preimmune serum gave some labelling of the cell surface but not of the Golgi apparatus. It was clear that the labelling was not simply in a single cisterna and in fact was found on both sides of a stack though not necessarily in every cisterna. (Fig. 3.12B). Labelling was unaffected by up to 0.5 M methylmannose and 0.5 M methylgalactose suggesting that carbohydrate antibodies were not interfering with the labelling pattern within the Golgi stack.

This result however, was not such clear cut evidence against polarity as it initially seemed. The labelling was also performed in a strain of *S.pombe* deleted for the GalT (*gma-12*) and labelling was still found specifically in the Golgi stacks (Fig. 3.12C). A point of interest was that the distribution of staining was changed. In the deletion strain of cells most of the labelling appeared to be at the dilated rims of Golgi cisternae whereas in wild type cells the labelling was both in the central cisternal region and in the dilated rims (Fig. 3.13B).

Recent work (T. Chappell *pers. comm.*) has shown that there is a second galactosyl transferase which was found by low stringency hybridization using a probe from the α -1,2-galactosyltransferase. These enzymes share substantial homology particularly in the catalytic region. The protein made to raise the antiserum was β -galactosidase fused to this luminal enzyme domain. It therefore seems that there is at least one cross reactive species which is blurring the issue of polarity when assessed by immuno-electron microscopy. The availability of the data from the mutant GalT deletion strain did however show that differential distribution of markers in the stack could be observed indicating some level of compartmentalization within the organelle.

3.3.2. Factors affecting the morphology of Golgi stacks in wild type cells

Effect of temperature on Golgi apparatus

Temperature is known to affect the secretory pathway in mammalian cells and certain temperatures cause a block in the flow of secretory traffic at specific points. For example, lowering the temperature to 20°C greatly slows the exit of material from the TGN and proteins amass there (Griffiths and Simons, 1986). Lowering the temperature further to 15°C causes an earlier block with secretory proteins accumulating in an expanded CGN compartment (Lippincott-Schwartz, et al., 1990; Saraste and Kuismanen, 1984).

The effect of a range of temperatures on the Golgi apparatus was assessed. Cells from an overnight culture were inoculated into fresh medium and incubated at various temperatures overnight. Cultures were then fixed using permanganate and processed for electron microscopy. Looking at random fields of cells revealed no obvious accumulation of ER or other compartments. Quantitation of the numbers of cisternae is shown in figure 3.14. No clear differences between any of the temperatures in the numbers of cisternae in stacks were found and the Golgi apparatus remained stacked in all instances.

Effect of medium on Golgi apparatus

Another factor that I thought might affect the Golgi stack in wild type cells was the medium in which the cells grow. *S.pombe* cells are normally grown in either a complex, rich medium of yeast extract (YES) or a defined minimal medium (DMM). The rate of cell growth in rich medium is faster with a generation time of 3 hours at 25°C compared to 4 hours when in DMM. Another slight difference between the cells is that the cell wall is thicker when cells are grown in rich medium and more difficult to

Figure 3.14. The effect of temperature on the size of Golgi stacks

Cells were incubated overnight at a range of temperatures from 4°C to 36°C. They were then fixed using potassium permanganate and processed for e.m. Sections of cells were selected randomly ($n > 100$) and every cisternae in a cell section scored according to the number of other cisternae with which it was associated.

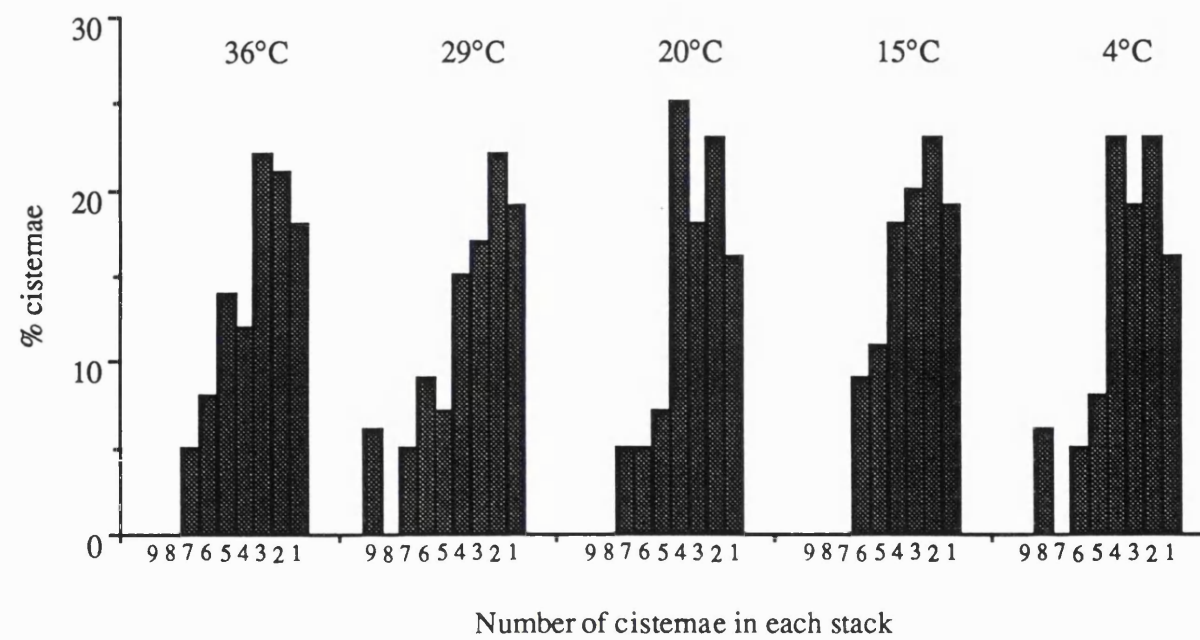
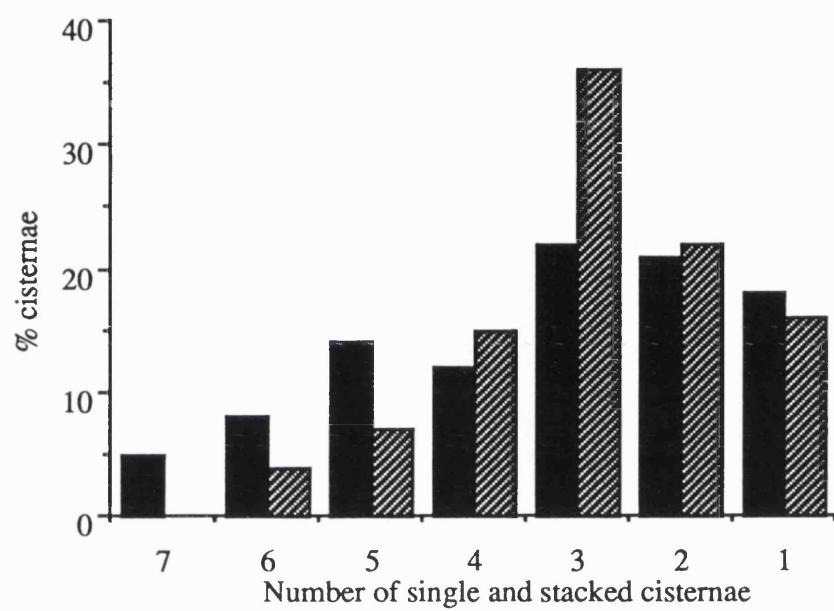


Figure 3.15. The effect of growth medium on Golgi stacks

Cells were grown to log phase in either rich medium (YES, ■) or minimal medium (DMM, ▨). They were then permanganate fixed and processed for e.m. Sections of cells were selected randomly ($n > 100$) and every cisternae in a cell section scored according to the number of other cisternae with which it was associated.



digest with novozym and zymolyase. Since the carbohydrates in these cells were more extensive and possibly more complex I decided to investigate whether this had any bearing on the morphology of the Golgi apparatus itself.

Cells were inoculated from an overnight culture into either rich or defined medium and grown for at least 4 generation times. Cells were then fixed in permanganate and processed for e.m. The cisternae in each preparation were counted. Figure 3.15 shows that there was no dramatic effect due to the medium of incubation. There does appear to be a shift towards smaller stacks when in minimal medium, with 3 cisternae per stack being predominant. Cells grown in rich medium have 41% of their cisternae in stacks comprised of more than 3 cisternae compared with only 26% when cells were grown in a defined medium. There is not an increase in the number of single cisternae or of two associated cisternae in these cells. At the time, the magnitude of this effect was not considered great enough to warrant further investigation.

3.4. Discussion

The Golgi apparatus in *S.pombe* is clearly an organelle comprised of stacked, flattened cisternae and so resembles that of mammalian cells. Other characteristics are not shared. For example, the mammalian cell has a single, juxtanuclear Golgi apparatus whilst in *S.pombe* many stacks could be seen and these were dispersed throughout the cell. The mammalian Golgi apparatus is polarized both in its morphology and in the distribution of resident enzyme markers whilst in *S.pombe* there was little or no polarity observed though there did seem to be some differential compartmentalization of enzyme markers. The tools described in this chapter allowed me to undertake wider investigations and to study the behaviour of the Golgi apparatus under conditions that were known to affect this organelle in mammalian cells.

Chapter 4

**Stacking of Golgi
cisternae requires
intact microtubules**

4.1. Introduction

It was recognized over ten years ago that the breakdown of microtubules in mammalian cells was accompanied by the disassembly of the Golgi apparatus (reviewed in Warren, 1993). On treatment of cells with the anti-microtubule agent nocodazole, rather than remaining a single juxta-nuclear organelle the Golgi apparatus was observed by immunofluorescence, as a disperse but punctate stain throughout the cell cytoplasm (Burke, et al., 1982). Electron microscopy of these cells revealed that the Golgi firstly broke down into many (>250) small stacks which were no longer confined to the nuclear region, this was then followed by vesiculation of these small stacks into vesicles and clusters of vesicles (Lucocq, et al., 1989). Nocodazole acts by preventing the formation of the mitotic spindle, so causing the cells to become arrested in mitosis (Zieve, et al., 1980). The use of a nocodazole block has been widely used to study the form of the Golgi apparatus at mitosis. The drug can be washed out to allow cells to proceed through mitosis then into interphase. Reassembly of the Golgi apparatus from the vesicles was observed at the onset of telophase (Lucocq, et al., 1989).

Since the blocking of cells early in mitosis had such a dramatic effect on the morphology of the Golgi apparatus in mammalian cells it was of interest to know whether these changes were mimicked by the Golgi apparatus in *S.pombe*.

4.2. Results

4.2.1. The effect of nocodazole on *S.pombe* cells

Experiments reported by Walker, (1982) indicated that the effect of nocodazole on *S.pombe* growth was minimal. This work documented only the effect of nocodazole on cell number and its effects on the actual microtubules were not addressed. The work showed that fission yeast cells were able to continue increasing cell number in the presence of the drug, thus indicating that mitotic spindles could still be formed and daughter nuclei separated.

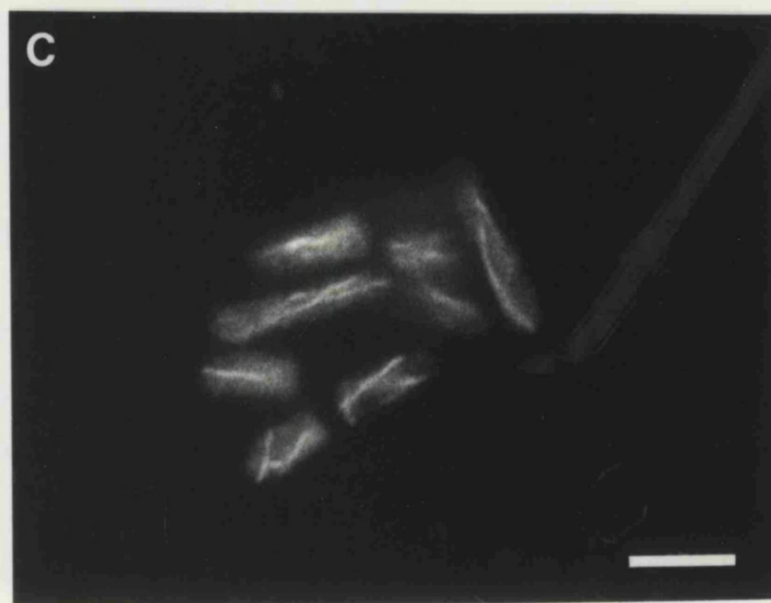
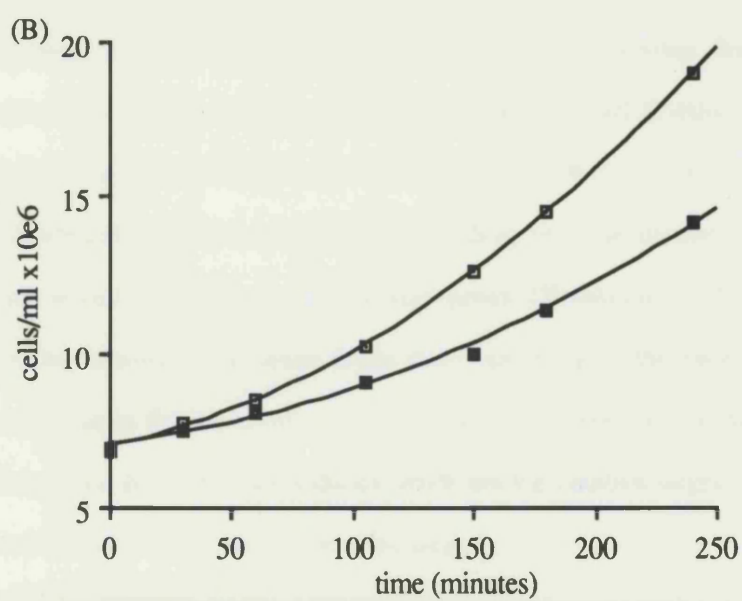
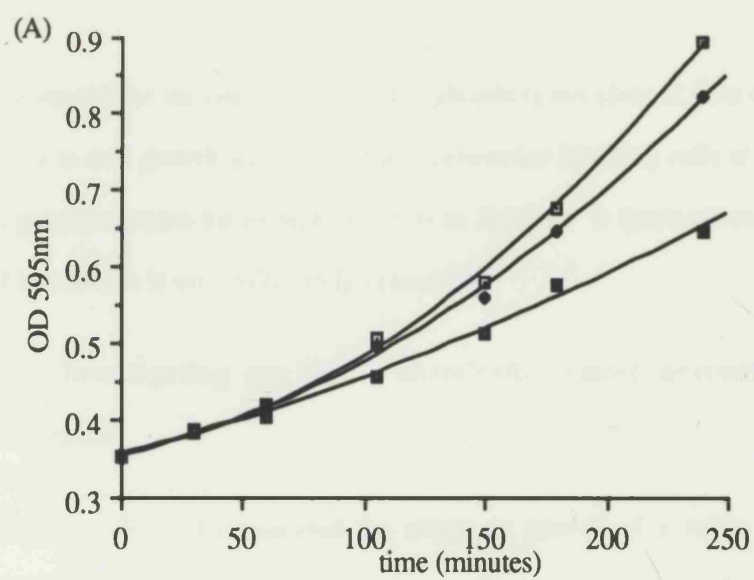
I decided to try and repeat growth experiments on the effect of nocodazole and also to couple these with immunofluorescence data using antibodies against tubulin (TAT1).

The effect of nocodazole on growth was assessed by cell counting with a haemocytometer and by following turbidity changes. This would account for cell number changes (haemocytometry) and changes in cell volume not necessarily accompanied by increasing cell number (turbidity). Cells were grown to log phase and nocodazole added at 0-50 $\mu\text{g/ml}$ (levels of less than 1 $\mu\text{g/ml}$ cause inhibition in mammalian cells). Cells were incubated, and measurements made for a generation time. The results are shown in Figs 4.1A and B. There did appear to be an effect of nocodazole on the growth of cells but there was clearly not a strong mitotic block, nor were the cells altered phenotypically from untreated cells (data not shown).

Immunofluorescence was performed on methanol fixed cells after 30 minutes exposure to 25 $\mu\text{g/ml}$ nocodazole. Intact cytoplasmic microtubules could be seen in most cells. Other cells contained mitotic spindles (Fig. 4.1C).

Figure 4.1. The effect of nocodazole on fission yeast.

Cells were grown to log phase and nocodazole added to the culture. The effect of the drug on cells was monitored. (A) Cell growth was followed by measuring changes in turbidity at OD_{595nm}. Levels of nocodazole assayed were 0 µg/ml (□), 5 µg/ml (♦), and 50 µg/ml (■). (B) Cell number changes were followed using a haemocytometer. This was performed on cells incubated in the absence (□) or presence (■) of 50 µg/ml nocodazole. (C) The effect of nocodazole (50 µg/ml) on microtubules was assessed by fixing cells which had been exposed for 1 hour to the drug and labelling cells with antibodies against tubulin (TAT1). Bar = 9 µm



The reason for the small effect by nocodazole is not clear. It does cause an arrest in cell growth and division in *S.cerevisiae* blocking cells at mitosis. A possible reason for its lack of action in *S.pombe* is that a necessary site of interaction is not sufficiently conserved.

4.2.2 Investigating the use of chemically related alternatives to nocodazole

Walker, (1982) also assessed the effect on growth of a range of anti-microtubular drugs which are chemically related to nocodazole and members of the benzimidazole family of anti-helminthic drugs. He showed that several of these could be used to arrest cell division in cells. Of the drugs that elicited an inhibition of cell division, benomyl and thiabendazole (TBZ) were used to make drug resistant mutants some of which were later shown to lie in tubulin genes. (Yamamoto, 1980). It was therefore assumed that these drugs were operating in the same way as nocodazole in the mammalian cell. No work was produced on the actual effect of the drugs on microtubules which are the putative targets since no suitable antibody was available at the time.

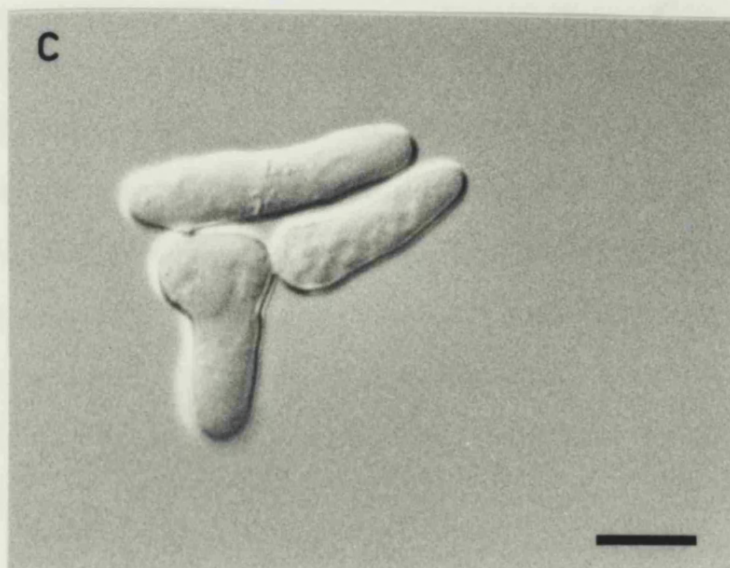
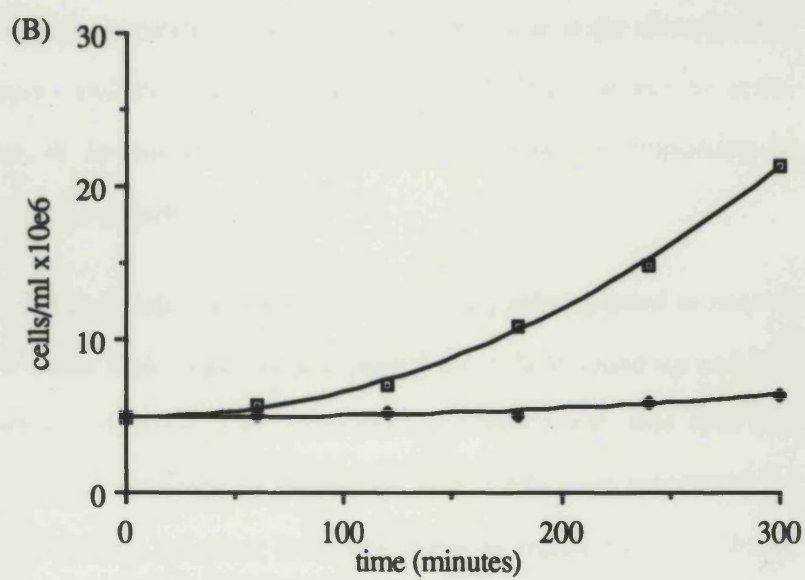
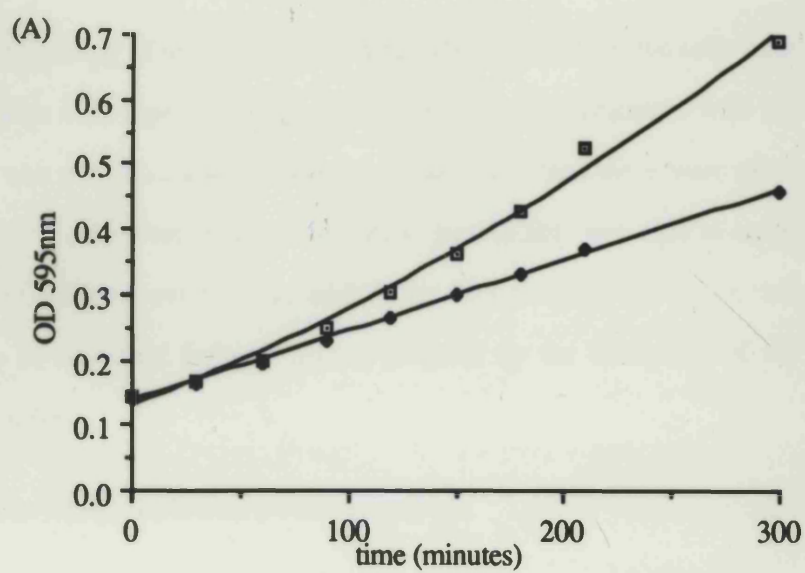
I have characterized the effect of the drug, thiabendazole on fission yeast cells in terms of changes it causes to growth, microtubules and the Golgi apparatus.

4.2.3. The effect of TBZ on growth and division

Cells were grown to log phase and TBZ added at 100 µg/ml. Cells were incubated for several hours and readings made to follow cell number (haemocytometry) and cell volume (turbidity OD_{595 nm}). The cells were still able to grow though the level of growth diminished with time (Fig. 4.2A). Cell division was however almost completely inhibited (Fig. 4.2B).

Figure 4.2. The effect of TBZ on fission yeast

Cells were grown to log phase and TBZ added to the culture. (A) Cell growth was followed by measuring changes in turbidity at OD_{595nm} in the absence (□) or presence (◆) of 100 µg/ml TBZ. (B) Cell number changes were followed using a haemocytometer for cells incubated in the absence (□) or presence (◆) of 100 µg/ml TBZ. (C) Cells treated with TBZ for 3 hours were observed using Nomarski optics. They were morphologically changed being longer and sometimes mis-shapen. Bar = 8 µm



Light microscopy of the cells treated with TBZ revealed that the cells were longer than wild type cells (Fig. 4.2C). After 3 hours treatment with the drug it was not uncommon to see mis-shaped cells and these were often branched. It was clear however that most growth that was able to occur after TBZ addition was from the ends of the cells showing that the normal polarity of secretion was not greatly affected by the disruption of the microtubules.

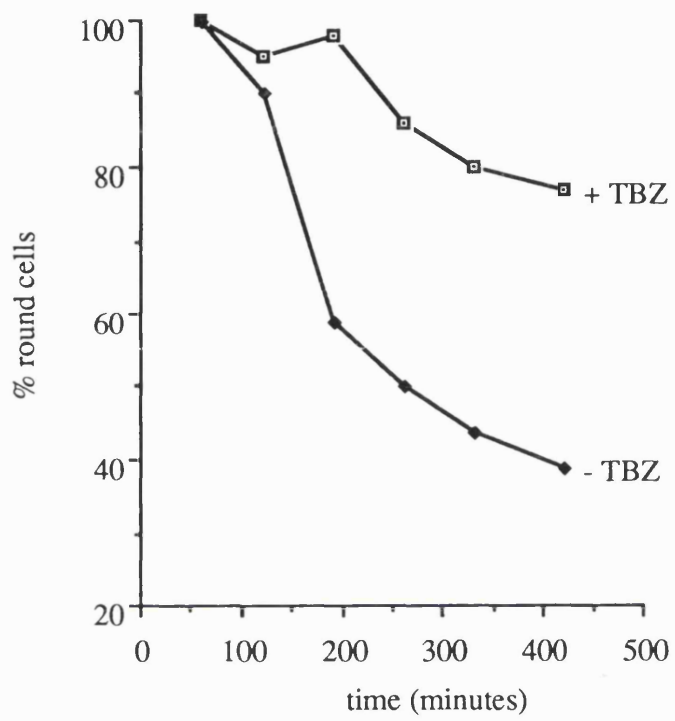
4.2.4. The effect of TBZ on polarized growth

Since cell growth still seemed to mainly occur at the ends of cells this suggested that microtubules did not play a major role in the directionality of transport and that the more important role may be due to actin. However, it is possible that microtubules could be important in establishing the polarity in a cell.

To test this hypothesis log phase cells were firstly spheroplasted to remove their cell walls. This treatment also caused the cells to round up and lose their normal rod shape. The spheroplast population was then split and incubated in the presence or absence of TBZ. Cells were monitored for when they lost the spherical form and began to regain their rod shape. Cells began this reversion process after about 3 hours and the proportion of rounded cells decreased rapidly from this point. Wild type cells in the presence of TBZ did begin to become less rounded. This was however at a much slower rate than with the untreated cells. Furthermore, few if any cells achieved the normal rod shape for cells within the following 12 hours (Fig. 4.3). This result suggested that although cytoplasmic microtubules do not seem to be necessary for directed secretion once the polarity in a cell is already established, they may have an important role when the polarity has been disrupted.

Figure 4.3. The effect of TBZ on reverting spheroplasts.

Log phase cells were treated to remove their cell walls so that the normal cylindrical shape was lost and cells became spherical. The cells were then suspended in growth medium including 1.2 M sorbitol (for osmotic support) in the absence (◆) or presence (▣) of 100 µg/ml TBZ. Cells were then monitored for loss of this spherical shape.



4.2.4 The effect of TBZ on microtubules

Log phase cells were treated for up to 4 hours with TBZ at varying levels. At levels of TBZ $\geq 50 \mu\text{g/ml}$ the cytoplasmic microtubules that stretch from one end of the cell to the other (Fig. 4.4A) disappeared completely leaving only one or two dots that most likely represented the spindle pole bodies (Fig. 4.4B). The effect of TBZ on microtubules was assessed from 0-100 $\mu\text{g/ml}$. At levels of $\geq 500 \mu\text{g/ml}$ the cells were unable to grow at all and died. At 10 $\mu\text{g/ml}$ there was a partial effect but with a significant number of cells still containing cytoplasmic microtubules. Figure 4.5A shows the effect of the different levels of TBZ on microtubules in cells as assessed by fluorescence microscopy.

A time course for the disruption was undertaken with 100 $\mu\text{g/ml}$ TBZ being applied to log phase cells. Disassembly of microtubules in the presence of TBZ occurred with a half-time of less than 10 minutes. Furthermore, the TBZ could be washed out and after 4 hours of treatment and the effect shown to be completely reversible (Fig. 4.5B). Reassembly was equally rapid with cytoplasmic microtubules reforming within 10 minutes.

4.2.5. Effect of TBZ on the Golgi apparatus - morphological changes

Since TBZ seemed to mimic nocodazole in terms of its effect on the microtubules it was of interest to see whether it would cause any disruption to the Golgi apparatus in fission yeast.

Immunofluorescence microscopy.

Log phase cells were treated for 4 hours with TBZ at 100 $\mu\text{g/ml}$. TBZ caused an increase in the cytoplasmic fluorescence and in the number of

Figure 4.4. The effect of TBZ on microtubules by immunofluorescence

Log phase cells were incubated for 4 hours at 32°C in the absence (A) or presence (B) of 100 µg/ml TBZ then fixed and labelled with antibodies to microtubules followed by secondary antibodies coupled to rhodamine.

Bar = 10 µm.

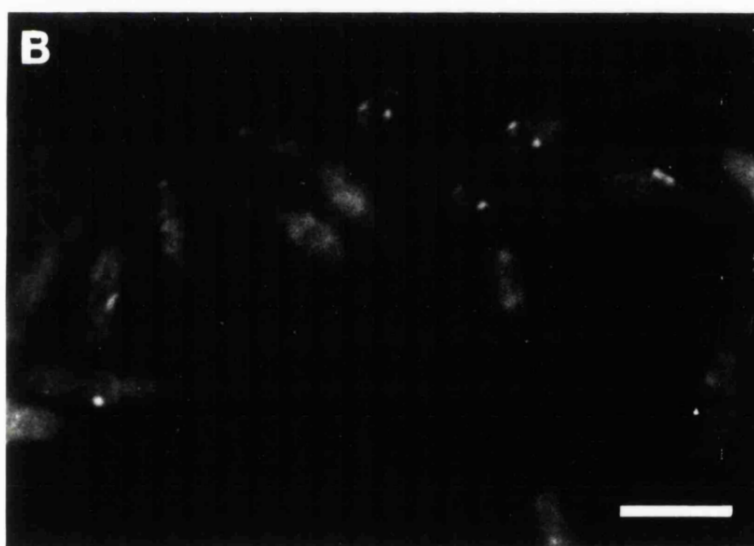
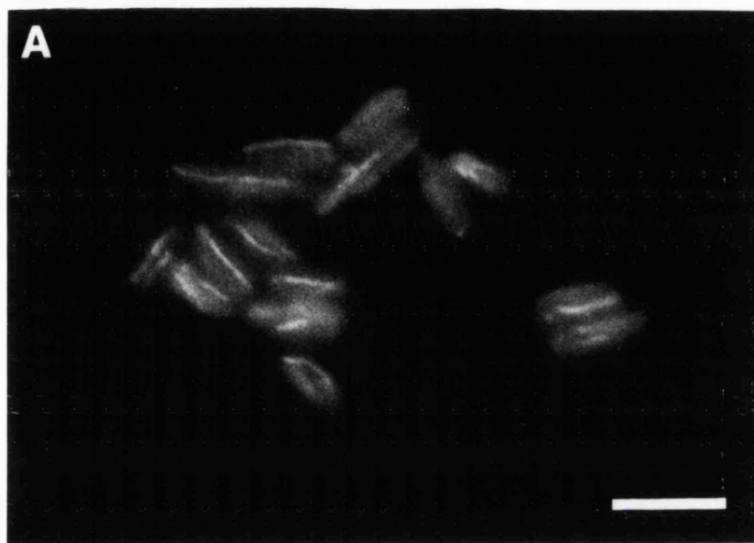
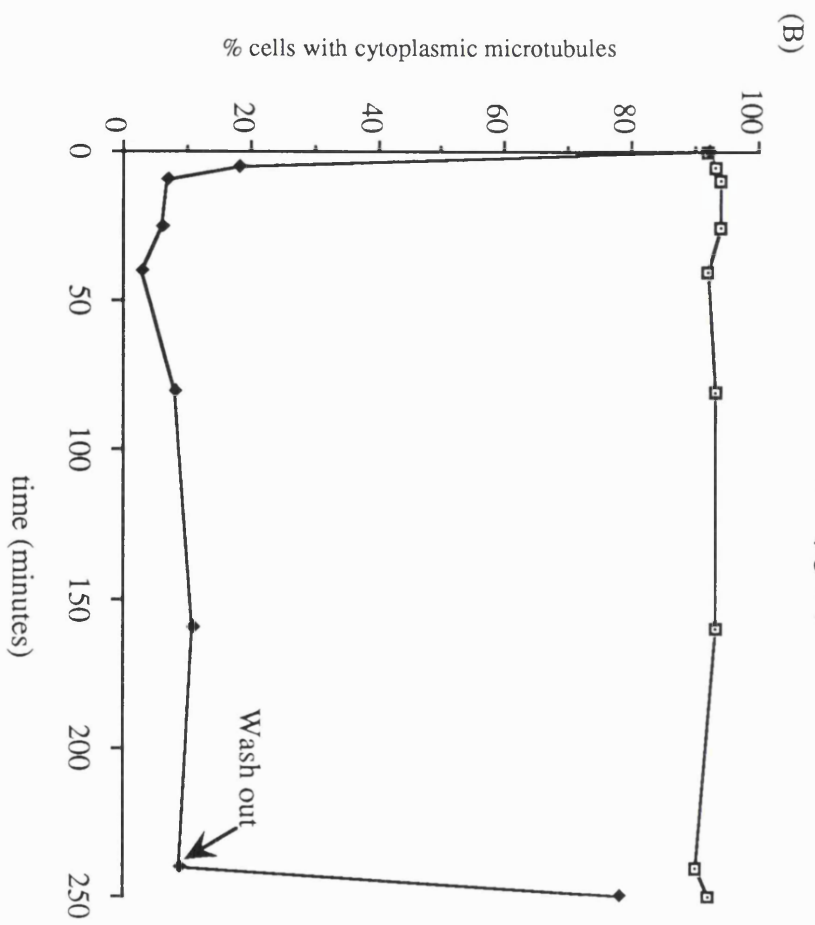
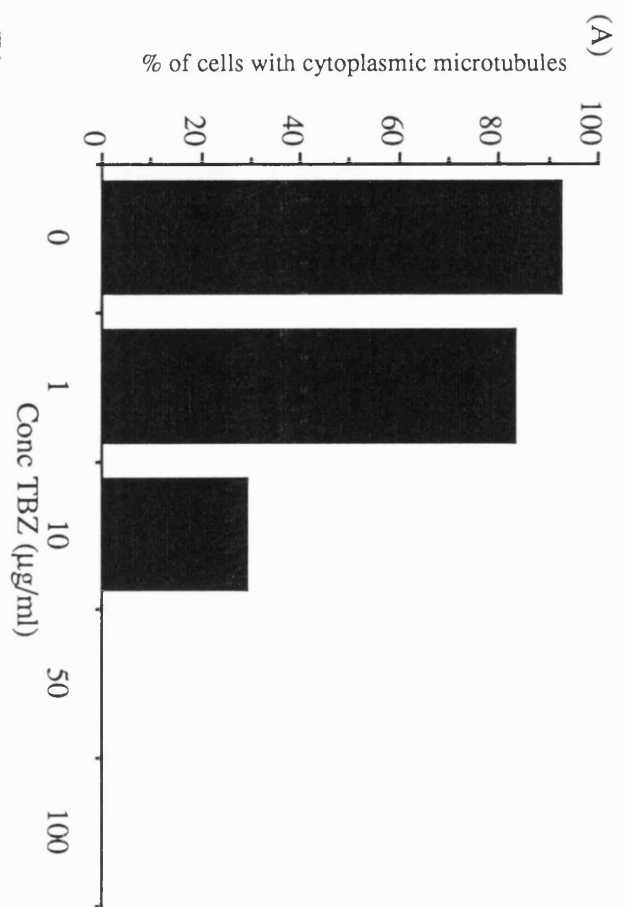


Figure 4.5. Microtubule disassembly in fission yeast.

(A) Log phase cells were treated with 0, 1, 10, 50, or 100 $\mu\text{g/ml}$ TBZ for 3 hours. They were then fixed in methanol and processed for immunofluorescence. Cells were labelled overnight with antibodies to microtubules and for 4 hours with secondary antibodies conjugated to rhodamine. Cells were mounted and the percentage of cells with cytoplasmic microtubules was counted. 200 cells were scored.

(B) Log phase cells were incubated in the absence (\square) or presence (\blacklozenge) of 100 $\mu\text{g/ml}$ TBZ. Samples were taken over a 4 hour time course and these cells fixed and processed for immunofluorescence with labelling for microtubules. After 4 hours the cells incubated with TBZ were harvested, washed and resuspended in fresh medium. 10 minutes after TBZ removal a sample of cells was processed for immunofluorescence and labelled with the anti-tubulin antibodies. Cells were mounted and the percentage of cells containing cytoplasmic microtubules counted.



Golgi stacks (Fig. 4.6). The staining pattern however remained punctate and no general dispersion of stain was seen. Since the number of Golgi stacks in a cell increases as cells grow (see Fig. 3.7) the increase in stack number observed in this case may be explained by the average increase in the length of the cells in a TBZ treated population.

Electron microscopy

TBZ had a dramatic effect on the Golgi apparatus when examined by electron microscopy. At low power most sections through untreated cells showed one or more transverse sections through Golgi stacks (Fig. 4.7A). After treatment with TBZ for 4 hours, few if any stacks remained (Fig. 4.7B). Figures 4.7C-F show high power images of the Golgi at increasing times after treatment. The clear impression is that the Golgi unstacks yielding individual cisternae which do not appear to break down further.

This result was not the consequence of using permanganate to fix the cells. Permanganate was used because it gives a high level of membrane contrast however it does so by removing large parts of the cytoplasm. TBZ could simply have made the Golgi more sensitive to disruption by permanganate. Samples were therefore fixed conventionally, using glutaraldehyde and formaldehyde. The contrast was lower but, as can be seen in figure 4.8, the effect of TBZ was still the same.

Other organelles were also examined for an effect of TBZ. The mitochondria, vacuoles and nuclear envelope were all unaffected. The peripheral ER was mostly unaffected though the lumen was sometimes slightly dilated.

Figure 4.6. The effect of TBZ on the Golgi apparatus by immunofluorescence

Log phase cells were incubated for 4 hours at 32°C in the absence (A) or presence (B) of 100 µg/ml TBZ then fixed and labelled with antibodies to the GalT fusion protein followed by secondary antibodies coupled to rhodamine. Bar = 10 µm.

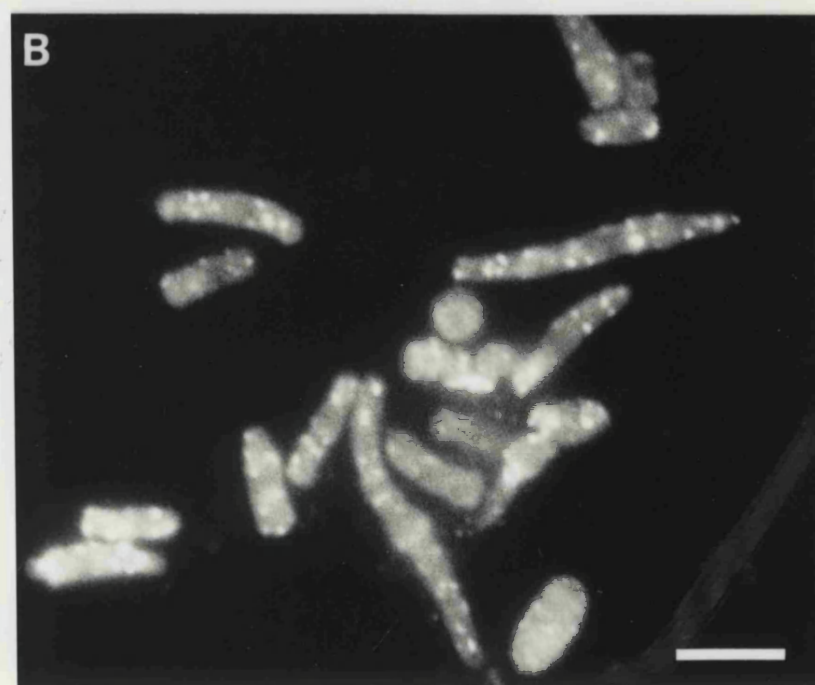
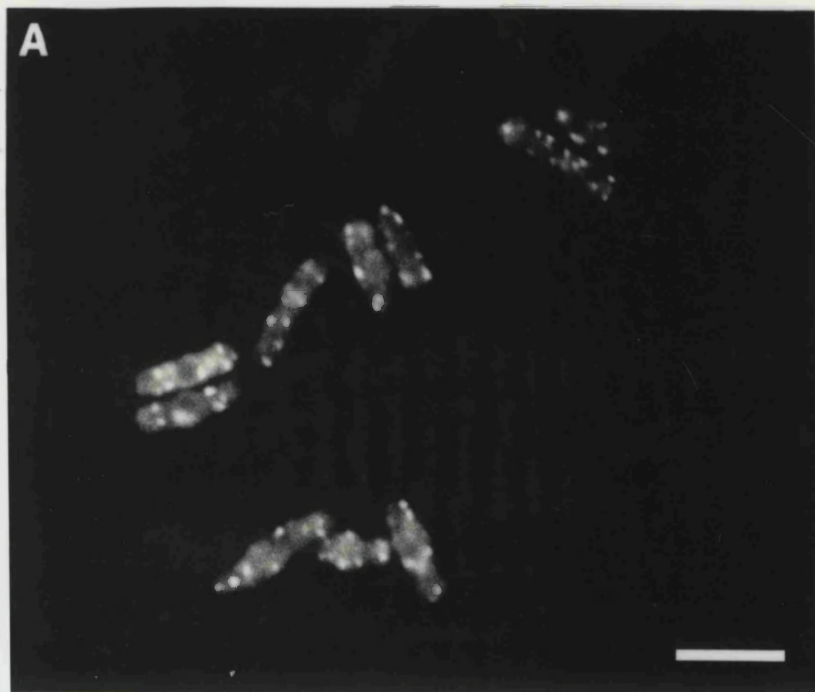


Figure 4.7. Effect of TBZ on the Golgi apparatus in permanganate fixed cells

Log phase cells were incubated at 32°C for 4 hours in the absence (A) or presence (B-F) of 100 µg/ml TBZ then fixed in potassium permanganate and prepared for electron microscopy. (A, B) Low magnification images of whole cells. Note the absence of Golgi stacks (G) in the presence of TBZ. (C-F) High magnification images of the Golgi region at increasing times after TBZ treatment (C = 0 mins.; D = 60 mins.; E= 120 mins.; F = 240 mins.). Bars (A,B) =1 µm, (C-F) = 0.25 µm. Arrowheads indicate possible single cisternae generated in the break down of the Golgi stacks.

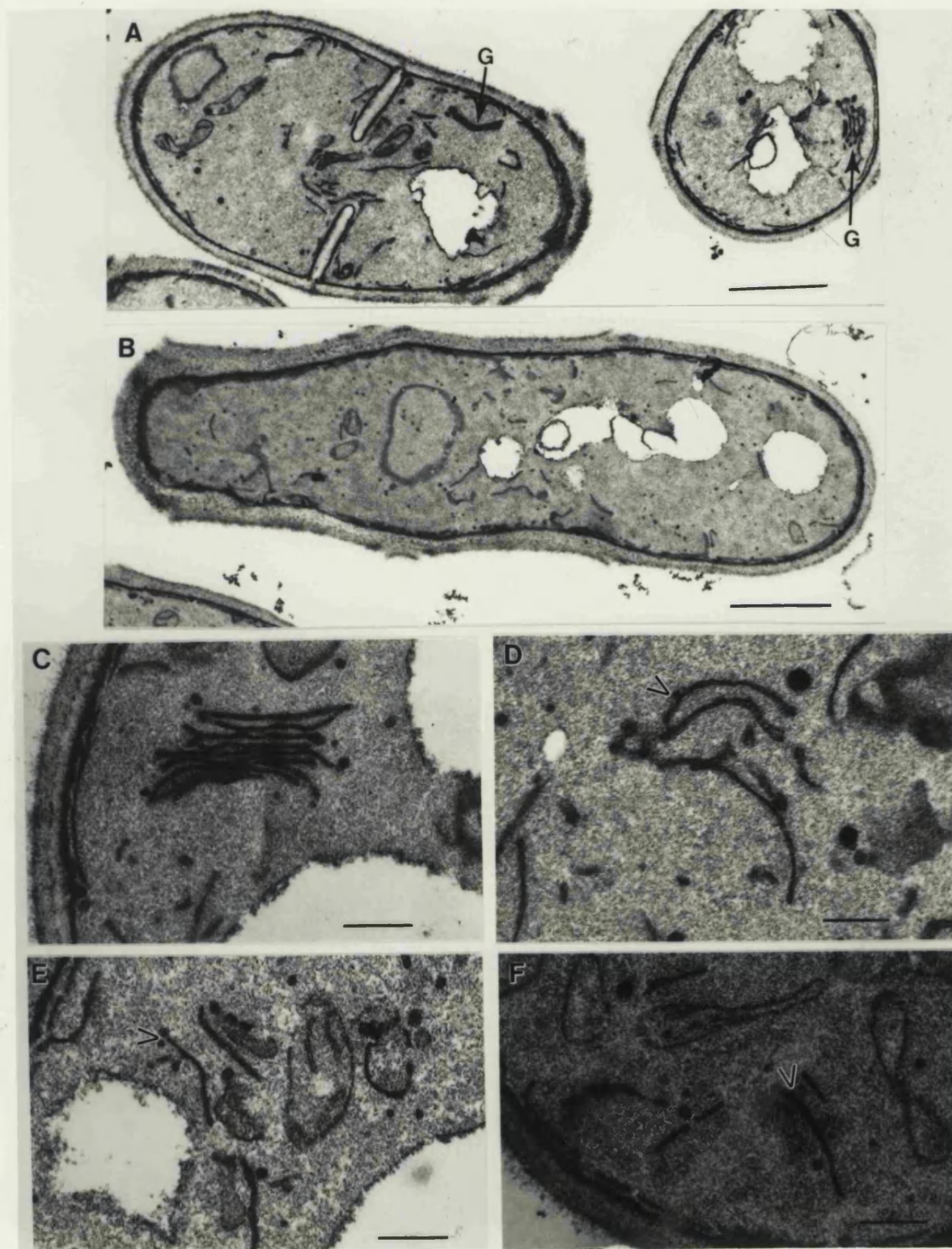
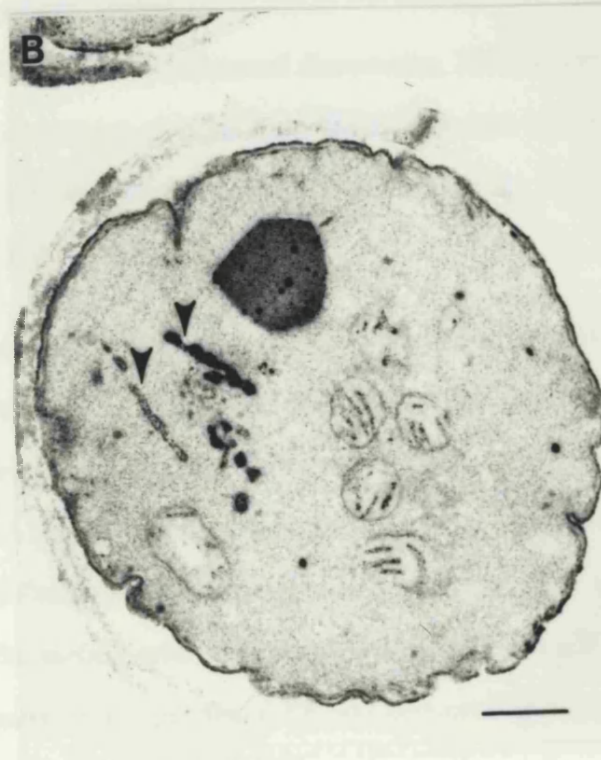
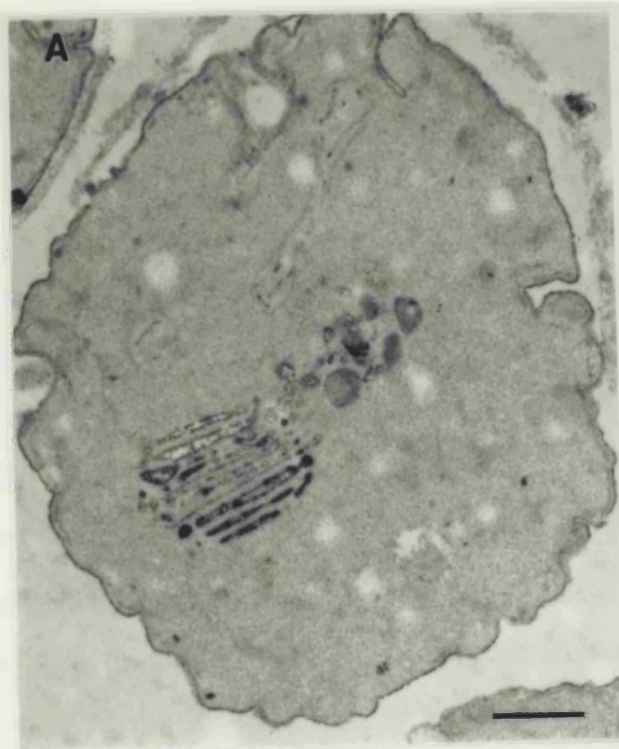


Figure 4.8. Effect of TBZ on the Golgi apparatus in glutaraldehyde / paraformaldehyde fixed cells

Log phase cells were incubated at 32°C in the absence (A) or presence (B) of 100 µg/ml TBZ for 4 hours then fixed in glutaraldehyde and paraformaldehyde and prepared for electron microscopy. Note the Golgi stacks in A and the presence of only single cisternae after TBZ treatment in B (marked with arrowheads). Bar = 0.4 µm.



4.2.6. Effect of TBZ on the Golgi apparatus - quantitation

Unstacking

The effect of TBZ on cisternal stacking was quantitated in two ways. Cells were selected randomly and every cisterna in these cells was counted and scored according to the size of stack in which it was found. Single cisternae were also scored. As shown in figure 4.9, TBZ had a dramatic effect on the number of cisternae in the stack, particularly on those stacks with three or more cisternae. In the absence of TBZ nearly 80% of identifiable cisternae were present in stacks, this dropped to about 30% after 4 hours of treatment with 100 $\mu\text{g/ml}$ TBZ. There was a corresponding rise in single cisternae from about 20% to 70%. The intermediate levels of TBZ gave partial breakdown of the Golgi stack. The changes described occurred without any significant change in the absolute number of cisternae per cell section (from 4.6 to 4.0 cisternae/cell section) arguing strongly that TBZ causes cisternal dissociation. Furthermore, the average length of all cisternae changed from 62 mm ± 9 before treatment to 58 mm ± 7 afterwards arguing that single cisternae were the final products and further breakdown did not occur.

Identification of single cisternae relied largely on morphological criteria and they could often be confused with internal ER (that fraction of the ER which does not underlie the plasma membrane and does not surround the nucleus). A second method which relied on measurements of the surface density of Golgi and ER membranes was therefore used to confirm the results. The surface area of randomly chosen Golgi stacks, internal ER, nuclear envelope and peripheral ER was measured by point counting and expressed as a percentage of the area of the cell cytoplasm, calculated in the same way. Single Golgi cisternae were included in the measurements of internal ER. As shown in figure 4.10 there was a 12% increase in the

Figure 4. 9. The effect of TBZ on the number of cisternae in the stack

Log phase cells were incubated at 32°C for 4 hours in the absence or presence of up to 100 µg/ml TBZ then fixed in potassium permanganate and prepared for electron microscopy. Random cell sections (n=150) were scored for the number of cisternae in each Golgi stack at the indicated levels of TBZ.

1

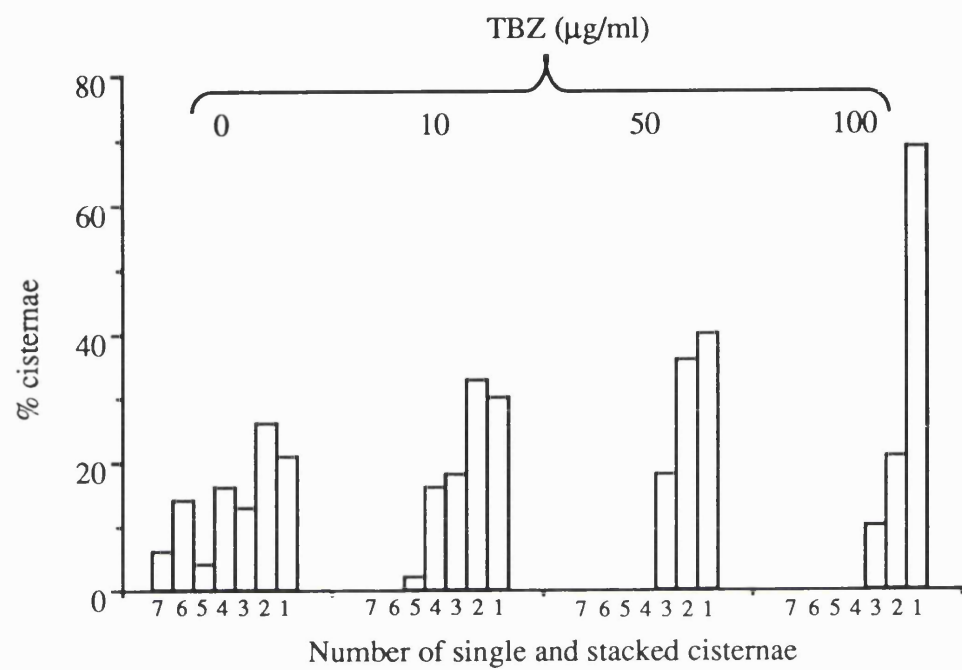
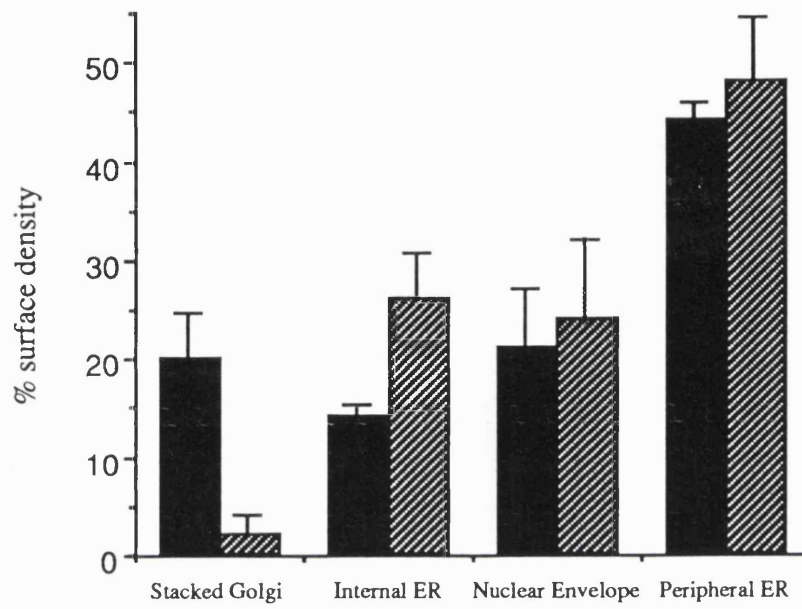


Figure 4.10. Effect of TBZ on the surface density of Golgi stacks and ER

Log phase cells were incubated at 32°C for 4 hours in the presence (▨) or absence (■) of 100 µg/ml TBZ then fixed in potassium permanganate and prepared for electron microscopy. The surface density of peripheral ER, nuclear envelope, internal ER and Golgi stacks were calculated. Note that the increase in surface density of internal ER was similar to the fall in Golgi stacks whereas there was little change in the surface density of both peripheral ER and the nuclear envelope.



surface density of internal ER, similar to the 18% fall in stacked Golgi membrane. The increase in internal ER was most likely due to an increase in single Golgi cisternae because the surface density of ER did not change. Both the nuclear envelope and the peripheral ER were little affected by treatment with TBZ (Fig. 4.10).

Kinetics of disassembly and reassembly

A time course monitored by e.m was carried out on log phase cells to which 100 µg/ml TBZ had been added.

Cisternal unstacking took slightly longer than the disassembly of microtubules with a half-time of 20-25 minutes (Fig. 4.11A). The effect was completely reversible after 4 hours of treatment. When TBZ was washed out and cells resuspended in fresh medium the stacks reformed with a half time of between 30 and 60 minutes. (Fig. 4.11B).

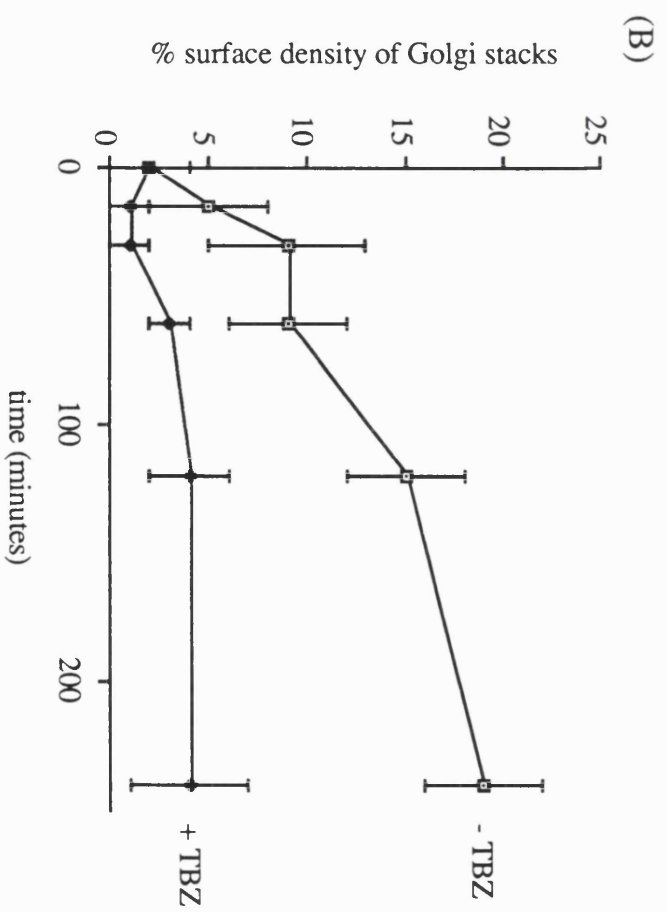
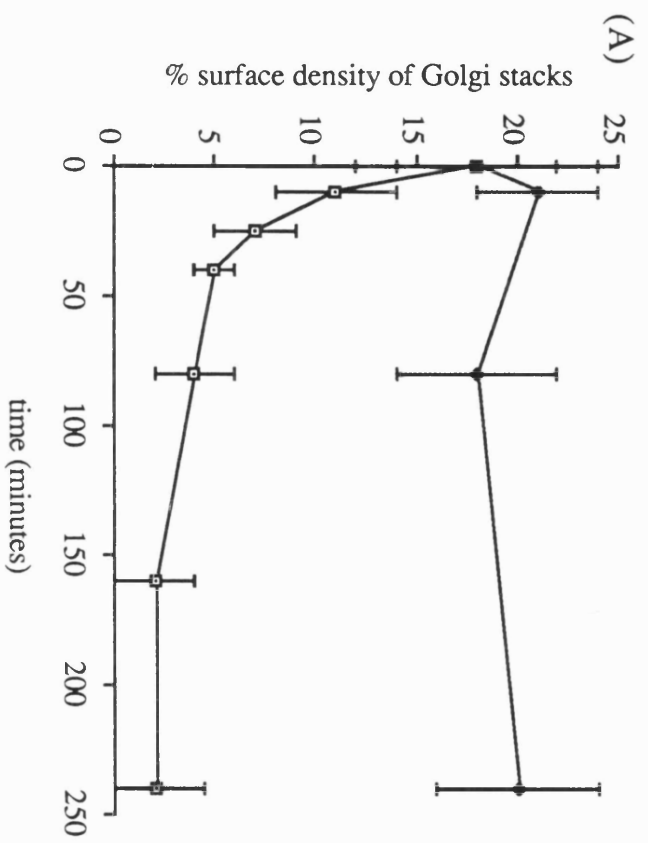
4.2.7. Tubulin mutants

At this stage in the study it seemed appropriate to investigate the nature of the observed effect on the Golgi apparatus. The effect was different from that seen with nocodazole on mammalian cells since the stacks appeared to come apart with TBZ rather than fragment and form smaller stacks. It was not possible to test the effect of TBZ on mammalian cells since at saturated stock concentration of 30 mg/ml when added to culture cells at 100 µg/ml the DMSO in the control sample alone caused cell death.

Tubulin mutants are available in *S.pombe* and some of these were used to address this problem.

Figure 4.11. Effect of TBZ on the surface density of Golgi stacks

(A) Log phase cells were incubated at 32°C for increasing times in the absence (◆) or presence (▣) of 100 µg/ml TBZ then fixed in potassium permanganate and prepared for electron microscopy. At each time point the percentage of the surface area of the cell occupied by Golgi stacks (% surface density) was calculated. (B) After incubation for 4 hours in the presence of TBZ half of the cells were maintained in the presence of TBZ (◆) whilst the other half of the cells were washed free (▣). The incubation was continued for a further 4 hours.



nda3 - conditional β - tubulin mutant

The *nda3* mutant (Umesono, et al., 1983) has a cold-sensitive mutation which blocks cells in mitosis at the non-permissive temperature. Some mutant alleles of this gene also confer resistance to microtubule-disrupting drugs of the benzimidazole which included TBZ. (Umesono, et al., 1983). Sequencing the gene showed it to be 75% homologous to that for chicken β -tubulin (Hiraoka, et al., 1984).

nda3 - the effect of TBZ on microtubules

nda3 cells were grown to log phase and inoculated with 100 μ g/ml TBZ. Growth of cells was still apparent though it was diminished when compared to wild type. The microtubules were analyzed by immunofluorescence using the antibody, TAT1. Before TBZ addition, 88% of *nda3* cells contained cytoplasmic microtubules and the remaining 12% had mitotic spindles. After 1 hour in the presence of TBZ 78% of cells still contained cytoplasmic microtubules. This compared to wild type cells where a fall from 90% to less than 10% was detected.

Since TBZ can be added to these cells without causing disruption of the microtubules I could address the question of whether the effect of TBZ on the Golgi apparatus was direct or whether it required microtubule breakdown. Furthermore, at 20°C the cells become blocked in mitosis with no cytoplasmic microtubules, a second means to investigate the effect of the lack of microtubules on the Golgi apparatus.

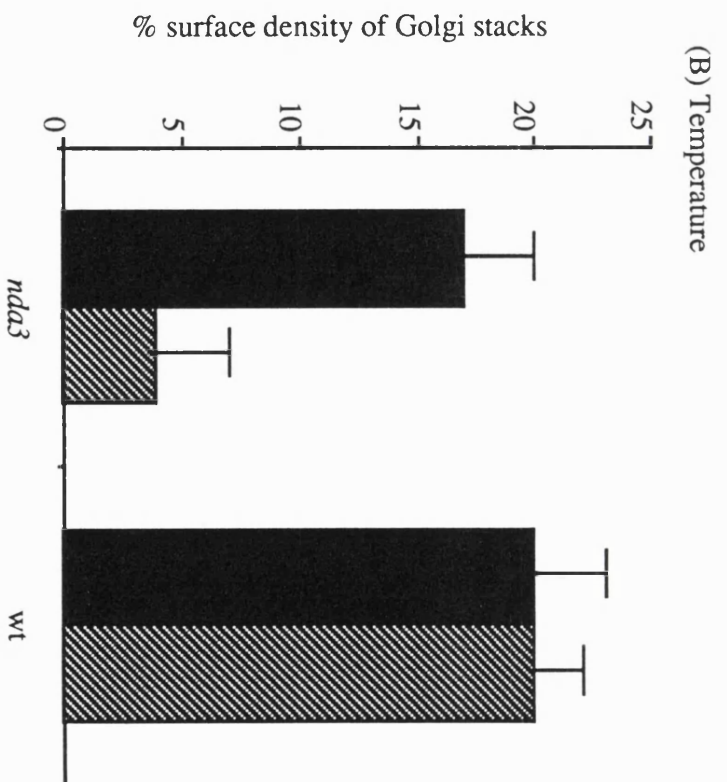
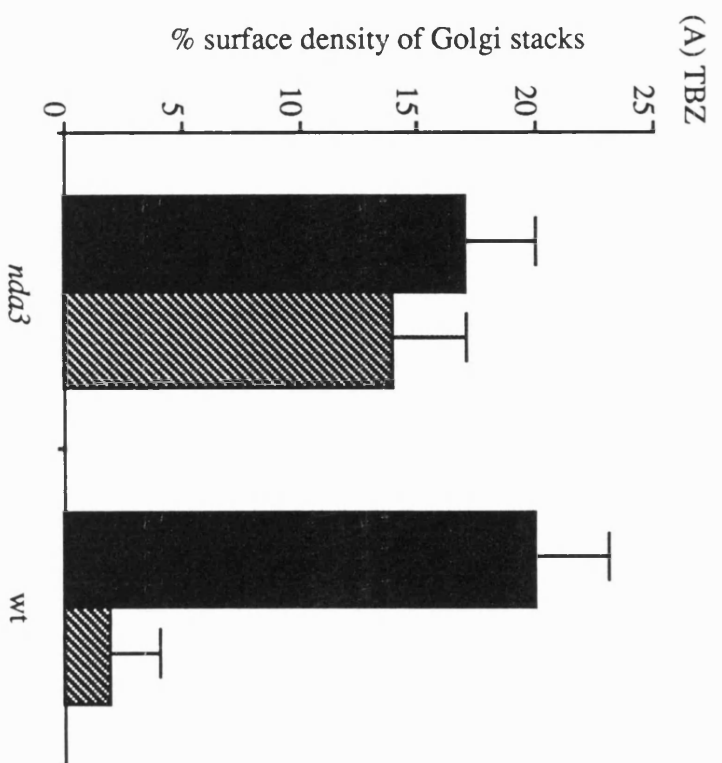
nda 3 - Effects on the Golgi apparatus

When grown at the permissive temperature of 32°C, TBZ had little effect on the surface density of Golgi stacks (Fig. 4.12A). The surface density fell from 17% to 14% whereas that of wild-type cells fell from 20% to 2%.

Figure 4.12. Effect of TBZ and temperature on stacking in the *nda3* mutant

(A) Wild type (wt) and *nda3* cells were incubated at 32°C for 4 hours in the absence (■) or presence (▨) of 100 µg/ml TBZ then fixed in potassium permanganate, prepared for electron microscopy and the surface density of Golgi stacks calculated. Note that TBZ had little effect on Golgi stacking in *nda3* cells.

(B) Wt and *nda3* cells were incubated for 4 hours at either 32°C (■) or 20°C (▨) then fixed in potassium permanganate, prepared for electron microscopy and the surface density of Golgi stacks calculated. Note that unstacking occurred in the *nda3* mutant at the non-permissive temperature (20°C).



However, when the cells were shifted to the non-permissive temperature of 20°C the mutant β -tubulin was unable to form a mitotic spindle so the cells became blocked in mitosis. After 10 hours incubation at 20°C, the surface density of Golgi stacks fell from 17% to 4% (Fig. 4.12B). In marked contrast, wild type cells were unaffected by this change in temperature (Fig. 4.12B).

nda2 - conditional α -tubulin mutant

Similar experiments were carried out on the *nda2* mutant which carries a mutation in the α -tubulin gene (Toda, et al., 1984). The strain used, *nda2-KM52*, is sensitive to TBZ and, at the permissive temperature behaved in the same way as wild-type cells. Figure 4.13 shows *nda2* cells incubated in the absence (A) or presence (B) of TBZ. Note the lack of Golgi stacks following treatment and the increase in short lengths of membrane.

4.2.8. The functional consequences of microtubule disruption and Golgi unstacking

The effect of TBZ on cells in addition to microtubule breakdown, seemed to be an unstacking of cisternae of the Golgi apparatus. This unexpected result led us to initiate investigations into the consequences of unstacking in *S.pombe* with a view to elucidating a possible role for stacking of Golgi cisternae.

Effect on cell growth and secretion of acid phosphatase

The effect of cisternal unstacking on Golgi function was measured in two ways. Cell growth could be used to measure Golgi function since growth would be prevented if plasma membrane and cell wall components were not secreted by the cell. The growth of cells after addition of TBZ was shown in figure 4.2A. This showed that the growth rate was barely

Figure 4.13. Effect of TBZ on Golgi stacks in *nda2* cells

nda2 cells were grown to log phase at 32°C with shaking. Cells were then incubated for a further 4 hours in the absence (A) or presence (B) of 100 µg/ml TBZ. Cells were fixed using 2% permanganate and processed for electron microscopy. Note the lack of stacks after addition of TBZ.
Bar = 1.2 µm



affected for at least 2 hours, much longer than the time taken to break down the microtubules and unstack the Golgi apparatus.

The secretion of acid phosphatase was also measured. Spheroplasts were prepared and these were incubated for 3 hours at 32°C in the absence or presence of TBZ. The amount of acid phosphatase secreted into the medium was measured. As shown in figure 4.14 secretion of acid phosphatase was relatively unaffected by TBZ. Only after 2 hours of treatment did significant differences become apparent.

Effect on protein synthesis and cell proteins

A) Protein synthesis

Subsequent experiments to these using TBZ, showed that an inhibition of protein synthesis could disrupt the Golgi apparatus (described in Chapter 5). As a result of this observation I tested whether TBZ itself was affecting protein synthesis and so mediating its effect by this route.

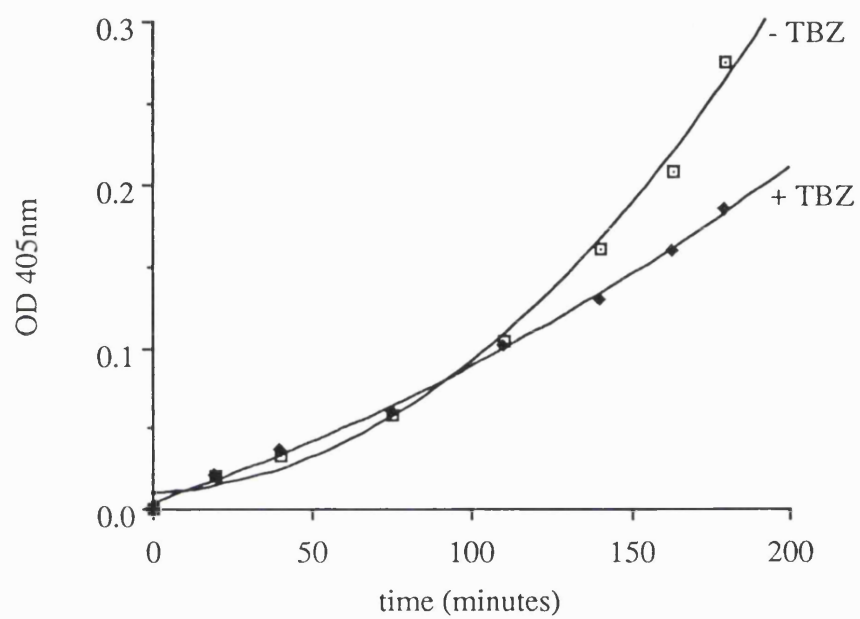
One reason that a slight effect might be expected is that the cells in the presence of TBZ became arrested in mitosis. In mammalian cells this period of the cell cycle is noted for the reduction in protein synthesis levels. In *S.pombe* the synthesis of protein is continuous throughout the cell cycle but there is variation in its rate with one report of a sharp drop in the rate of protein synthesis for a short time in mitosis (Mitchison, 1991)

Cells were grown to log phase and split into four cultures. TBZ was added to two of these. Cells were labelled using ³⁵S-trans-label for 30 minute periods either immediately after addition of TBZ or after cells had been incubated with TBZ for 2 hours. This then showed whether there was an immediate effect of TBZ on protein synthesis or whether the effect was gradual.

Figure 4.14. The effect of TBZ on the secretion of acid phosphatase.

Spheroplasts were incubated at 32°C in the absence (▣) or presence (◆) of TBZ and the secretion of acid phosphatase into the medium monitored using the substrate *p*-nitrophenylphosphate.

†



The data are shown in figure 4.15A. TBZ does seem to have an effect on protein synthesis in fission yeast. In the first 30 minutes the effect is small and would not be expected to be in any way responsible for the changes noted morphologically over this period after TBZ addition. After 2 hours the changes become more significant and the level of reduction in protein synthesis probably accounts for most, if not all of the decrease in the rate of cell growth noted from this time. The change in the level of protein synthesis is most likely due to the cells becoming blocked at mitosis.

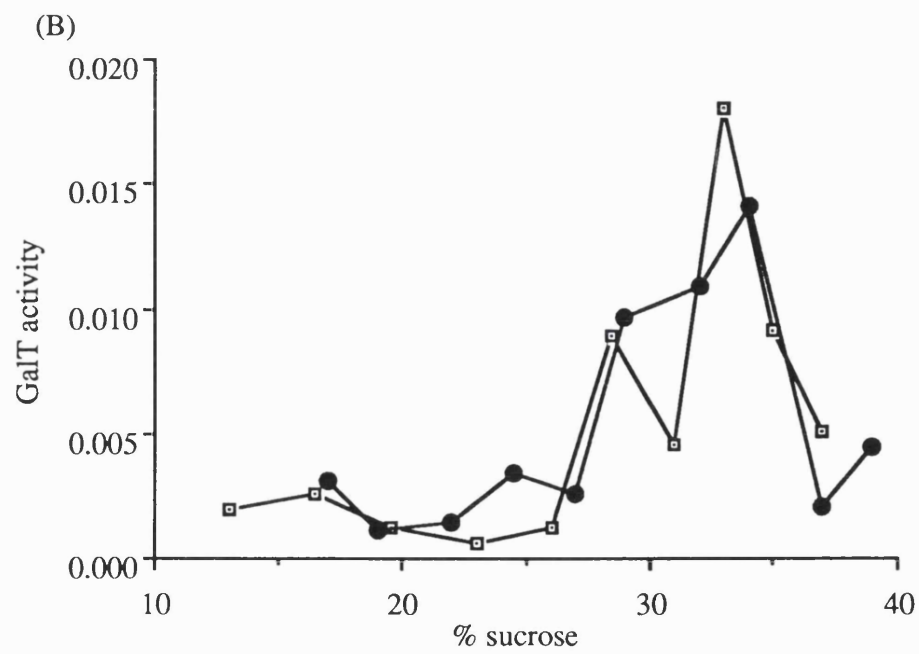
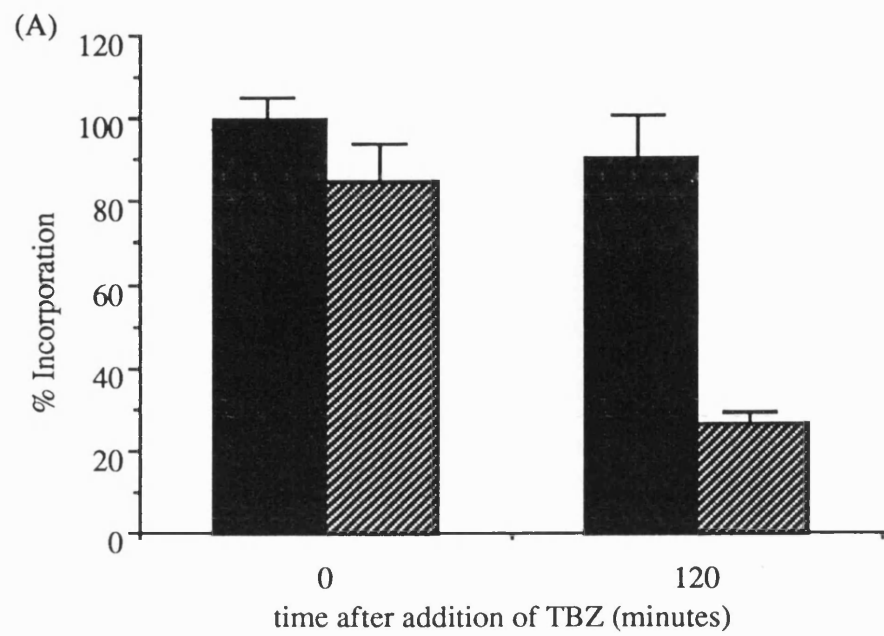
B) GalT

The morphological affect of TBZ on the Golgi apparatus was to cause the dissociation of Golgi cisternae. It was of interest then, to assess the affect this structural change had, if any, on the resident enzymes of the organelle. To assess whether the Golgi marker protein, GalT, remained in a compartment of the same density, its activity was assayed from sucrose¹ gradient fractions. Cells were grown to log phase and TBZ added at 100 µg/ml to half the culture for 3 hours. Homogenates were prepared from an equal volume of cells and applied to the top of a continuous sucrose gradient (0.5 M to 1.8 M). The gradients were centrifuged overnight to equilibrium. Fractions were taken and assessed for % sucrose. The GalT activities of the samples were measured in the presence and absence of the assay substrate, methylmannose. This background level was deducted before calculating the activity of each fraction. Fig. 4.15B shows the activities of the samples after incubation of cells in the presence or absence of TBZ. The activity in both cases was found between 29 and 34% (0.9-1.1M) sucrose. This indicated that the GalT remained in a compartment of the same density after Golgi cisternal dissociation and had not been redistributed to another cell compartment such as the ER, which would be found at a different density.

Figure 4.15. The effect of TBZ on cell proteins

(A) The effect of TBZ on new protein synthesis was assayed by measuring the incorporation of ^{35}S -trans label into protein either immediately after or two hours after TBZ was added. Both treated (▨) and untreated (■) cells were assessed.

(B) Homogenates were made from cells incubated in the absence (□) or presence (●) of 100 $\mu\text{g/ml}$ TBZ for 3 hours. The homogenates were spun to equilibrium in a sucrose gradient, fractions collected and assayed for galactosyltransferase activity (nmol/min/ μl).



4.3. Discussion

The characterization of the effect of TBZ on fission yeast showed that there is a strict correlation between the presence of microtubules in *S.pombe* and the presence of Golgi stacks. Microtubules were broken down either using TBZ or by shifting the *nda3* mutant to the non-permissive temperature. Golgi stacks disappeared under both conditions. Furthermore, the *nda3* mutant at the permissive temperature was resistant to TBZ and under these conditions the Golgi stacks were unaffected. This shows that the effect of TBZ on Golgi stacks is a consequence of its action on microtubules and cannot be attributed to a side effect of the drug.

The effect of microtubule breakdown was to convert stacks of cisternae to single cisternae. Two methods were used to quantitate the effect and both showed that the stacked Golgi apparatus disappeared but there was a concomitant rise in the level of short lengths of membrane with dilated rims proposed to be single cisternae.

The only data that do not, at first sight, fit the interpretation are the immunofluorescence images in figure 4.6B. GalT is present in most cisternae in the Golgi stack (Fig. 3.12 and Chappell et al., submitted), so unstacking should have caused a 2-3 fold increase in the number of labelled structures in each cell. An increase was observed but this was in line with the increase in cell length caused by the inhibition of cell division. The simplest explanation is to suggest that unstacked cisternae do not migrate far from the original stack and so cannot be resolved as separate structures by immunofluorescence microscopy. Evidence in support of this view comes from images such as those seen in figure 4.7 E,F where unstacked cisternae remain clustered together.

These results then pose the question of how the breakdown of microtubules could cause unstacking. One obvious possibility is that the microtubules act as stacking proteins. However, microtubules have a width of 250Å, which is wider than the intercisternal space in *S.pombe* (see Table 3.1). In addition, there was no co-localization of the Golgi with microtubules by immunofluorescence microscopy (Fig. 3.6 and data not shown). It is of course possible that the microtubules are linked to stacking proteins but they would only have access to those at the cisternal edges so it is difficult to see how they could control stacking. In addition, none of the known microtubule-binding proteins have been located to the intercisternal space.

Another possibility is suggested by work on the budding yeast, *S.cerevisiae*. In these cells the Golgi exists mostly as single cisternae (Preuss, et al., 1992) yet certain secretory (*sec*) mutants accumulate what appear to be Golgi stacks (Novick, et al., 1981; Svoboda and Necas, 1987). implying that a stacking mechanism exists but the Golgi spends most of its time as single cisternae. These cisternae may move around the cell on microtubules. Microtubules bind to Golgi membranes (Corthésy-Theulaz, et al., 1992; Ho, et al., 1989) and are known to move membranes from one part of a cell to another (Schroer and Sheetz, 1991). Since a stacking mechanism exists this suggests that the cisternae need to come together occasionally, perhaps for the purpose of exchanging material by vesicle-mediated transport. Movement along microtubules would ensure that cisternae have the opportunity for stacking and once they had exchanged material the cisternae could separate and move back onto microtubules. Providing the time spent together was much less than the time spent travelling the Golgi appear morphologically as single cisternae.

In *S.pombe* the cisternae would spend longer together and less time travelling on microtubules so that most of the Golgi would appear to be stacked. However, in the absence of microtubules, when the cisternae separate, they would be unable to go anywhere. This would explain unstacking and why the single cisternae appear clustered together (Fig. 4.7E,F). Such clustering could also help explain why the effect on growth and secretion of acid phosphatase was limited. Sufficient association could still occur to permit vesicle-mediated transport.

This model does not explain why the stack is a transient rather than a stable structure as it appears to be in mammalian cells. Whatever the reason, this system may provide a means of testing functions that might depend on the stacking of Golgi cisternae.

Chapter 5

Inhibition of protein synthesis disrupts the Golgi apparatus in fission yeast

5.1. Introduction

Whilst investigating the unstacking of Golgi cisternae caused by TBZ (see Chapter 4) I decided to test whether the reassembly of the stacks after removal of the drug required protein synthesis. Cells were washed free from TBZ and incubated in the presence or absence of cycloheximide. Analysis by e.m. however revealed that control samples, treated with cycloheximide alone had no recognizable Golgi stacks. This was an unexpected result since the morphology of the Golgi apparatus in mammalian cells is not affected by similar treatments (Green, et al., 1981; Jamieson and Palade, 1968) though there is one report in plant cells showing a similar though less striking effect (Picton and Steer, 1983).

I have investigated this effect showing that it is specific for the Golgi apparatus and the products of disruption appear to be small vesicles. The effect is reversible and not dependent on the type of protein synthesis inhibitor used. All of the data point to a component of the fusion machinery that turns over very quickly in *S.pombe* cells.

5.2. Results

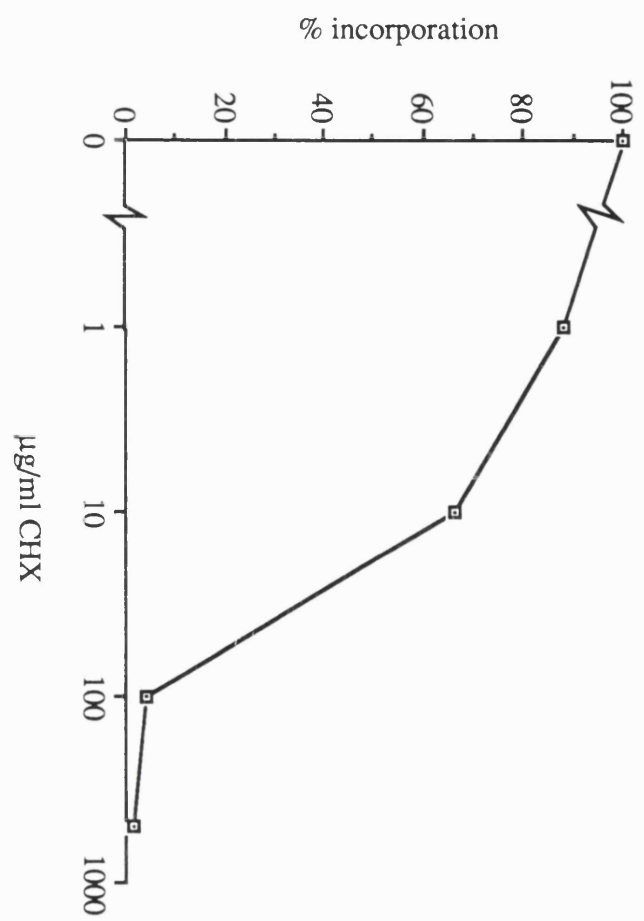
5.2.1. Inhibitors

Two inhibitors were applied to cells in order to eliminate the possibility of any side effects each might have on processes other than protein synthesis. Anisomycin (ANS) was used at 100 µg/ml as recommended by Yamamoto (1990). Cycloheximide (CHX) was titrated as shown in figure 5.1. 100 µg/ml was sufficient to inhibit >95% of protein synthesis over the 3 hour period.

Figure 5.1. Dose dependent inhibition of protein synthesis by CHX

Log phase cells were incubated in the presence of ^{35}S -trans label and increasing levels of CHX for 3 hours. Incorporation was measured after acid precipitation and boiling.

1



These levels of both ANS and CHX completely inhibited any cell growth as shown by the lack of increase in turbidity or cell number as assessed by haemocytometry (Fig. 5.2A-C). They also had no apparent effect on the cells under phase or using Nomarski optics (data not shown).

5.2.2. Immunofluorescence microscopy

When antibodies to the GalT/ β -gal fusion protein were used to stain untreated cells of *S.pombe* the fluorescence staining pattern was as observed previously (Fig. 3.6) with 10-20 punctate spots per cell depending on the cell size (Fig. 5.3A). When this antibody was used to label cells pretreated with cycloheximide or anisomycin the usual staining pattern was no longer perceived. After incubation with the antibiotics there were few if any discrete spots in cells (Figs. 5.3B-E). In a time course monitored by fluorescence the number of spots in the cells was reduced from 10-20 at the outset to 5-10 after 1 hour and to 0-3 over a 3 hour period. Thus, the change was gradual over the time monitored and was accompanied by a concomitant rise in cytoplasmic staining. The staining in the cells was excluded from vacuoles which are distinguishable by light microscopy with phase optics and from the nucleus as shown by non co-localization with the DNA stain DAPI.

The vacuoles did not appear to be grossly altered in their morphology after treatment with CHX or ANS. After three hours in the presence of the antibiotics cell vacuoles were visualized by staining with the dye 5(6)-carboxy-2'7'-dichlorofluorescein diacetate (CDCFDA). In addition the ER retained its structure when CHX treated cells were stained for the ER resident protein BiP (data not shown)

Figure 5.2. The effect of protein synthesis inhibitors on cell growth.

Cells were grown to log phase and then inoculated with protein synthesis inhibitors. Growth was monitored by turbidity changes and by haemocytometry. (A) Cells were incubated in the presence or absence of CHX at 0 $\mu\text{g/ml}$ (\square), 1 $\mu\text{g/ml}$ (\blacklozenge), 10 $\mu\text{g/ml}$ (\blacksquare), 100 $\mu\text{g/ml}$ (\blacklozenge). The effect on cell growth was followed by measuring the turbidity (B) Cells were incubated in the presence (\blacklozenge) or absence (\square) of CHX and the effect assessed by counting cell number with a haemocytometer. (C) Cells were incubated in the presence or absence of ANS at 0 $\mu\text{g/ml}$ (\square), 10 $\mu\text{g/ml}$ (\blacklozenge), 20 $\mu\text{g/ml}$ (\blacksquare), 50 $\mu\text{g/ml}$ (\blacklozenge), 100 $\mu\text{g/ml}$ (\blacksquare) and the effect of the drug on cell growth assessed by following turbidity changes at OD 595nm .

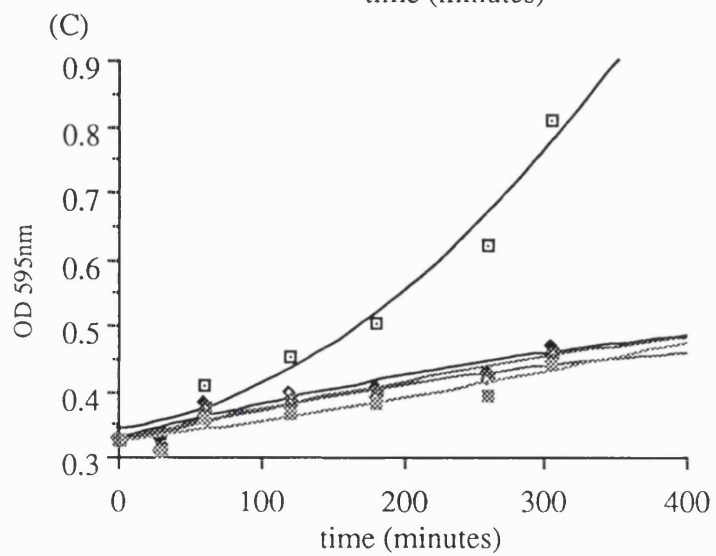
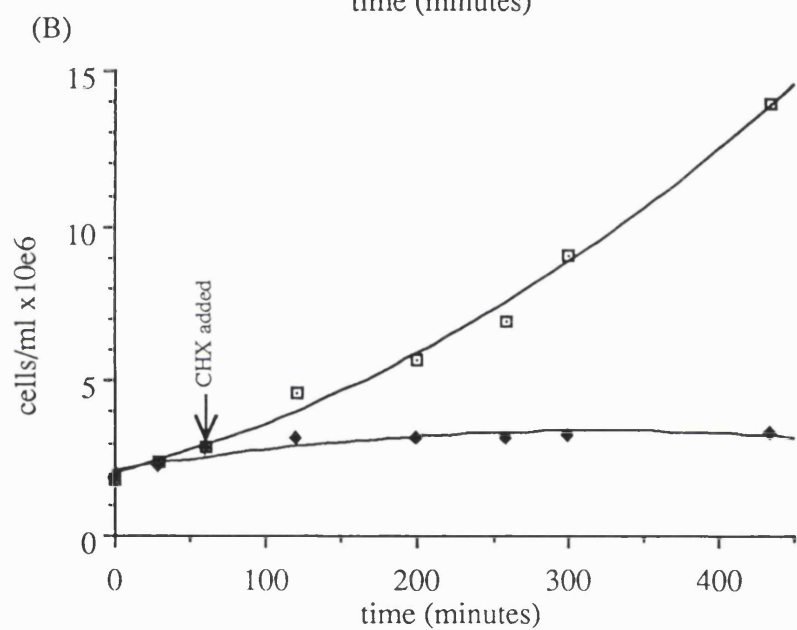
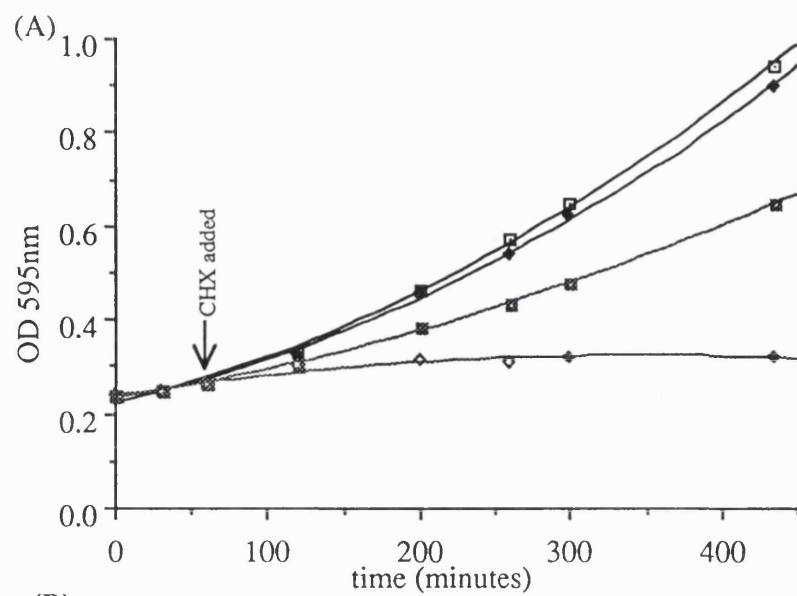
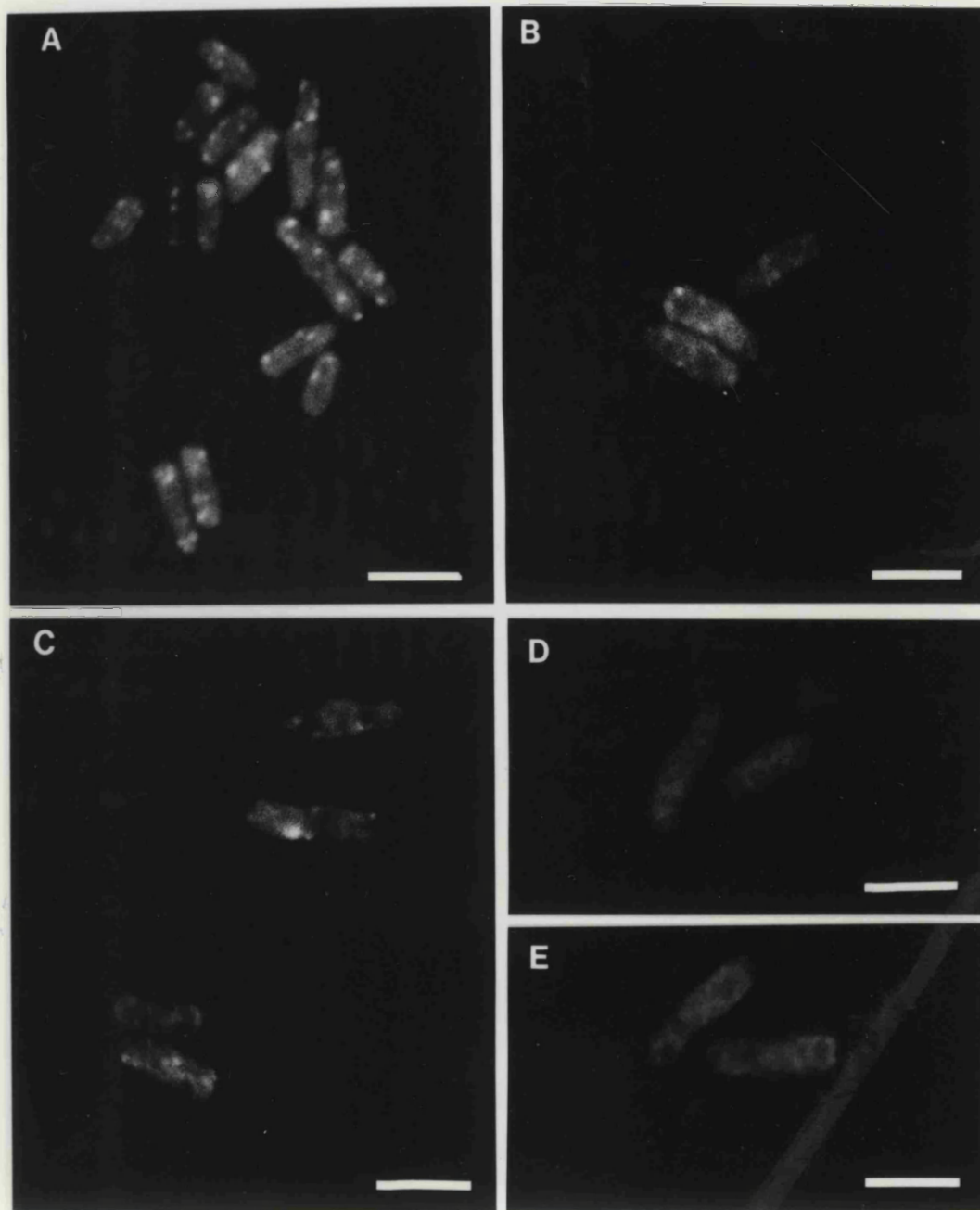


Figure 5.3. Appearance of the Golgi apparatus by immunofluorescence microscopy after treatment with protein synthesis inhibitors

Log phase cells were either (A) untreated; (B) treated with ANS for 3 hours; (C) treated with CHX for 1 hour; (D,E) treated with CHX for 3 hours. They were then fixed and labelled with anti-GalT antibodies followed by rhodamine conjugated secondary antibodies. Bar = 10 μ m.



5.2.3. Electron microscopy

To allow more detailed observations to be made, cells were analyzed by electron microscopy following the inhibition of protein synthesis. Following treatment of cells with the inhibitors the most apparent change was in the number of stacks of Golgi cisternae indicating that the effect is selective for these membranes. Before CHX addition 73% of cells observed in randomly selected sections contained clear stacks of cisternae. This was reduced to 14% of the population after 3 hours of treatment. Furthermore, any stacks which were seen were composed of fewer cisternae and the cisternae were shorter. The average cisternal length in a stack fell from $0.67\ \mu\text{m} \pm 0.03$ to $0.36\ \mu\text{m} \pm 0.02$. These stacks with fewer and shorter cisternae may represent intermediates in breakdown of the Golgi apparatus in cells (Figs. 5.4D-F). Other changes which were detectable at the level of electron microscopy included a slight dilation of the ER and some coalescence of the vacuoles.

Stereology, employing the disector method was used to quantitate the electron microscopy data obtained by permanganate fixation of treated and untreated cells. The categories of membrane assessed were: nuclear envelope, peripheral ER, internal ER (all non-peripheral stretches of membrane in a cell that were judged not to be mitochondrial or vacuolar) and stacked Golgi cisternae. The data show a substantial alteration in the level of stacked cisternae in cells following exposure to either CHX or ANS. The change was not immediate with a reduction in the level of stacked Golgi membrane on CHX addition from 18% to 6% after 1 hour and to 2% over the 3 hour period (Fig. 5.5A). The effect of ANS on Golgi stacks was equally dramatic with a reduction in stacked cisternae from 16% to 2% (Fig. 5.5B). The amount of nuclear envelope and peripheral ER per unit cell volume remained roughly constant whilst the internal ER

Figure 5.4. Appearance of the Golgi apparatus after treatment with CHX by electron microscopy on permanganate fixed cells.

Log phase cells were incubated at 32°C in the absence (A) or presence (B-F) of CHX then fixed in potassium permanganate for visualization by electron microscopy. (A, B) Low power images of whole cells. Note the absence of Golgi stacks in the presence of CHX; (C-F) High power images of the Golgi region at increasing times after CHX treatment (C= 0 mins.; D= 60 mins.; E,F= 180 mins.). In D-F note the shortened and disrupted Golgi stacks, possible intermediates in breakdown of the Golgi apparatus. G = Golgi apparatus. Bar (A,B) = 1 μm . (C-F) = 0.1 μm .

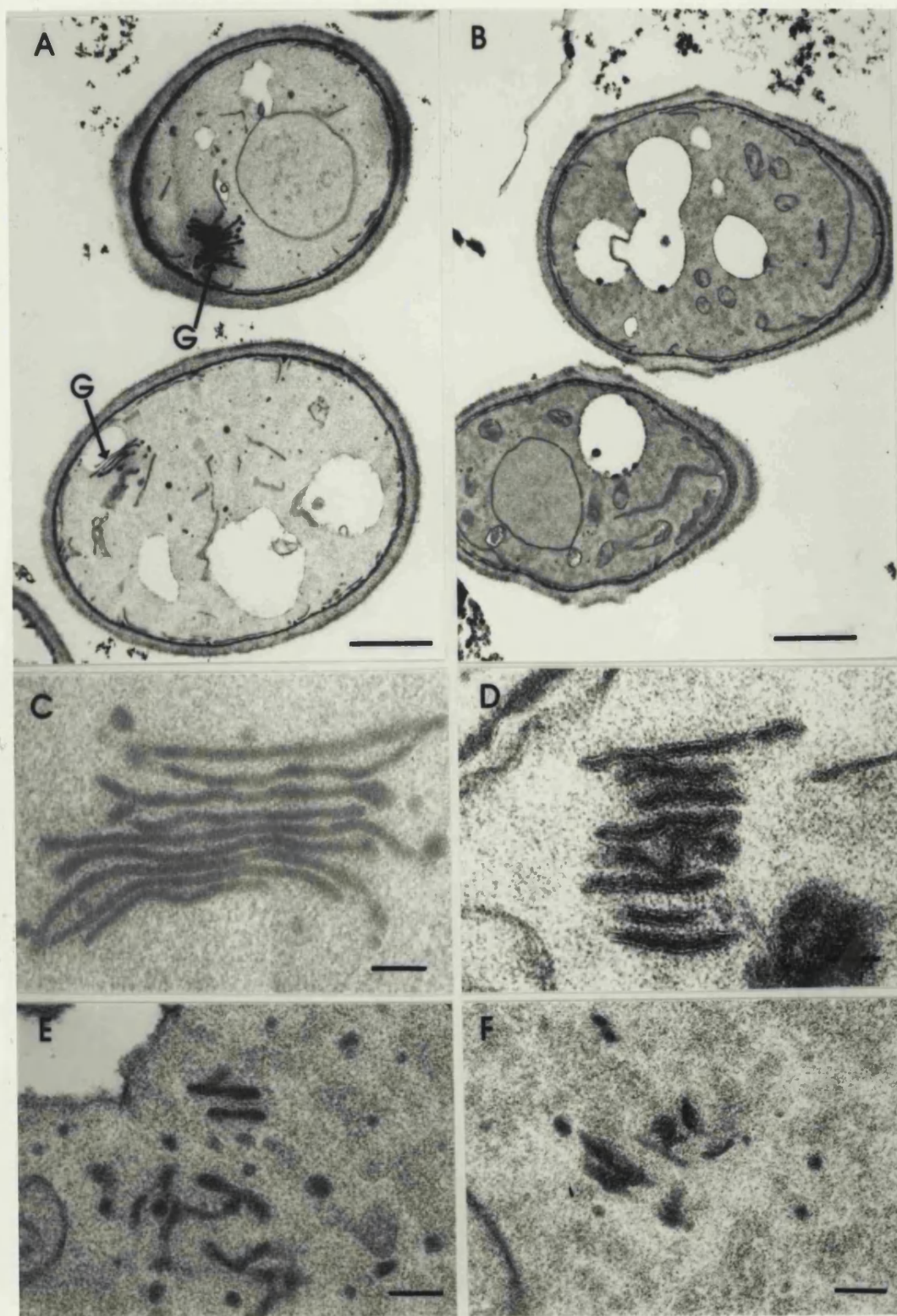




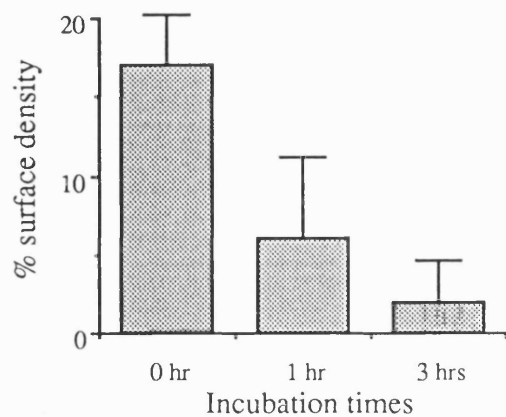


Figure 5.5. Effect of inhibition of protein synthesis on the surface densities of internal membranes.

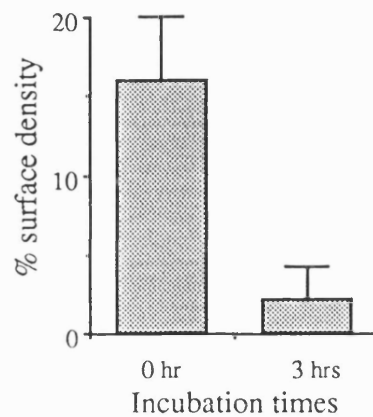
Log phase cells were treated with either CHX (A,C) or ANS (B) for up to 3 hours, then fixed with potassium permanganate and processed for electron microscopy. The surface densities of the Golgi stacks (A,B) and the ER (C) were measured.

Golgi apparatus =  ; nuclear envelope =  ; peripheral ER =  ;
internal ER =  Results are presented as the mean \pm standard deviations.

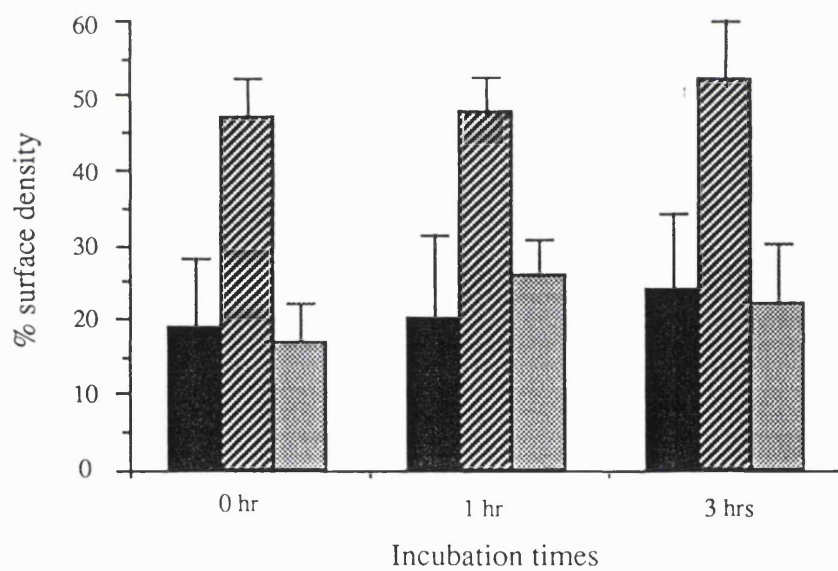
(A) CHX on Golgi stacks



(B) ANS on Golgi stacks



(C) CHX on ER membranes



showed some fluctuation with an initial increase in its level concomitant with the onset of Golgi apparatus breakdown followed by a slight fall (Fig. 5.5C).

To ensure that these morphological changes were not artefacts associated with the harsh fixation conditions of permanganate a more conventional fixation procedure was used which is less disruptive to cellular architecture. This glutaraldehyde/paraformaldehyde based method gave good preservation of Golgi structure in control preparations and supported the aforementioned findings with few stacks observed in a population of cells following treatment with cycloheximide or anisomycin. Some structures, which could represent disassembling Golgi stacks or intermediates in this process were seen (Fig. 5.6).

5.2.4. Changes in Cell Proteins

GalT

A biochemical assay was used to ascertain whether the activity of the GalT was impaired during the disruption of the Golgi apparatus. The measurable activity of GalT fell to about half of its initial level over the background measured with no substrate present (Fig. 5.7). The other half of the activity was not found on the surface of intact cells indicating that GalT, at least in its active state, was not being transported to the cell surface on breakdown of the stack. The assay was also performed on cell extracts made in the absence and presence of CHX. High speed pellets were assayed and again about half of the activity was detected. The remaining 50% was not found in the cytosol (data not shown).

Immuno-electron microscopy using the antibody GTF2, which had shown good labelling of the Golgi apparatus in wild type cells, was attempted on cells pretreated with CHX. There did not appear to be any labelling

Figure 5.6 Appearance of the Golgi apparatus in cells treated with CHX by electron microscopy of glutaraldehyde/paraformaldehyde fixed cells.

Log phase cells were incubated in the presence of CHX for 3 hours. Cells were fixed using 3% glutaraldehyde and 0.5% paraformaldehyde, then post fix osmicated to enhance visualization of Golgi membranes. At low magnification no Golgi stacks were seen (A). Possible Golgi breakdown products are depicted in B and C. Bar = 0.7 μm (A) ; 0.25 μm (B,C).

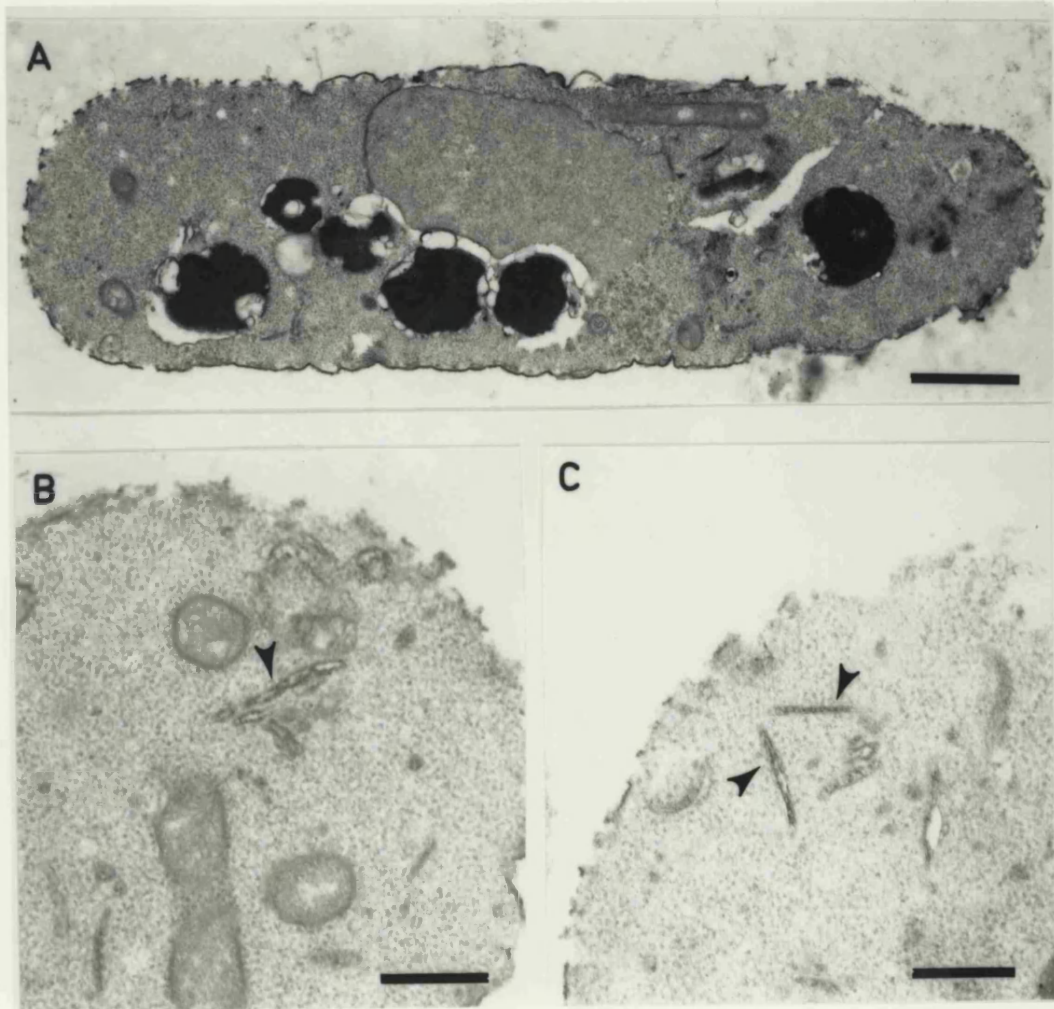
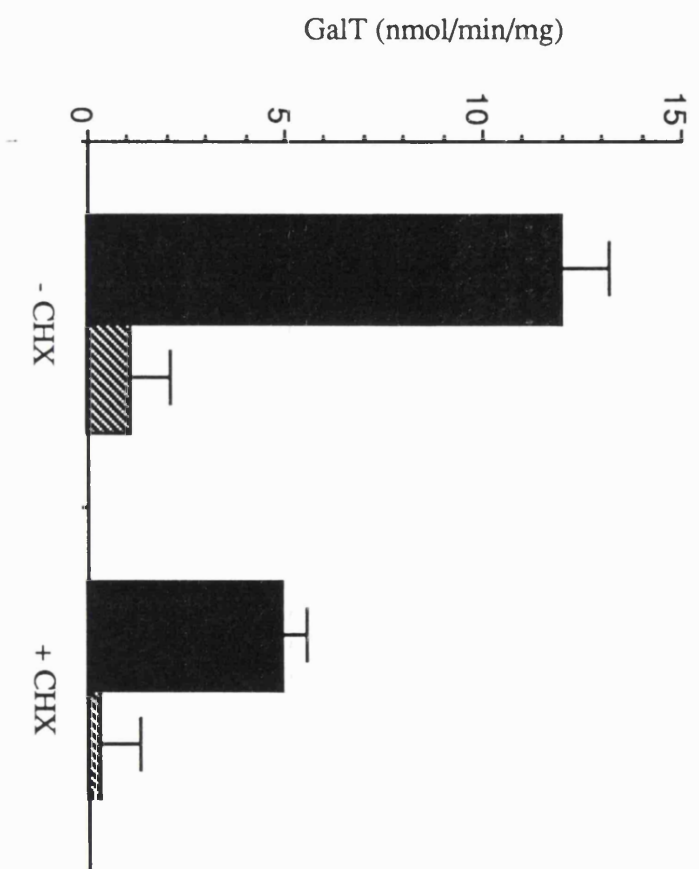


Figure 5.7. The effect of CHX on GalT in cells

GalT activity present in equivalent numbers of cells was measured following incubation of *S.pombe* cells with or without CHX for 3 hours. The assay was performed on permeabilized (■) and intact cells (▣) using the substrate methylmannose. Background values in the absence of methylmannose were subtracted.



attributable to a specific organelle and the overall level of labelling was very low (data not shown). However, it should be noted that labelled vesicles would be very difficult to distinguish over non-specific cytoplasmic labelling due to their size and the reduced membrane contrast in immuno e.m.

Acid Phosphatase.

A secretory protein, acid phosphatase, was blotted in homogenates prepared from cells which had been incubated in the absence or presence of CHX. In untreated cells there was a 72kD form of the protein which is the ER core-glycosylated form (Schweingruber, et al., 1986a) and higher molecular weight forms due to processing of these oligosaccharides. On deglycosylation by Endo H treatment the major form was 54kD. When the cells were treated with CHX the 72kD form was barely visible whilst higher molecular weight forms of the protein were still present. The major deglycosylated species was again 54kD (Fig. 5.8). This indicated that proteins were able to exit the ER in the presence of CHX but the higher molecular weight species were unable to leave cells. Pulse chase experiments demonstrating glycosylation and secretion of acid phosphatase have shown that the protein is fully glycosylated with a $t_{1/2}$ of 10 minutes and the level of labelled protein begins to fall after 20 minutes due to secretion from the cell (Schweingruber, et al., 1986a).

Hexokinase.

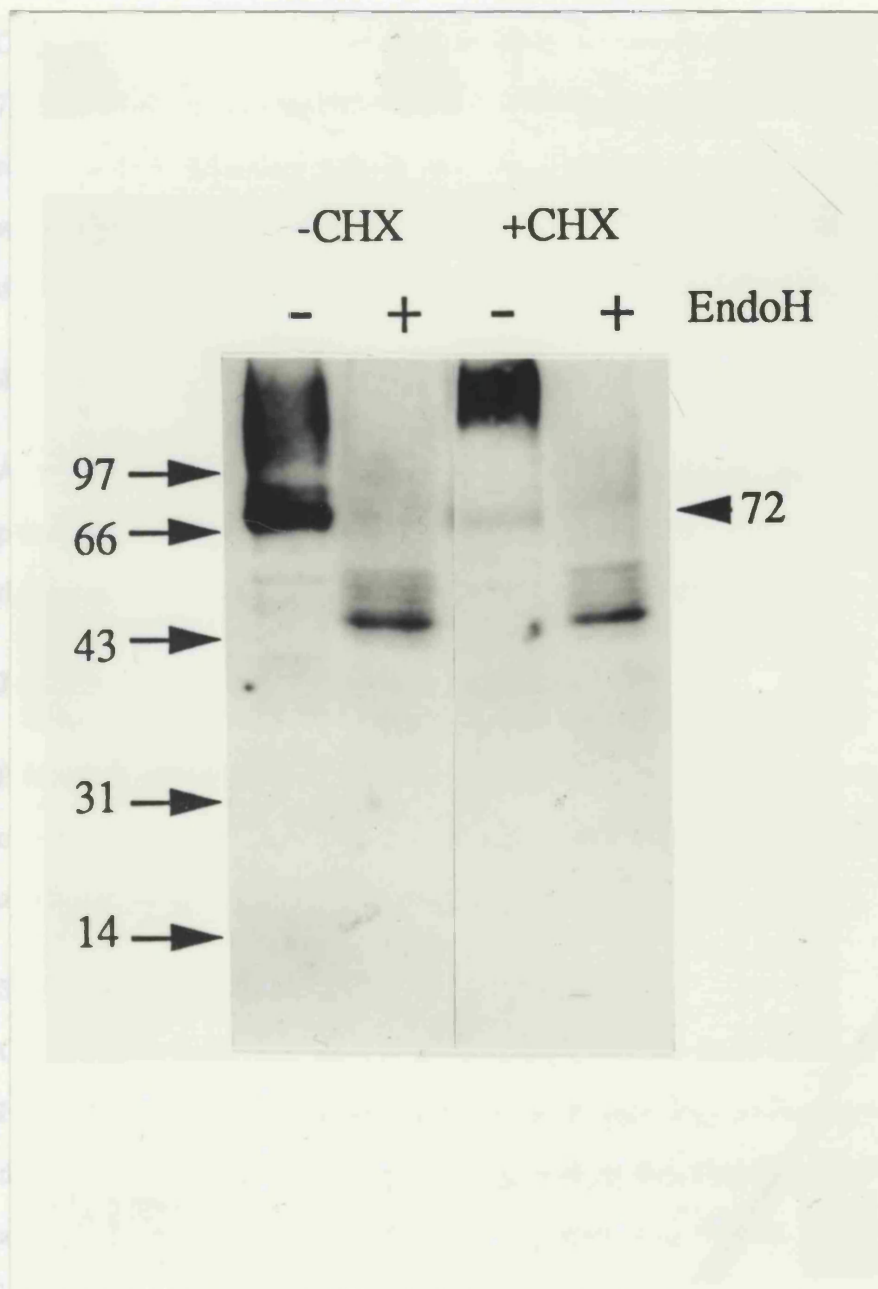
The activity of a cytoplasmic enzyme, hexokinase, was monitored for changes in its activity following a 3 hour incubation with CHX. Its activity was measured in whole and permeabilized cells and also in cell homogenates. No change in its activity was detectable (Table 5.1).

Figure 5.8. Loss of the ER form of acid phosphatase following incubation of cells with CHX

Log phase cells were incubated for 3 hours in the absence or presence of CHX. Extracts were prepared and run on a gel before blotting for acid phosphatase with a monoclonal antibody, 7B4. Note the dramatic reduction in the 72kD, ER form, of the protein in the presence of CHX.

Tubulin

The amount of tubulin remaining in cells after a 3 hour incubation with



Endonuclease H (EndoH)

Cells also resumed growth after CHX removal or escaped by toxicity changes. However, cells that were exposed to CHX for 3 hours exhibited a lag before growth resumed and attained a rate comparable to that of a population of cells that was not exposed to the drug (Fig. 53A).

Tubulin.

The amount of tubulin remaining in cells after a 3 hour incubation with CHX was assessed by Western blotting using the monoclonal antibody 7B4. The antibody was applied to blots of cell homogenates prepared from cells treated or not treated with the antibiotic. The level of tubulin in cells was only slightly reduced over the time of CHX addition. Laser densitometry from blots showed the levels to be $78\% \pm 10\%$ (Table 5.1).

BiP.

A resident protein of the ER, BiP, was probed for in extracts from cells pretreated with CHX. No significant differences were detectable between the amount of BiP from treated and untreated extracts (Table 5.1).

Total cell protein.

Ponceau-S staining of whole cell extracts when blotted showed no observable changes between extracts made from cells treated in the absence or the presence of CHX (data not shown).

5.2.5. Disruption of the Golgi apparatus is reversible

Cells were washed free of CHX and resuspended in fresh medium. Following permanganate fixation and processing, stereology showed that the Golgi stacks could be reassembled and were at the original level of about 20% membrane surface density by 3 hours after removal of the inhibitor (data not shown).

Cells also recommenced growth after CHX removal as assessed by turbidity changes. However, cells that were exposed to CHX for 3 hours exhibited a lag before growth reinitiated and attained a rate comparable to that of a population of cells that was not exposed to the drug (Fig. 5.9A).

Table 5.1. The effect of CHX on cell proteins

Cells were treated for 3 hours with or without 100 $\mu\text{g/ml}$ CHX. Hexokinase was measured in a coupled enzyme assay using glucose as the substrate for the initial reaction and NADP as the cofactor for the second. The activity was measured spectrophotometrically. The levels of the tubulin and the ER resident protein, BiP, were assessed by laser densitometry from blots probed with appropriate antibodies (TAT 1 for tubulin, and JARM13 for BiP).

Protein	- CHX	+ CHX
Hexokinase	70 \pm 6 mU/mg	68 \pm 6 mU/mg
BiP	100 \pm 9%	93 \pm 12%
Tubulin	100 \pm 9%	78 \pm 10%

This lag was also observed for the secretion of acid phosphatase. This protein is normally secreted from cells at a low rate and becomes enmeshed in the amorphous cell wall carbohydrates. In this assay the cell wall was removed and the secretion of acid phosphatase into the medium was measured. The lag for the production and secretion of the acid phosphatase was about 1 hour, after which the rate of production of acid phosphatase was comparable to that from untreated cells (Fig. 5.9B).

5.3. Discussion

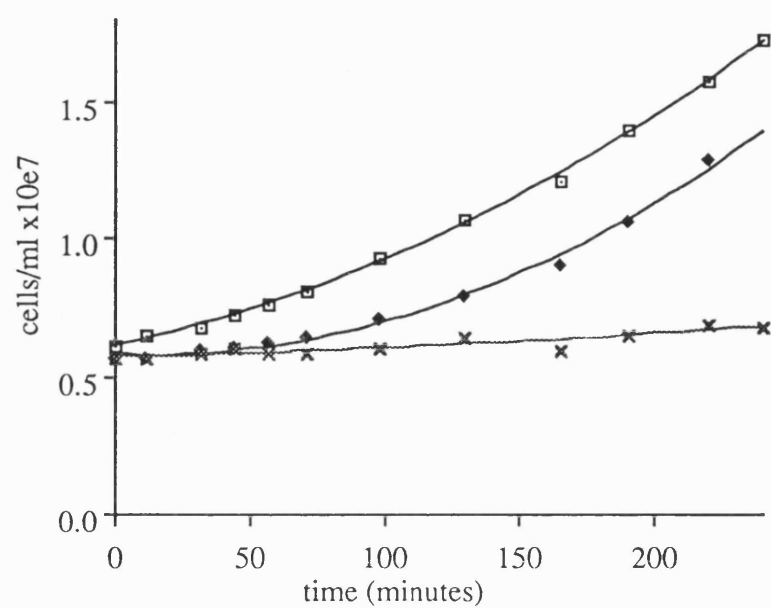
Inhibition of protein synthesis has a dramatic effect on the morphology of the Golgi apparatus in *S.pombe*. Treatment with either CHX or ANS caused almost complete disappearance of the Golgi apparatus both by immunofluorescence and electron microscopy. Quantitation showed a 10-fold decrease in surface density of Golgi membranes over a 3 hour incubation and the activity of GalT fell by 50%. This effect was reversible and restricted to the Golgi apparatus. None of the other cellular organelles were significantly affected either in their morphology or content of marker proteins.

Several lines of evidence point to small vesicles as the product of the breakdown process. The bright spots of labelled Golgi visible in untreated cells by immunofluorescence microscopy were replaced by an increased cellular staining that was restricted to the cytoplasm. Similar cytoplasmic staining is seen in mammalian cells when the Golgi undergoes complete vesiculation at mitosis (Burke, et al., 1982). The GalT that remained at the end of the incubation was found in the high speed, not the low speed pellet after homogenisation, consistent with it being contained in small vesicles.

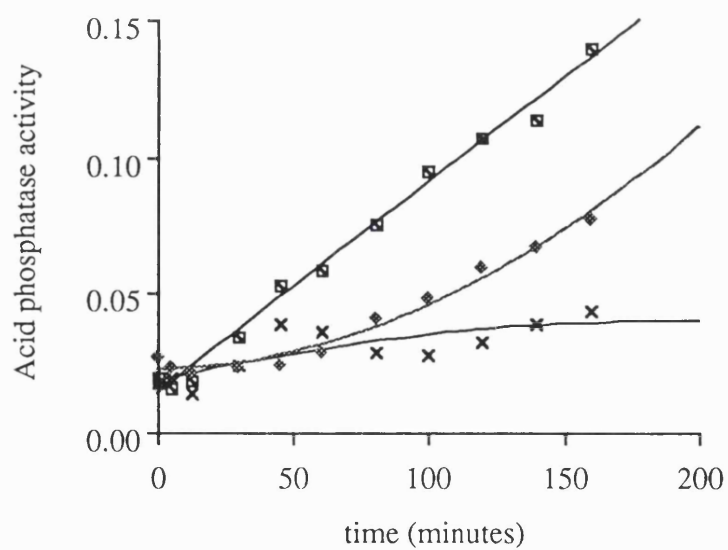
Figure 5.9. Reversibility of the inhibition

Log phase cells were incubated in the presence or absence of CHX for 3 hours and spheroplasts made. Half of the treated population was then washed and resuspended in fresh medium. (A) Reinitiation of cell growth as measured by an increase in turbidity at OD_{595nm}. Cells were either untreated (□); treated for 3 hours and then CHX was washed out (◆); or incubated with CHX throughout the whole time course (×). (B) Secretion of a specific enzyme, acid phosphatase, assessed spectrophotometrically at OD_{405nm} with the phosphatase substrate, *p*-nitrophenyl phosphate. Again cells were either untreated (□); treated for 3 hours and then CHX was washed out (◆); or incubated with CHX throughout the whole time course (×). The change in absorbance at OD_{405nm} was divided by the cell number to correct for cell growth during the incubation. after homogenisation, consistent with it being contained in small vesicles.

(A) Growth



(B) Secretion



Lastly, vesicle-like structures with a diameter between 100 and 300 nm could be seen after treatment with CHX (Figs. 5.4 E and F).

Vesicles could be generated by budding in the absence of fusion. Vesicles usually bud from the dilated rims of Golgi cisternae and fuse with the next cisterna in the stack towards the trans side (Rothman and Orci, 1992). If, after inhibition of protein synthesis, they continued to bud but can no longer fuse (Fig. 5.10) this would explain the conversion of the stack of cisternae to small vesicles. Intermediates with cisternae of variable but shorter length would be expected and were found (Figs. 5.4 D and E).

Since vesicles also bud from the ER and fuse with the cis Golgi (Balch, et al., 1986; Beckers, et al., 1989) this model would not explain why the surface density of the ER remained unchanged by the treatment (Fig. 5.5C). Continued budding without fusion should have caused the ER to vesiculate in the same manner as the Golgi stack. If, however, the inhibition of fusion is a general phenomenon then the fusion of retrograde vesicles with the ER would also be stopped (Fig. 5.10). Several components of the transport machinery are membrane proteins which must be recycled by vesicles (Sweet and Pelham, 1992). If these are not delivered by the retrograde pathway back to the ER vesicles will no longer be able to bud. This would explain why the surface density of the ER remained unchanged.

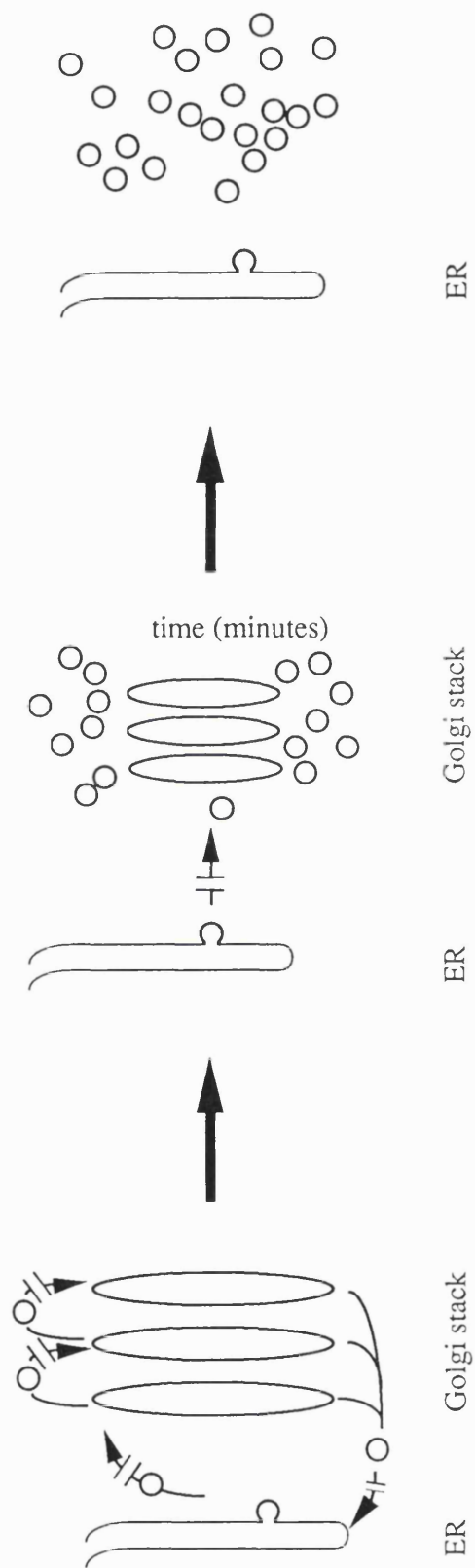
Despite the immediate cessation of protein synthesis caused by CHX and ANS the time taken for the Golgi apparatus to vesiculate was several hours. Furthermore, transport out of the ER occurred at early times as shown by the disappearance of the ER form of acid phosphatase (Fig. 5.8). Earlier work had shown that intracellular transport is not directly coupled to continued protein transport (Jamieson and Palade, 1968; Green, et al., 1981). This strongly suggests that the inhibition of protein synthesis only

Figure 5.10. Disassembly of the Golgi stack by inhibition of fusion

(A) Fusion of transport vesicles with their acceptor compartments becomes blocked due to the high lability of an essential component for the fusion mechanism.

(B) Cisternae of Golgi stacks become shortened as budding alone can occur. Export from the ER is shut off, possibly by the exhaustion of a necessary component that would normally be recycled. The ER thus maintains its size.

(C) Budding of the Golgi stacks continues until it is totally vesiculated.



indirectly affects the fusion machinery. The most likely possibility is that one or more components of this machinery are particularly labile and turn over very rapidly in the cell.

As the transport components that have been identified in mammals (Rothman and Orci, 1992) and *S.cerevisiae* (Pryer, et al., 1992) are identified in *S.pombe*, it should be possible to check their stability to see if they are the components responsible for the effect on the Golgi apparatus caused by inhibition of protein synthesis.

Chapter 6

The effect of Brefeldin A on the Golgi apparatus in *S.pombe*

6.1 Introduction

Brefeldin A was first isolated as an antiviral antibiotic (Tamura, et al., 1968) however it was later realized that the drug had a major effect on secretion in treated cells causing inhibition at an early step in the secretory pathway (Misumi, et al., 1986; Takatsuki and Tamura, 1985). By biochemical approaches and by immunofluorescence it was apparent that proteins normally resident in the Golgi apparatus were found in the ER. Initially this was taken to mean that these proteins were unable to exit the ER and so were accumulating at the earlier compartment. Biochemical characterization of these proteins however showed them to have received modifications characteristic of those generated by Golgi enzymes (Lippincott-Schwartz, et al., 1989). Further observation showed that no recognizable Golgi stacks were present in treated cells and that a wide range of markers for the Golgi apparatus had redistributed to the ER (Doms, et al., 1989; Lippincott-Schwartz, et al., 1989). Proteins of the trans Golgi network did not redistribute to the ER (Chege and Pfeffer, 1990). The morphological events that characterize the breakdown of the Golgi apparatus and its redistribution into the ER in BFA treated cells have been studied in detail. Within minutes of adding BFA to cells Golgi markers are no longer localized by immunofluorescence to a compact juxta-nuclear region. Cisternae appear first to swell and then to extend long processes out to the cell periphery. These Golgi derived tubules extend along microtubules. After 10 minutes these tubules are no longer visible and Golgi markers instead show a punctate reticular structure. These observations led Klausner (1992) to suggest that BFA inhibits the outward flow of traffic from the ER/Golgi mixed system whilst at the same time enhancing a retrograde pathway involved in the movement of Golgi membrane back to the ER.

The effect of Brefeldin A in other cell types has not been widely documented. A marked response was found when the drug was added to plant cells. In both suspension culture cells and root tissues of maize (*Zea mays*) BFA caused a reversible distortion and dissociation of the Golgi stacks coupled with the appearance of numerous cytoplasmic vesicles (Satiat-Jeunemaitre and Hawes, 1992). The effect of BFA in *S.cerevisiae* has not been reported but the phenomenon of retrograde transport from the Golgi apparatus to the ER is the subject of intensive investigation (Pelham, 1991; Lewis and Pelham, 1992a,b). Several proteins defined by various *sec* mutations have highlighted the requirement by cells for such a pathway. The consequences of enhancing the retrograde pathway in terms of Golgi morphology have not been reported presumably because of the difficulty in distinguishing the normal appearance of the Golgi apparatus in *S.cerevisiae* from strands of ER in the cytoplasm.

Since Brefeldin A has such a dramatic effect on the morphology of the Golgi apparatus in cells, and because I had tools available to observe and quantitate such changes I decided to see whether any changes resembling those in either mammalian cells or plant cells occurred when it was added to cultures of *S.pombe*.

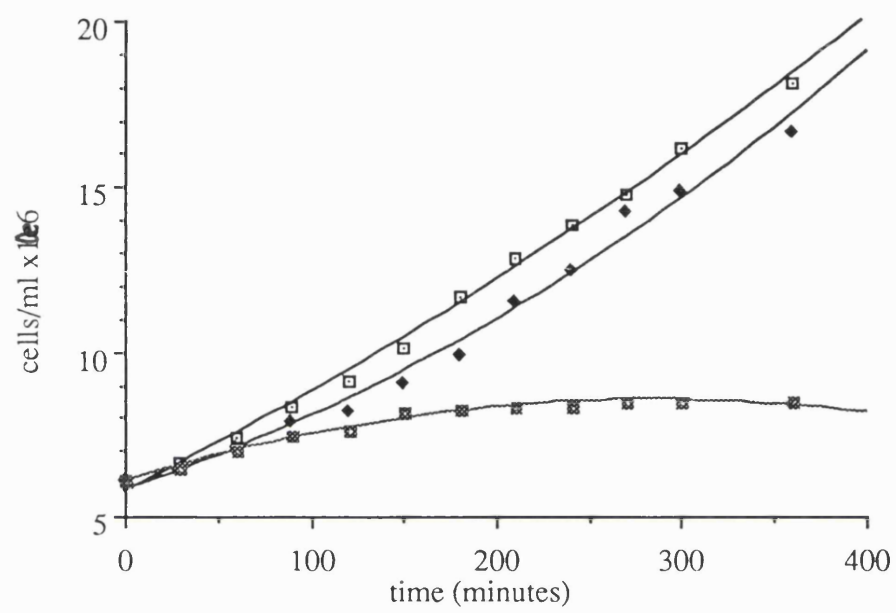
6.2. Results

6.2.1. Effect on growth

Brefeldin A from 0-200 µg/ml was added to log phase cells in suspension and the effect on cell number and growth monitored. Levels of 200 µg/ml completely inhibited cell growth and division (Fig. 6.1). Plated colonies were replica plated to YES plates containing levels of BFA of 0, 50, 100 and 200 µg/ml. The growth at 50 µg/ml was less than wild type but cells

Figure 6.1 The effect of BFA on growth

BFA, at various levels was added to log phase cells growing in rich medium. Cell growth was monitored by changes in OD_{595nm}. Levels assayed were 0 µg/ml (■), 20 µg/ml (♦) and 200 µg/ml (■).



were able to grow and form new colonies. At both 100 µg/ml and 200 µg/ml growth was completely abrogated. A level of BFA for future experiments was taken as 100 µg/ml since this was the lowest level tested that caused growth inhibition.

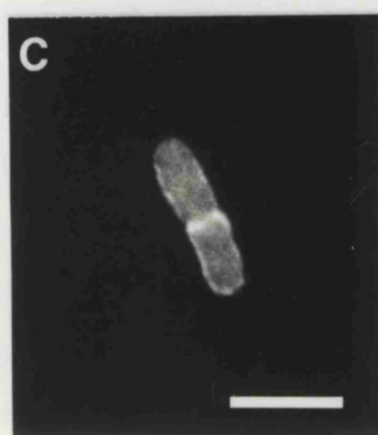
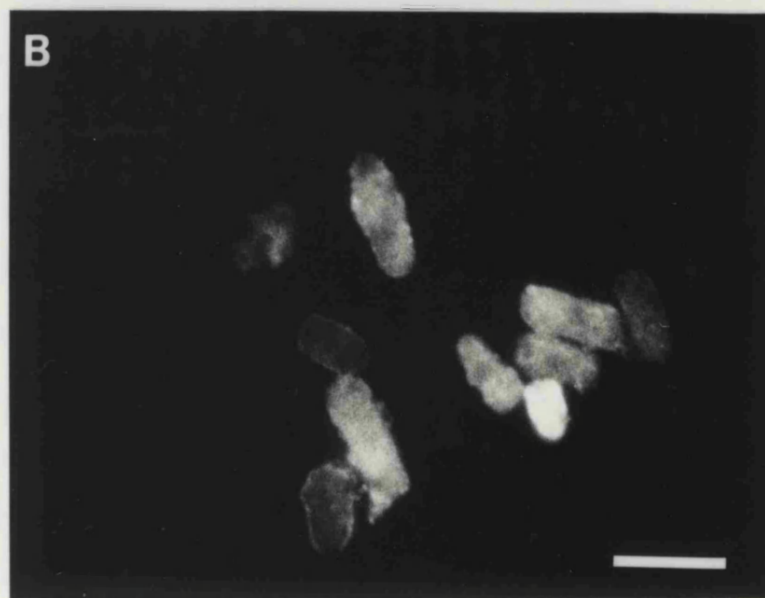
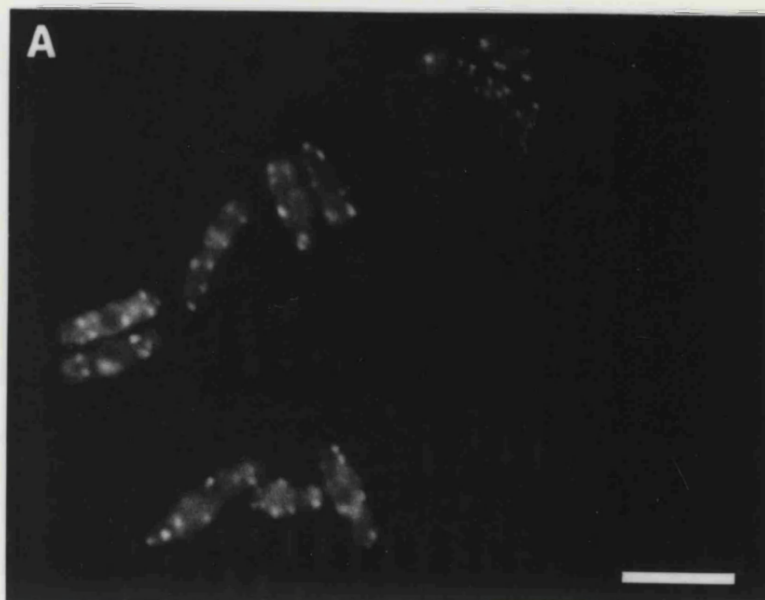
6.2.2 Immunofluorescence

BFA was added at 100 µg/ml to log phase cells and the cultures shaken for a further 3 hours. The cells were fixed and labelled with GTF2. The normal Golgi apparatus staining pattern of several spots per cell was not observed in cells treated with BFA. Instead, there was a much weaker stain mostly at the cell periphery (Fig. 6.2). Focusing through these cells gave the impression of a reticulum (Fig. 6.2C) with regular patterning such as that seen for the ER marker protein, BiP (Pidoux and Armstrong, 1992). However, there was no nuclear envelope staining nor was there any clear staining of the strands of internal ER which emanate from the nuclear envelope, cross the cytoplasm and link to the more extensive peripheral ER which underlies the plasma membrane. It was clear however that the compartment in which the marker protein was normally found had been severely disrupted to the extent that no punctate staining was seen after BFA treatment. It should be recognized that in this procedure only a single, or small number of related proteins are being recognized and their localization may not reflect that of all Golgi apparatus proteins.

The TAT1 antibody was also used to label cells and showed clear microtubules in the cytoplasm of the cells exposed to BFA. These looked the same as in untreated cells. (data not shown).

Figure 6.2 Immunofluorescence staining for the Golgi apparatus following BFA treatment

Log phase cells were treated for 3 hours with 100 $\mu\text{g/ml}$ BFA, then fixed using methanol and processed for immunofluorescence. Cells were labelled overnight with the primary antibody GTF2 against the Golgi marker protein, GalT. (A) shows untreated cells with characteristic punctate staining. (B,C,D) show cells treated with BFA. Note the increase in staining at the periphery of cells. Bars = 11 μm (A) and 9 μm (B,C,D).



6.2.3. Electron microscopy and quantitation

Log phase cells treated for either 1 hour or 3 hours with BFA were fixed in permanganate and observed by electron microscopy. The images obtained did not clarify the issue of what had become of the Golgi apparatus. After 1 hour there was a large number of rounded up, extended, beaded structures in cells. (Fig. 6.3 D,E) They bore a strong resemblance to membranes of the Golgi apparatus and in some cases the structures contained partial stacks. (Fig. 6.3 D) These, more beaded structures are sometimes seen in untreated cells though in far fewer cases. In untreated cells about 6% of Golgi observed in a population of 100 cells were similar to this form compared to 60% when cells were treated for 1 hour with BFA. After 3 hours some of these beaded structures were still seen though there was less Golgi membrane apparent in the cells.

These observations were quantitated by point counting from electron micrographs. As in previous cases the membranes assessed were Golgi stacks and membranes of the ER (nuclear envelope, peripheral ER and internal ER). It should be noted that unless the membranes were exactly juxtaposed, the dissector method of quantitation, which I used, would not recognize membranes derived from the Golgi apparatus as Golgi stacks but rather as internal ER which, as counted, included all lengths of membrane in cells which were not recognizably from another organelle *e.g.* mitochondria or vacuoles.

The results from the quantitation were clear. The level of stacked Golgi membrane fell from about 18% of membrane counted to 6% after 1 hour and 2% after 3 hours (Fig. 6.4). The shift from a stacked structure to a distended and distorted one and then to an apparent loss of the Golgi membrane was in part reflected in the quantitation of ER membrane. The level, particularly of internal ER increased as the stacks became

Figure 6.3. Electron microscopy of permanganate fixed cells pretreated with BFA.

Log phase cells were incubated for up to 3 hours in the absence^(A,C) or presence^(B,D,E,F) of 100 µg/ml BFA, fixed using permanganate and processed for e.m. (A, C) show a low and high magnification respectively, of untreated cells. (D,E) show distorted Golgi stacks after cells were exposed to the drug for 1 hour. (F) shows a highly fenestrated and tubular structure near the cell periphery which may be Golgi in origin. Bar = 1.2 µm (A,B); 0.3 µm (C-F).

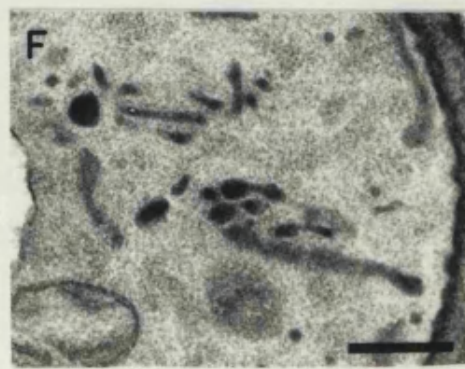
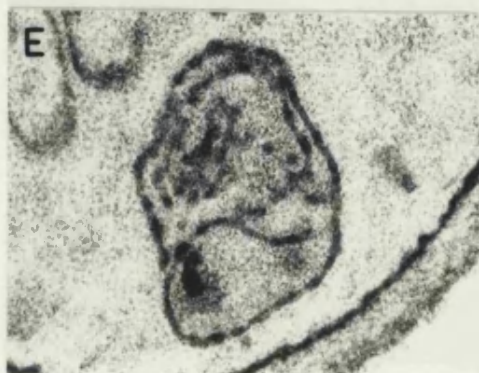
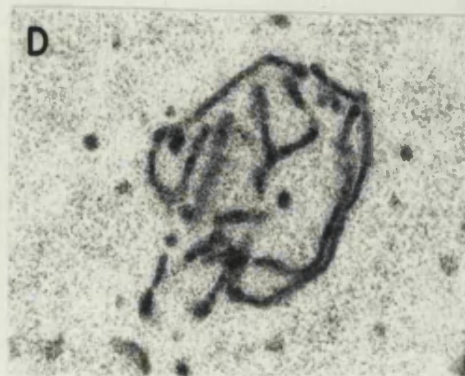
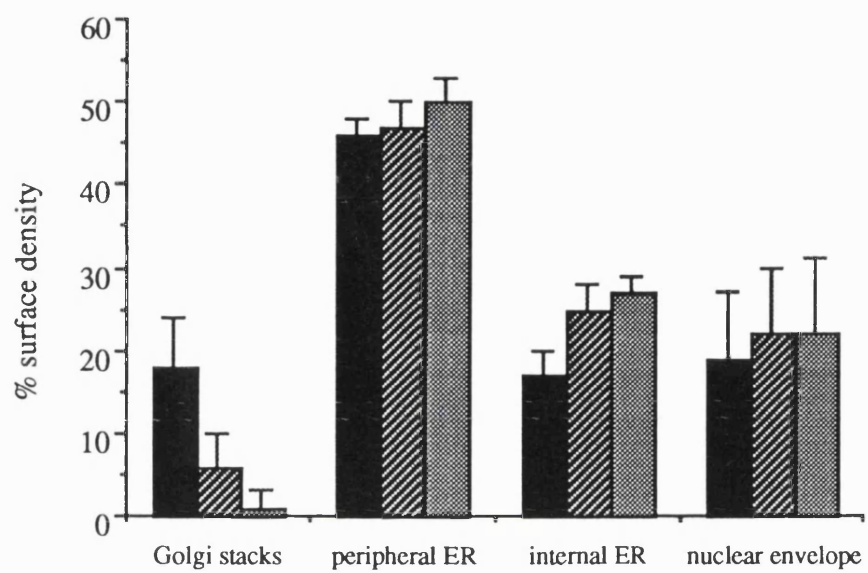


Figure 6.4. Quantitation of the effect of BFA on Golgi stacks and the ER.

Cells were grown to log phase and BFA added to 100 µg/ml. Samples were taken and fixed using permanganate. The fixed pellets were processed and embedded in Epon. Sections were cut and random electron micrographs taken and the state of the membranes in the cell sections quantitated. Samples were taken at 0 hours (■), 1 hour (▨), and 3 hours (▩) after addition of BFA.



dissociated from one another and formed extended beaded structures which would be scored as ER structures. The level remained high however, even when the beaded structures were no longer prevalent indicating the membrane was largely incorporated into existing ER structures. In fact the increase in the level of all ER membranes combined could account for the total loss of Golgi stack. This quantitation would suggest that the Golgi stacks break down via an intermediate of beaded, tubulovesicular structures and then somehow become incorporated into ER membranes.

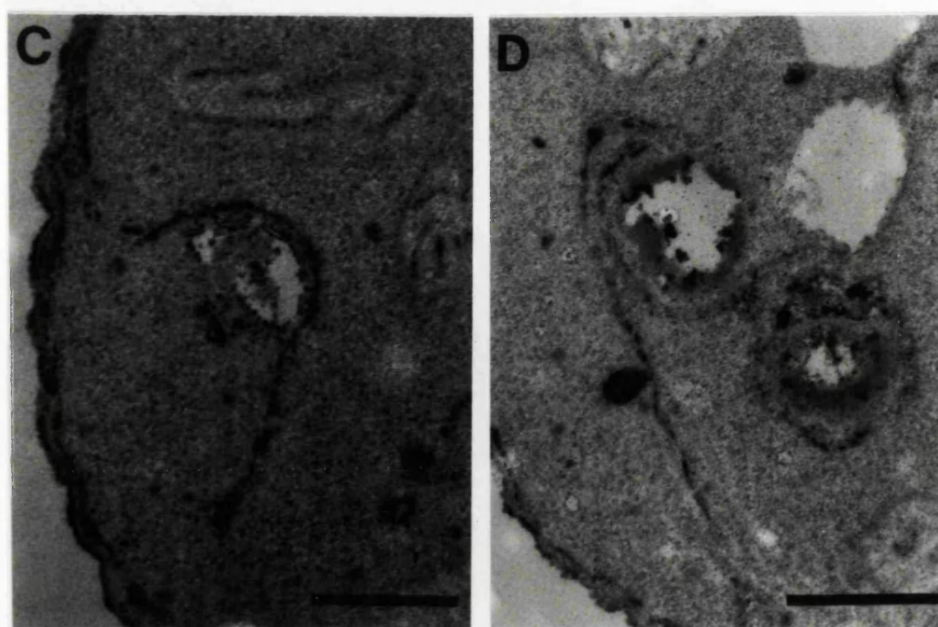
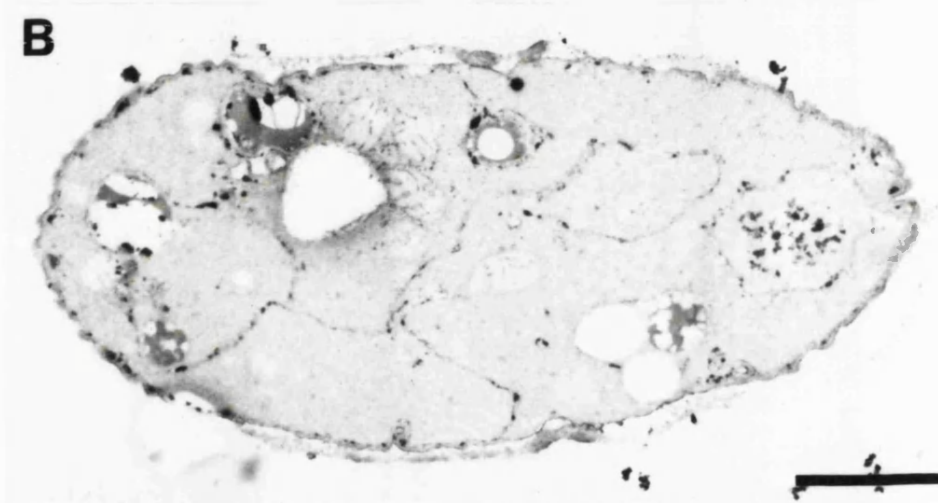
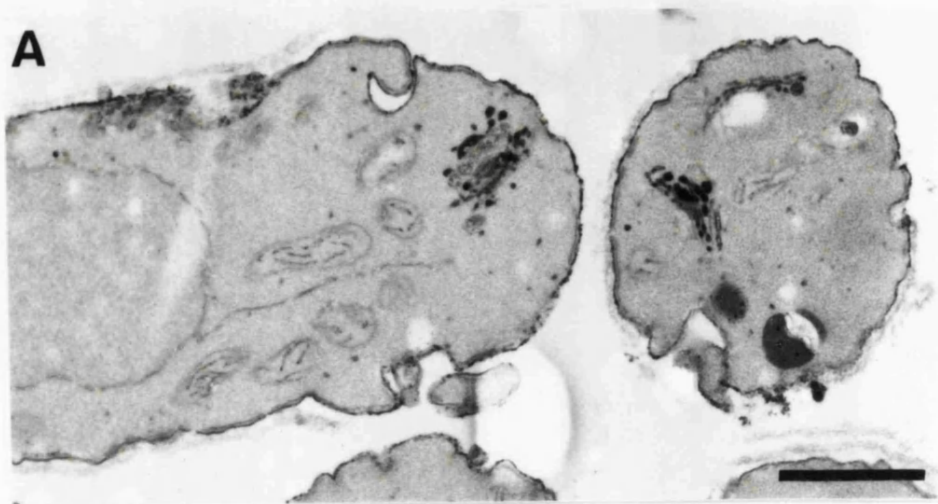
Other fixation techniques were used in an attempt to strengthen the impressions gained from the initial observations. Cells were again treated for 3 hours with 100 µg/ml BFA. When fixed with 3% PFA and 2% glutaraldehyde no stacks were seen at all. A few beaded structures were observed near the periphery of cells (data not shown). Using the fixative of 3% glutaraldehyde and 0.5% PFA the images obtained were very striking. The cells had been post fixed in osmium which in untreated cells stains the Golgi apparatus more heavily than other membranes. In the treated cells no Golgi stacks were observed at all (Fig. 6.5). Rather, strong staining was seen in the ER. Osmium staining was seen of lengths of membrane in the cell cytoplasm which was most likely to be internal ER, at the cell periphery and also of the nuclear envelope. It was difficult to discern any membrane which looked clearly Golgi derived since no membranes with dilated rims were seen. If the osmium was reflecting the position of any specific Golgi derived protein or lipid this result would suggest a relocation of certain of the Golgi components to the ER.

6.2.4. Reversibility of the BFA effect on the Golgi apparatus

The effect of BFA on both plant and mammalian systems is completely reversible. It was important therefore to test whether the changes induced

Figure 6.5. Electron microscopy of glutaraldehyde / paraformaldehyde fixed cells pretreated with BFA.

Log phase cells were incubated for 3 hours in the absence or presence of 100 $\mu\text{g/ml}$ BFA, fixed using 3% glutaraldehyde and 0.5% paraformaldehyde and processed for electron microscopy. A and B show pictures of whole cells in untreated and treated cultures, respectively. Whilst C and D show possible Golgi redistribution to the ER. Bar = 1.25 μm (A,B) = 0.3 μm (C,D)



in fission yeast were also reversible and not artefacts associated with very sick cells. It was also relevant because the levels of BFA used were high compared to those used on mammalian culture cells (100 µg/ml vs. 2-5 µg/ml) so the effects could just be due to extreme levels of the drug. Against this idea though were two points. One was that the levels used on the experiments in plants which were shown to be reversible used levels of 200 µg/ml BFA and also in fission yeast, levels of BFA greater than 50 µg/ml were required to have any marked effect on growth and by implication on secretion (see 6.2.1).

BFA at 100 µg/ml was added to log phase cells and incubated at 30°C for 3 hours. A sample was taken and permanganate fixed for electron microscopy. The cells were then washed free of BFA and resuspended in fresh medium. The cells were allowed to grow for a further 3 hours with shaking. After this time cells were taken and permanganate fixed.

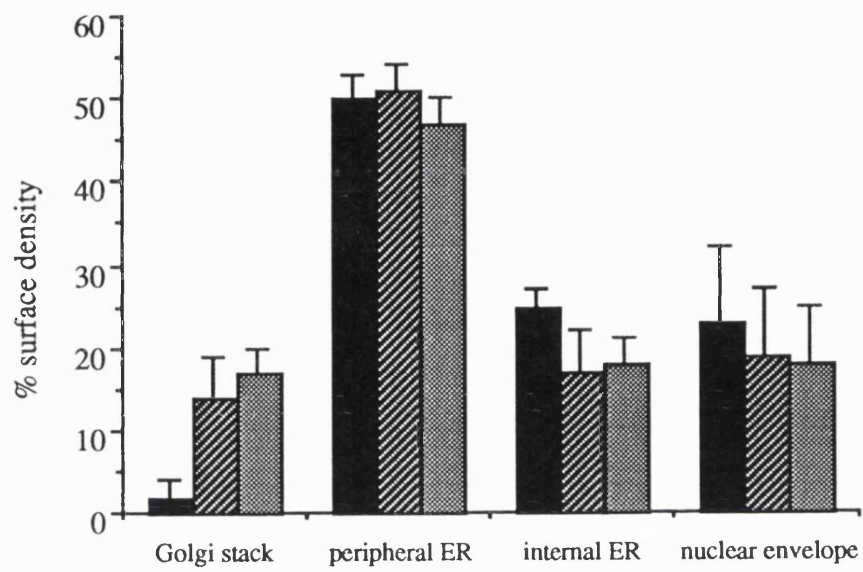
From observation of random fields of cells it was apparent that the effect of BFA was reversible since Golgi stacks could be seen. The electron microscopy was quantitated and is shown in figure 6.6. The level of stacked Golgi membrane was completely restored by 3 hours after removal of the drug. Following BFA treatment 2% of the membrane scored as Golgi stacks whereas after 3 hours in fresh medium the level was 18%. This was the same as the initial level of 18% in untreated cells.

6.2.5. Effect on Golgi marker proteins

The only marker protein that is available for the Golgi apparatus is that used previously, GalT. If the position of its activity were to change on a sucrose gradient it would imply that its position in the cell might also have changed. Cells were grown to log phase and BFA added at 100 µg/ml for 3

Figure 6.6. Quantitation of the reversibility of the BFA effect.

Log phase cells were treated for 3 hours with 100 $\mu\text{g/ml}$ BFA with shaking at 30°C. The cells were then pelleted, washed and resuspended in fresh medium in the absence of BFA. Samples were taken after this time and cells were fixed using permanganate and the samples processed for electron microscopy. Electron micrographs were taken at random and the level of Golgi and ER membrane in each quantitated. The samples assessed were taken at 0 hours (■), 2 hours (▨) and 3 hours (▩) after removal of BFA.



hours. Cell homogenates were then made and loaded onto gradients. The gradients were run overnight and fractions collected and their protein concentration, their sucrose level and their GalT activity measured.

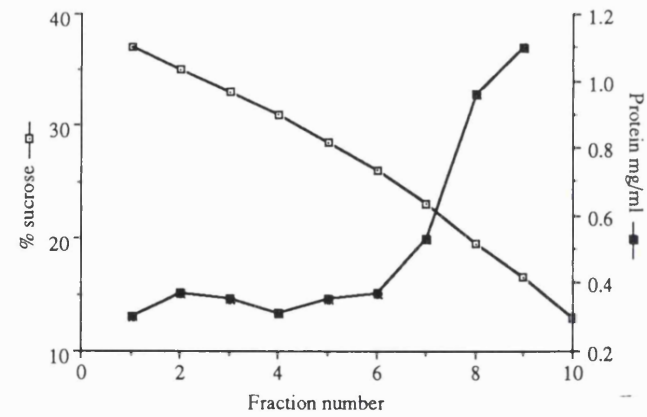
Untreated cells had two peaks of GalT activity at 28-29% and at 33% (Fig. 6.7A). The major peaks of GalT activity after BFA treatment were at 39-37% (Fig. 6.7B) and at 31%. A smaller peak at 24% sucrose was also noted.

To address whether the peak at a higher density co-localized with any other markers the fractions were run on gels and blotted. The ER resident protein BiP was probed for using a polyclonal antibody, JARM13. Control homogenate fractions were also run and blotted. The blots were analyzed by laser densitometry. Control samples for BiP had a peak at the highest density on the gradient of 37% and a second peak at 33% sucrose whereas the BFA sample had a predominant peak at 39-37% with a smaller peak at a much lower density of 20-24% sucrose. (Fig 6.7). By comparison with fractionation in *S.cerevisiae* (Antebi and Fink, 1992) the more dense peak was most likely to represent the ER. This suggested that in the control sample BiP was found in both the ER and in the more dense Golgi fraction whereas in the BFA treated homogenate it was predominantly in the ER and the Golgi peak was much reduced. The major peaks of GalT activity and BiP levels did not coincide in the untreated cells. However, after incubation with BFA the main GalT activity appeared to have shifted on the sucrose gradient and was recovered in a fraction which had the same density as the compartment where BiP was found, presumably the ER.

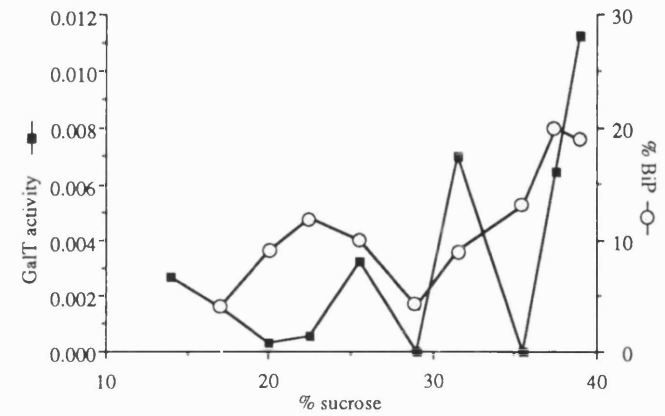
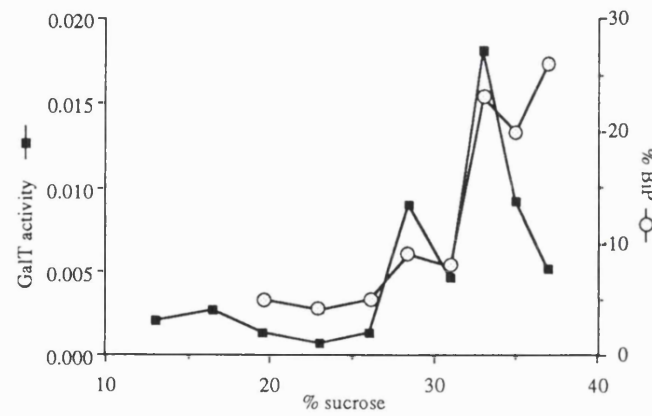
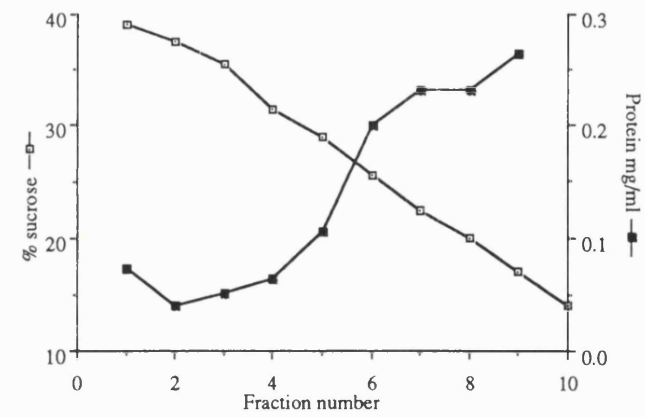
Figure 6.7. The effect of BFA on the localization of cell proteins

Cells were grown to log phase and then incubated in the absence (A) or presence (B) of BFA at 100 $\mu\text{g/ml}$ for 3 hours. Cell homogenates were then made and loaded onto gradients. The gradients were run overnight and fractions collected. Each fraction was measured for its protein concentration (\blacksquare), its sucrose density (\blacksquare), and its GalT activity (\blacksquare)(nmol/min/ μl). Samples of the fractions were loaded onto gels and these blotted and probed with antibodies against an ER resident protein, BiP. The levels of BiP in each sample were assessed by laser densitometry (\bigcirc).

(A) Control



(B) Brefeldin A



6.3. Discussion

These experiments demonstrated that Brefeldin A can induce a striking effect in the morphology of the Golgi apparatus in fission yeast cells. At the level of immunofluorescence, using antibodies to the Golgi protein, GalT, the normal punctate staining pattern was no longer observed. Instead a cytoplasmic staining was seen with more intense staining at the cell periphery. In many cases the staining at the periphery appeared to be reticular bearing some resemblance to the ER staining obtained with antibodies to the ER resident protein, BiP. However, the immunofluorescence pattern with this marker did not show staining of the nuclear envelope nor of the strands of ER which span the cytoplasm between the nuclear envelope and peripheral ER.

By electron microscopy, after 3 hours the stacks seemed to have completely disappeared. There did however appear to be a general change in Golgi morphology before they were no longer detected. In permanganate fixed cells, extended, beaded structures were seen in a large percentage of cell sections. These structures were reminiscent of the distorted Golgi stacks seen when maize cells were treated with similar levels of BFA (Satiat-Jeunemaitre and Hawes, 1992). The number of these distended Golgi then declined and after 3 hours few if any were seen. The stereology data suggest that much of the membrane may have been incorporated into the ER and there was a rise in levels of all ER quantitated. By analogy with the TBZ data (chapter 4) the rise in ER could be attributed to the Golgi stacks coming apart. However, observation of more than 200 cell sections indicated an increase in long membrane lengths rather than the short 'cisternal' lengths which were prevalent after TBZ treatment.

A second fixation technique which used osmium staining to enhance visualization of the Golgi apparatus showed a very striking change after treatment of cells with BFA. Golgi stacks were distinct entities before addition of the drug. However after 3 hours no stacks were seen but heavy staining of what appeared to be strands of ER in the cytoplasm, the nuclear envelope and the peripheral ER were apparent.

All methods are highly suggestive of Golgi breakdown with redistribution to the ER and so may highlight a similar mode of action of BFA in both yeast and mammalian cells. That the effect seems to be slower in fission yeast (hours rather than minutes) might be due to the involvement of microtubules. In mammalian cells there is an extensive microtubular network and membrane tubules can be seen to emanate from the Golgi cisternae along the microtubules towards the cell periphery and ultimately to the ER. In cells with disrupted microtubules the redistribution of markers to the ER is much slower. Maybe, the lack of a dense network of microtubules in *S.pombe* precludes their use in this retrograde pathway and so the whole process is more gradual. In this work the mechanism for retrieval, whether by a vesicular means or by tubules was not addressed.

The patterns of redistribution of Golgi markers in *S.pombe* also differed with GalT seemingly limited more to the periphery whilst osmium staining was found throughout the ER compartment. These disparities may reflect a preference for different subcompartments of the Golgi apparatus to redistribute to specific regions of the ER.

Chapter 7

Changes in the Golgi apparatus of mutant strains of *S.pombe*

1

7.1. Introduction

The ease of generating mutant yeast strains has been one of the great advantages of using these organisms. A mutation in a specific molecule can cause a pathway to become blocked and for the phenotypic effect of such a change to be observed. Genetic analysis of such mutations has provided valuable *in vivo* corroboration of some concepts derived from biochemical studies of mammalian intercompartmental transport *in vitro* (Clary, et al., 1990b; Kaiser and Schekman, 1990; Rothman and Orci, 1992; Wilson, et al., 1989). Other mutations have defined unrecognized activities (Hicke and Schekman, 1989; Semenza, et al., 1990).

Originally, most mutations were made by exposing populations of cells to mutagens and then selecting for certain phenotypic changes. This approach is essential to create mutations in new genes. If, however, the gene of interest has already been cloned by another method specific mutations can be made in the coding sequence to generate point mutations at certain sites. This latter approach allows genes to be mutated without the need for a recognizable phenotype.

The mutant strains that I used were largely generated by wholesale mutation followed by phenotypic screening. For example in *S.pombe*, *nda3* (Chapter 4) was selected for by isolating cold sensitive mutant strains which were defective in their partitioning of nuclear material; *cdc* mutants (section 7.3) were found by a screen for temperature sensitive strains which grew to an abnormally long length without dividing, indicating a defective cell cycle. The mutant, *ypt1-1*, (section 7.2), on the other hand was generated by replacing the normal *ypt1* gene with a specifically mutated form of the gene.

Several mutant strains were studied in the course of my work to see whether the changes the mutations imposed on the cell by blocking certain pathways, in any way interfered with the morphology of the Golgi apparatus.

7.2. Secretory mutants

7.2.1. Background

Mutations in the secretory pathway might be expected either to have an effect on, or to directly involve the Golgi apparatus, since this is a major organelle in the pathway.

The secretory pathway has been studied in far more detail in the yeast, *S.cerevisiae* than in *S.pombe* and the genetics of the pathway are more fully discussed in section 1.5.2. Many mutants of secretion (called *sec* mutants) have been isolated and some of these *sec* mutants caused the accumulation of membrane in cells, which on occasion had the appearance of Golgi membrane. In particular, *sec7* seemed to cause a defect associated with the Golgi apparatus (Novick, et al., 1981; Franzusoff and Schekman, 1989). However, changes associated with the Golgi were not always easy to discern because of the problems of identifying this organelle in wild type cells of *S.cerevisiae*.

Far fewer secretory mutants have been found in *S.pombe* and no successful screen for a full range of such mutants has been performed. Most mutants defective in the secretory pathway are associated with the small GTP-binding proteins. Several of the *rab/ypt* family of genes have been isolated in *S.pombe* mostly by cloning homologues of *S.cerevisiae* or mammalian counterparts (Miyake and Yamamoto, 1990; Fawell, et al.,

1992) and these have in some cases been shown to affect specific stages of secretion.

YPT1 has been studied in *S.cerevisiae* and mutations in this gene cause a phenotype reminiscent of early secretion defective mutants, including accumulation of membranes and vesicles as well as a defect in secretion and incomplete glycosylation of invertase (Segev, et al., 1988; Becker, et al., 1991). Immunofluorescence against the YPT1 protein showed punctate staining which was changed in the *sec7* mutant at the non-permissive temperature, indicating it was associated with the Golgi apparatus (Segev, et al., 1988).

A temperature sensitive conditional mutation was made by Mark Craighead (in the laboratory) in the yeast strain 556 (^{leu1-32 ade6-M216 ura4-D18} ~~leu⁻ ade⁻ his⁻~~ h⁺). The gene, *ypt1* was specifically targeted and replaced by a copy of the gene which had a point mutation in the GTP binding site such that it was unable to function at the restrictive temperature of 37°C. The strain carrying the mutant allele was named *ypt1-1*. I used this strain to investigate changes in the Golgi apparatus when the secretory pathway was disrupted at this early stage.

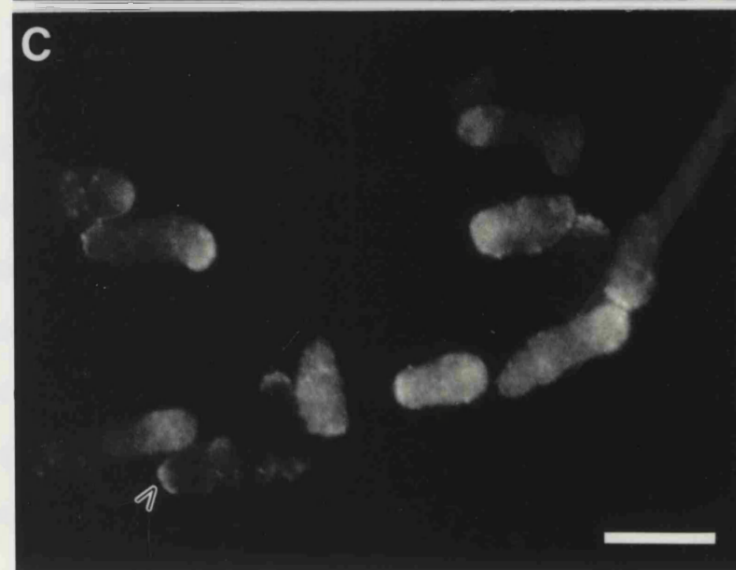
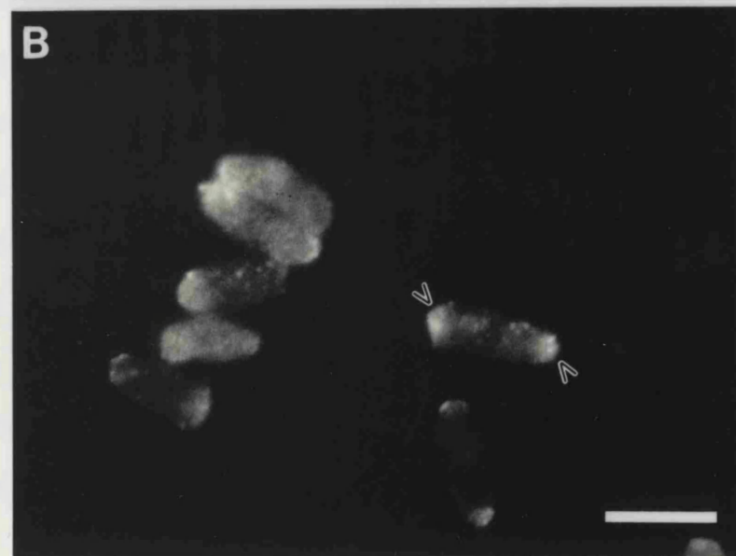
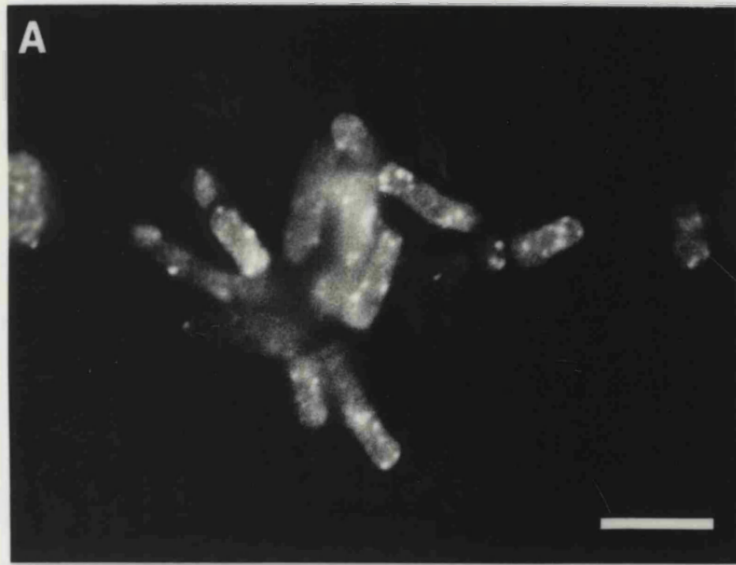
7.2.2. Results

Immunofluorescence staining of ypt1-1 cells.

Cells were grown at the permissive temperature overnight. Half of the culture was then shifted to the restrictive temperature for 4 hours. Cells were fixed and processed for e.m. The mutant cells were fatter and slightly longer than wild type cells at all temperatures and this phenotype was more exaggerated at 37°C. Staining for the Golgi marker protein, GalT gave a very striking change between 30°C and 37°C. Figure 7.1A shows the staining in cells at 30°C. It resembles that found in wild type cells with

Figure 7.1 The effect of a temperature shift on *ypt1-1* cells

Ypt1-1 cells were grown at the permissive temperature overnight into log phase. The culture was then shifted to the restrictive temperature for 4 hours. Samples were taken before and after the shift and fixed in methanol before processing for immunofluorescence. Cells were labelled using the GTF antibodies. (A) shows cells at 30°C with a disperse and punctate staining pattern. (B,C) show cells after 4 hours at the restrictive temperature. Note the decrease in the number of discrete spots and the increase in end labelled cells. Bar = 10 µm



several spots in each cell. There were between 7 and 15 'spots' counted per cell in a population of 100 cells. However, at 37°C (Fig. 7.1B,C) the punctate stain was mostly absent and instead there was a weak cytoplasmic stain often with intense staining at one or both ends of the cell. The end staining reflects the positions in the cell where secretory traffic would normally be targeted.

Electron microscopy and quantitation of the effect.

To gain a more detailed insight into the changes noted by immunofluorescence *ypt1-1* cells were grown to log phase and half of the culture shifted to 37°C for four hours. Cells were then fixed in permanganate and processed for e.m. At the non-restrictive temperature Golgi stacks could be seen in many cell sections (Fig. 7.2A). After 4 hours at the restrictive temperature few Golgi stacks could be seen at all (Fig. 7.2B). Some structures which were not normally apparent in cells could be seen. These were small membrane bound organelles with a profile diameter of 100-250 nm. Their function and origin have not been further investigated.

The changes observed were quantitated using the stereological grid method. Figure 7.3 shows the changes in the level of ER and stacked Golgi in cells. The level of Golgi stack fell substantially from 14% of the membrane quantitated at 30°C to 2% after 4 hours at the non-permissive temperature. Other membranes were not altered to this extent. The levels of nuclear envelope and peripheral ER were barely changed whilst the slight increase in internal ER was not sufficient to account for the loss of membrane from the Golgi apparatus. The overall level of membrane quantitated fell by 9% indicating that most of the Golgi material was not redistributing to organelles which could be quantitated using these methods.

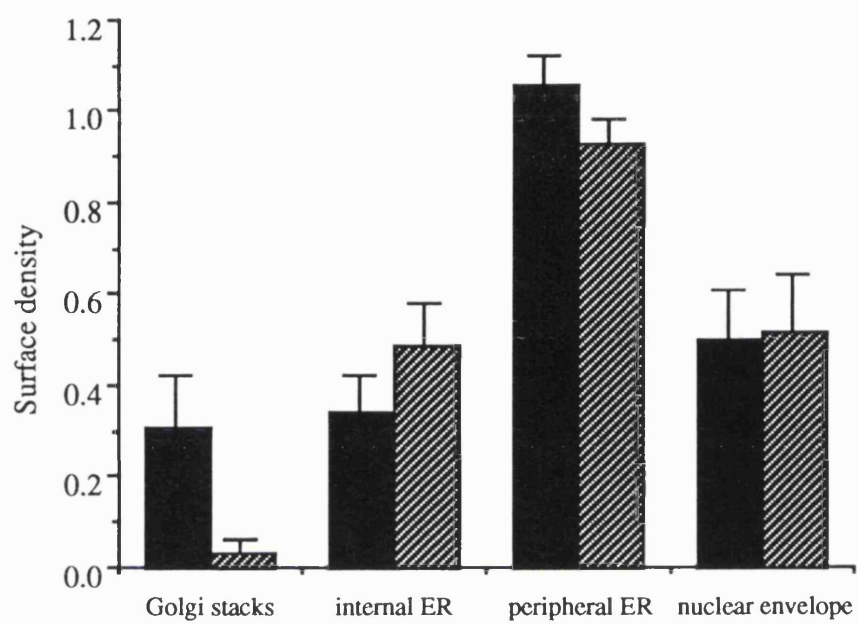
Figure 7.2. Electron microscopy of permanganate fixed *ypt1-1* cells at the permissive and restrictive temperatures

Cells were grown at the permissive temperature of 30°C overnight and then half of the culture was shifted for 4 hours to the restrictive temperature of 37°C. Cells were then fixed using permanganate and processed for e.m. (A) shows a cell at the permissive temperature whilst (B) shows the effect of a shift to 37°C. Golgi stacks and the organelles which appear after the temperature shift are denoted by G and O respectively. Bar = 0.75 µm



Figure 7.3 The surface density of Golgi stacks and ER in *ypt1-1* cells

Ypt1-1 cells were grown to log phase and half the culture shifted to the restrictive temperature for 4 hours. Samples were taken from the culture at 30°C (■) and that at 37°C (▨) and fixed using permanganate. The fixed pellets were processed and embedded in Epon. Sections were cut and random electron micrographs taken and the state of the membranes in the cell sections quantitated. Note the reduction in the level of Golgi stacks after shifting cells to 37°C.



7.2.3. Discussion

A block in secretion at an early stage of the secretory pathway caused the Golgi apparatus in *S.pombe* to disassemble. By immunofluorescence the normal punctate staining pattern was disrupted and instead there was a low level cytoplasmic stain with intense staining towards the ends of cells. By e.m stacks of Golgi cisternae were scarce and quantitation from electron micrographs indicated that the Golgi apparatus had virtually disappeared. The material did not seem to be redistributing to the ER since these membrane systems did not show sufficient increase to account for the loss of Golgi membrane.

The immunofluorescence staining pattern resembled most closely a vesicular staining pattern such as that seen in mammalian cells after cells have entered metaphase (Burke et al. 1982). The staining of one or both ends of the cell indicated that vesicles or fragments of the Golgi apparatus were generated and then possibly being transported along normal membrane traffic routes to the points of growth in cells. Cells in the sample which were early in the cell cycle would only have been secreting from one end of the cell, whereas those cells which had passed the NETO (new end take off) point in the cell cycle would have had both ends stained.

The simplest model to explain the observations is that *ypt1* is involved in co-ordinating certain fusion events at some post-ER stage. When the mutant form is expressed vesicles continue to bud but are unable to fuse at the next step. Eventually the Golgi apparatus buds itself away.

This model is very similar to that proposed to explain the effects of CHX on the Golgi apparatus (Chapter 5, Fig. 5.10). The only significant

difference between the outcomes of the two treatments was in the pattern of immunofluorescence staining. With CHX there was no evidence of end labelling indicating no targeting of the vesicles.

This could easily be explained if, in the CHX model the proposed labile component of fusion was normally associated with molecules responsible for targeting. If the fusion component was depleted the targeting molecule could no longer bind to vesicles and they would remain disperse in the cytoplasm.

In the case of ypt1 the most likely function it might have in the pathway would be in GTP hydrolysis to allow a specific step of fusion to proceed (Bacon, et al., 1989). If it was unable to perform this step then no fusion could occur at this site. Vesicles would therefore accumulate. Molecules related to ypt1 may be able to bind weakly to the vesicles and allow some level of targeting in cells, e.g. to the plasma membrane. The association would not however, be strong enough or sufficiently specific to permit fusion.

7.3. Cell cycle mutants

7.3.1. Background

In mammalian cells the most dramatic morphological change associated with the Golgi apparatus is at entry into mitosis. The Golgi apparatus breaks down firstly into small stacks at prophase and this is followed by a complete vesiculation by metaphase (Maul and Brinkley, 1970; Colman, et al., 1985; Sathananthan, et al., 1985; Warren, 1993). The Golgi remains in this state until after anaphase when it reassembles (Lucocq, et al., 1989). Cells can be blocked in metaphase by incubating cells in the presence of

nocodazole, which prevents formation of the mitotic spindle (Zieve, et al., 1980), and the breakdown products of the Golgi apparatus studied. My work using the related drug, thiabendazole is recorded in chapter 4. That work indicated that there was no breakdown into small stacks nor vesiculation after its removal. However, a system not using drugs could provide complementary evidence for the maintenance of stacks in the normal cell cycle.

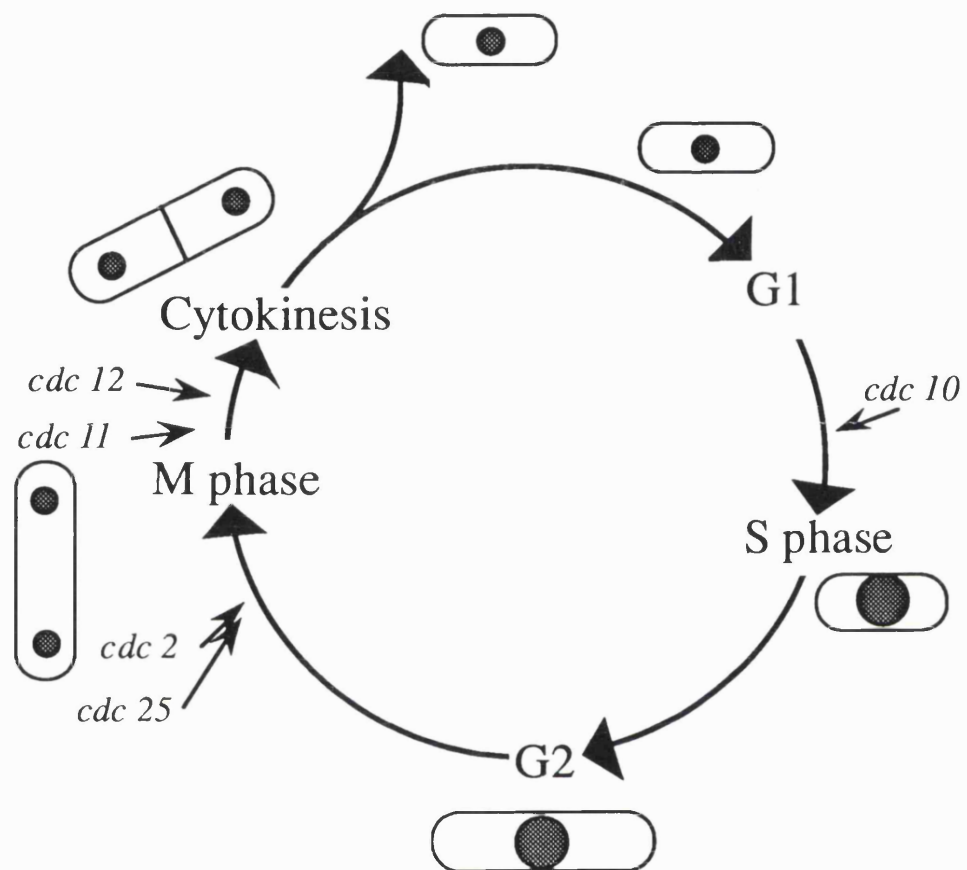
The use of cell cycle mutants also allowed another point of interest to be addressed. This was concerned with the growth and production of new organelles. It was not clear whether the number of Golgi stacks depended on the volume of the cell, and so as cells grew more Golgi stacks would be generated, or whether there was a specific point in the cell cycle at which all new Golgi material would be synthesized and the number of Golgi stacks doubled. The work mentioned in Chapter 3 (see Fig. 3.6) suggested that the number of Golgi stacks increased with cell size. However, the classes of cells distinguishable from each other i.e. just divided, nuclei condensed but septum not formed, and nuclei divided and septum virtually formed, did not account for much of the cell cycle, only for early G1, early mitosis and late mitosis/cytokinesis. By using various cell cycle mutants the stages of the cycle that could be distinguished was greater.

The cell division cycle (*cdc*) mutants were isolated as recessive temperature sensitive mutants which were unable to complete the cell division cycle at the restrictive temperature (Nurse, et al., 1976). The original mutants defined genes involved in nuclear division, septum formation and DNA synthesis.

I used a range of *cdc* mutants (see Fig. 7.4 for the point in the cell cycle at which they act) to try and discern whether blocks in the pathway affected the number or the morphology of the Golgi stacks in cells.

Figure 7.4 The cell cycle in *S.pombe*

The cell cycle in *S.pombe* is comprised of distinct G1, S, G2 and M phases. A class of mutant was found which was unable to divide due to a block in its cell cycle. The position at which some of these cell division cycle (*cdc*) mutants block is marked on this schematic diagram.



7.3.2. Results

Immunofluorescence of cdc mutants

Mutants blocking in G1 (*cdc10*), late G2 (*cdc2*) and between mitosis and cytokinesis (*cdc11*) were selected to look at the number of Golgi stacks in cells when they were shifted to the non-permissive temperature. Figure 7.5 shows immunofluorescence staining for GalT in the cells after 4 hours at 36°C. In all cases there were more spots representing Golgi stacks than in wild type cells or than at the permissive temperature (data not shown). Thus when cells were blocked the number of Golgi stacks did not remain static but increased regardless of the point of inhibition.

The number of Golgi 'spots' in cells was counted for these mutants at the permissive and restrictive temperatures. Figure 7.6 shows the average number of stacks in the different mutants. In all cases as the cell size increased, so the number of Golgi stacks was augmented. The number of stacks in the *cdc10* mutants was slightly less but this was reflected in their size, being somewhat smaller than either *cdc2* or *cdc11* after 4 hours at the non-permissive temperature.

Electron microscopy of cdc mutants

Several mutants were selected to look for morphological changes associated with mitosis. Initially, mutants *cdc2* (late G2), *cdc11* (early septation), and *cdc12* (late septation) were chosen to represent various stages before and after mitosis. Cells were grown at the permissive temperature and shifted for 4 hours to 36°C, then fixed using permanganate. The cisternae in cells ($n \geq 100$) were then scored for their association with other cisternae. Using these mutants there were no striking difference when compared to wild type cells at the same

Figure 7.5. Staining for the Golgi apparatus in *cdc* mutants

Various *cdc* mutant strains were grown at 25°C overnight to log phase. These were then shifted to the non-permissive temperature of 36°C for 4 hours to allow the mutant phenotype to be expressed. Cells were then fixed and processed for immunofluorescence. Cells were labelled with the antibody against the Golgi marker protein, GalT. (A) *cdc2* which blocks in late G2 (B) *cdc10* which blocks in G1 (C) *cdc11* which blocks early in septum formation. Bar = 12 µm

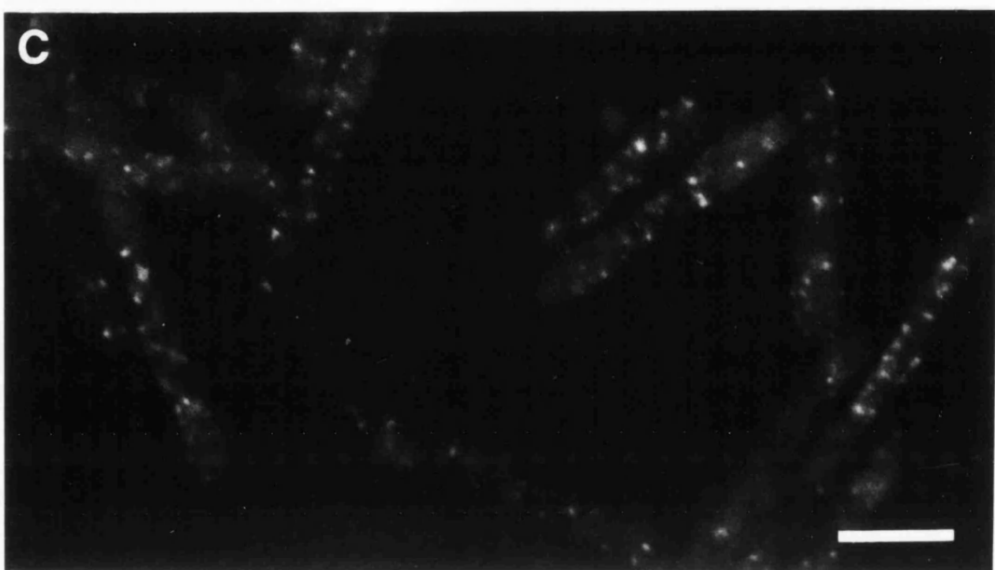
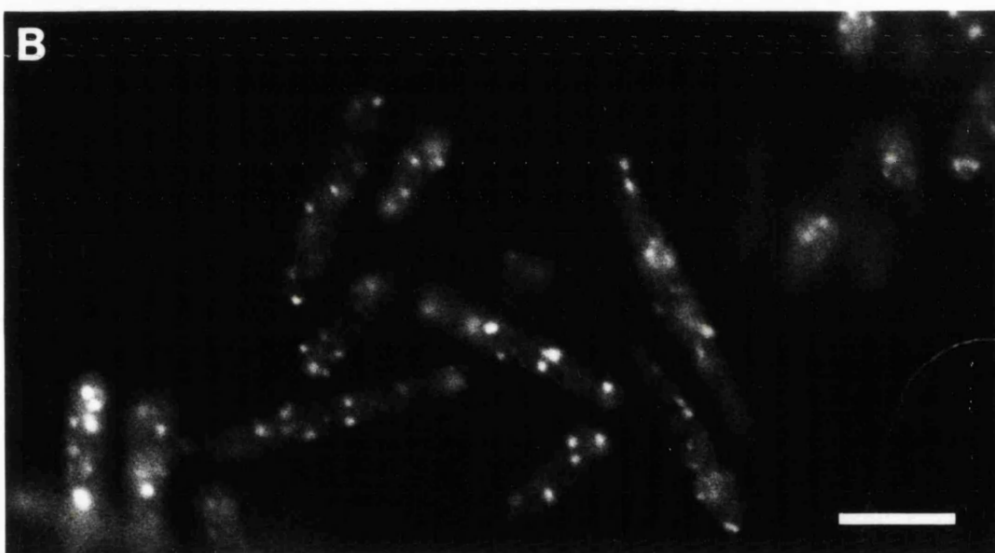
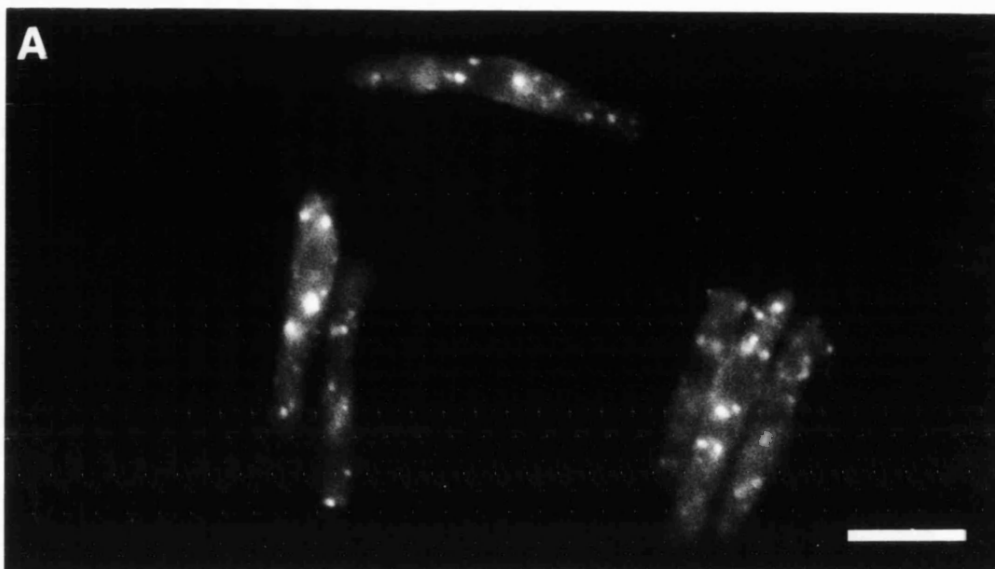
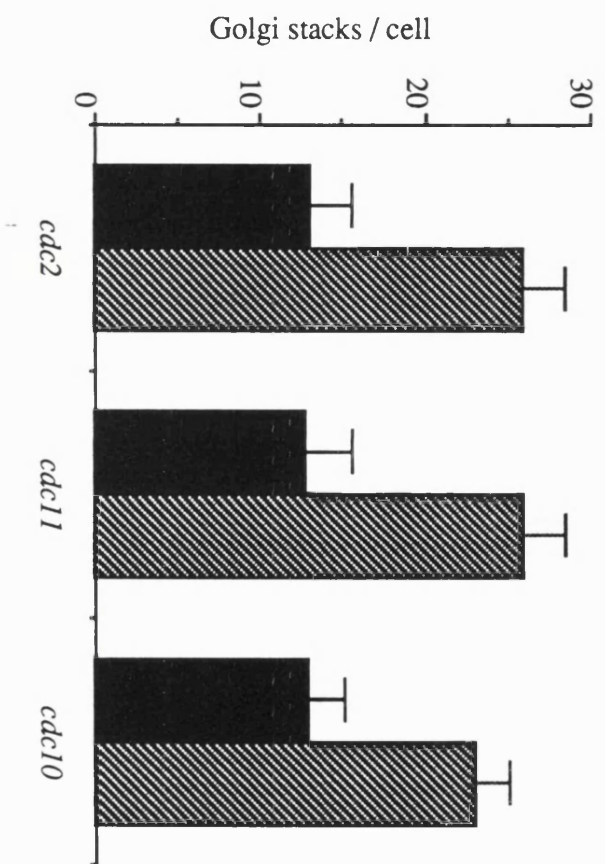


Figure 7.6 Comparison between the number of Golgi stacks at the permissive and restrictive temperature for certain *cdc* mutants.

The *cdc* strains, *cdc2*, *cdc11* and *cdc10* were grown at the permissive temperature (■) and then shifted^{for 4 hours} to the restrictive temperature (▨). Cells were fixed and processed for immunofluorescence. Cells were labelled using the GTF antibody. Golgi stacks in cells were counted by focusing through cells. The number of Golgi stacks per cell was recorded.



temperature (Fig. 7.7).

One mutant which was particularly useful for the problem of cells entering mitosis was *cdc25*. This strain blocks tightly when cells are shifted to 36°C and cells are released with reasonable synchrony when the culture is returned to the permissive temperature (MacNeill and Nurse, 1989). This mutant was used in a time course to monitor any changes as cells passed from late G2 (the point of the *cdc25* block), into mitosis. As shown in figure 7.8, there was a slight effect on the Golgi apparatus on release from the block. The level of stacking fell from an initial level of 17% quantitated membrane to only 9%. The level of stack remained fairly low until about half an hour after the release when it was almost back at the original level. This period of time corresponds to the cells entering and proceeding through mitosis. By 60 minutes the cells had fully formed septa or had just undergone cytokinesis.

7.3.3. Discussion

The data showed that there was an effect on the Golgi apparatus associated with cells entering mitosis. However, the period spent in mitosis is relatively short so any disassembly whether into vesicles or to single cisternae would be unlikely to be observed at the level of immunofluorescence. It was not clear whether the Golgi apparatus was unstacking or vesiculating since the breakdown was only partial and would be difficult to quantitate with the methods developed. Possibly, changes would be quantifiable if a much smaller grid was used for the stereology but since it was clear that some stacks persisted and there was no total Golgi apparatus breakdown as found with mammalian cells, I did not pursue this investigation further. One point of interest is that during

Figure 7.7 The effect of a cell cycle block on Golgi apparatus morphology

cdc strains which block near mitosis were grown to log phase and then shifted to the restrictive temperature. After 4 hours cells were fixed using permanganate and processed for e.m. Random cells were observed and the cisternae in each cell counted and scored as to the size of Golgi stack in which they were found. Strains observed were *cdc2* (G2/M block), *cdc11* (early septation block), and *cdc12* (late septation block).

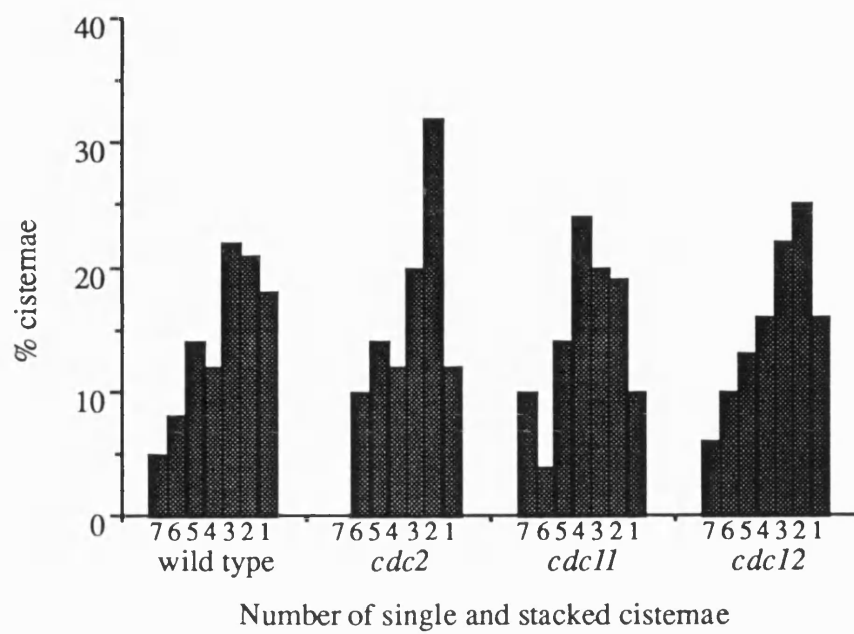
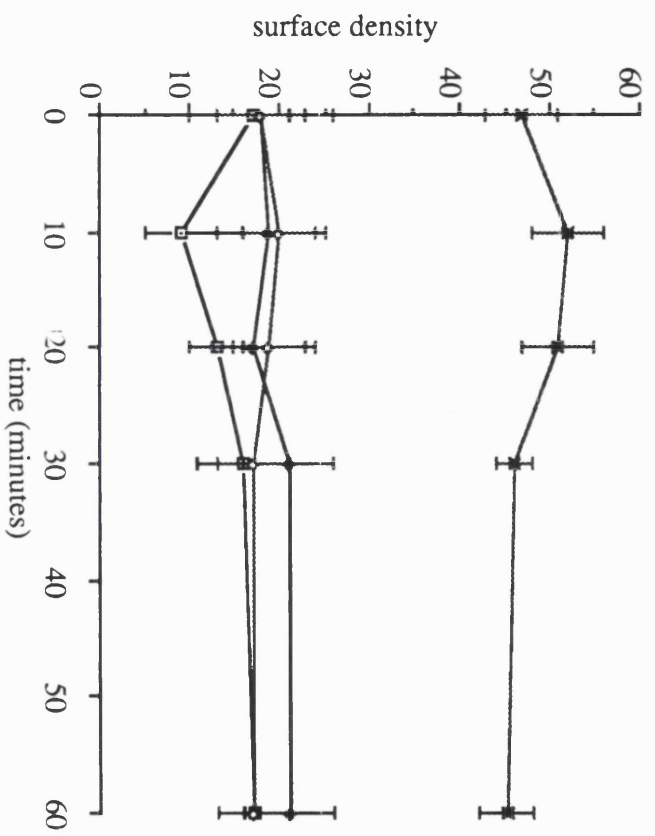


Figure 7.8 Quantitation of the surface density of ER and Golgi membranes in *cdc25* cells after release from a 36°C block.

cdc25 cells were grown to log phase and then shifted to the restrictive temperature of 36°C for 4 hours. The culture was then shifted back to the permissive temperature and samples taken over the next 60 minutes. Cells were fixed using permanganate and processed for e.m. Micrographs were taken of random sections and analysed using the disector, for Golgi stack (■), nuclear envelope (◆), peripheral ER (×), and internal ER (◇).



mitosis there would be a lack of cytoplasmic microtubules, a factor already shown to affect Golgi stacking (chapter 4). The level of breakdown over this period of entry into mitosis was comparable to the level of disruption in the first 20-30 minutes after TBZ addition.

Chapter 8

Recognition of the Golgi apparatus in *S.pombe* by antibodies raised to mammalian Golgi structures

8.1. Introduction

Most of the work discussed thus far indicates that the Golgi apparatus in *S.pombe* does not behave in the same manner as the Golgi of mammalian cells when challenged with certain drugs or in response to physiological changes associated with the cell cycle. It remains however, that the Golgi apparatus in both has a distinct stacked structure and certain aspects of this structure may be expected to have been conserved.

A different approach was taken to see whether certain structural components of the Golgi apparatus were preserved between the organelle in rat liver cells and in fission yeast.

An antibody was raised, by Paul Slusarewicz in the laboratory, against a preparation of rat liver Golgi which had been extracted with Triton-X100. The extraction procedure was monitored by electron microscopy and after the Triton treatment some Golgi-like structures remained. It was proposed that these structures could be some sort of proteinaceous matrix involved in Golgi stacking. Further experiments have now shown that this matrix binds medial Golgi enzymes from rat liver Golgi homogenates. A polyclonal antiserum (TEX, Triton extracted) was raised to the structures and used in immunofluorescence on mammalian cells. The pattern of staining was shown, by co-localization with known markers, to be of the Golgi apparatus.

The results described in this chapter are the observations made using the TEX antibody on fission yeast cells.

8.2. Results

8.2.1. Western Blotting

Homogenates were made from log phase wild type cells. These were separated on a 10% gel and blotted. Homogenates were probed with the preimmune serum and with the TEX immune serum (third bleed) at a dilution of 1 in 50.

Figure 8.1 shows the bands obtained on these blots. Several bands were seen with the preimmune and immune serum. The clear band at 40kDa and the fainter bands at 95kDa and 130kDa were not detected using the preimmune serum showing them to be specific.

The blot was repeated several times on different homogenate preparations. On all occasions the same pattern of banding was seen though the weaker bands varied in intensity.

8.2.2. Immunofluorescence microscopy

Since at least one specific protein was recognized on a blot it was of interest whether the pattern of staining would resemble that seen with the GTF antibodies against the fission yeast Golgi marker, GalT.

Log phase cells were fixed using methanol and, after blocking the cells were incubated with the antibody at a range of dilutions overnight (1 in 10 to 1 in 500). Secondary antibodies were applied (rhodamine-conjugated goat anti rabbit) before the cells were washed and mounted. Figure 8.2A shows the staining pattern obtained with the antibody used at 1 in 25 dilution. The staining is punctate and there are several spots labelled in each cell. The level of staining was good and the spots were clearly discrete. The background staining in the cell was slightly higher but in

Figure 8.1. Western blotting *S.pombe* homogenates with TEX.

Homogenates were prepared from log phase cells and run out on SDS PAGE. The gels were blotted and after blocking of non-specific sites were incubated with the TEX antibody (1:50 dilution). Bands were detected using the p-nitro blue tetrazolium / 5-bromo,4-chloro,3-imidoyl phosphate system with alkaline phosphatase conjugated secondary antibodies. Arrows show bands recognized by the TEX immune serum but not with the preimmune serum.

1

Figure 8.1 Blotting *S.pombe* homogenates with the TEX1 antiserum

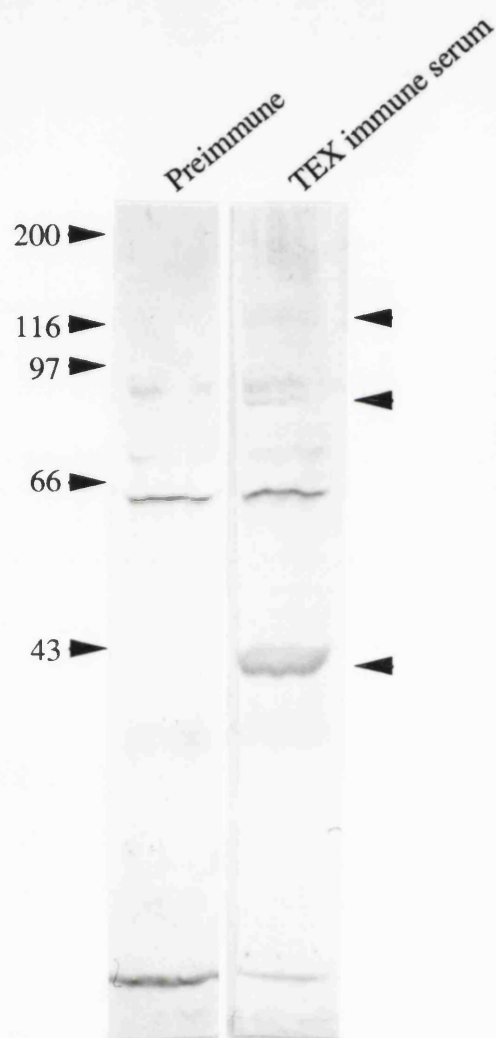
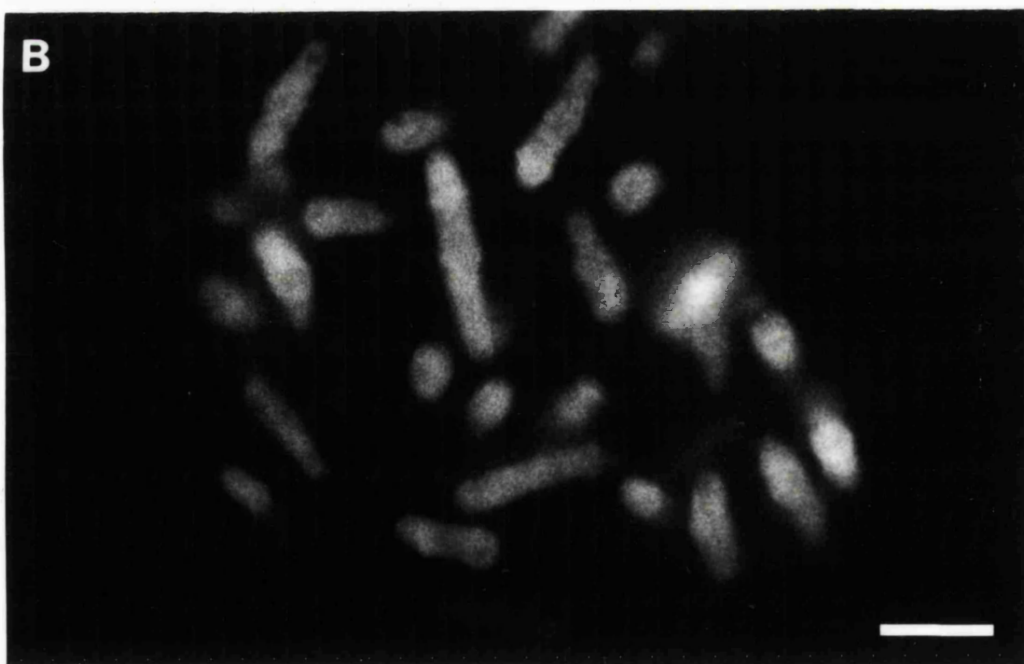
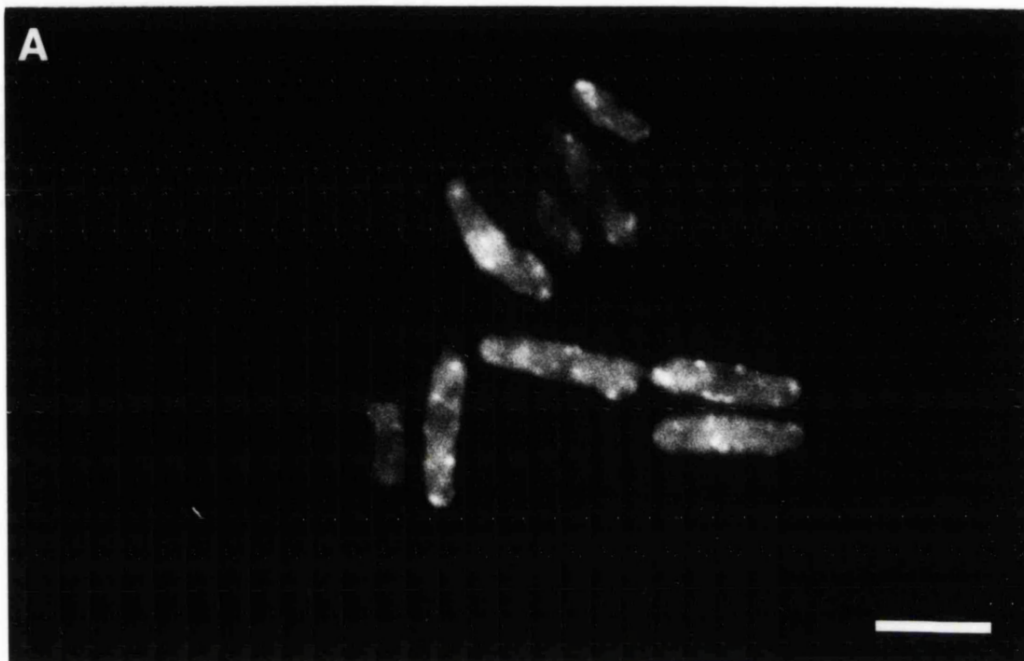


Figure 8.2. Immunofluorescence with the TEX antiserum on wild type cells.

Log phase cells were fixed and processed for immunofluorescence. Cells were incubated overnight with the TEX antiserum at 1 in 25 dilution (A) or with the preimmune serum (B). After washing the antibodies were incubated with rhodamine-conjugated secondary antibodies. Bar = 10 μ m



other respects the staining was similar to that obtained using GTF antibodies (Fig. 3.6).

The pattern of staining was highly suggestive of the antibodies recognizing a specific Golgi apparatus component. As a test of specificity the cells were also labelled with the preimmune serum at a range of concentrations from 1 in 10 to 1 in 500 dilution (Fig. 8.2B).

8.2.3. Factors affecting the TEX staining pattern

Since the staining does appear to be specific for the Golgi apparatus it was intriguing to discover whether factors affecting the GTF staining pattern would also disrupt that of the TEX antibodies. Two conditions that were investigated in the course of the study had a dramatic impact on the staining as seen by immunofluorescence. These were, the addition of inhibitors of protein synthesis (cycloheximide and anisomycin), and a temperature shift in the secretory mutant *ypt1-1* from 30°C to 37°C.

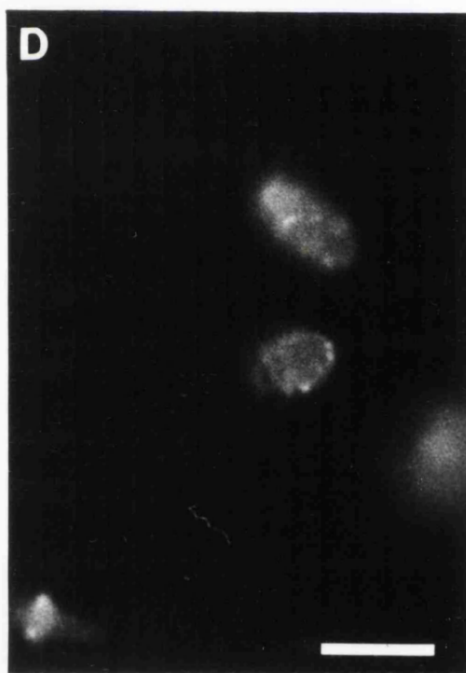
Effect of protein synthesis inhibitors.

Cells were grown to log phase and both CHX and ANS separately added at 100 µg/ml for a 3 hour period to cultures. Cells were routinely fixed and incubated with TEX antibody (1 in 25 dilution). When this antibody was used to label cells pre-treated with cycloheximide or anisomycin the usual staining pattern was no longer observed. After incubation with the antibiotics there were few if any discrete spots in cells (Fig. 8.3A). The control samples in the experiment looked the same as those shown in figure 8.2A. This was further evidence that the Golgi was being specifically recognized since from the electron microscopy quantitation on cells treated with CHX and ANS the effect they caused was selective for this compartment (see Fig.5.5).

Figure 8.3. Factors affecting the TEX staining pattern.

Log phase cells were treated with anisomycin (A) or cycloheximide (B) for 3 hours, a time known to cause disruption of the GalT staining in cells, then fixed and processed for immunofluorescence using the TEX antiserum. Bar = 11 μm

Ypt1-1 cells were grown at 30°C and then shifted to 37°C for 4 hours to allow expression of the mutant phenotype. Cells were fixed and processed for immunofluorescence. (C) and (D) show staining in the cells at 37°C using the TEX antibody. Bar = 9 μm .



Effect of a temperature shift in ypt1-1.

The mutant strain *ypt1-1* was grown to log phase at 30°C. The culture was then shifted to 37°C for 4 hours to allow the mutant phenotype to be expressed. The cells were then fixed and stained using the TEX antibody. Again the staining resembled that obtained with the GTF antibodies. Punctate staining was clear at 30°C but much reduced at 37°C (Fig. 8.3D).

8.3. Discussion

The results presented here are highly suggestive of a shared epitope between the Golgi stacks in rat liver Golgi cells and fission yeast. No other antiserum to general or specific components of the Golgi apparatus has been shown to exhibit cross reactivity over such a broad evolutionary range.

Attempts were made to provide irrefutable evidence of Golgi labelling but the antibody did not bind successfully in immuno-e.m. experiments. Furthermore an attempt to achieve double labelling using the GalT gene tagged with the myc-epitope (recognized by a specific monoclonal antibody, 9E10) in conjunction with the TEX antiserum was not successful.

Chapter 9

Concluding Remarks

9.1 Summary introduction

The aim of this project was to study the Golgi apparatus in a simple organism which would also be tractable for genetic studies. This should facilitate our understanding of this complex organelle and how its distinctive stacked structure could relate to its function.

In the course of this work I have revealed numerous similarities as well as disparities between the two systems. Several of the findings indicate that certain aspects of Golgi apparatus structure in *S.pombe* are well conserved and strongly suggest that the further study of the Golgi in this organism would reveal components necessary for maintenance of the stacked Golgi form.

9.2. Structural conservation between the mammalian and fission yeast Golgi apparatus

On the basis of the characterization of the Golgi apparatus in wild type *S.pombe* cells comparisons can be drawn with the organelle in mammalian cells.

The major similarity is the appearance of the stack structure consisting of apposed cisternae with dilated rims. The number of cisternae in a stack is comparable with between four and seven most common for both mammalian cells and in fission yeast. However, in fission yeast the number can be quite variable within a cell with stacks of between two and nine existing in a single organism. Mammalian cells seem to have a variable number of cisternae in a stack but this number is usually constant

within a particular cell type. For example the stack in HeLa cells has three cisternae.

The stack size is extremely similar with the size of a single stack measuring about 0.5-1 μm in *S.pombe* and in mammalian cells about 1 μm , when measured in transverse section. The arrangement of these stacks in the cell is however different. The situation in fission yeast resembles that in plants with the stacks dispersed throughout the cell. In mammalian cells these stacks are linked together by tubules to form a single copy organelle. This structure is located in the juxtanuclear region of the cell. This difference means that the study of the Golgi apparatus in *S.pombe* might be able to shed light on the subject of stacking but other overlying complexities such as the reason for linking stacks or for localizing the Golgi apparatus near the nucleus could not be addressed. This however, can be considered as an advantage of such a system since it would allow a single problem to be investigated in relative isolation.

One factor that is clear in the mammalian Golgi apparatus is the polarity of the stack. Proteins from the ER enter at the cis face and traverse the Golgi in a uni-directional manner to the trans face where they are sent to the plasma membrane or are diverted to the lysosomes or secretory granules. At each stage within the Golgi stack the proteins may be post translationally modified. The compartments of the stack are biochemically distinct allowing a series of modifications to be performed. The presence of several of the resident enzymes has been determined by immunolocalization and this has demonstrated the differential localization of enzymes in the stack. As well as a functional polarity the two sides of the Golgi apparatus are also visually different. The trans face contains clathrin on its surface and is more reticular in nature. The situation in *S.pombe* does not appear to be so clear. No compartments corresponding

to the CGN or to the TGN have been morphologically identified. There is as yet no marker which has been used that shows a cisternally restricted localization. Some evidence for the existence of subcompartments came from immunolocalization of GalT (see chapter 3.3.1. and Fig. 3.12.). This did not show any polarity in its own localization but in a GalT deletion strain the antibody cross reacted with another Golgi protein which had a different distribution within the stack, being found primarily in the dilated rims. This protein was however still in most cisternae in the stack. The recent cloning of other Golgi proteins (T.Chappell, *pers. comm.*) and the availability of epitope tagging might allow this issue to be resolved relatively soon.

One interesting similarity between the mammalian and the fission yeast Golgi apparatus was highlighted by the cross reactivity of an antibody between the two systems. The antibody had been raised to rat liver Golgi stacks after extraction with Triton-X100 (see chapter 8). In mammalian cells, by immunofluorescence, exclusively Golgi apparatus staining was observed. When the antibody was applied to fission yeast cells the staining was extremely similar to that obtained with antibodies to the Golgi marker, GalT. Furthermore, staining was affected by factors which had been shown by electron microscopy to disrupt the Golgi apparatus. This indicated that certain epitopes associated with the Golgi apparatus structure have been conserved over the period of evolutionary divergence.

9.3. The Golgi apparatus at mitosis and the effect of microtubule disruption

The most dramatic morphological change observed for the Golgi apparatus in mammalian cells is at the onset of mitosis. The Golgi firstly fragments into about 250-300 small stacks which are dispersed in the cytoplasm. As mitosis progresses these stacks break down further into vesicles and clusters of vesicles. This end result of Golgi break down can be induced by the addition of nocodazole to cells. This drug has the effect of disrupting the microtubule network in cells so producing an effect similar to the onset of mitosis. It prevents formation of a mitotic spindle which is necessary for mitosis to proceed. This allows large numbers of cells, effectively in mitosis, to accumulate. The Golgi apparatus after treatment is found in the form of vesicles and clusters of vesicles. Cell cycle changes using mutant fission yeast strains and the effect of microtubule disrupting drugs were investigated with regard to their effect on the Golgi apparatus.

Nocodazole was added to fission yeast cells but it had relatively little effect on the cells (see 4.2.1). A related drug, thiabendazole (TBZ), was however, shown to have the desired effect on microtubules causing a rapid and reversible disruption of cytoplasmic microtubules. The effect on the Golgi apparatus was however different. There was no breakdown into smaller stacks nor an obvious vesiculation of the structure. Rather, the stack appeared to come apart yielding single cisternae. In the absence of a stack the cells were still able to secrete material though whether the secreted proteins were modified to the same extent could not be assayed due to the lack of markers for different stages in processing.

This process of unstacking could now be investigated more fully to try and elucidate the components of the Golgi apparatus which make it susceptible

to TBZ treatment. Further studies on the impact of the unstacking with regard to the functioning of the Golgi apparatus could be performed particularly as more stages of processing in this yeast are recognized and markers for these reactions detected.

The effect of entry into mitosis was also assessed in cell cycle mutants. In particular, the strain *cdc25*, can be shifted to the non-permissive temperature and the cells become blocked in late G2 phase. Cells can then be shifted back to the permissive temperature when they enter mitosis. The state of the Golgi apparatus was monitored in these cells. There was a decline in the level of stacked Golgi cisternae concomitant with mitosis but some stacks could be seen throughout mitosis and there was no evidence of wide scale vesiculation. This indicated that in fission yeast, as has been noted for plant cells, there is no wholesale break down of the Golgi apparatus at mitosis. The use of *S.pombe* to study the Golgi apparatus would therefore not be relevant for studying processes associated with the vesiculation observed at mitosis.

9.4. The effect on the Golgi apparatus of blocking the secretory pathway

Two areas of study gave some insight into the effect of blocking the secretory pathway on the Golgi apparatus in fission yeast. The work described in chapter 5 analyzed the effect of a block in new protein synthesis. Addition of protein synthesis inhibitors, cycloheximide (CHX) or anisomycin (ANS), caused the Golgi apparatus to fragment to such an extent that stacks of cisternae could no longer be seen in cells. Quantitation of membranes indicated that the Golgi apparatus had completely broken down into vesicles or small fragments. A model was

proposed to account for the observations which suggested that some component necessary for transport vesicles to fuse was rapidly turned over and in the presence of the drugs could not be replaced. The Golgi continued to bud but vesicles that formed were not able to fuse. Since fusion was inhibited components required for budding from the ER would not be able to return by the retrieval mechanism and so budding from this compartment would cease so preserving most of the structure of the ER. Thus, this indirect disruption of transport resulted in the break down of the Golgi apparatus.

A second area of study also shed light on the effect of transport on the structure of the Golgi apparatus. The mutant strain *ypt1-1* is defective in transport from the ER to the Golgi and possibly at intra-Golgi stages. When shifted to its non-permissive temperature the Golgi apparatus breaks down in a similar fashion to that seen with CHX. This therefore reaffirmed the observation that a block early in the secretory pathway can cause a massive perturbation in the structure of the Golgi apparatus.

9.5. The effect of Brefeldin A on the Golgi apparatus

The effect of the anti-fungal agent Brefeldin A (BFA) on the Golgi apparatus in mammalian cells is very dramatic. Within a few minutes of drug addition the stacks of cisternae are no longer visible and enzyme markers of the cis, medial and trans compartments are instead found in the ER. Whether this process in anyway resembles a physiological pathway for retrograde transport from the Golgi to the ER is not known. However, it was interesting to see the effect BFA had on the Golgi in *S.pombe*. The effect, as far as it could be quantitated was very similar to that observed in mammalian cells. The Golgi apparatus disappeared and most evidence

suggested that the material redistributed to the ER. This suggests that the components of the Golgi apparatus that are affected by BFA are largely conserved.

9.6. Summary

During the course of my work I have made an intensive investigation of the Golgi apparatus in the fission yeast. Initially, I made a detailed analysis of the organelle in wild type cells using immunofluorescence and electron microscopy. Antibodies were raised to a fusion protein that I constructed and these were shown to label the Golgi apparatus by immuno-electron microscopy. I then used these tools to study morphological changes in the Golgi apparatus under a range of conditions.

My research can be summarized as follows:

- 1) I have developed a system which causes the reversible unstacking of cisternae in the cell. This may allow a fuller understanding of the role of the stack to be assessed.
- 2) I have demonstrated the lability of a fusion component which if not continually synthesized results in breakdown of the Golgi apparatus.
- 3) I have shown that the action of BFA in *S.pombe* resembles the effect in mammalian cells with Golgi disruption and redistribution of markers to the ER.
- 4) In an early secretory pathway mutant, *ypt1-1*, I have shown that a block in the pathway leads to disruption of the Golgi apparatus.

5) In cell cycle mutants I have established that there is no wholesale vesiculation of the Golgi apparatus at mitosis as is observed in mammalian cells.

6) Specific cross reactivity with an antibody to mammalian Golgi structures showed that some epitopes have been conserved over the evolutionary period of divergence from *S.pombe* to mammalian cells.

This study has highlighted many aspects of the Golgi structure that were before unrecognized and further research at a genetic level could reveal molecules which play essential roles in the maintenance of the stacked structure. Such work would in turn increase our understanding of how the complex structure of the Golgi apparatus relates to its function.

1

Acknowledgements

I would like to thank my supervisor, Graham Warren, for his help and assistance over the years that I have been in his lab. My thanks also to the other members of the Cell Biology group, both past and present, who have provided support and advice during this time. In particular, I am extremely grateful to Rose Watson who has given so much excellent advice and assistance on the electron microscopy front, Maria Pierce for her help and friendship whilst she was in the lab, Deborah MacKay for encouragement, advice and excellent English grammar when required and Ginny Kieckbusch for always being around with a good and cheerful word.

I would also like to acknowledge my London University supervisor, Jeremy Hyams who was an inspiration, especially at the outset of the project.

To Paul Nurse I would like to express my gratitude for good advice just when needed and for giving me the opportunity to meet with other yeast scientists.

Beyond the laboratory is where my greatest thanks must be given, to those people who have borne the brunt of my frustrations when they have all had many of their own. Hopefully, they will be around to share in any future successes and still bear with me in my failures.

To my husband, James, who had a hard job to keep me smiling throughout writing up, but managed to succeed.

To all my family, especially my parents for unending support and encouragement when everything seemed doomed to failure. Without them it would have been a much harder task.

References

- Achstetter, T., Franzusoff, A., Field, C. and Schekman, R. (1988). *SEC7* encodes an unusual, high molecular weight protein required for membrane traffic from the yeast Golgi apparatus. *J.Biol. Chem.* **263**, 11711-11717.
- Alfa, C., Fantes, P., Hyams, J., McLeod, M. and Warbrick, E. (1993). Experiments with fission yeast; a laboratory course manual. Cold Spring Harbor Laboratory Press
- Antebi, A. and Fink, G.R. (1992). The yeast Ca^{2+} ATPase homologue, PM1, is required for normal Golgi function and localizes in a novel Golgi-like distribution. *Mol Biol. Cell* **3**, 633-654.
- Aves, S.J., Durkacz, B.W., Carr, A. and Nurse, P. (1985). Cloning, sequencing and transcriptional control of the *Schizosaccharomyces pombe* *cdc 10* "start" gene. *EMBO J.* **4**, 457-463.
- Bacon, R.A., Salminen, A., Ruohola, H., Novick, P. and Ferro-Novick, S. (1989). The GTP binding protein Ypt1 is required for transport in vitro: the Golgi apparatus is defective in *ypt1* mutants. *J. Cell Biol.* **109**, 1015-1022.
- Balch, W.E., Dunphy, W.G., Braell, W.A. and Rothman, J.E. (1984). Reconstitution of the transport of protein between successive compartments of the Golgi measured by the coupled incorporation of N-acetylglucosamine. *Cell* **39**, 405-416.
- Balch, W.E., Wagner, K.R. and Keller, D.S. (1986). ATP-coupled transport of vesicular stomatitis virus G protein between the endoplasmic reticulum and the Golgi. *J.Biol.Chem.* **261**, 14681-14689.
- Balch, W.E. (1992). From G minor to G major. *Curr. Biol* **2**, 157-160.
- Ballou, C. (1976). Structure and biosynthesis of the mannan component of the yeast cell envelope. *Advances in Microbial Physiology* **14**, 93-158.

- Bankaitis, V.A., Aitken, J.R., Cleves, A.E. and Dowhan, W. (1990).** An essential role for a phospholipid transfer protein in yeast Golgi function. *Nature* **347**, 561-562.
- Banta, L.M., Robinson, J.S., Klionsky, D.J. and Emr, S.D. (1988).** Organelle assembly in yeast: characterization of yeast mutants defective in vacuolar biogenesis and protein sorting.
- Barr, F.A., Leyte, A., Molliner, S., Pfeuffer, T., Tooze, S.A. and Huttner, W.B. (1991).** Trimeric G proteins of the trans Golgi network are involved in the formation of constitutive secretory vesicles and immature secretory granules. *FEBS Lett.* **293**, 1-5.
- Bause, E. and Lehle, L. (1979).** Enzymatic N-glycosylation and O-glycosylation of synthetic peptide acceptors by dolichol sugar linked derivatives in yeast. *Eur. J. Biochem.* **101**, 531-540.
- Becker, J., Tan, T.J., Trepte, H.H. and Gallwitz, D. (1991).** Mutational analysis of the putative effector domain of the GTP-binding Ypt1 protein in yeast suggests specific regulation by a novel GAP activity. *EMBO J.* **10**, 785-792.
- Beckers, C.J.M., Block, M.R., Glick, B.J. and Rothman, J.E. (1989).** Vesicular transport between the endoplasmic reticulum and the Golgi stack requires the NEM-sensitive protein. *Nature* **339**, 397-398.
- Behrens, N.H., Parodi, A.J. and Leloir, L. (1971).** Glucose transfer from dolichol monophosphate glucose: the product formed with endogenous microsomal acceptor. *Proc. Natl. Acad. Sci. USA* **68**, 2857-2860.
- Behrens, N.H., Carminatti, H., Stanelloni, R.J., Leloir, L. and Canarella, A.I. (1973).** Formation of lipid bound oligosaccharides containing mannose. Their role in glycoprotein synthesis. *Proc. Natl. Acad. Sci. USA* **70**, 3390-3394.

- Bennett, M.K., Calakos, N. and Scheller, R.H. (1992).** Syntaxin: a synaptic protein implicated in docking of synaptic vesicles at presynaptic active zones. *Science* **257**, 255-259.
- Blobel, G. and Dobberstein, B. (1975).** Transfer of protein across membranes. I. Presence of proteolytically processed and unprocessed nascent immunoglobulin light chains on membrane bound ribosomes of murine myeloma. *J. Cell Biol.* **67**, 835-851.
- Blomfield, J., Simson, J.A., Martinez, A.M. and Martinez, J.R. (1983).** Ultrastructural responses by Golgi apparatus to rat submandibular gland to β -adrenergic, α -adrenergic, and cholinergic stimulation. *Exp. Mol. Pathol.* **38**, 170-182.
- Braell, W.A., Balch, W.E., Dobberty, D.C. and Rothman, J.E. (1984).** The glycoprotein that is transported between successive compartments of the Golgi in a cell free system resides in stacks of cisternae 1984. *Cell* **39**, 511-524.
- Brands, R., Snider, M.D., Hino, Y., Park, S.S., Gelboin, H.V. and Rothman, J.E. (1985).** Retention of membrane proteins by the endoplasmic reticulum. *J. Cell Biol.* **101**, 1724-1740.
- Bressan, G.M. and Stanley, K.K. (1987).** pUEX, a bacterial expression vector related to pEX with universal host specificity. *Nuc. Acids Res.* **15**, 10056-10057.
- Burgess, T.L. and Kelly, R.B. (1987).** Constitutive and regulated secretion of proteins. *Ann. Rev. Cell Biol.* **3**, 243-293.
- Burke, B., Griffiths, G., Reggio, H., Louvard, D. and Warren, G. (1982).** A monoclonal antibody against a 135kDa Golgi membrane protein. *EMBO J.* **1**, 1621-1628.
- Burke, J., Pettitt, J.M., Schachter, H., Sarkar, M. and Gleeson, P.A. (1992).** The transmembrane and flanking sequences of β -1,2-N-

acetylglucosaminyl transferase I specify medial Golgi localization. *J. Biol. Chem.* **267**, 24433-24440.

Chappell, T. and Warren, G. (1989). A galactosyltransferase from the fission yeast, *Schizosaccharomyces pombe*. *J. Cell Biol.* **109**, 2693-2702.

Chege, N.W. and Pfeffer, S.R. (1990). Compartmentation of the Golgi complex : Brefeldin A distinguishes trans-Golgi cisternae from the trans Golgi network. *J. Cell Biol.* **111**, 893-899.

Chen, L.B. (1988). Mitochondrial membrane potential in living cells. *Annu. Rev. Cell Biol.* **4**, 155-181.

Clary, D.O. and Rothman, J.E. (1990a). Purification of three related peripheral membrane proteins needed for vesicular transport. *J. Biol. Chem.* **265**, 10109-10117

Clary, D.O., Griff, I.C. and Rothman, J.E. (1990b). SNAPs, a family of NSF attachment proteins involved in intracellular membrane fusion in animals and yeast. *Cell* **61**, 709-721.

Cluett, E.B. and Brown, W.J. (1992). Adhesion of Golgi cisternae by proteinaceous interactions: intercisternal bridges as putative adhesive structures. *J. Cell Sci.* **103**, 773-784.

Colman, A., Jones, E.A. and Heasman, J. (1985). Meiotic maturation in *Xenopus* oocytes: a link between the cessation of protein secretion and the polarized disappearance of Golgi apparatus. *J. Cell Biol.* **101**, 313-318.

Copeland, C.S., Doms, R.W. and Bolzau, E. (1986). Assembly of influenza haemagglutinin trimers and its role in intracellular transport. *J. Cell Biol.* **103**,

Corthésy-Theulaz, I., Pauloin, A. and Pfeffer, S.R. (1992). Cytoplasmic dynein participates in the centrosomal localization of the Golgi complex. *J. Cell Biol.* **118**, 1333-1346.

d'Enfert, C., Barlowe, C., Nishikawa, S., Nakano, A. and Schekman, R. (1991). Structural and functional dissection of a membrane

glycoprotein required for vesicle budding from the endoplasmic reticulum. *Mol. Cell Biol.* **11**, 5727-5734.

Dahms, N.M. and Hart, G.W. (1986). Influence of quaternary structure on glycosylation. *J. Biol. Chem.* **261**, 13186-13196.

Dalton, A.J. and Felix, M.D. (1954). Cytologic and cytochemical characteristics of the Golgi substance of epithelial cells of the epididymis - in situ, in homogenates and after isolation. *Am. J. Anat.* **94**, 171-207.

Dalton, A.J. and Felix, M.D. (1957). Electron microscopy of the mitochondria and the Golgi complex. *Symp. Soc. Exp. Biol.* **10**, 148-159.

Dean, N. and Pelham, H.R.B. (1990). Recycling of proteins from the Golgi compartment to the ER in yeast. *J. Cell Biol.* **111**, 369-377.

DeLaFuente, G. and Sols, A. (1970). The kinetics of yeast hexokinase in the light of the induced fit involved in binding of its sugar substrate. *Eur. J. Biochem* **16**, 234-239.

DeShaies, R.J., Sanders, S.L., Feldheim, D.A. and Schekman, R. (1991). Assembly of yeast Sec proteins involved in translocation into the endoplasmic reticulum into a membrane bound multisubunit complex. *Nature* **349**, 806-808.

Doms, R.W., Russ, G. and Yewdell, J.W. (1989). Brefeldin A redistributes resident and itinerant Golgi proteins to the endoplasmic reticulum. *J. Cell Biol.* **109**, 61-72.

Dunphy, W.G., Fries, E., Urbani, I.J. and Rothman, J.E. (1981). Early and late functions associated with the Golgi apparatus reside in distinct compartments. *Proc. Natl. Acad. Sci. USA* **78**, 7453-7457.

Dunphy, W.G. and Rothman, J.E. (1983). Compartmentation of asparagine-linked oligosaccharide processing in the Golgi apparatus. *J. Cell Biol.* **97**, 270-275.

Dunphy, W. and Rothman, J. (1985). Compartmental organization of the Golgi stack. *Cell* **42**, 13-21.

- Farquhar, M.G. and Palade, G.E.** (1981). The Golgi apparatus (complex) - (1954-1981) - from artifact to centre stage. *J. Cell Biol.* **91**, 77s-103s.
- Fawell, E., Bowden, S. and Armstrong, J.** (1992). A homologue of the ras-related *CDC42* gene from *Schizosaccharomyces pombe*. *Gene* **114**, 153-154.
- Franke, W.W., Kartenbeck, J., Zentgraf, H., Scheer, U. and Falk, H.** (1971). Membrane to membrane cross-bridges. A means to orientation and interaction of membrane faces. *J. Cell Biol.* **51**, 881-888.
- Franke, W.W., Kartenbeck, D.J., Krien, S., VanderWoude, W.J., Scheer, U. and Morre, D.J.** (1972). Inter- and intra-cisternal elements of the Golgi apparatus. A system of membrane to membrane cross-links. *Z.Zellforsch Mikrosk. Anat.* **132**, 365-380.
- Franzusoff, A. and Schekman, R.** (1989). Functional compartments of the yeast Golgi apparatus are defined by the *sec7* mutation. *EMBO J.* **8**, 2695-2702.
- Franzusoff, A., Lauze, E. and Howell, K.E.** (1992). Immuno-isolation of Sec7p-coated transport vesicles from the yeast secretory pathway. *Nature* **355**, 173-175.
- Friend, D.S. and Murray, M.J.** (1965). Osmium impregnation of the Golgi apparatus. *Am. J. Anat.* **117**, 135-150.
- Fries, E. and Rothman, J.E.** (1980). Transport of vesicular stomatitis virus glycoprotein in a cell free extract. *Proc. Natl. Acad. Sci. USA* **77**, 3870-3874.
- Gallop, P.M., Pa, M.A. and Hensen, E.** (1982). Boradeption: A new procedure for transferring water insoluble agents across membranes. *Science* **217**, 166-169.

- Gething, M.J., McCammon, K. and Sambrook, J. (1986).** Expression of wild type and mutant forms of influenza haemagglutinin: the role of folding in intracellular transport. *Cell* **46**, 939-950.
- Glick, B.S. and Rothman, J.E. (1987).** A possible role for acyl-coenzymeA in intracellular protein transport. *Nature* **326**, 309-312.
- Goldberg, D. and Kornfeld, S. (1983).** Evidence of extensive subcellular organization of asparagine-linked oligosaccharide processing and lysosomal enzyme phosphorylation. *J. Biol. Chem.* **258**, 3159-3165.
- Golgi, C. (1898).** Sur la structure des cellules nerveuses. *Arch. Ital. Biol.* **30**, 60-71.
- Graham, T.R. and Emr, S.D. (1991).** Compartmental organization of Golgi specific protein modification and vacuolar protein sorting events defined in a yeast *sec 18* (NSF) mutant. *J. Cell Bio.* **114**, 207-218.
- Green, J., Griffiths, G., Louvard, D., Quinn, P. and Warren, G. (1981).** Passage of viral membrane proteins through the Golgi complex. *J.Mol.Biol.* **152**, 663-698.
- Griffiths, G., Warren, G., Stuhfauth, I. and Jockusch, B.M. (1981).** The role of clathrin coated vesicles in acrosome formation. *Eur. J. Cell Biol.* **26**, 52-60.
- Griffiths, G., Brands, R., Burke, B., Louvard, D. and Warren, G. (1982).** Viral membrane proteins acquire galactose in trans Golgi cisternae during intracellular transport. *J. Cell Biol.* **95**, 781-792.
- Griffiths, G. and Simons, K. (1986).** The trans-Golgi network : sorting at the exit site of the Golgi complex. *Science* **234**, 438-443.
- Griffiths, G., Fuller, S.D., Back, R., Hollinshead, M., Pfeiffer, S. and Simons, K. (1989).** The dynamic nature of the Golgi complex. *J.Cell Biol.* **108**, 277-297.

- Groesch, M.E., Ruohola, H., Bacon, R., Rossi, G. and Ferro-Novick, S.** (1990). Isolation of a functional vesicular intermediate that mediates ER to Golgi transport in yeast. *J. Cell Biol* **111**, 45-53.
- Hardwick, K. and Pelham, H.R.B.** (1992). SED5 encodes a 39kD Integral membrane protein required for vesicular transport between the ER and the Golgi complex. *J. Cell Biol.* **119**, 513-521.
- Havelkova, M. and Mensik, P.** (1966). The Golgi apparatus in the regenerating protoplasts of *Schizosaccharomyces*. *Naturwissenschaften* **21**, 562.
- Hicke, L. and Schekman, R.** (1989). Yeast Sec23p acts in the cytoplasm to promote protein transport from the endoplasmic reticulum to the Golgi complex in vivo and in vitro. *EMBO J.* **8**, 1677-1684.
- Hiraoka, Y., Toda, T. and Yanagida, M.** (1984). The NDA3 gene of fission yeast encodes β -tubulin: A cold sensitive *nda3* mutation reversibly blocks spindle formation and chromosome movement. *Cell* **39**, 349-358.
- Ho, W.C., Allan, V.J., van Meer, G., Berger, E.G. and Kreis, T.E.** (1989). Reclustering of scattered Golgi elements occurs along microtubules. *Eur. J. Cell Biol.* **48**, 250-263.
- Huttner, W.B.** (1987). Protein tyrosine sulphation. *Trends. Biol. Sci.* **12**, 361-363.
- Jackson, M., Nilsson, T. and Peterson, P.A.** (1990). Identification of a consensus motif for retention of transmembrane proteins in the endoplasmic reticulum. *EMBO. J.* **9**, 3153-3162.
- Jackson, M.R., Nilsson, T. and Peterson, P.A.** (1993). Retrieval of transmembrane proteins to the endoplasmic reticulum. *J. Cell Biol.* **121**, 317-334.
- Jamieson, J.D. and Palade, G.E.** (1967). Intracellular transport of secretory proteins in the pancreatic exocrine cell. II. Transport to condensing vacuoles and zymogen granules. *J. Cell Biol.* **34**, 577-596.

- Jamieson, J.D. and Palade, G.E.** (1968). Intracellular transport of secretory proteins in the pancreatic exocrine cell: III. Dissociation of intracellular transport from protein synthesis. *J.Cell Biol.* **39**, 580-588.
- Johnson, B., Calleja, G., Yoo-B., Zuker, M. and McDonald, I.** (1982). Cell division : Key to cellular morphogenesis in the fission yeast *Schizosaccharomyces*. *Int.Rev.Cytol.* **208**, 167-208.
- Johnson, L.M., Bankaitis, B.A. and Emr, S.D.** (1987). Distinct sequence determinants direct intracellular sorting and modification of a yeast vacuolar protease. *Cell* **48**, 875-885.
- Julius, D., Brake, A., Blair, L., Kunisawa, R. and Thorner, J.** (1984). Isolation of the putative structural gene for the lysine-arginine cleaving endopeptidase required for processing of yeast prepro alpha factor. *Cell* **37**, 1075-1089.
- Kaiser, C.A. and Schekman, R.** (1990). Distinct sets of *SEC* genes govern transport vesicle formation and fusion early in the secretory pathway. *Cell* **61**, 723-733.
- Karecla, P.I. and Kreis, T.E.** (1992). Interaction of membranes of the Golgi complex with microtubules in vitro. *Eur, J, Cell Biol.* **57**, 139-146.
- Karnovsky, M.J.** (1965). A formaldehyde-glutaraldehyde fixative of high osmolality for use in electron microscopy. *J.Cell Biol. (Abstracts)* **27**, 137.
- Kelleher, D.J., Kreibich, G. and Gilmore, R.** (1992). Oligosaccharyltransferase activity is associated with a protein complex composed of ribophorins I and II and a 48kD protein. *Cell* **69**, 55-65.
- Kelly, R.B.** (1985). Pathways of protein secretion in eucaryotes. *Science* **230**, 25-32.
- Klausner, R.D., Donaldson, J.G. and Lippincott-Schwartz, J.** (1992). Brefeldin A: Insights into the control of membrane traffic and organelle structure. *J. Cell Biol.* **116**, 1071-1080.

- Klionsky, D.J. and Emr, S.D. (1989).** Membrane protein sorting: biosynthesis, processing and sorting of a yeast vacuolar alkaline phosphatase. *EMBO J.* **8**, 2241-2250.
- Klionsky, D.J. and Emr, S.D. (1990).** A new class of lysosomal/vacuolar protein sorting signals. *J. Biol. Chem.* **265**, 5349-5352.
- Klut, M.E., Stockner, J. and Bisalputra, T. (1989).** Further use of fluorochromes in the cytochemical characterization of phytoplankton. *Histochem.J.* **21**, 645-650.
- Kornfeld, R. and Kornfeld, S. (1985).** Assembly of asparagine linked oligosaccharides. *Ann. Rev. Biochem.* **54**, 631-664.
- Lang. (1984).** Lysosomal enzyme phosphorylation. *J. Biol. Chem.* **259**, 14663-14671.
- Lazzarino, D.A. and Gabel, C.A. (1988).** Biosynthesis of the mannose 6-phosphate recognition marker in transport impaired mouse lymphoma cells. *J. Biol. Chem.* **263**, 10118-10126.
- Lewis, M.J. and Pelham, H.R.B. (1990).** A human homologue of the yeast HDEL receptor. *Nature* **348**, 162-163.
- Lewis, M.J. and Pelham, H.R.B. (1992a).** Sequence of a second human KDEL receptor. *J. Mol. Biol.* **226**, 913-916.
- Lewis, M.J. and Pelham, H.R.B. (1992b).** Ligand-induced redistribution of a human KDEL receptor from the Golgi complex to the endoplasmic reticulum. *Cell* **68**, 353-364.
- Lippincott-Schwartz, J., Yuan, L.C., Bonifacino, J.S. and Klausner, R.D. (1989).** Rapid redistribution of Golgi proteins into the ER in cells treated with Brefeldin A : evidence for membrane cycling from Golgi to ER. *Cell* **56**, 801-813.
- Lippincott-Schwartz, J., Donaldson, J.G., Schweizer, A., Berger, E.G., Hauri, H.P., Yuan, L.C. and Klausner, R.D. (1990).** Microtubule

dependent retrograde transport of proteins into the ER in the presence of Brefeldin A suggests an ER recycling pathway. *Cell* **60**, 821-836.

Lipsky, N.G. and Pagano, R.E. (1985). A vital stain for the Golgi apparatus. *Science* **235**, 747.

Lodish, H.F., Kong, N., Hirani, S. and Rasmussen, J. (1987). A vesicular intermediate in the transport of hepatoma secretory proteins from the rough endoplasmic reticulum to the Golgi complex. *J. Cell Biol.* **104**, 221-230.

Lodish, H. (1988). Transport of secretory and membrane glycoproteins from the rough endoplasmic reticulum to the Golgi. *J. Biol. Chem.* **263**, 2107-2110.

Lucocq, J.M., Berger, E. and Warren, G. (1989). Mitotic Golgi fragments in HeLa cells and their role in the Golgi reassembly pathway. *J. Cell Biol.* **109**, 463-474.

Luft. (1956). Permanganate: a new fixative for electron microscopy. *J. Biophys. Biochem. Cytol.* **2**, 799.

Machamer, C.E., Doms, R.W., Bole, D.G., Helenius, A. and Rose, J.K. (1990). Heavy chain binding protein recognizes incompletely disulphide bonded forms of vesicular stomatitis virus G protein. *J. Biol. Chem.* **265**, 6879-6883.

MacNeill, S. and Nurse, P. (1989). Genetic interactions in the control of mitosis in fission yeast. *Curr.Genet.* **16**, 1-6.

Malholtra, V., Orci, L., Glick, B., Block, M.R. and Rothman, J.E. (1988). Role of an N-ethylmaleimide sensitive transport component in promoting fusion of transport vesicles with csterane of the Golgi stack. *Cell* **54**, 221-227.

Mans, R.J. and Novelli, G.D. (1961). Measurement of the incorporation of radioactive amino acids into protein by a filter paper disk method. *Arch. Biochem. Biophys.* **94**, 48-53.

- Maul, G.G. and Brinkley, B.R.** (1970). The Golgi apparatus during mitosis in human melanoma cells in vitro. *Cancer Res.* **30**, 2326-2335.
- Melancon, P., Glick, B.S., Malholtra, V., Weidman, P.J., Serafini, T., Gleason, A.M., Orci, L. and Rothman, J.E.** (1987). Involvement of GTP binding 'G' proteins in transport through the Golgi stack. *Cell* **51**, 1053-1062.
- Misumi, Y., Miki, A., Takatsuki, A., Tamura, G. and Ikehara, Y.** (1986). Novel blockade of brefeldin A of intracellular transport of secretory proteins in cultured hepatocytes. *J. Biol. Chem.* **261**, 11398-11403.
- Mitchison, J.M.** (1991).in *Molecular Biology of the fission yeast* Ed. Nasim, Young, and Johnson. Academic Press.
- Miyake, S. and Yamamoto, M.** (1990). Identification of the ras related , YPT family genes in *Schizosaccharomyces pombe*. *EMBO J.* **9**, 1417-1422.
- Mollenhaur, H.H.** (1965). An intercisternal structure in the Golgi apparatus. *J.Cell Biol.* **24**, 504-511.
- Mollenhaur, H.H. and Morre, D.J.** (1991). Perspectives on Golgi apparatus form and function. *J.Electr.Microsc.Tech.* **17**, 2-14.
- Moreno, S., Sanchez, Y. and Rodriguez, L.** (1990). Purification and characterization of the invertase from *S.pombe*. *Biochem. J* **267**, 697-702.
- Moreno, S., Klar, A. and Nurse, P.** (1991). Molecular Genetic Analysis of fission yeast, *Schizosaccharomyces pombe*. *Methods Enzymol.* **194**, 795-833.
- Moskalewski, S. and Thyberg, J.** (1992). Synchronized shift in localization of the Golgi complex and the microtubule organizing centre in the terminal phase of cytokinesis. *J. Submicrosc. Cytol. Pathol.* **24**, 359-370.

- Munro, S. and Pelham, H.R.B.** (1987). A C-terminal signal prevents secretion of luminal ER proteins. *Cell* **48**, 899-907.
- Munro, S.** (1991). Sequences within and adjacent to the transmembrane segment of α -2,6-sialyltransferase specify Golgi retention. *EMBO.J.* **10**, 3577-3588.
- Murata, M., Itoh, T.J., Kagiwada, S., Hishida, R., Hotani, H. and Ohnishi, S.** (1992). Interaction of the Golgi membranes isolated from rat liver with microtubules in vitro. *Biol. Chem.* **75**, 127-134.
- Newman, A.P. and Ferro-Novick, S.** (1987). Characterization of new mutants in the early part of the yeast secretory pathway isolated by [3 H] mannose suicide selection. *J. Cell Biol.* **105**, 1587-1594.
- Newman, A.P., Groesch, M.E. and Ferro-Novick, S.** (1992). Bos1p, a membrane protein required for ER to Golgi transport in yeast, co-purifies with the carrier vesicles and with Bet1p and the ER membrane. *EMBO. J.* **11**, 3609-3617.
- Nguyen, T.H., Law, D.T. and Williams, D.B.** (1991). Binding protein BiP is required for translocation of secretory proteins into the endoplasmic reticulum in *S.cerevisiae*. *Proc. Natl. Acad. Sci. USA* **88**, 1565-1569.
- Niehhs, C. and Huttner, W.B.** (1990). Purification and characterization of tyrosylprotein sulfotransferase. *EMBO. J* **9**, 35-42.
- Nilsson, T., Jackson and Peterson, p.A.** (1989). Short cytoplasmic sequences serve as retention signals for transmmbrane proteins in the endoplasmic reticulum. *Cell* **58**, 707-718.
- Nilsson, T., Lucocq, J.M., MacKay, D. and Warren, G.B.** (1991). The membrane spanning domain of β -galactosyltransferase specifies trans Golgi localization. *EMBO. J* **10**, 3567-3575.
- Nilsson, T., Pypaert, M., Hoe, M., Slusarewicz, P., Berger, E. and Warren, G.** (1993). Overlapping distribution of two glycosyltransferases in the Golgi apparatus of HeLa cells. *J. Cell Biol.* **120**, 5-13.

- Novick, P., Field, C. and Schekman, R. (1980).** Identification of 23 complementation groups required for post-translational events in the yeast secretory pathway. *Cell* **21**, 205-215.
- Novick, P., Ferro, S. and Schekman, R. (1981).** Order of events in the yeast secretory pathway. *Cell* **25**, 461-469.
- Novikoff, A.B. and Goldfisher, R. (1961).** Nucleoside diphosphatase activity in the Golgi apparatus and its usefulness in cytological studies. *Proc. Natl. Acad. Sci. USA* **47**, 802-810.
- Nurse, P., Thuriaux, P. and Naysmyth, K. (1976).** Genetic control of the cell division cycle in the fission yeast *Schizosaccharomyces pombe*. *Mol. Gen. Genet.* **146**, 167-178.
- Orci, L., Ravazola, M., Amherdt, M., Louvard, D. and Perrelet, A. (1985).** Clathrin immunoreactive sites in the Golgi apparatus are concentrated at the trans pole in polypeptide hormone secreting cells. *Proc. Natl. Acad. Sci. USA* **82**, 5385-5389.
- Orci, L., Glick, B.S. and J.E., R. (1986).** A new type of vesicular coated carrier that appears not to contain clathrin; its role in transport within the Golgi stack. *Cell* **46**, 171-184.
- Orci, L., Malholtra, V., Amherdt, M., Serafini, T. and Rothman, J.E. (1989).** Dissection of a single round of vesicular transport: sequential intermediates for intercisternal movement in the Golgi stack. *Cell* **56**, 357-368.
- Orci, L., Tagaya, M., Amherdt, M., Perrelet, A., Donaldson, J.G., Lippincott-Schwartz, J., Klausner, R.D. and Rothman, J.E. (1991).** Brefeldin A, a drug that blocks secretion, prevents the assembly of non-clathrin coated buds on Golgi cisternae. *Cell* **64**, 1183-1195.
- Orlean, P., Kuranda, M.J. and Albright, C.F. (1991).** Analysis of glycoproteins from *S.cerevisiae*. *Meth. Enzymol.* **194**, 682-697.

- Pagano, R.E., Sepanski, M.A. and Martin, O.C.** (1989). Molecular trapping of a fluorescent ceramide analogue at the Golgi apparatus of fixed cells. *J.Cell Biol.* **109**, 2067-2079.
- Palade, G.** (1975). Intracellular aspects of the process of protein synthesis. *Science* **189**, 347-358.
- Paulik, M., Nowack, D.D. and Morre, D.J.** (1988). Isolation of a vesicular intermediate in the cell free transfer of membrane from transitional elements of the endoplasmic reticulum to the Golgi apparatus. *J.Biol. Chem.* **263**, 17738-17748.
- Pelham, H.R.B.** (1989a). Control of protein exit from the endoplasmic reticulum. *Ann.Rev.Cell Biol.* **5**, 1-23.
- Pelham, H.R.B.** (1989b). Heat shock and the sorting of luminal ER proteins. *EMBO.J* **8**, 3171-3176.
- Pelham, H.R.B.** (1991). Recycling of proteins between the endoplasmic reticulum and Golgi complex. *Curr. Opin. Cell Biol.* **3**, 585-591.
- Peter, F., Nguyen-Van, P. and Soling, H.D.** (1992). Different sorting of Lys-Asp-Glu-Leu proteins in rat liver. *J. Biol. Chem.* **267**, 10631-10637.
- Picton, J.M. and Steer, M.W.** (1983). The effect of cycloheximide on dictyosome activity in *Tradescantia* pollen tubes determined using cytochalasin D. *Eur.J.Cell Biol.* **29**, 133-138.
- Pidoux, A.L. and Armstrong, J.** (1992). Analysis of the BiP gene and identification of an ER retention signal in *Schizosaccharomyces pombe*. *EMBO J.* **11**, 1583-1591.
- Plutner, H., Cox, A.D., Pind, S., Khovravi-Far, R., Bourne, Schwaninger, R., Der, C.J. and Balch, W.E.** (1991). Rab1b regulates vesicular transport between the endoplasmic reticulum and successive Golgi compartments. *J. Cell Biol* **115**, 31-43.

- Preuss, D., Mullholland, J., Franzusoff, A., Segev, N. and Botstein, D.** (1992). Characterization of the *Saccharomyces* Golgi complex through the cell cycle by immunoelectron microscopy. *Mol. Biol. Cell* **3**, 789-803.
- Pringle, J.R., Preston, R.A., Adams, A.E.M., Stearns, T., Drubin, D.G., Haarer, B.K. and Jones, E.W.** (1989). Fluorescence Microscopy Methods for Yeast. *Methods Cell Biol.* **31**, 357-435.
- Pryer, N., Wuestehube, L.J. and Schekman, R.** (1992). Vesicle mediated protein sorting. *Ann. Rev. Biochem.* **61**, 471-516.
- Rexach, M.F. and Schekman, R.W.** (1991). Distinct biochemical requirements for the budding, targeting and fusion of ER derived transport vesicles. *J. Cell Biol.* **114**, 219-229.
- Reynolds, E.C.** (1963). The use of lead citrate at high pH as an electron opaque stain in electron microscopy. *J. Cell Biol.* **17**, 208-212.
- Robbins, E. and Gonatas, N.K.** (1964). The ultrastructure of a mammalian cell during the mitotic cycle. *J. Histochem. Cytochem.* **12**, 704.
- Roberson, R.W. and Fuller, M.S.** (1988). Ultrastructural aspects of the hyphal tip of *Sclerotium rolfii* preserved by freeze substitution. **146**, 143-149.
- Roberts, C.J., Pohlig, G., Rothman, J.H. and Stevens, T.H.** (1989). Structure, biosynthesis and localization of peptidyl aminopeptidase B, an integral membrane glycoprotein of the yeast vacuole. *J. Cell Biol.* **108**, 1363-1373.
- Rose, J.K. and Doms, R.W.** (1988). Regulation of protein export from the endoplasmic reticulum. *Ann. Rev. Cell Biol.* **4**, 257-288.
- Roth, J. and Berger, E.G.** (1982). Immunocytochemical localization of galactosyltransferase in HeLa: codistribution with thiamine pyrophosphatase in trans Golgi cisternae. *J. Cell Biol.* **92**, 223-229.

- Rothblatt, J.A., DeShaies, R.J., Sanders, S.L., Daum, G. and Schekman, R. (1989).** Multiple genes are required for proper insertion of secretory proteins into the endoplasmic reticulum in yeast. *J. Cell Biol.* **109**, 2641-2652.
- Rothman, J.E. (1981).** The Golgi apparatus: two organelles in tandem. *Science* **213**, 1212-1219.
- Rothman, J.E., Miller, R.L. and Urbani, L.J. (1984a).** Intercompartmental transport in the Golgi complex is a dissociative process: facile transfer of membrane protein between two Golgi populations. *J. Cell Biol.* **99**, 260-271.
- Rothman, J.E., Urbani, L.J. and Brands, R. (1984b).** Transport of proteins between cytoplasmic membranes of fused cells: correspondence to processes reconstituted in a cell free system. *J. Cell Biol.* **99**, 248-259.
- Rothman, J.E. (1987).** Protein sorting by selective retention in the endoplasmic reticulum and Golgi stack. *Cell* **50**, 521-522.
- Rothman, J.E. (1989a).** Polypeptide chain binding proteins catalysts of protein folding and related processes in cells. *Cell* **59**, 591-601.
- Rothman, J.H., Howald, I. and Stevens, T.H. (1989b).** Characterization of genes required for protein sorting and vacuolar function in the yeast *Saccharomyces cerevisiae*. *EMBO. J* **8**, 2057-2065.
- Rothman, J.E. and Orci, L. (1992).** Molecular dissection of the secretory pathway. *Nature* **355**, 409-415.
- Russell, P. and Nurse, P. (1986).** *cdc25⁺* functions as an inducer in the mitotic control of fission yeast. *Cell* **45**, 145-153
- Sambrook, J., Fritsch, E.F. and Maniatis, T. (1989).** in *Molecular Cloning: a laboratory manual*. New York: Cold Spring Harbor Laboratory Press.

- Saraste, J. and Kuismanen, E. (1984).** Pre- and Post- Golgi vacuoles operate in the transport of Semliki Forest virus membrane glycoproteins to the cell surface. *Cell* **38**, 535-549.
- Sathananthan, A.H., Ng, S.C., Chia, C.M., Law, H.Y., Edirisinghe, W.R. and Ratnam, S.S. (1985).** The origin and distribution of cortical granules in human oocytes with reference to Golgi, nucleolar, and microfilament activity. *Ann. N.Y. Acad. Sci.* **442**, 251-264.
- Satiat-Jeunemaitre, B and Hawes, C. (1992).** Reversible dissociation of the plant Golgi apparatus by Brefeldin A. *Biol Cell* **74**, 325-328.
- Schacter, H. (1986).** Biosynthetic controls that determine the branching and microheterogeneity of protein bound oligosaccharides. *Biochem. Cell Biol.* **64**, 163-181.
- Schroer, T.A. and Sheetz, M.P. (1991).** Functions of microtubule based motors. *Ann. Rev. Physiol.* **53**, 629-652.
- Schweingruber, A.M., Schoenholzer, F., Keller, L., Schwaninger, R., Trachsel, H. and Schweingruber, M.E. (1986a).** Glycosylation and secretion of acid phosphatase in *Schizosaccharomyces pombe*. *Eur. J. Biochem* **158**, 133-140.
- Schweingruber, M.E., Fluri, R., Maundrell, K., Schweingruber, A.M. and Dumermuth, E. (1986b).** Identification and characterization of thiamin repressible acid phosphatase in yeast. *J.Biol.Chem.* **261**, 15877-15882.
- Seeger, M. and Payne, G.S. (1992).** A role for clathrin in the sorting of vacuolar proteins in the Golgi complex of yeast. *EMBO.J.* **11**, 2811-2818.
- Segev, N., Mulholland, J. and Botstein, D. (1988).** The yeast GTP binding YPT1 protein and a mammalian counterpart are associated with the secretion machinery. *Cell* **52**, 915-924.

- Semenza, J.C., Hardwick, K.G., Dean, N. and Pelham, H.R.B. (1990).** ERD2 , a yeast gene required for the retrieval of luminal ER proteins from the secretory pathway. *Cell* **61**, 1349-1357.
- Serafini, T., Orci, L., Amherdt, M., Brunner, M., Kahn, R.A. and Rothman, J.E. (1991a).** ADP-ribosylation factor is a subunit of the coat of Golgi derived COP-coated vesicles: a novel role for a GTP binding protein. *Cell* **67**, 239-253.
- Serafini, t., Stenbeck, G., Brecht, A., Lottspeich, F., Orci, L. and Rothman, J.E. (1991b).** A coat subunit of Golgi derived non-clathrin coated vesicles with homology to the clathrin coated vesicle coat protein β -adaptin. *Nature* **349**, 215-220.
- Serrano, R.C., Gancedo, J.M. and Gancedo, C. (1973).** Assay of yeast enzymes in situ. A potential tool in regulation studies. *Eur.J.Biochem.* **34**, 479-482.
- Sewall, T.C., Roberson, R.W. and Pommerville, J.C. (1989).** Identification and characterization of Golgi equivalents from *Allomyces macrocygnus*. *Exp. Mycology* **13**, 239-252.
- Shim, J., Newman, A.P. and Ferro-Novick, S. (1991).** The *BOS1* gene encodes an essential 27k putative membrane protein that is required for vesicular transport from the ER to the Golgi complex in yeast. *J. Cell Biol.* **113**, 55-64.
- Sjöstrand, F.S. and Hanzon, V. (1954).** Ultrastructure of Golgi apparatus of exocrine cells of mouse pancreas. *Exp. Cell Res.* **7**, 415-429
- Slot, J.W. and Geuze, H.J. (1983).** Immunoelectron microscopic exploration of the Golgi complex. *J. Histochem. Cytochem.* **31**, 1049-1056.
- Smith, D. and Svoboda, A. (1972).** Golgi apparatus in normal cells and protoplasts of *Schizosaccharomyces pombe*. *Microbios* **5**, 177-182.

- Sollner, T., Whiteheart, S.W., Brunner, M., Erdjument-Bromage, H., Geromans, S., Tempst, P. and Rothman, J.E.** (1993). SNAP receptors implicated in vesicle targeting and fusion. *Nature* **362**, 318-323.
- Sterio, D.C.** (1984). The unbiased estimation of numbers and sizes of arbitrary particles using the disector. *J. Microsc.* **134**, 127-136.
- Stevens, T., Esmo, B. and Schekman, R.** (1982). Early stages in the yeast secretory pathway are required for transport of carboxypeptidase Y to the vacuole. *Cell* **30**, 439-448.
- Streiblova, E., Hasek, J. and Jelke, E.** (1984). Septum patterns in ts mutants of *Schizosaccharomyces pombe* defective in genes *cdc3*, *cdc4*, *cdc8*, and *cdc12*. *J Cell Sci* **69**, 47-65.
- Südhof, T.C. and Jahn, R.** (1991). Proteins of synaptic vesicles involved in exocytosis and membrane recycling. *Neuron* **6**, 665-677.
- Svoboda, A. and Necas, O.** (1987). Ultrastructure of *Saccharomyces cerevisiae* cells accumulating Golgi organelles. *J. Basic Microbiol.* **27**, 603-612.
- Sweet, D. and Pelham, H.R.B.** (1992). The *Saccharomyces cerevisiae* *SEC20* gene encodes a membrane glycoprotein which is sorted by the HDEL retrieval system. *EMBO J.* **11**, 423-432.
- Swift, S. and Machamer, C.E.** (1991). A Golgi-retention signal in a membrane spanning domain of coronavirus-E1 protein. *J. Cell Biol.* **115**, 19-30.
- Takatsuki, A. and Tamura, G.** (1985). Brefeldin A, a specific inhibitor of intracellular translocation of Vesicular Stomatitis virus G protein: intracellular accumulation of high mannose type G protein and inhibition of its cell surface expression. *Agric. Biol. Chem.* **49**, 899-902.
- Tamura, G., Ando, K., Suzuki, S., Takatsuki, A. and Arima, K.** (1968). Antiviral activity of brefeldin A and Verrucaric acid. *J. Antibiotics* **21**, 160-161.

- Tartakoff, A.M. and Vassalli, P. (1983).** Lectin binding sites as markers of Golgi subcompartments: proximal to distal maturation of oligosaccharides. *J. Cell Biol.* **97**, 1243-1248.
- Thyberg, J. and Moskalewski, S. (1985).** Microtubules and the organization of the Golgi complex. *Exp.Cell Res.* **159**, 1-16.
- Toda, T., Adachi, Y., Hiroaka, Y. and Yanagida, M. (1984).** Identification of the pleiotropic cell division cycle gene *NDA2* as one of two different alpha tubulin genes in *Schizosaccharomyces pombe*. *Cell* **37**, 233-242.
- Tong, P.Y., Gregory, W. and Kornfeld, S. (1989).** Ligand interactions of the cation independent mannose 6-phosphate receptor. *J. Biol. Chem.* **264**, 7962-7969.
- Tong, P.Y. and Kornfeld, S. (1989).** Ligand interactions of the cation dependent mannose 6-phosphate receptor. *J.Biol. Chem.* **264**, 7970-7975.
- Turner, F.R. and Whaley, W.G. (1965).** Intercisternal elements of the Golgi apparatus. *Science* **147**, 1303-1304
- Umesono, K., Toda, T., Hayashi, S. and Yanagida, M. (1983).** Two cell division cycle genes *NDA2* and *NDA3* of the fission yeast, *S.pombe* control microtubular organization and sensitivity to anti mitotic benzimidazole compounds. *J.Mol.Biol.* **168**, 271-284.
- Valls, L.A., Hunter, C.P., Rothman, J.H. and Stevens, T.H. (1987).** Protein sorting in yeast: the localization determinant of yeast vacuolar carboxypeptidase Y resides in the propeptide. *Cell* **48**, 887-897.
- Valls, L.A., Winther, J.R. and Stevens, T.H. (1990).** Yeast carboxypeptidase Y vacuolar targeting signal is defined by four propeptide amino acids. *J.Cell Biol.* **111**, 361-368 .
- van Rijn, H.J.M., Linneman, W.A.M. and Boer, P. (1975).** Localization of acid phosphatase in protoplasts from *Saccharomyces cerevisiae*. *J. Bacteriol.* **123**, 1144-1149.

- von Figura, K. and Hasilik, A. (1986).** Lysosomal enzymes and their receptors. *Ann. Rev. Biochem.* **55**, 167-193
- Walker, G. (1982).** Cell cycle specificity of certain antimicrotubular drugs in *S.pombe*. *J. Gen.Microbiol.* **128**, 61-71.
- Walworth, N.C., Goud, B., Kastan-Kabcenell, A. and Novick, P. (1989).** Mutational analysis of SEC4 suggests a cyclical mechanism for the regulation of vesicular traffic. *EMBO.J.* **8**, 1685-1693.
- Warren, G. (1993).** Membrane partitioning during cell division. *Annu. Revs. Biochem.* in press,
- Weisman, L., Bacallao, R. and Wickner, W. (1987).** Multiple methods of visualizing the yeast vacuole permit evaluation of its morphology and inheritance during the cell cycle. *J.Cell Biol.* **105**, 1539-1547.
- Wiedmann, M., Huth, A. and Rapoport, T.A. (1984).** *Xenopus* oocytes can secrete bacterial β -lactamase. *Nature.* **309**, 637-639.
- Wieland, F.T., Gleason, M.L., Serafini, T.A. and Rothman, J.E. (1987).** The rate of bulk flow from the endoplasmic reticulum to the cell surface. *Cell* **50**, 289-300.
- Williams, D.B. and Lennarz, W.J. (1984).** Control of asparagine-linked oligosaccharide processing: studies on bovine pancreatic ribonuclease B. *J. Biol. Chem.* **259**, 5105-5114.
- Willingham, M.C., A.V., R., Galo, M.G., Wehland, J., Dickson, R.B., Schlegel, R. and Pastan, I.H. (1981).** Receptor mediated endocytosis in cultured fibroblasts. *J. Histochem. Cytochem.* **27**, 1003-1013.
- Wilson, D.W., Wilcox, C.A., Flynn, G.C., Chen, E., Kuang, W.J., Henzel, W.J., Block, M.R., Ullrich, A. and Rothman, J.E. (1989).** A fusion protein required for vesicle mediated transport in both mammalian cells and yeast. *Nature* **339**, 355-359.

Wong, S.H., Low, S.H. and Wong, W. (1992). The 17-residue transmembrane domain of the β -galactoside α 2,6-sialyltransferase is sufficient for Golgi retention. *J. Cell Biol.* **117**, 245-258.

Yamamoto, M. (1980). Genetic analysis of resistant mutants to antimitotic benzimidazole compounds in *Schizosaccharomyces pombe*. *Mol.Gen.Genet.* **180**, 231-234.

Yamamoto, A., Masaki, R. and Tashiro, Y. (1985). Is cytochrome P-450 transported from the endoplasmic reticulum to the Golgi apparatus in rat hepatocytes? *J.Cell Biol.* **101**, 1733-1740.

Yamamoto, K.K. and Pellegrini, M. (1990). Ribosome subunit to polysome ratios affect the synthesis of rRNA in *Drosophila* cells. *Biochemistry* **29**, 11029-11032.

Zahraoui, A., Touchot, N., Chardin, P. and Tavitian, A. (1989). The human rab genes encode a family of GTP-binding proteins related to yeast YPT1 and SEC4 products involved in secretion. *J.Biol.Chem* **264**, 12394-12401.

Zieve, G.W., Turnbull, D., Mullins, J.M. and McIntosh, J.R. (1980). Production of large numbers of mitotic mammalian cells by use of the reversible microtubule inhibitor nocodazole. *Exp. Cell Res.* **126**, 397-405.